AD

USAAVLABS TECHNICAL REPORT 68-9

T63 REGENERATIVE ENGINE PROGRAM

By

Edward J. Privoznik

May 1968

U. S. ARMY AVIATION MATERIEL LABORATORIES
FORT EUSTIS, VIRGINIA

CONTRACT DA 44-177-AMC-293(T)

ALLISON DIVISION - GENERAL MOTORS

INDIANAPOLIS, INDIANA

205

DEPARTMENT OF THE ARMY

U S ARMY AVIATION MATERIEL LABORATORIES

FORT EUSTIS VIRGINIA 23604

This report was prepared by the Allison Division of General Motors Corporation under the terms of Contract DA 44-177-AMC-[illegible](T), and describes design features of the regenerator and modifications performed on the basic T63 engine and fuel controls as well as modifications made to the YOH-6A aircraft. Test data are presented for the regenerator, regenerative engine, and the YOH-6A aircraft powered with the regenerative T63 engine.

The object of this contractual effort was to conduct experimental flight testing of a regenerative T63 engine to investigate engine/regenerator performance and fuel control response in an experimental aircraft installation and to assess installation and operational problems associated with regenerative engine systems.

This program demonstrated the feasibility of a regenerative engine as a powerplant for aircraft operation. Results indicate that application of a regenerative engine can provide a significant improvement in aircraft range capability and in fuel logistics. The world's first known flight of an aircraft obtaining its sole power from a regenerative engine was demonstrated during this program.

The conclusions and recommendations contained herein are concurred in by this Command.

Disclaimer

When Government drawings, specifications, or other data are used for any purpose other than in connection with a definitely related Government procurement operation, the United States Government thereby incurs no responsibility nor any obligation whatsoever; and the fact that the Government may have formulated, furnished, or in any way supplied the said drawings, specifications, or other data is not to be regarded by implication or otherwise as in any manner licensing the holder or any other person or corporation, or conveying any rights or permission, to manufacture, use, or sell any patented invention that may in any way be related thereto.

The findings in this report are not to be construed as an official Department of the Army position unless so designated by other authorized documents.

Disposition Instructions

Destroy this report when no longer needed. Do not return it to the originator.

Task 1M121401A14413
Contract DA-44-177-AMC-293(T)
USAAVLABS Technical Report 68-9
May 1968

T63 REGENERATIVE ENGINE PROGRAM

EDR 5380

by
Edward J. Privoznik

Prepared By
Allison Division • General Motors
Indianapolis, Indiana

for
U. S. ARMY AVIATION MATERIEL LABORATORIES
FORT EUSTIS, VIRGINIA

ABSTRACT

Application of regeneration to the small gas turbine engine can provide a significant improvement in Army aircraft range capability and in fuel logistics. However, very little is known about regenerator performance when tested under actual operating conditions. This is especially true of regenerative engine-aircraft compatibility. The program was oriented toward gaining this experience.

The program was divided into three phases. Phase I consisted of the design and fabrication of the regenerator and required engine modifications. Phase II encompassed the engine testing required to ensure the flight worthiness of the regenerative engine. Phase III included modifications of a YOH-6A helicopter and flight test of the regenerative engine powered aircraft throughout its operating range.

The test program demonstrated the feasibility of a regenerative engine as a powerplant for aircraft operation. A horsepower-to-weight ratio of 1.62 and a maximum specific range of 1.25 miles per pound of fuel were demonstrated. The addition of a regenerator increased the specific range of the YOH-6A aircraft by 25.7%. The performance at altitude agreed with the originally predicted values obtained by means of a computer program.

The transient response of the regenerative engine powered aircraft was similar to that obtained using the prototype T63-A-5 nonregenerative engine.

TABLE OF CONTENTS

LIST OF ILLUSTRATIONS

LIST OF TABLES

LIST OF SYMBOLS

θ = Ratio of compressor inlet temperature to standard sea level temperature

θ_A = Ratio of compressor inlet temperature to standard altitude temperature

δ = Ratio of compressor inlet pressure to standard sea level pressure

δ_A = Ratio of compressor inlet pressure to standard altitude pressure

$\frac{HP}{\sqrt{\theta}\,\delta}$ = Horsepower corrected to standard day conditions

$\frac{W_f}{\sqrt{\theta}\,\delta}$ = Fuel flow corrected to standard day conditions—lb/hr

$\frac{N}{\sqrt{\theta}}$ = Rotational speed corrected to standard day conditions—rpm

$\frac{W_a\sqrt{\theta}}{\delta}$ = Airflow corrected to standard day conditions—lb/sec

sfc = Specific fuel consumption—lb/fuel/horsepower-hour

K_4 = Gas producer turbine flow factor

R_t = Turbine expansion ratio

R_c = Compressor pressure ratio

η_T = Turbine efficiency—%

η_c = Compressor efficiency—%

η = Regenerator effectiveness—%

$\frac{\Delta P}{P} \cdot 100$ = Pressure loss—%

P_{T_2} = Compressor inlet total pressure—in. Hg abs

P_{T_3} = Compressor discharge total pressure—in. Hg abs

$P_{T_{3.5}}$ = Regenerator air outlet total pressure—in. Hg abs

P_{T_4} = Burner outlet total pressure—in. Hg abs

P_{S_7} = Regenerator gas inlet static pressure—in. Hg abs

P_{S_8} = Regenerator gas outlet static pressure—in. Hg abs

T_{T_2} = Compressor inlet total temperature—°F

T_{T_3} = Compressor discharge total temperature—°F

$T_{T_{3.5}}$ = Regenerator air outlet total temperature—°F

T_{T_5} = Gas producer turbine outlet temperature—°F

T_{T_7} = Regenerator gas inlet total temperature—°F

T_{T_8} = Regenerator gas outlet total temperature—°F

N_1 = Gas producer speed—rpm

N_2 = Power turbine speed—rpm

INTRODUCTION

Application of regeneration to the small gas turbine can provide a significant improvement in Army aircraft range capability and in fuel logistics. However, very little is known about regenerator performance under actual operating conditions. This is especially true of regenerative engine-aircraft compatibility. The program was oriented toward gaining this experience.

Parametric studies have been made to determine the optimum regenerator effectiveness for light helicopter applications. These studies have shown that although specific fuel consumption decreases as regenerator effectiveness increases, the higher regenerator effectiveness requires a substantially greater size and weight, which lower the fuel-carrying capacity of the aircraft for a given gross weight. In terms of aircraft performance, the optimum regenerator effectiveness lies between 50% and 75%. Within this range of effectiveness, the final design effectiveness for any particular installation is dependent on the trade-off between engine weight, physical size, and engine specific fuel consumption. For this test program, it was necessary to adapt a regenerator to an existing T63 engine for installation in an existing YOH-6A helicopter. Under these conditions, the target effectiveness was 60% with a total pressure drop of 4.86%.

The program was divided into three phases. Phase I consisted of the design and fabrication of the regenerator and required engine modifications. A "bolt-on" type regenerator requiring a minimum of engine and aircraft modifications was designed and fabricated by AiResearch Manufacturing Division of Garrett Corporation. Phase II encompassed the engine testing required to ensure the flightworthiness of the regenerative engine. Phase III included modification of a YOH-6A helicopter and the flight test of the regenerative engine powered aircraft throughout its operating range.

SUMMARY

1. The regenerative engine produced 300 hp with a specific fuel consumption of 0.555 at takeoff and Military power rating (TOT = 1380°F). This is 7% above program target horsepower and 0.9% below program target specific fuel consumption. The basic engine without the regenerator exceeded specification by approximately 2%.

2. The regenerator performance met or exceeded the program target values of 60% effectiveness and 9.86% total pressure drop. Regenerator weight was 50.2 lb.

3. The total engine weight was 184.5 lb, resulting in a horsepower-to-weight ratio of 1.62.

4. The engine successfully completed a 50-hr flightworthiness test without difficulty. All parts were found to be in excellent condition. The maximum performance depreciation of 2.1% occurred at 75% normal power. This depreciation is well within the allowable limits.

5. At takeoff and Military power (1380°F TOT), the engine performance at altitude agreed closely with calculated performance. Horsepower ranged from 2% to 6% above calculated, and specific fuel consumption ranged from 1% below to 2% above the calculated performance.

6. Bypassing the exhaust side of the regenerator did not increase the horsepower at 1380°F because of excessive pressure drop in the bypass system. With a regenerator specifically designed for a bypass system, the pressure drop could be reduced.

7. The maximum specific range of the regenerative powered helicopter was 1.25 mile/lb of fuel compared to 0.99 mile/lb of fuel for the nonregenerative powered helicopter. This is a 25.7% improvement in range.

8. Installation losses of the regenerative engine in the YOH-6A were 2.2% in horsepower and 1.8% in specific fuel consumption. This loss is comparable with that of the nonregenerative engine.

9. An operational control system for the regenerative engine was made using existing nonregenerative control components.

10. Aircraft control response during transient and steady-state operation was adequate for the test program. Additional control work is required to provide transient response close to that of the T63-A-5A nonregenerative engine.

11. Compartment temperatur s were 27° to 96° F higher than those with the nonregenerative engine. Although compartment temperatures were still within limits for the test program, hot day operation will require insulation on the regenerators to reduce compartment temperatures. Estimated weight of the insulation is 4 lb.

12. Infrared measurements of the regenerative powered aircraft indicated a marked reduction in the infrared signature from the "tail-on" position. Infrared radiation test results will be published by Naval Weapons Test Center.

13. A total test time of 121 hr 50 min was accumulated on three sets of hardware. The maximum time on one set of hardware was 63 hr 30 min. Of this total test time, 21 hr 5 min flight test time was accumulated on the third set of regenerators.

CONCLUSIONS AND RECOMMENDATIONS

The test data obtained during this program has demonstrated the feasibility of a regenerative engine as a powerplant for aircraft operation. No serious problems (i.e., abnormal engine depreciation or excessive thermal inertia) were encountered during the program. In addition, the regenerator has demonstrated the capability of withstanding the temperature transients associated with engine operation.

However, there are areas which should be investigated. Additional endurance time should be accumulated on the existing hardware. The area of carbon fouling and dust ingestion should be investigated. No problem with carbon fouling was encountered in this program, but a specific test schedule should be run which will tend to build up carbon. Carbon buildup should be greatest after long periods at low power. The effects of sand and dust ingestion should also be investigated. A regenerator should tolerate the same dust environment as the basic engine.

It should be kept in mind that the regenerative engine resulting from this program is not the optimum regenerative engine cycle. To obtain the maximum benefit from the regenerator, the engine should operate at a constant temperature. Variable turbine nozzles or power transfer can provide this mode of operation. With constant-temperature operation, the specific fuel consumption at low horsepower is significantly reduced, resulting in the flat specific fuel consumption curve characteristic of most regenerative engine performance studies. Any further regenerative engine programs should consider variable geometry or power transfer.

REGENERATOR DESIGN AND FABRICATION

PRELIMINARY DESIGN

A major consideration in design of the regenerator was achievement of favorable performance in the envelope available with both flow maldistribution and pressure losses held to a minimum. The relatively high duct velocity pressures required that abrupt changes in flow direction and flow area be avoided to achieve low pressure losses. This philosophy was followed in the design of the regenerator, although restrictions of duct locations, sizes and overall envelope required some compromise.

A core no-flow dimension that is large relative to one or two of the other core flow dimensions generally results in a lightweight core whereas a small no-flow dimension results in a heavier core. For a given heat exchanger core, as the no-flow dimension is reduced, the mass velocity on both sides of the core increases directly. If the core matrix is unchanged, then the flow dimensions on both sides of the core must be increased to reduce the pressure drops. Although the core velocity pressure decreases with the square of the increase in flow width on one side of the core, the corresponding increase in flow length on the other side of the core causes the pressure drop to decrease at a slower rate than the flow width increases. Since the surface area of the core increases the temperature effectiveness also increases, requiring a change in heat exchanger surface to a less restrictive and less compact heat transfer surface. As a result, a smaller portion of the pressure drop is utilized in the heat transfer portion of the core and the parasitic losses are larger. This relationship is shown in Figure 1.

The problem of a small no-flow dimension is inherent in most aircraft heat exchanger applications where space is restricted. This was also true with the T63 application. For the T63 application, a maximum no-flow dimension was attained by designing the core in the form of a ring or annulus. This design concept lends itself to packaging in a compact configuration and to reasonable duct designs that minimize both flow maldistribution and pressure loss. See Figure 48.

The final regenerator flow configuration is a two-pass folded cross-flow design. Figure 2 shows the gas and airflow paths through the regenerator. Two regenerators, a left-hand and a right-hand, are required for each engine. The two regenerators are defined as a ship set. Air enters the regenerator through the air inlet duct from the engine compressor, turns

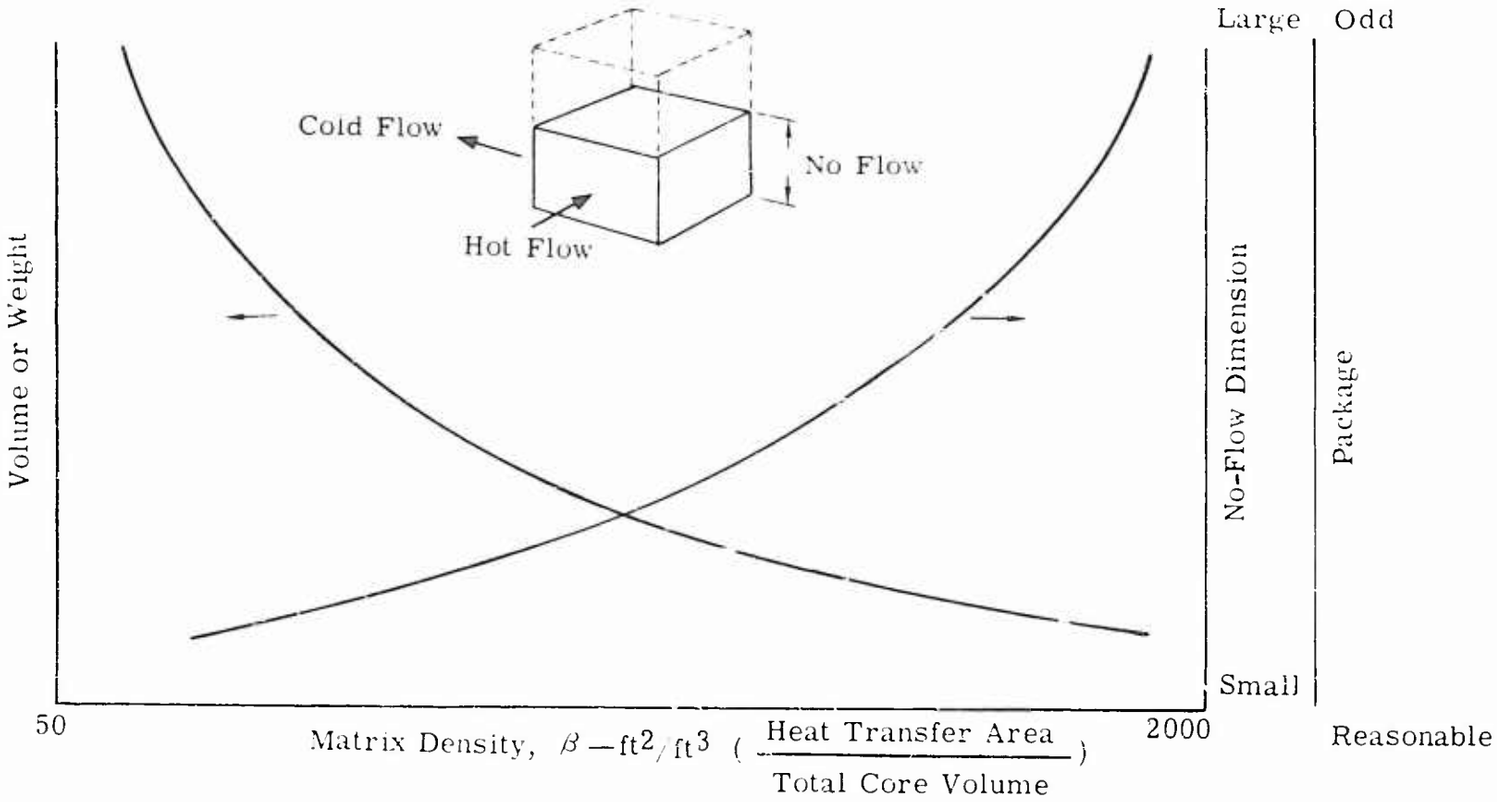

Figure 1. Heat Exchanger Parameters.

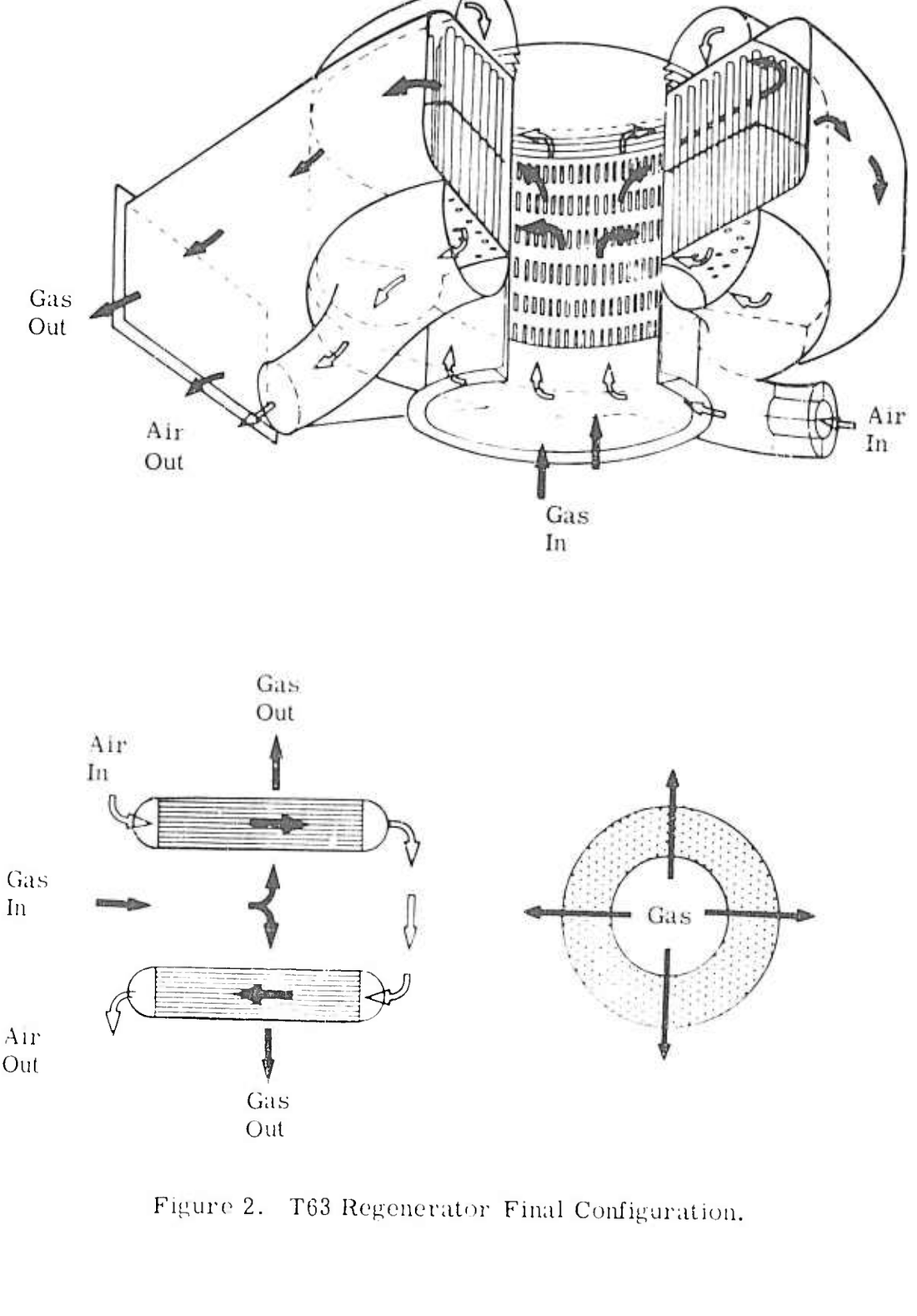

Figure 2. T63 Regenerator Final Configuration.

through a moderate angle, expands in the diffuser section, and expands into the air inlet manifold of the regenerator. The diffuser is a cone-shaped insert in the air inlet duct and serves to reduce the expansion losses into the air inlet manifold. The air enters half of the regenerator core tubes and passes to a toroidal turning pan. From the turning pan, air enters the remaining half of the core tubes for the second core pass and passes into the air return manifold. The air is then contracted into the air outlet duct and is turned at two 45-degree angles before exit from the regenerator.

Flow maldistribution on the air side is minimized by orientating the core relative to the air inlet and air outlet ducting. Figure 3 illustrates this effect. With the headers arranged as shown in Figure 3A, a preferential flow will occur at the core inlet and outlet. Flow at the extreme ends of the header will be minimized because of the sharp turning required. The selected header orientation is illustrated in Figure 3B. This configuration balances the pressure losses of the inlet and outlet headers and results in a uniform air-side distribution.

Exhaust gas enters the regenerator from the engine exhaust duct and makes a single radial pass across the core tubes. The gas is collected in an annular gas outlet manifold and passes through a square duct to the helicopter exhaust ducting. With this arrangement, a preferential gas flow path would exist through the core if uniform core tube spacing were used. The flow path would be through the core adjacent to the outlet duct opening. This effect is minimized by spacing the core tubes in both the exhaust gas flow and core no-flow directions. The tubes are more closely spaced at the outlet side of the manifold and farther apart on the opposite side of the core. The optimum core tube spacing was determined by an AiResearch computer program.

Figure 4 shows the general arrangement of the T63 core. The core tubes are arranged in an annular configuration with a variable tube matrix density around the core. The tube pattern is a staggered design. For reference purposes, the core has been divided into various sectors from I to VI. The core geometry is symmetrical about the centerline with core sector I identical with core sector I', etc. Sector IV is divided into IV-A and IV-B since this portion of the core incorporates the first-to-second pass split.

The core matrix density is greatest adjacent to the gas outlet duct (Sectors IV, V, VI and VI') and decreases in the core no-flow direction to a minimum at Sectors I and I'. Due to [illegible] geometry, the core [illegible]

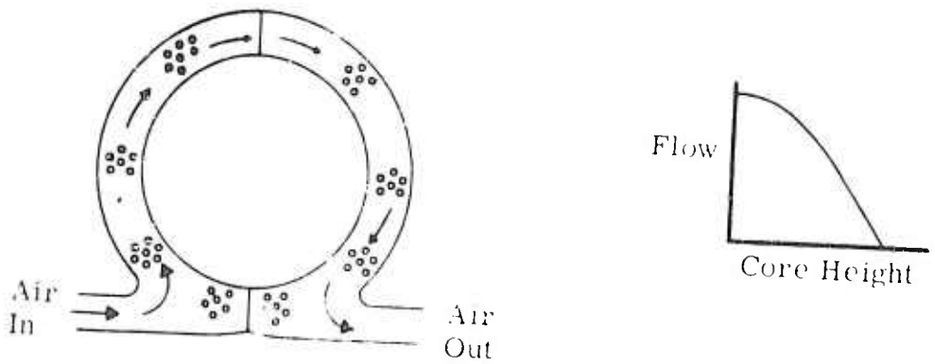

A. Poor Air-side Distribution

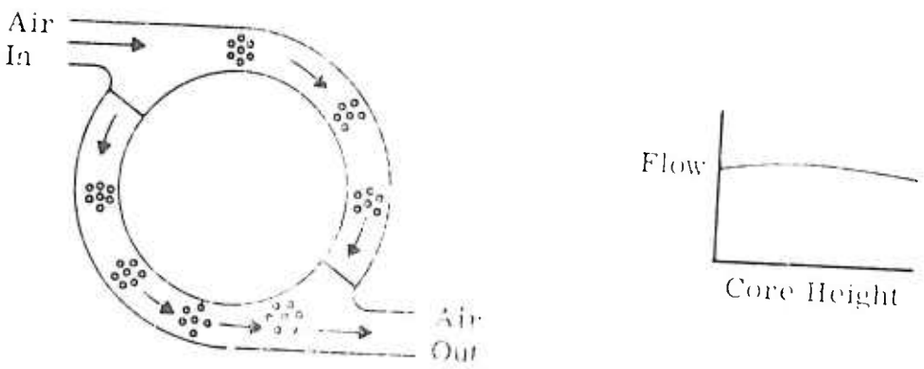

B. Improved Air-side Distribution

Figure 3. Air-Side Distribution.

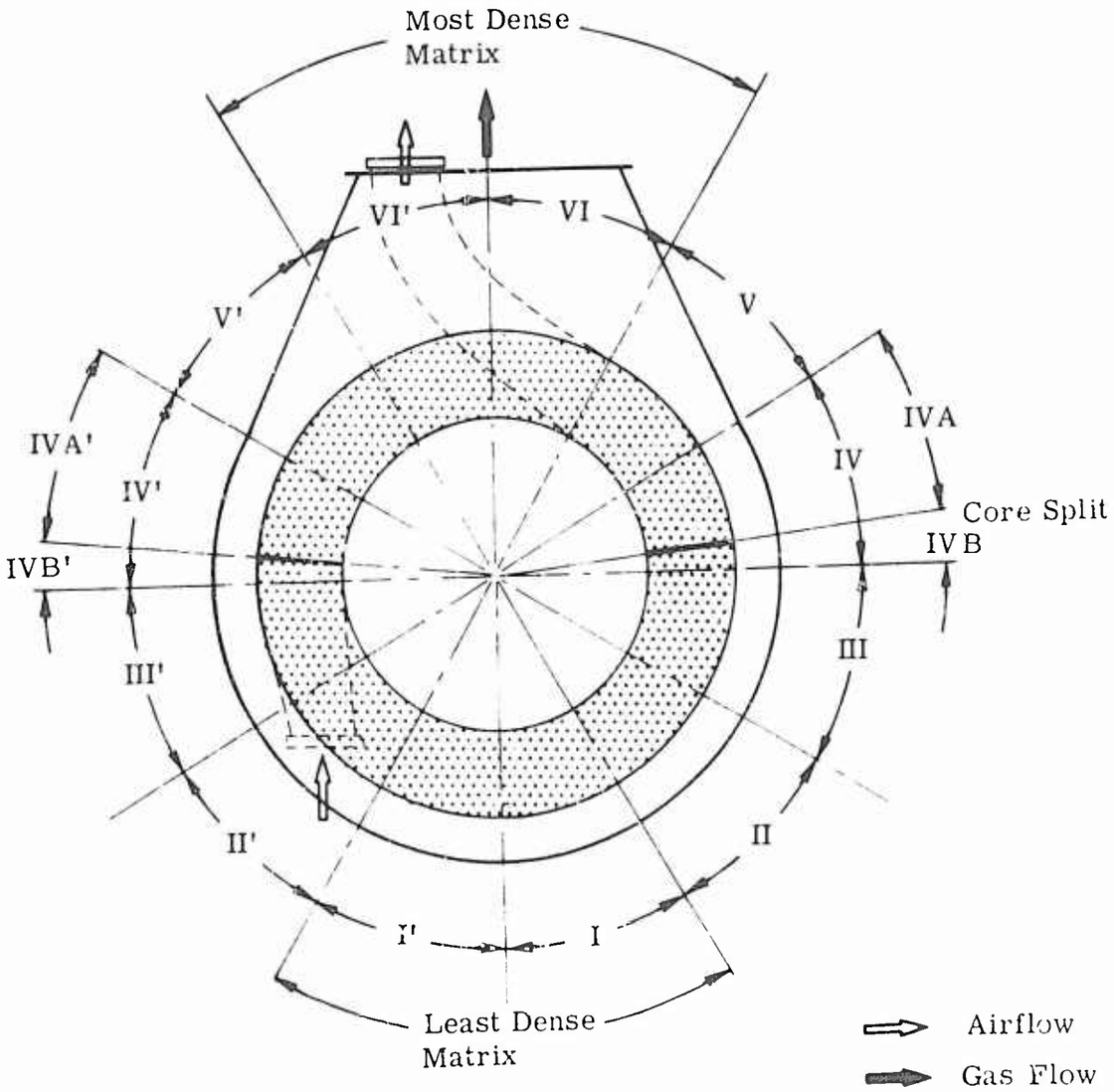

Figure 4. Tube Pattern Arrangements.

also decreased in the gas flow direction from a maximum at the inner diameter to a minimum at the outer core diameter. This core arrangement was designed and optimized using the AiResearch tubular heat exchanger program. The program considered different tube diameters, tube spacing, and types of tubes. All of the tube patterns investigated were of the staggered type

The T63 regenerator is fabricated entirely of Type 347 stainless steel; the core tubes are brazed with braze alloy per AMS 4778. The CRES 347 material was selected as that best suited for this application based on structural requirements, good corrosion resistance in the high temperature JP-4 combustion products atmosphere, and relative ease of fabrication. The corrosion-resistant properties of CRES 347 have been substantiated by its use in a number of AiResearch regenerator applications. Corrosion studies of CRES 347 were conducted during the development program for the Allison T78 regenerator. In these studies, CRES 347 specimens were subjected to stressed salt spray and high temperature (1400 F) JP-4 combustion product atmospheres. The test results verified the selection of CRES 347 as the basic core materials of the T78 regenerator.

Four types of vibration were considered in the design of the regenerator:

- Structure-borne vibration originating from the engine and rotor rotating assemblies
- Air and gas acoustic pressure fluctuations originating at the turbine or compressor blade passages and transmitted to the regenerator by the flowing fluid
- External acoustic airborne noise from the engine or rotor
- Aerodynamic excitation of the tubes in the core

The structure-borne vibration is the more critical, and the fundamental frequencies of the unit (such as rigid-body mode of the unit on the mounting flanges, core fundamental frequencies, etc) were designed to be outside the most prevalent exciting frequency ranges.

The vibration that results from the acoustic pressure fluctuations are critical only in the design of the thin-gage sheet metal manifold. Experience has shown that the relatively flat areas of manifolds are particularly subject to this type of excitation. This problem can easily be improved by local stiffening or by the use of damping material. The relatively flat areas of the gas outlet manifold were designed to incorporate parent metal stiffeners to avoid this problem.

The only type of aerodynamically excited vibration that is of concern in the regenerator is that induced by the vortex shedding off the tubes that may tend to excite the core tubes individually. In the regenerator design, the free length of the tubes was reduced by a spacer plate through which all the tubes pass. The spacer plate is not attached to the surrounding structure. Since the natural frequency of the tubes varies with the tube length, the tendency towards excitation is decreased by the spacer plate because the effective tube length is decreased.

Vibration stresses and combined steady and vibrating stresses were designed to be within the allowable envelope of a Goodman-type diagram for the regenerator material at the appropriate temperature level. The boundary of the envelope was established by the endurance limit stress and yield strength of the material.

The first set of regenerators was subjected to preliminary vibration testing at Allison. No major problems were encountered. The principal regenerator resonance frequencies with vertical excitation were at 44, 58, and 105 cps. The left-hand module exhibited a pitching and yawing motion with respect to the engine. As a result of this motion, the air inlet duct rotated in the compressor outlet casting while the air outlet duct sustained an oscillatory motion at the root. The amplitude of the movements was comparatively small. The right-hand module was steady during the test.

A 1/16 × 1/2 in. tie strip was added between the gas outlet manifolds of the two regenerators. Another 1/16 × 1/2 in. tie strip was added between each regenerator gas outlet flange and the engine. With the tie strips in place, the vibration scan was repeated. The amplitude of the motions was reduced to negligible levels and the resonant frequencies were shifted to 75, 106, 121, and 310 cps.

Horizontal excitation in the direction of the engine axis yielded resonant frequencies of small amplitude at frequencies of 75 to 85, 105, and 120 to 150 cps. The core tubes were not excited by this testing.

STRESS ANALYSIS

Thermal stresses in the regenerator may be divided into two types: steady state and transient. Steady-state thermal stresses exist in the regenerator during most of its operational life, while transient thermal stresses are imposed only during startups, shutdowns, and load changes and, therefore, occur for relatively shorter periods of time.

In the regenerator design, steady-state thermal stresses have been reduced to a minimum by the selection of a unit that is free to expand along its centerline from a fixed reference at the gas inlet mounting flange. Because of the flow arrangement through the regenerator, there is an inherent radial and circumferential thermal gradiert in the manifold and the core tubes. The core tubes near the center of the unit that are exposed to the incoming hot gas operate at a higher temperature than the core tubes on the outer diameter of the core, and each pass of the regenerator core operates at different temperatures. The incoming air in the first pass is relatively cooler and results in a lower tube temperature in the first pass core tubes. The relatively higher air temperature of the second pass results in higher tube temperatures in the second pass. These temperature differentials cause differential tube growths from the inner to the outer header diameter and a maximum differential tube growth across the core at the transition from the first air pass to the second air pass. The header has been split and a bellows incorporated in the design to lower the core tube stress in these areas.

A critical stress area in the regenerator is at the first inside tube rows. These tubes are subjected to the hot incoming gas and tend to grow at a faster rate than the core tubes at outer diameters. A bellows is incorporated between the core header and the air-side return header. The bellows incorporates the desired flexibility into the core and decreases the loading on the inner tubes. The air inlet-outlet header plate is also designed to provide the desired radial flexibility in the core. To oppose the air-side pressure loading on the header inner tubes, a perforated cylinder is attached on the gas side between the air return header and the gas inlet duct. A secondary purpose of the perforated cylinder is to act as a heat shield for the first rows of core tubes on the gas side. Core tube failure of the inner rows is further avoided by using plain, undimpled, 0.006-in. wall tubes in the first three inner core rows.

The core tube arrangement is shown by Figure 5. As may be seen in Figure 5 the core tube matrix density has been selected to promote uniform gas flow through the core. Sectors IV and IV' of Figure 5 include a split between the air inlet and air outlet sides of the core. The header was split in these two areas because the temperature gradient between the air inlet and air outlet sides of the core results in excessive local tube stressing. Sufficient flexibility could not be designed into the header in these areas to prevent the overstress in adjacent tubes. Leakage across to the gas side is prevented by the use of a thin, flexible, metal sealing sheet. This design, then, incorporates the desired flexibility [illegible]

Tube Description

Length 4.90 in.
Tube Rows = 25
Total Tubes = 5490
Tube OD = 0.10 in.

	Rows 1, 2, 3 24 and 25	Rows 4 through 23
Tube Wall (in.)	0.006	0.004
Tube Surface	Plain	Ring Dimple

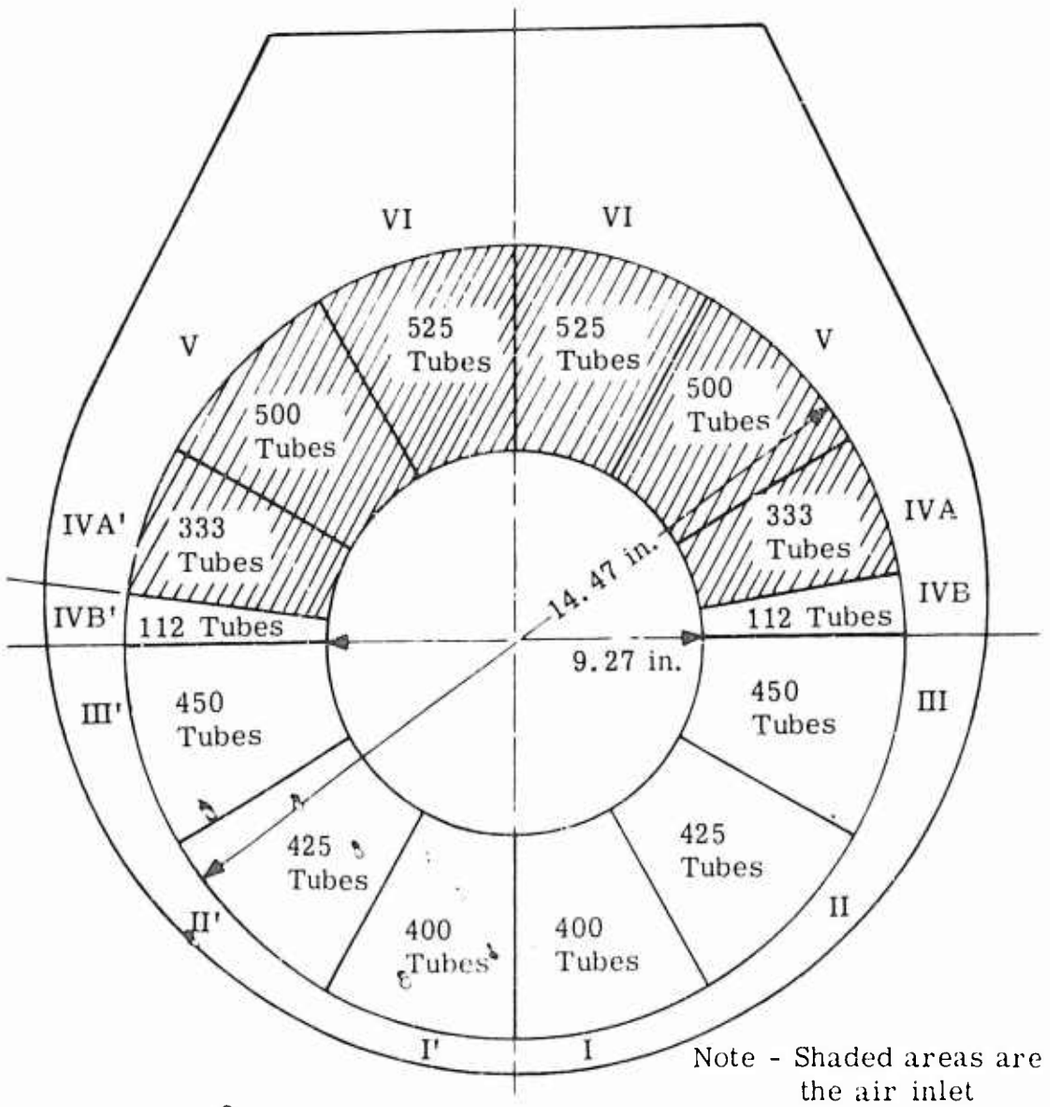

Note - Shaded areas are the air inlet core sections.

Figure 5. Regenerator Core Description.

header at these points to allow a difference in the relative expansion of the adjacent core tubes. The gap in the core tubes that results from the incorporation of the split header was blocked off using sections of plain triangular fins.

The tube metal temperature differential at the first and second air passes was investigated to determine if the loads imposed on the adjacent core tubes would be excessive if a solid header were used. Figure 6 shows the temperature differential between adjacent tubes on either side of the split at the inside and outside diameters. At the core outside diameter, a differential of 423°F occurs at seven seconds at a flow of 1.39 lb/sec and a steady-state temperature differential of 141°F. Figures 7 and 8 show the peak transient and steady-state differentials at the division between the first and second passes in the core radial direction. These curves show that the entire second pass tends to grow more than the entire first pass.

Based on actual test data, the maximum allowable compressive load for the dimpled tube is 9.6 lb. The induced compressive load resulting from a temperature differential between the first and second passes can be calculated. The induced compressive load was found to be 0.1068 times the temperature differential. For a 9.6-lb load, the maximum allowable temperature differential is 90°F. Therefore, both the transient (423°F) and the steady-state (141°F) temperature differentials are in excess of the allowable 90°F and required a split header to reduce the tube loads to an acceptable level.

For the header analysis, only the steady-state condition was considered because it was assumed that the header plates, having a relatively high thermal inertia, will slowly come up to steady-state condition without being affected by transient peaks. The average radial temperature gradient for the air return header plate was obtained by using the mean gas and air temperature on either side of the header plate. Based on the mean radial temperature gradient, the tangential and radial stresses in the header were calculated. Figure 9 shows the results of this calculation and that the stress distribution is of an acceptable level.

The pressure loads in the core header were obtained using the critical speed beam computer program. The analysis was made at Sector I of the core. Figure 10 shows the header bending stresses and indicates that the maximum header bending stress occurs at approximately the 24th tube row. The calculation assumed a header thickness of 0.08 in. at the outer edge and 0.05 in. thickness at the center. It was further assumed that a bellows was incorporated at the inner edge of the header. The requirement for the bellows is discussed later. The maximum header bending stresses obtained are listed in Table I.

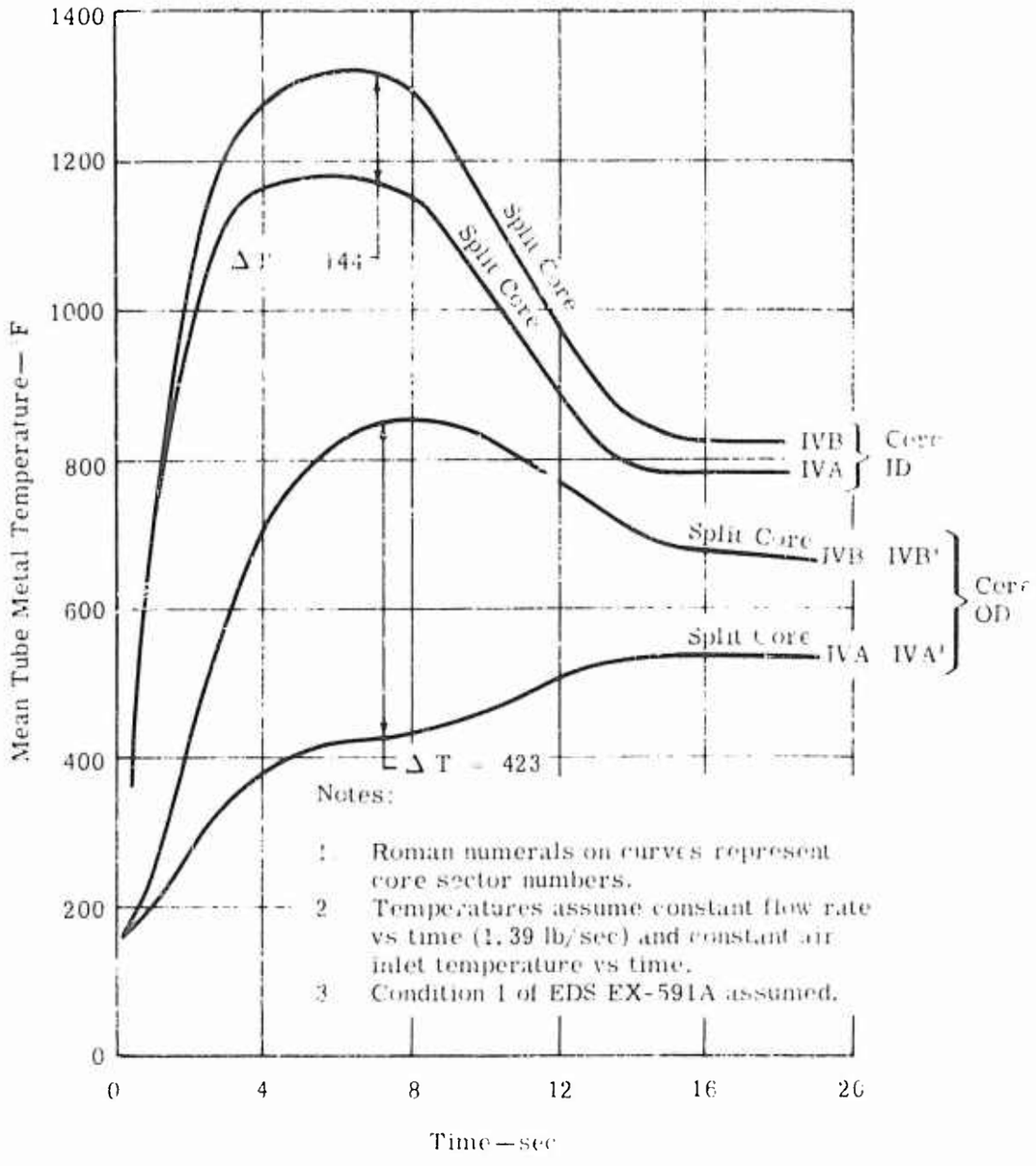

Figure 6. Temperature Differential Across the Header Split at the Core OD and ID.

Notes

1. Roman numerals on curves represent core sector numbers.
2. Temperatures assume constant flow rate vs time (1.39 lb/sec) and constant air inlet temperature vs time.
3. Condition 1 of EDS EX-591A assumed.

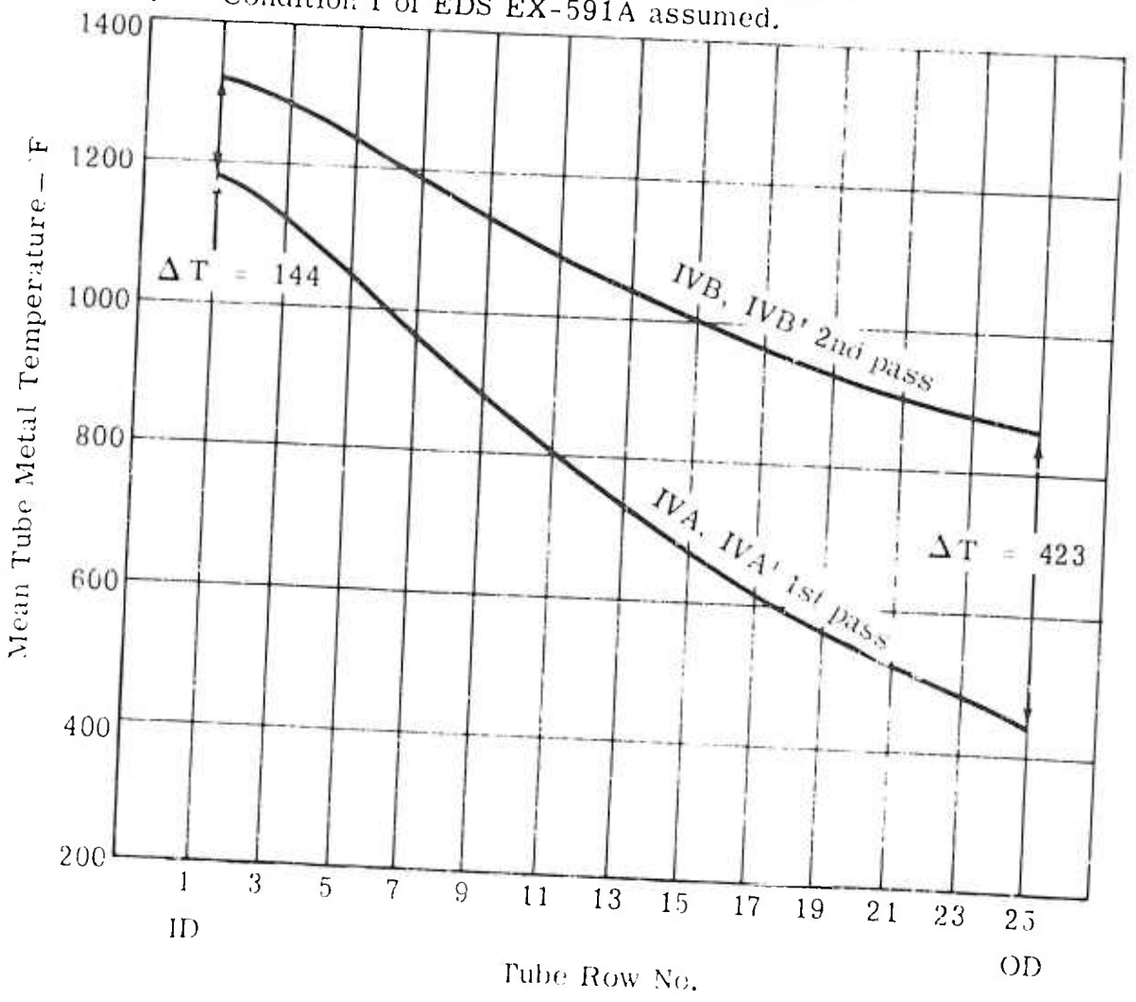

Figure 7 Maximum Tube Temperature Differential Across the Header Split Between the First and Second Pass.

Notes:

1. Roman numerals on curves represent core sector numbers.
2. EDS Condition 1 at 17.6 sec assumed (steady state across split)

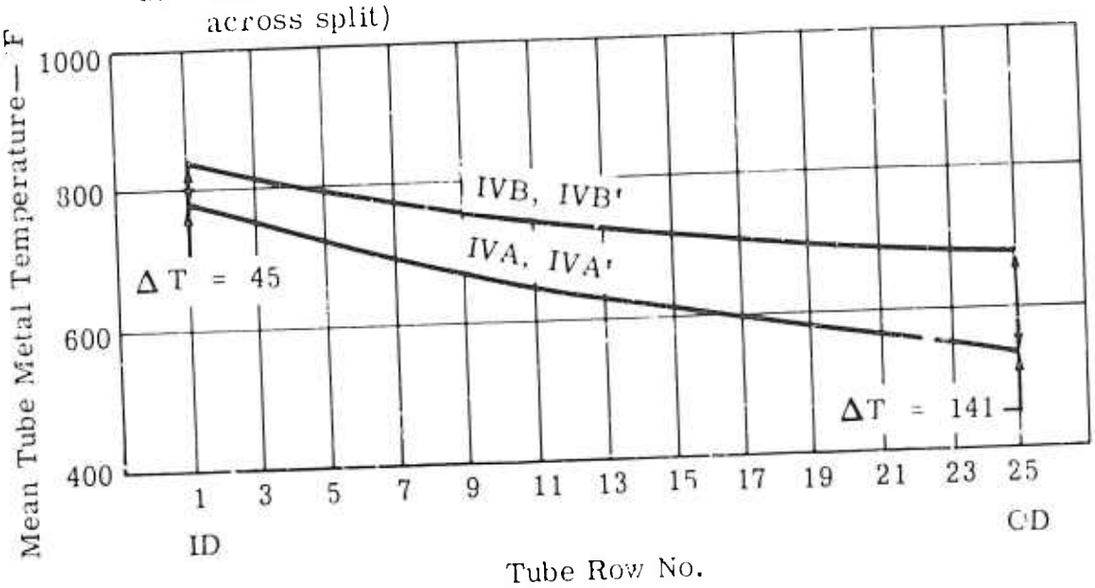

Figure 8. Steady-State Temperature Differential Across the Core Split.

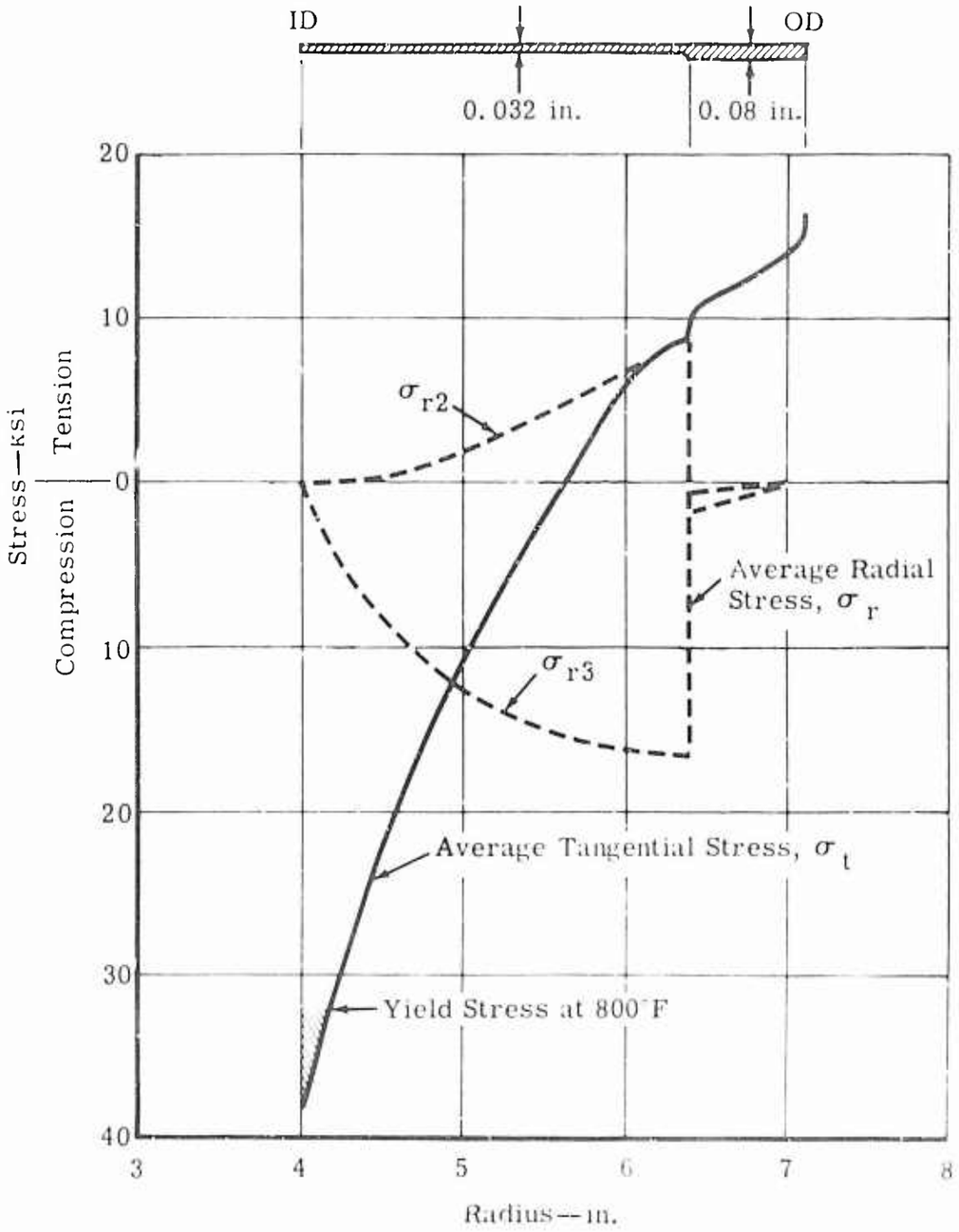

Figure 9. Steady-State Thermal Stresses in the Retort Header Plate Due to 200°F Radial Temperature Differential.

Notes:

1. Load with 110 psig internal pressure.
2. Tube Numbers 1, 2, 24 and 25 have 0.006-in. walls.

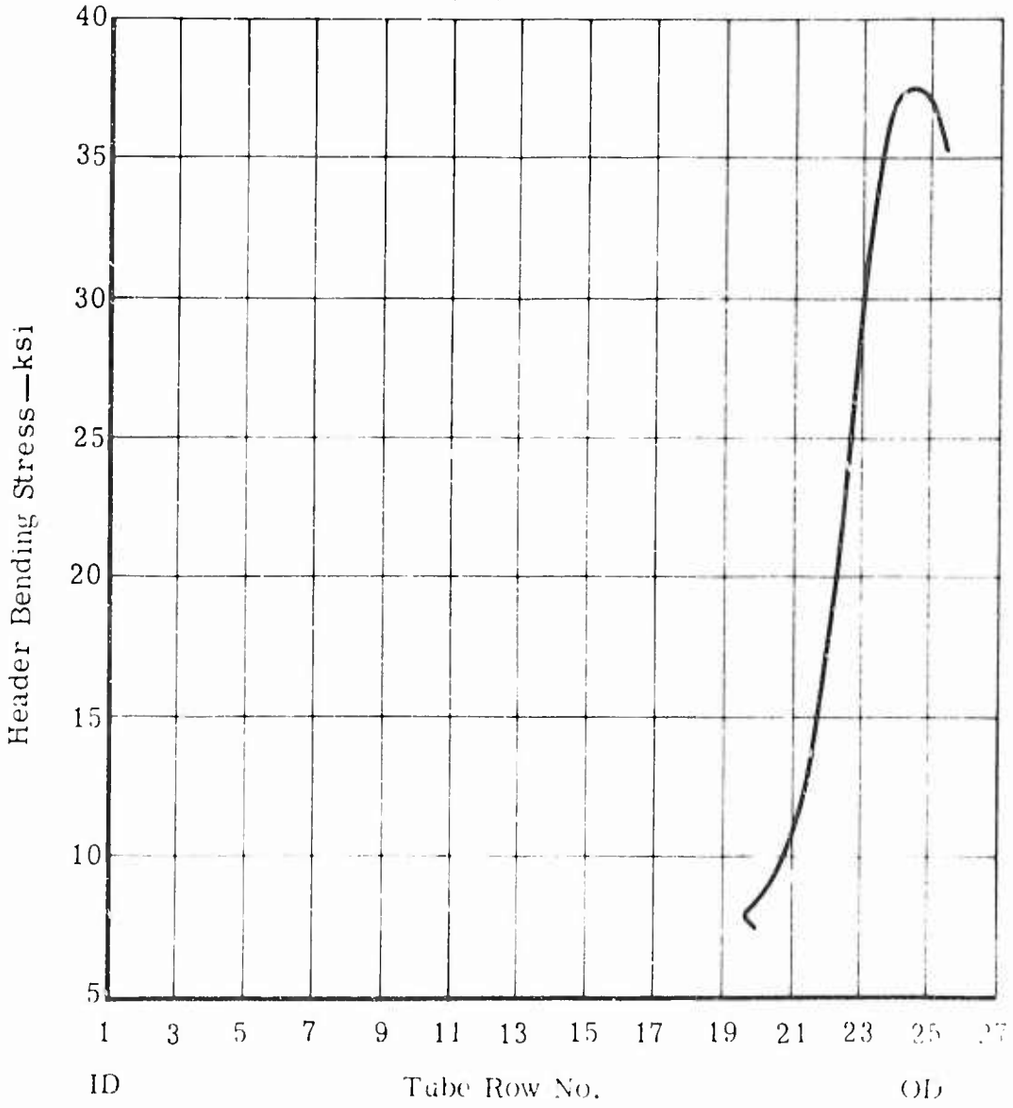

Figure 10. Header Bending Stress from Internal Pressure.

TABLE I.

[illegible] HEADER BENDING STRESSES

[illegible]	Temperature (°F)	Maximum Bending Stress (psi)	CRES 347 Tensile Yield Stress (psi)	Safety Margin
	1000	24,200	30,000	0.24
	500	24,700	32,000	0.30
	[illegible]	24,200	32,500	0.085

[illegible] to the above stress analysis using the effect of speed [illegible] progress. The analysis was based on the Section I data [illegible] which, being the most dense, would incur the highest loads [illegible] these core tube loading distributions operated. The allowable [illegible] were those of 0.005 in./in. tube and 0.004 in./in. tube [illegible] the core. Table II exceeds the tube stress margins, [illegible] tube loads for both operating and [illegible] allowable tube loads are based on actual test [illegible]

[illegible] program was applied to give the core tube loads at [illegible] points [illegible] steady state temperature profile across the tube [illegible] The program also considered the torsional resistance against header [illegible] from the ring of the scrubbers and return manifold. Figure 12 shows the most severe radial temperature profile at Section 1 for the 0.70 [illegible] condition occurring at three seconds after startup. Figure 13 shows the resultant tube loadings that represent the most severe tube [illegible] in the core. The loadings are in excess of the [illegible] allowable tube loads. These predicted tube loads were then incorporated [illegible] the deflection of the air return manifold under pressure and the air [illegible] accumulator header. The bellows permits the header to de- [illegible] as shown in Figure 14 so that the air return manifold

[illegible] deflected, the header was assumed to act as a disk [illegible] (Figure 15).

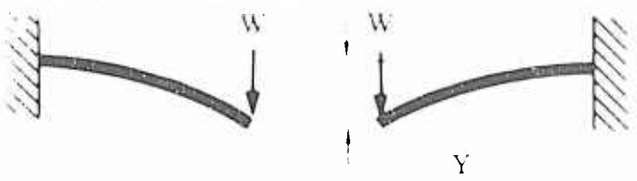

Notes:

1. Load with 110 psig internal pressure.
2. Tube numbers 1, 2, 24 and 25 have 0.006-in. walls.

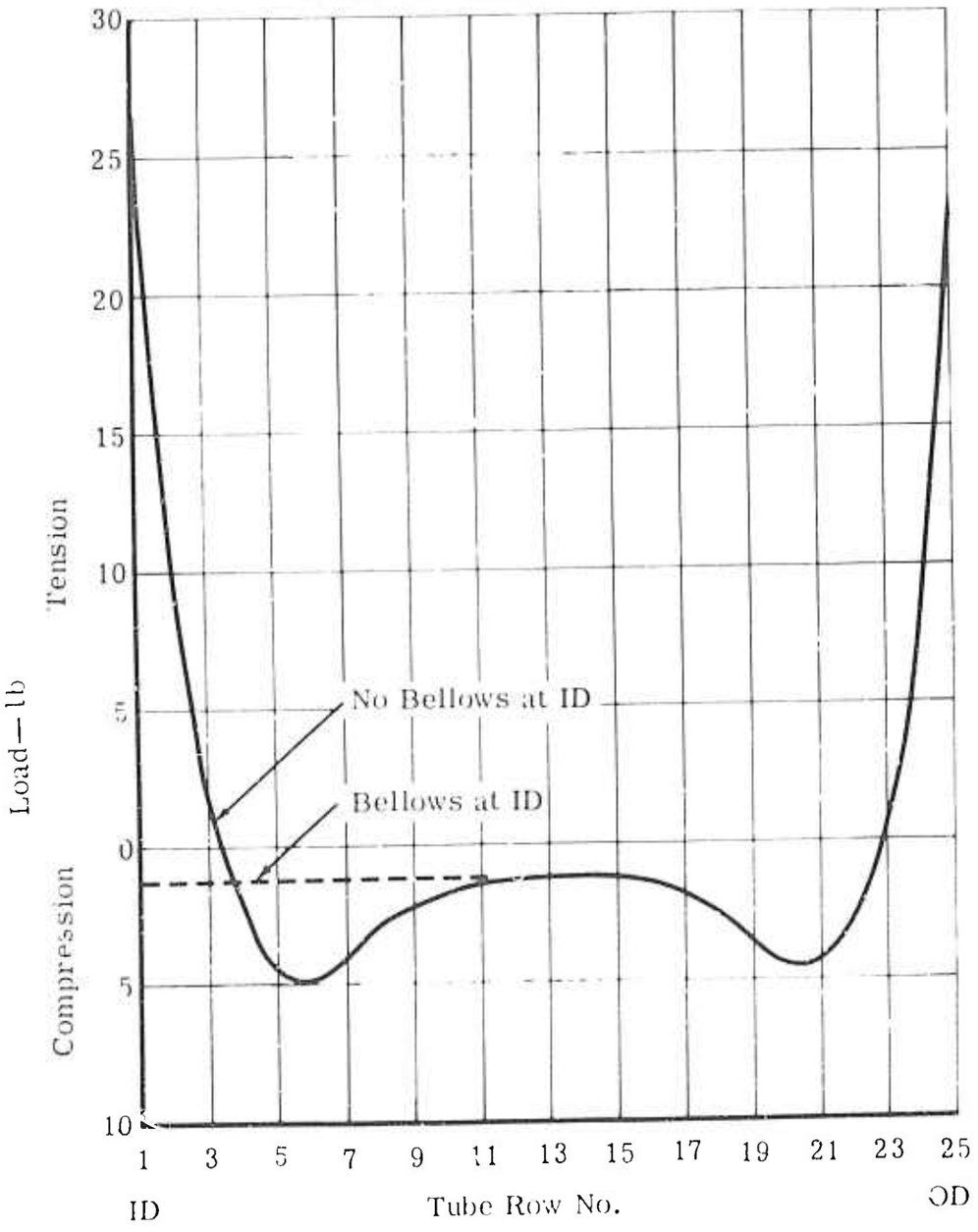

Figure 11. Typical Distribution of Tube Loading Due to Internal Pressure.

TABLE II.
CORE TUBE PRESSURE LOADS

Tube Item No.	Tube Wall (in.)	EDS Condition	Pressure Load (lb) Tension	Compression	Allowable Load (lb)	Load Safety Margin	Pressure Membrane (psi)	Allowable Membrane (psi)	Membrane Safety Margin
Long-Term Pressure Load: 72.3 psig at 100° F Operating Temperature									
1	0.006	2	17.45	– –	48.2	0.40	0.0685	0.528	OK
3	0.004	2	0.74	– –	34.7	OK	0.0203	0.45	OK
5	0.003	2	– –	3.41	8.13	OK			
Long-Term Pressure Load: 86.1 psig at 80° F Operating Temperature									
1	0.006	2	20.72	– –	85.5	0.73	0.0778	0.67	OK
3	0.004	2	0.85	– –	15.72	OK	0.0282	0.462	OK
5	0.003	3	– –	4.84	9.49	OK			
Short-Term Pressure Load: 130 psig at Room Temperature									
1	0.006	Proof	31.2	– –	48.5	0.40	0.122	0.825	OK
3	0.004	Proof	1.33	– –	19.4	OK	0.363	0.593	OK
5	0.003	Proof	– –	6.09	11.36	0.865			

* Tube 1 is No. 1 at the core ID

Notes:

1. Tube temperatures during startup transient at 3 sec.
2. Flow = 0.7 lb/sec.
3. ΔT = 1290 - 374 = 916°F.
4. Tube rows 1, 2, 24 and 25 have 0.006-in. walls.
5. This profile (at sector 1) gives the highest tube loads for the regenerator.

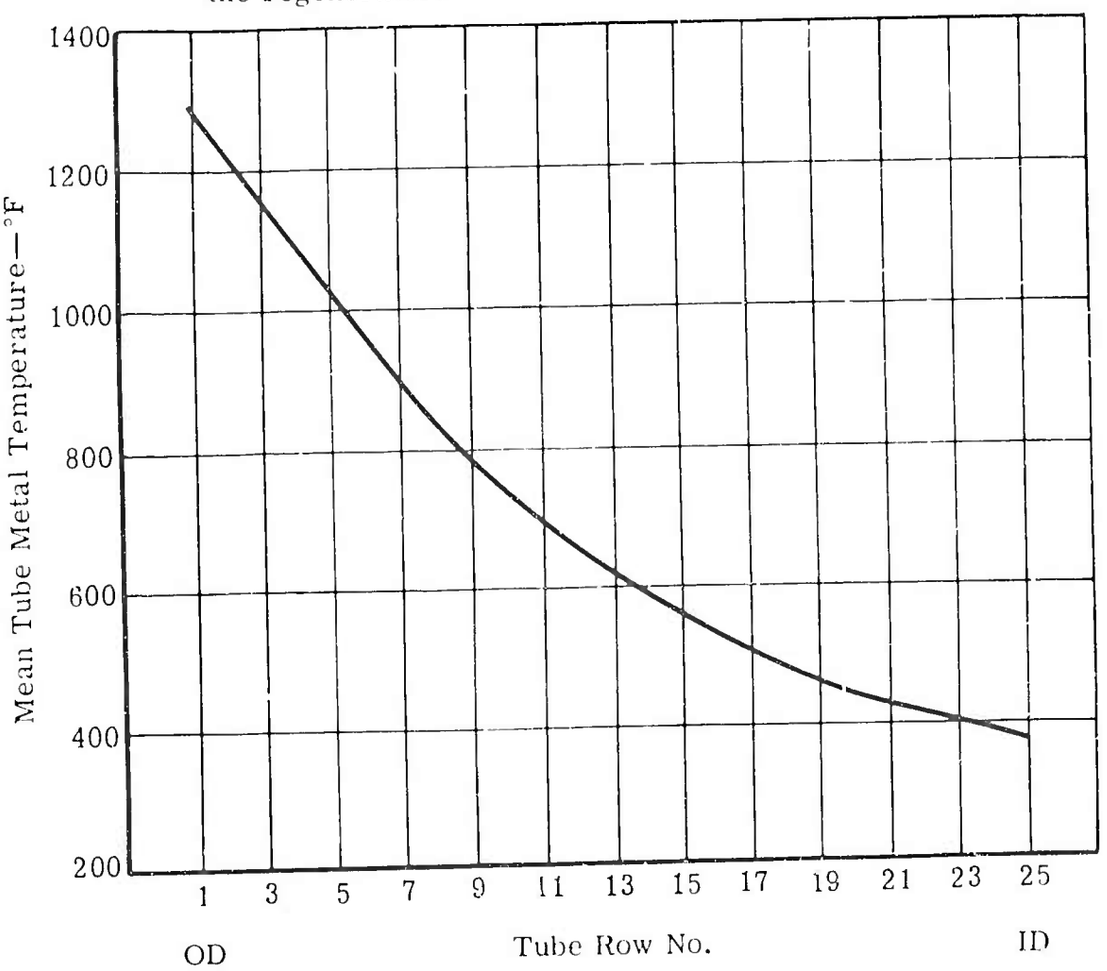

Figure 12. Core Sector I Tube Temperatures.

Notes:

1. Tube loads during startup transient at 3 sec without bellows at ID on return header.
2. Flow = 0.7 lb/sec.
3. Return pan torsional stiffness factor = 6300 in.-lb/in./rad.
4. ΔT = 1290 - 374 = 916 F.
5. Tube rows 1, 2, 24 and 25 have 0.006-in. walls.
6. Allowable tube loads are at 1200°F.

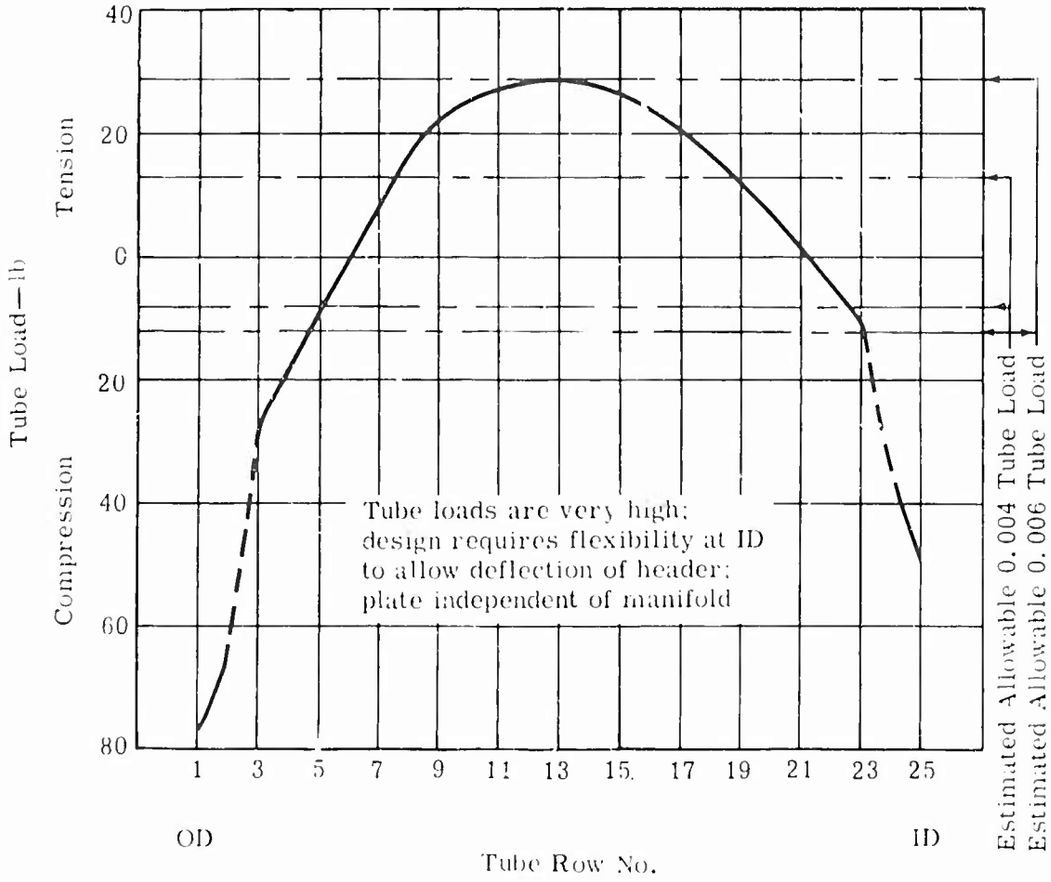

Figure 13. Core Sector I Tube Loads.

Calculations show that the bellows reduces the tube loads, caused by the radial temperature gradient, to an acceptable level. The maximum tube stress was 26,300 psi.

During the testing of the first set of regenerators (P/N 182330-1-1 and 182330-2-1) at Allison, excessive leakage was experienced on the regenerator air side. A posttest examination of the units revealed that a number of core tubes were cracked on the inner rows of the core of both units, or those rows of tubes which see the highest exhaust gas temperatures.

On return of the test units to AiResearch, core leakage tests revealed that tube cracking had also occurred in the third, fourth, and fifth inside core rows. The tube cracks appeared in the first dimple at a location where the dimple runs out tangent to the tube OD on the header side of the dimple. The cracks were random at either the top or the bottom of the tubes.

A dimensional statistical comparison of tube dimples was made to compare a new tube (selected at random), a cracked tube, an uncracked tube removed from the inner core rows, and an uncracked tube removed from the outer core tube rows. The results of this comparison were inconclusive since all of the tubes appeared to be within new tube dimensions and tolerances.

Sample tubes taken from the regenerator core were also sectioned and examined for excessive thinning or deterioration at the dimple areas. No excessive thinning or corrosion was detected. Thinning at the tube dimples was about 0.0002 in. Some of the failed tubes examined showed braze alloy "run-down" into the ID of the tube, and the alloying penetration was from 25% to 50% of the tube wall. Thickness of the alloy was about 0.001 in. This amount of braze penetration could reduce parent metal strength by as much as 75%. Since some of the tubes that failed did not have the braze "run-down," it was concluded that brazing could not be the total cause of the tube failures.

The first two tube rows in the core appeared to have been running at a much higher temperature than the remainder of the core. Also, the first tube rows appeared to have seen some bowing and buckling that could have contributed to low cycle fatigue. The core was, however, designed to

withstand this type of loading. The individual tube tests in tension and compression conducted during the design phase of the program indicated that the tube bundle could withstand all of the engine conditions without failure. Failure could occur if the tubes were at a higher temperature than the maximum operating temperatures or if the bellows did not deflect properly and subjected the inner tube rows to loads that exceeded the design values.

A review of the design of the regenerator revealed that both of these conditions could have existed. The regenerator components adjacent to the bellows could have caused the bellows to hang up and impose an increased load into the inner core tubes. The proximity of the first bellows convolution to the inlets of the inner rows of the core tubes was such that a starvation of airflow to these tubes could occur. With reduced airflow in these tubes, the tube metal temperatures would have approached the gas inlet temperature of 1100°F. The resulting stress discontinuity in the core could result in failure of these tubes.

Based on the foregoing analysis, it was concluded that the probable causes of the inner core tube failures were both the restricted airflow to the inner core tubes and an increased load applied by the bellows as a result of the interference of the bellows with adjacent components. These conditions were corrected on subsequent configurations by increasing the inner core diameter and moving the first bellows convolution away from the core. This ensured that adequate flow was maintained through the inner core tubes. A sufficient clearance was introduced around the bellows to prevent the possibility of interference with adjacent components.

The stress analysis presented herein was based on the design of ship set No. 1 specifically and applied to the AiResearch Regenerator series defined on Outline Drawing 182330. Design improvements were incorporated between ship sets No. 1 and No. 2 and again between No. 2 and No. 3. All of these changes were of a type that increased structural integrity except in the case where the exhaust gas duct was changed from a curved to a rectangular shape. Since adequate similarity does exist between ship sets 1, 2, and 3, it was deemed not necessary to repeat the stress analysis for ship sets 2 and 3.

The second ship set configuration, identified as 182330-5-1 and 182330-6-1, was scheduled to be run on the engine for the 50-hr flightworthiness test. The unit was designed to correct the tube failure problems encountered with the first ship set and was further designed for lower pressure loss. The revisions incorporated in this unit are as follows.

- The bellows were redesigned to move the convolutions away from the tube bundle. This change permitted better flow distribution into the first core tube rows.

- The gap between the bellows and adjacent components was increased to a generous amount to prevent binding with a resulting loading of the inner tube rows.

- [illegible] tube support plate was added to the core approximately [illegible] between two core header plates. The tube support plate will [illegible] pressure drop by preventing the nesting tendency [illegible] core tubes.

- The tie rods used to support the header pressure loads were replaced with a perforated cylinder. The cylinder performs the same stress function but has the added feature of acting as a heat shield for the first row of core tubes that the gas sees.

- The core size was redefined to redistribute the same number of tubes in a larger diameter bundle. This change basically consisted of removing the first three inner tube rows and adding them to the outside diameter of the core. The increased no-flow length will result in a lower gas-side pressure drop core.

- The first three inner core tube rows were changed to plain, undimpled tubes with 0.006-in. walls. The first ship set had dimpled 0.004-in. wall tubes in these rows. The thicker plain tube provided increased core strength in this critical area.

- The gas outlet duct geometry was changed from an elliptical cross section to a rectangular cross section. This change provided an increased flow area for the outlet gas and a lower gas-side pressure loss.

- The air inlet diffuser length was increased to further decrease the air inlet diffusion losses.

- The core tube dimple depth was decreased by 38% to further reduce the air-side pressure losses.

- The gas outlet duct was reinforced by the addition of parent metal dimples to avoid acoustical vibration problems in the flat sections of the revised gas outlet duct. The dimples further provide reinforcement against the internal gas pressure.

Besides the changes already mentioned, several one-time changes were made to these units that would not be included on the flight hardware. Additional external stiffeners were used on the gas outlet ducting. The additional stiffening was required because of the high negative pressure to be imposed during the simulated 20,000-ft altitude test run in the Allison laboratory. This test point could impose negative pressure as high as 9 psi and collapse the duct. The additional stiffeners are not required for the flight test regenerators.

The unit also included instrumentation bosses and a removable exhaust gas bypass plate required for laboratory testing only.

PRESSURE DROP AND EFFECTIVENESS

Following the fabrication of the first regenerator configuration, a performance test was conducted at AiResearch in an attempt to verify the predicted performance of the unit. The unit tested was the left-hand unit. For testing purposes, a substitute modified air outlet duct was temporarily welded to the air outlet pan. The final air outlet duct had not been received from the vendor on schedule. The regenerator effectiveness was 59.7%.

A comparison of the test results obtained from this testing and the calculated performance revealed a much higher pressure drop on both the air and gas sides of the regenerator. To further isolate the areas of high pressure drop, the test regenerator was extensively instrumented.

The pressure drop test data, obtained from this testing, is presented in Table III corrected to the Condition 1 of Allison Specification EDS EX-581A. Because of the more complete instrumentation used for the isothermal test, the pressure drops obtained from this testing are felt to more accurately represent the actual regenerator losses.

To further isolate component pressure drops, the two core halves were tested independently without a return pan. The test units consisted only of the core and the inlet or outlet pan. In each case, the flow was introduced into the pan inlet or outlet. Thus, the flow through the second pass was reversed.

During the early fabrication phases of the regenerator, exhaust gas-side isothermal pressure drop tests were conducted. Isothermal tests were conducted with the core only, with the core and simulated collecting pan,

TABLE III

SHIP SET 1 (182330-1-1) PRESSURE LOSS TEST RESULTS—CONDITION 1

Test Description	Measured Total to Total $\sigma \Delta P$	Measured Static to Static $\sigma \Delta P$ (in. Hg)	Corrected Total to Total $\sigma \Delta P$ (psi)	Adjusted Specification EDS EN-3961A Condition 1 Total to Total ΔP (psi)	(%)
Original Regenerator Heat Transfer Test Results					
Air side	32.1 in. Hg		13.82	5.87	[illegible]
Exhaust gas side	34.[illegible] in. H_2O		0.[illegible]	7.22	[illegible]
Total					4.71
More Fully Instrumented Regenerator Isothermal Test Results					
Air side	28.0 in. Hg		14.[illegible]	5.[illegible]	[illegible]
Gas side	13.3 in. H_2O		0.480	3.[illegible]	[illegible]
Total					4.[illegible]
Air-side core first pass				0.[illegible]	0.[illegible]
Air-side core second pass				0.412	[illegible]
Air-side Isothermal Core and Header Pressure Drop Test Results					
Air-side core first pass	[illegible].26	[illegible].24	[illegible].[illegible]	0.[illegible]	0.[illegible]
Air-side core second pass (reverse flow)	[illegible].24	4.[illegible]0	[illegible].60	[illegible].[illegible]	[illegible]
Exhaust Gas-side Isothermal Pressure Drop Test Results With Simulated Collecting Pan					
Core without outlet pan				0.660	[illegible]
Core with outlet pan				1.[illegible]6	[illegible].[illegible]
Core with outlet pan and [illegible]				0.[illegible]4	[illegible].[illegible]

Notes:

1. Tested with air on both sides.
2. Air-side flow = 3.49 lb/sec = 83.4 lb/min
   Exhaust gas-side flow = 3.79 lb/sec = 87.4 lb/min
3. $\sigma = 17.3 \frac{P}{T}$

   where P = average pressure in. Hg
   T = average temperature °F

   Assumed Condition 1 densities, σ lbs
   Air side first pass σ = [illegible].77
   Air side second pass σ = [illegible].[illegible]7
   Air side [illegible] pass σ = [illegible].[illegible]7
   Gas side σ = 0.[illegible]
4. The total-to-total pressure drops are calculated from the static-to-static pressure drops of the test.

and with the core pac and inlet diffusion cone. The results of this testing corrected to Condition 1 are shown in Table III. Because of the results of this test, the gas inlet diffusion cone was eliminated from the gas inlet. As shown by this testing, the diffusion cone actually increased the gas-side pressure loss by a small amount.

Using the results of the aforementioned testing, the detailed air and gas pressure losses were established for the regenerator. A breakdown of these losses is presented in Table IV.

TABLE IV.

ESTIMATED COMPONENT PRESSURE LOSSES FOR SHIP SET NO. 1 (32,430 HP)

Component	Loss Coefficient	Total Pressure Drop (psi)	Condition 1 Total Pressure Drop (%)
Gas Side			
Inlet	1.0	0.201	2.7
Core		0.560	7.51
Outlet	0.65	0.233	3.14
Total	—	—	7.42
Air Side			
Inlet	1.0	2.[illegible]	3.43
Core Entrance	—	0.[illegible]76	0.[illegible]8
Core Matrix	[illegible]	0.[illegible]34	0.[illegible]8
Core Exit to Duct	—	0.[illegible]2	[illegible].[illegible]
Duct Header	0.[illegible]	0.[illegible]3	[illegible].[illegible]
Outlet Duct	0.47	0.062	0.56
Total			[illegible].[illegible]

The inability of the second pass matrix to [illegible] the [illegible] to the test data, [illegible] the [illegible] of the [illegible] [illegible]. Approximately 11 percent more air took the path of the [illegible] the core than through the rest of the second pass matrix. This [illegible] maldistribution accounts for the higher than predicted [illegible] drop in this pass and the lower than predicted heat transfer. The dynamic pressure head change in the [illegible] out of header was the main cause of the second pass maldistribution. Redesigned outlet ducting reduced this problem.

With the exception of the second air core pass, the test results showed that the core pressure drops were within 2% of that predicted for the design. The component pressure losses of Table IV show that the high unpredicted air- and gas-side pressure drops were mainly caused by the regenerator manifolding and ducting.

Based on the detailed pressure loss analysis, the regenerator ducting and manifolding were redesigned in an attempt to relieve the high pressure drop areas. Modifications were made to the air inlet diffuser and pan, the air outlet pan and duct, and the gas collector pan. The revisions were coordinated with Allison by the use of a wooden mock-up of the regenerator with installations of the mock-up on the engine to ensure that proper clearances were maintained for the engine installation. Figure 14 shows the wooden mock-up with cloth applied to the surfaces where the changes were made. The air inlet duct was modified by increasing the air inlet flange from 1.84 to 1.92 in. and incorporating a symmetrical, straight diffuser duct. A concentric diffuser cone was placed in the air inlet duct before the first turn in the duct. The entrance to the air distribution pan was enlarged and a re-entrant turn, leading to reduce flow to some of the core tubes, was eliminated. The interface section between the air outlet pan and the air outlet duct was enlarged and the air outlet duct was made constant, eliminating the diffusion in that area. The cross section of the gas collector pan was enlarged and its shape redesigned.

Following the modifications, the regenerator was again subjected to both isothermal and heat transfer performance testing at AiResearch. The test results, corrected to Condition I, are shown by Table V. The test results showed that the first cut manifold modifications have successfully reduced the pressure drop on the air side to the originally calculated value. The gas-side pressure drop was still higher than the calculated value but was considerably lower.

During the heat transfer testing of the regenerator, the air inlet diffuser cone failed. The cause of the failure was diagnosed to be aero-induced conical-type vibration resulting in fatigue and premature metal failure. The diffusers were replaced by a redesigned configuration. The redesigned configuration had a larger diameter inner cone which reduced the support spans and the metal gage was increased 50%.

The units were accepted after tests with the results as shown in Table VI, before shipment to Allison.

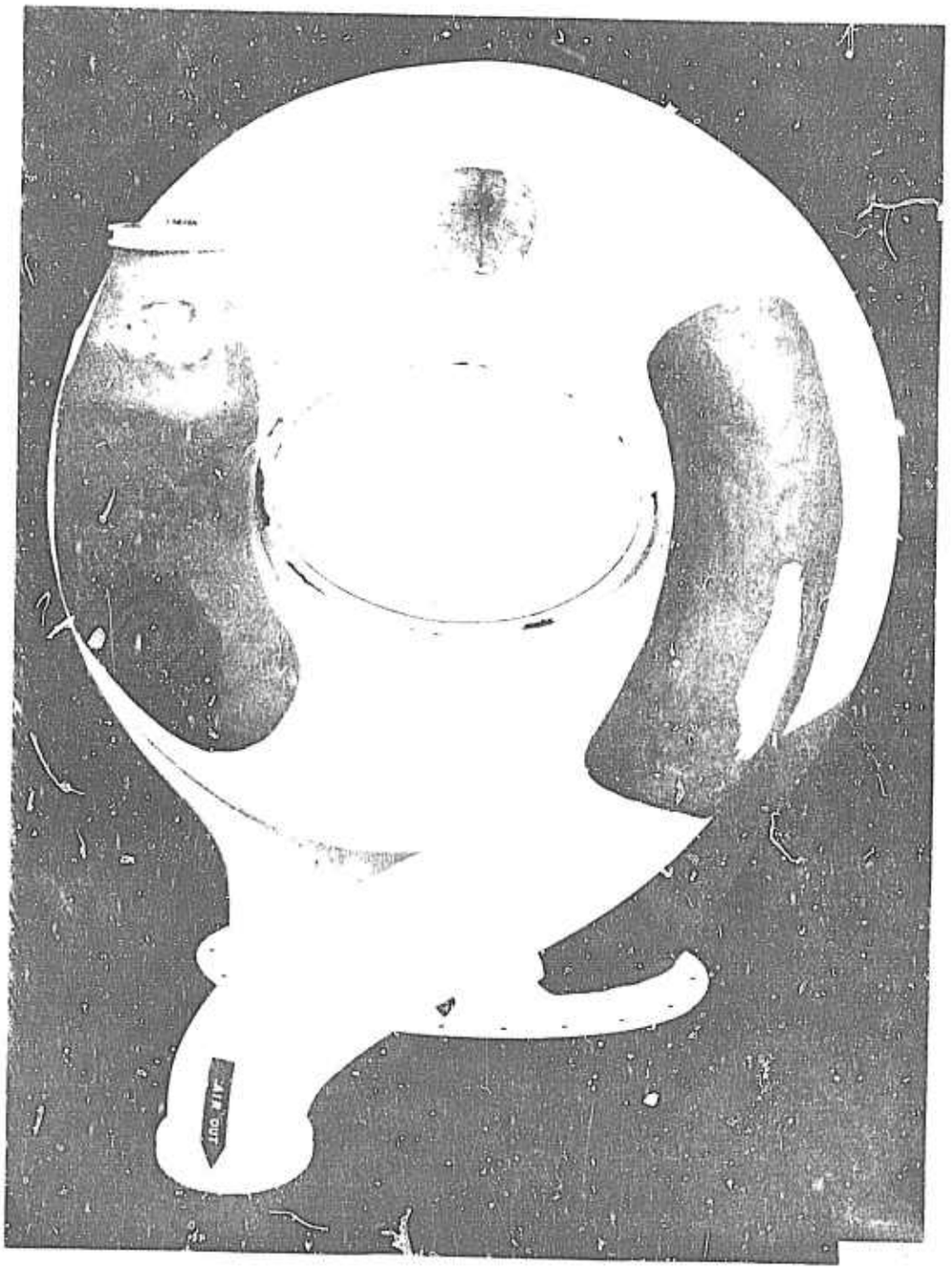

Figure 14. Revised Regenerator Mock-up.

TABLE V.

SUMMARY OF PERFORMANCE FOR SHIP SET NO. 1
(182330-1-1 AND 182330-2-1)—CONDITION 1

			Calculated	AiResearch Test (1)
Original Configuration	$\frac{\Delta P}{P}$	Gas Side, %	6.00	7.42
		Air Side, %	3.80	7.34
		Total, %	9.80	14.76
		Effectiveness, %	61.0	59.7

			AiResearch Test	Allison Test	AiResearch Test (3)
Following Duct Modifications (First Modification)	$\frac{\Delta P}{P}$	Gas Side, %	7.07	8.8	7.0
		Air Side, %	3.78 (2)	3.9	(4)
		Total, %	10.85	12.7	
		Effectiveness, %	61.1	60.1	(4)

			Calculated Performance Change	Allison Test
Following the Core Repair and Renovation (Second Modification)	$\frac{\Delta P}{P}$	Gas Side, %	-0.54	8.0
		Air Side, %	-0.22	3.9
		Total, %	-0.32	11.9
		Effectiveness, %	-0.72	60.1

(1) Effectiveness calculated from test results based on the average heat transferred.

(2) Isothermal pressure drop. The heat transfer pressure drop was invalid because of a damaged air inlet diffuser cone.

(3) AiResearch test results following the return of the regenerator from Allison

(4) Air-side pressure drop and effectiveness could not be determined because of excessive air-side leakage.

TABLE VI

ACCEPTANCE TEST RESULTS

	Leakage from Air Side (lb/sec at 150 psig)		Leakage from Gas Side (lb/sec at 2 psig)		External Leakage	Weight (lb)
	Measured	Allowable	Measured	Allowable		
P/N 382[illegible]-1 (left-hand)	0.00033	0.0042	0.0	0.007	0	21.80
P/N 382330-2-[illegible] (right-hand)	0.0017	0.0042	0.0	0.007	0	22.10

The weights in Table VI include two additional instrumentation bosses per unit as required by Allison. The weight increase due to the bosses is approximately 0.20 lb per unit.

Performance tests of these regenerators at Allison resulted in overall pressure drops that were higher and a lower effectiveness than that obtained at AiResearch. The Allison test results are shown in Table IV. In addition, a number of core tubes on the inner core rows of both regenerators failed during the testing. The units were returned to AiResearch for investigation and repair.

A systematic investigation was initiated in an attempt to isolate the pressure drop problem areas and to provide basic design data for the follow on regenerators. Leakage tests were conducted on the air side of both regenerators, and the leakage was excessive. The left-hand unit leakage was 12 lb/min at 115 psig, and the right-hand unit leakage was 7 lb/min 130 psig. The leakage was mainly in the area of the first two inner tube rows. An isothermal pressure drop test was conducted on the gas side the regenerator in an attempt to determine the cause of the increased gas side pressure drop at Allison. The pressure drop obtained duplicated the pressure drop obtained at AiResearch before shipping, indicating that the increased loss was the result of some other variable. The pressure drop, before shipping and after return from Allison are presented in Table V. Another possible source for the increased gas-side pressure drop was the gas flow into the regenerator from the engine. A Y shaped exhaust gas collector is used by Allison as a transition duct from the engine to the regenerator gas inlets. It was suspected that the inlet gas flow distribution may be affected by the gas collector and result in the higher gas-side pressure drop.

A gas collector duct was obtained from Allison for testing purposes. Isothermal pressure drop tests were run on both the left-hand regenerator and the right-hand regenerator and on the Allison gas collector duct. An overall isothermal test was then run with the gas collector and both regenerators. The gas collector pressure drop was then subtracted from the overall isothermal test results. The resulting isothermal pressure drop (of only the regenerators) was then compared to the average individual pressure drop of the regenerator. Both pressure losses were identical indicating that this gas collector duct configuration had a negligible effect on the regenerator gas-side pressure drop.

Based on the aforementioned testing, it was concluded that since the AiResearch testing was conducted at room temperature and the Allison testing was conducted at engine operating temperature, the higher Allison pressure drop may have been caused by either or both of the following

- [illegible] gas-side [illegible].

- [illegible] temperature in a gas that caused nesting, resulting in partial blockage of the gas flow.

Following the investigation of the failure of the first ship set, a program [illegible] was initiated to return the superheaters to Nelson to permit [illegible]. The cores were removed by removing all tubes [illegible] and tubes [illegible] as the header using a microcarbide [illegible]. The remaining core tubes [illegible] in Table VII were plugged.

TABLE VII

NUMBER OF CORE TUBES PLUGGED.

Row	Number of Times Plugged
[illegible]	[illegible]
[illegible]	[illegible]

[illegible] The operator [illegible] was increased to 730 psig and the mea[illegible] Deflection was 0.312 in. Upon removal of the pressure, the Rad indicator returned to zero indicating no [illegible] deformation had taken [illegible]

The estimated magnitude of the performance change in the regenerators is shown in Table V. Also shown in Table V are the performance values experienced by Allison during later engine tests. Since this regenerator did not incorporate a tube support plate, the Allison gas-side pressure losses were still relatively high, probably because of the nesting of the core tubes.

These regenerators subsequently successfully completed the preliminary engine developmental performance testing, which included engine starts, acceleration, and deceleration, with no depreciation in the regenerator performance.

Ship set No. 2, the 50-hr flightworthiness units, were reidentified with Parts No. 182330-5-1 (left-hand unit) and No. 182330-6-1 (right-hand unit). A discussion of the design improvements that were incorporated in this unit for performance and structural reasons has been previously presented.

Before the second ship set was shipped to Allison, a performance test was conducted on the left-hand unit (182330-5-1). The performance corrected to design Condition 1 is presented in Table VIII.

TABLE VIII.

RESULTS OF TEST ON LEFT-HAND UNIT (182330-5-1)

	$\sigma \Delta P$	σ	ΔP (psi)	$\Delta P/P$ (%)
Gas side	7.82 in. H_2O	0.419	0.6745	4.35
Air side	17.1 in. Hg	2.57	3.26	4.15
Effectiveness	87.7%			

Examination of the test regenerator following the initial performance testing revealed that the air inlet diffuser was broken. The broken diffuser was removed and the air-side isothermal test was repeated with no diffuser installed. It is this isothermal pressure drop value that is presented in Table VIII. Because of the limited time available, the air inlet diffuser cone was removed from both units before shipment to Allison. Based on the test results on the first ship set, which had a diffuser, the removal of the diffuser caused an increase in air-side pressure drop of 1.07% and a decrease in effectiveness of 1.1% at design Condition 1. The walls of the air inlet diffuser were increased from 0.010 to 0.020 in. to prevent a repetition of this failure on ship set No. 3. The weight penalty for this change was 0.034 lb.

The total pressure loss at Condition 1 (8.5%) was less than the maximum permitted by the Allison specification (9.86% maximum). The effectiveness (57.7%) of the unit, however, was less than that required by the specification (60.0%). The decreased effectiveness was anticipated since change in the core dimple depth sacrificed effectiveness to lower air-side pressure drop.

The units were acceptance tested, with the results as shown in Table IX, before shipment to Allison.

TABLE IX.

ACCEPTANCE TEST RESULTS AT AiRESEARCH

	Leakage From Air Side (lb/sec at 132 psig)		Leakage From Gas Side (lb/sec at 2 psig)		External Leakage	Weight (lb)
	Measured	Allowable	Measured	Allowable		
P/N 182330-5-1 (left hand)	< 0.00085	0.0042	< 0.00085	0.007	0	26.875
P/N 182330-6-1 (right hand)	< 0.00085	0.0042	< 0.00085	0.007	0	27.30

Since these units were scheduled for flightworthiness tests at Allison, the aforementioned weights include several items that are not required for the flight regenerators. The weight increase for these items is:

	Weight/unit (lb)
[illegible]	0.[illegible]
[illegible]	0.77
[illegible]	[illegible].21
[illegible]	[illegible].28

Ship set No. 3, the flight test units, was identified with Parts No. 182330-7-1 (left-hand unit) and No. 182330-8-1 (right-hand unit). These units were modified from the second ship set configuration to increase the effectiveness up to that required by the specification. The effectiveness of the core was increased by using a deeper dimple in the core tubes. The dimple used was of the same depth as that used for the original ship set No. 1 core. The stronger air inlet diffuser cone was included in the air inlet ducts. Both the gas exit duct channels and the gas bypass plate bolts were deleted. Stiffeners were added to the gas bypass plate to increase the stiffness of this member. Based on these changes and past testing, performance of this unit was estimated and is shown in Table X. The total estimated pressure drop at Condition 1 is 8.12% at an effectiveness of 60.7%. This indicates that this unit will meet the Allison specification requirements of 9.86% maximum pressure drop and 60% effectiveness.

TABLE X.
ESTIMATED PERFORMANCE OF SHIP SET NO. 3 AT CONDITION 1

		$\Delta P/P$, (%)
Gas Side		
Ship set No. 2 Test Results		4.35
Revised Core		-0.01
	Total	4.34
Air Side		
Ship set No. 2 Test Results		4.15
Valley Diffuser		-1.07
Revised Core		+0.70
	Total	3.78
Effectiveness		
Ship set No. 2 Test Result		57.7
Revised Core		+ 1.5
New Diffuser		+ 1.4
	Total	60.7

Tests to verify the performance of these units were not run at AiResearch prior to their delivery to Allison because of limited time available.

The completed units are shown in Figures 15 through 17. The acceptance test results are presented in Table XI.

TABLE XI

ACCEPTANCE TEST RESULTS

	Leakage from Air Side (lb/sec at 130 psig)		Leakage from Gas Side (lb/sec at 2 psig)		External Leakage	Weight (lb)
	Measured	Allowable	Measured	Allowable		
P/N 182330-7-1 (left hand)	0.0017	0.0042	0.0021	0.007	0	25.75
P/N 182330-8-1 (right hand)	0.0008	0.0042	0.0015	0.007	0	24.75

The weights in Table XI include instrumentation bosses not required on the flight unit. The weight increase due to the bosses is 0.30 lb/unit.

An outline drawing showing the final regenerator configuration is included at the back of this report. The estimated flightweight regenerator details, at specification Condition 1, are as follows:

Weight (lb)	25.45 (maximum)
Effectiveness (%)	60.7
Gas side $\Delta P/P$ (%)	1.34
Air side $\Delta P/P$ (%)	2.78
Total $\Delta P/P$ (%)	3.12

Some weight reduction could be realized with the quantity production of these units. This is illustrated by the one-pound variation between the weights of the left-hand and the right-hand regenerators. A greater part of this variation is the result of differences in the amounts of welding and

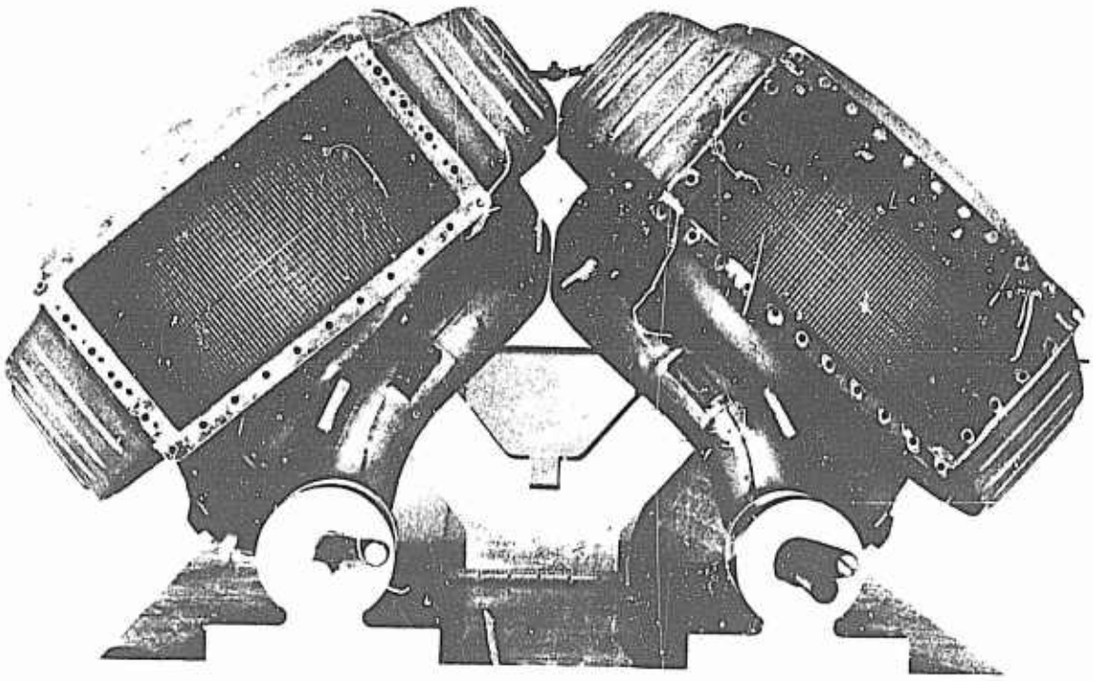

Figure 15. Regenerators P/N 182330-7-1 and 182330-8-1 (Ship Set 3)—Rear View.

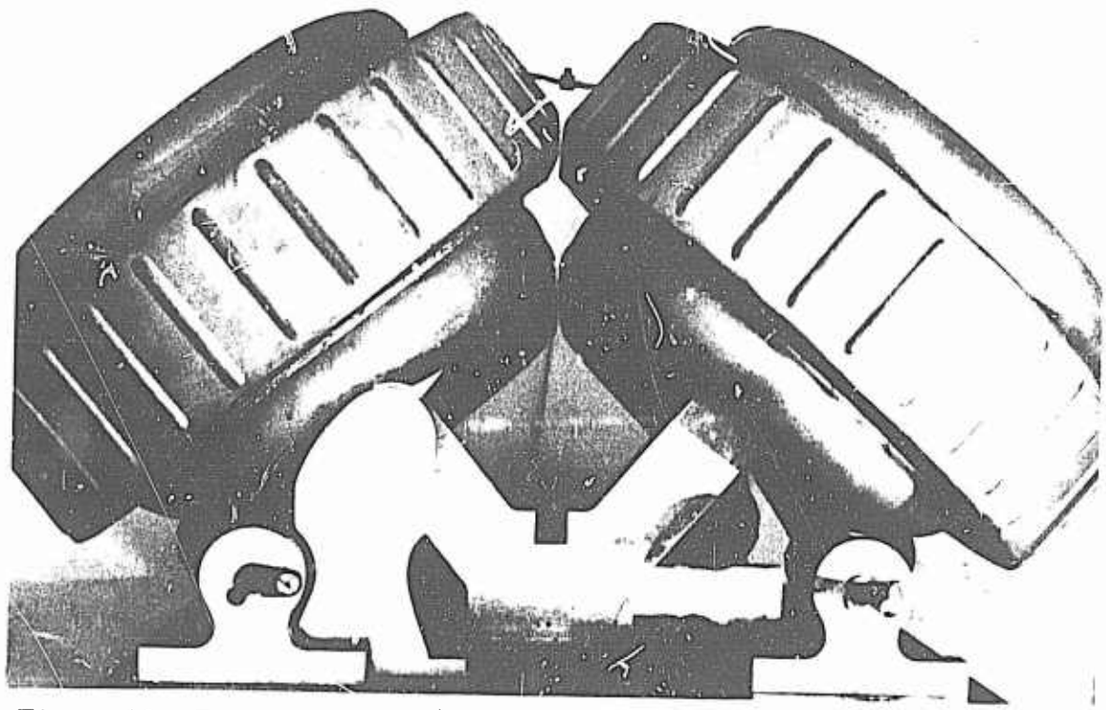

Figure 16. Regenerators P/N 182330-7-1 and 182330-8-1 (Ship Set 3)—Front View.

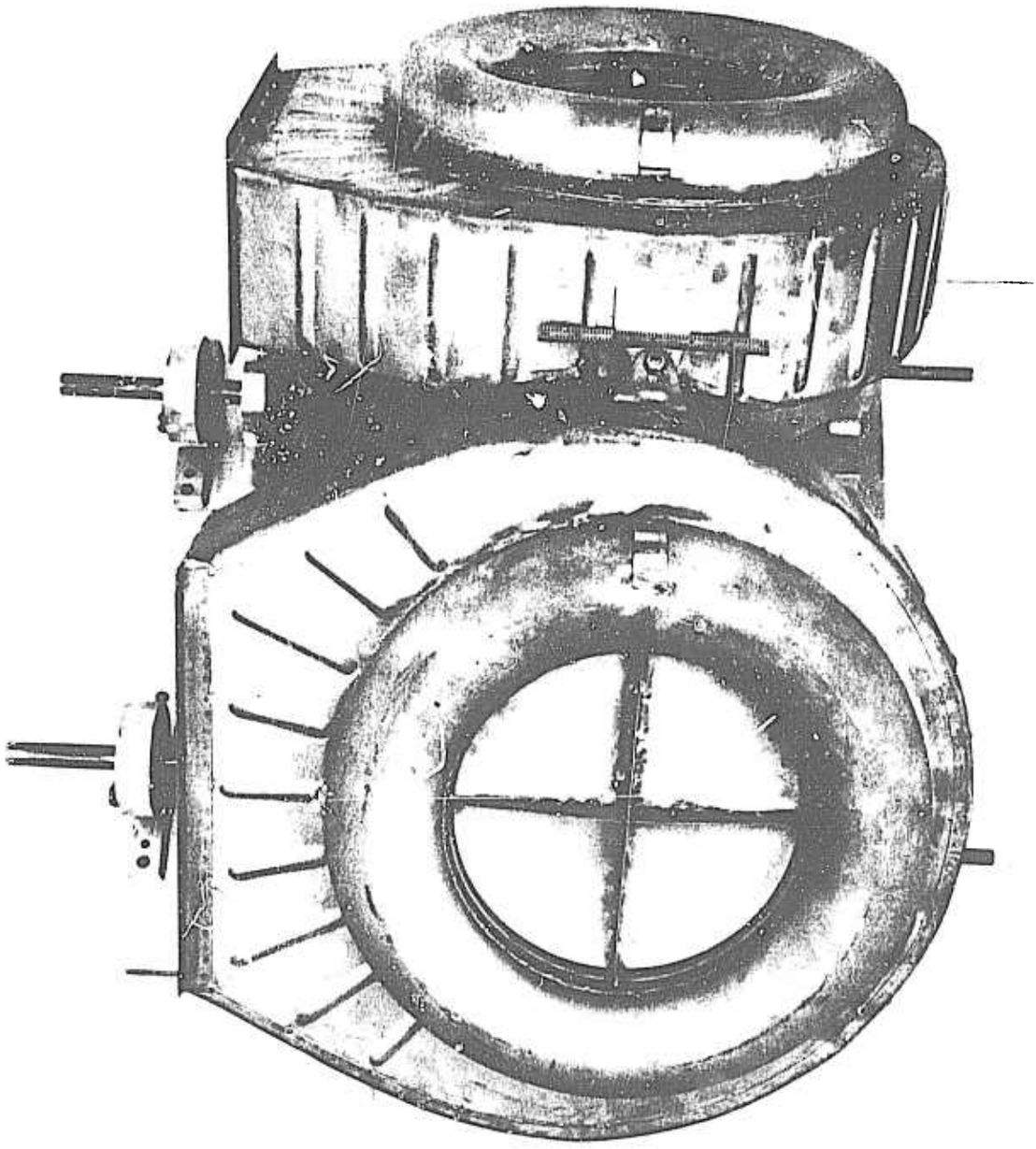

Figure 17. Regenerators P/N 182330-7-1 and 182330-8-1 (Ship Set 3)—Top View.

braze material. A number of areas have been welded on the flight test regenerators that would probably be formed in one piece with more sophisticated tooling. The degree of tooling sophistication is of course dependent on the production quantity.

A detailed weight analysis was performed wherein each detail drawing of the flight test version regenerator was reviewed.

The most significant weight influences were challenged first. The tube bundle must remain unchanged from the viewpoint of performance and structural integrity. The total quantity of tubes is dictated by performance requirements, and the use of 0.006-in. wall tubes in the core is dictated by structural necessity.

Similarly, all components were reviewed. It was ascertained that the weight prediction must remain at 25.45 lb (maximum) per regenerator module.

ENGINE MODIFICATION AND FABRICATION

ENGINE CONFIGURATION

The T63-A-5 regenerative engine was conceived as a configuration using a "bolt on" type regenerator and requiring a minimum of changes to the basic engine.

A standard T63-A-5 engine was converted to a functional T63-A-5A by installation of a compressor bleed system. The regenerators were designed to attach to the exhaust ducts by means of the same Marmon clamps now used to attach the aircraft exhaust ducts. The regenerator air inlet and outlet ducts replaced the existing air transfer tubes and used the same piston ring sealing arrangement at the compressor scroll and the outer combustion case. See figure 48.

An additional turbine cooling air manifold supplies cooling air to the first-stage turbine wheel. The control system uses the same control and power turbine governor with a revised schedule to accommodate the regenerative engine operating characteristics.

Figure 18 shows the T63-A-5 regenerative engine with the original mock-up regenerators installed.

Figure 18 T63-A-5 Regenerative Engine With Original Mock-up Regenerators Installed.

EXHAUST COLLECTOR STRESS ANALYSIS

The regenerators are attached to the exhaust collector by means of Marmon clamps. The stress produced in the exhaust duct by this added weight was calculated based on load requirements from Specification MIL-E-8593. The maximum design load is 15 g down, 3 g aft, and a side load equal to 1.5 g. Since the axes of the exhaust ducts are not mounted in a vertical direction, the downward g-force resulting from the weight of the regenerator unit must be resolved into components which coincide with or are perpendicular to the engine axis as shown in Figure 19.

The method used to determine if the possibility of buckling exists within the gas outlet ducts of the exhaust collector is taken from the "Handbook of Structural Stability" by George Gerard. The results show that the exhaust collector ducts will not fail by compressive buckling under the design loading conditions and have a margin of safety of 6.14.

In addition to axial compressive loading, bending moments about the major and minor axis of the ellipse are produced by the design loads. These additional bending moments must also be considered in combination with the axial compressive loads when calculating the critical buckling stress. The applied stress at the critical radius of curvature is 4340 psi at a section located 3.3 in. below the end of the duct. The critical buckling stress for the applied moment is 53,000 psi.

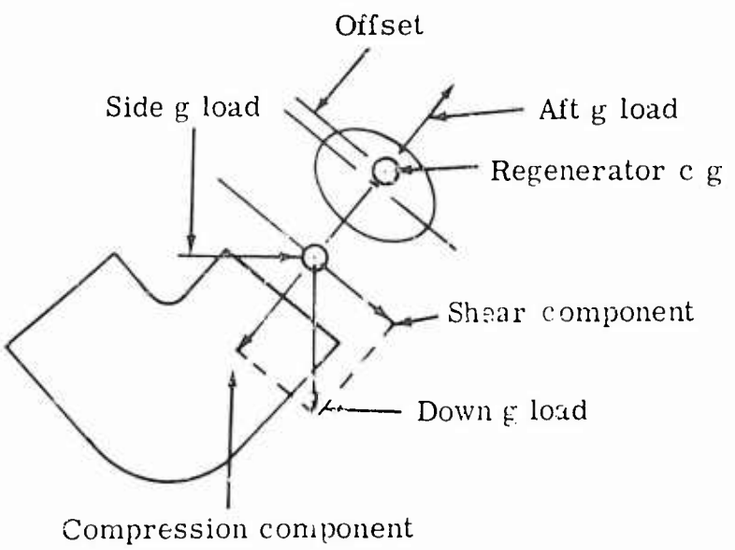

Figure 19. G-loads Resulting from Weight of Regenerator Unit.

In addition to the exhaust duct buckling stress, the stresses in the load carrying members of the exhaust collector assembly were investigated. Under a 1-g condition or normal operating condition, the maximum stress applied was 7225 psi to the upper member and -4672 psi to the lower member. For the 15-g load condition, the stresses were 79,740 and -53,637 psi, respectively.

Under the 15-g load condition, some yielding could be expected, but the stress would not exceed the ultimate strength of the material (105,000 psi). Since a 15-g load condition would occur only on an extremely hard landing, it was felt that the stress levels were acceptable and no modification of the exhaust collector would be required.

THERMAL GROWTH

The regenerator is mounted directly on top of the engine exhaust duct and is rigidly attached to the exhaust duct by means of a Marmon clamp. The growth of the regenerator relative to the engine will, therefore, occur between the regenerator air inlet duct and the compressor scroll and also between the regenerator air outlet duct and the outer combustion case. Piston ring seals on the regenerator air inlet and outlet ducts allow relative movement between the regenerator and the engine.

The relative growths between the engine and the regenerator are shown in Figure 20.

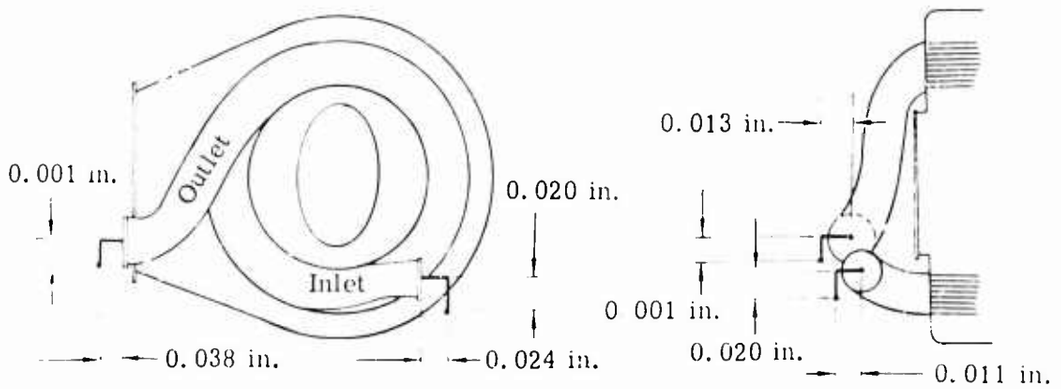

Figure 20. Relative Growths Between Engine and Regenerator.

In the axial direction, there is sufficient clearance to allow for the relative movement of the air inlet duct with respect to the compressor scroll. A snap ring in the outer combustion case locates the regenerator air outlet duct and transfers the air pressure load to the outer combustion case. The outlet duct is flexible enough to accommodate the 0.038-in. relative movement. In the plane perpendicular to the axis of the regenerator air outlet and air inlet tubes, the piston ring seals allow a 0.020 to 0.030-in. relative movement which is sufficient to accommodate the relative growth.

TURBINE COOLING AIR

The addition of the regenerator requires a change in the turbine cooling air circuit. In the T63-A-5, the cooling air for the first-stage turbine wheel and the second-stage balance piston is obtained internally from secondary air (burner inlet). With a regenerator, this temperature increases from 450° to 750°F, which makes it too hot for cooling air use. The initial cooling air circuit is shown in Figure 21.

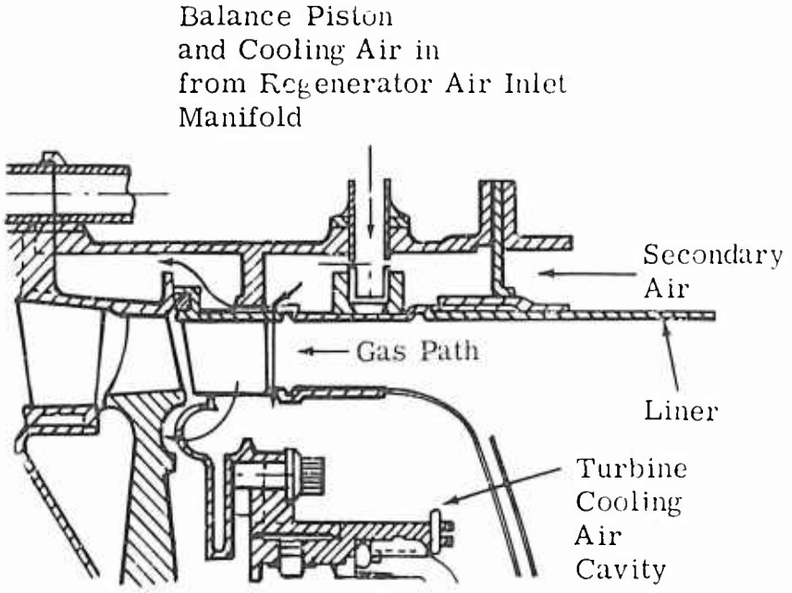

Figure 21. Initial Cooling Air Circuit.

A flange on the combustion liner, bolted between the gas producer and outer combustion case, blocked secondary air from the gas producer support. A cooling air manifold provided an external supply from the regenerator air inlet duct (450°F supply) through two No. 8 hoses for turbine cooling air and balance piston air. The T63-A-5 gas producer support has four bosses which were originally intended for turbine inlet thermocouples. Two of the bosses were blanked off and the other two were used for dummy thermocouples to position the first-stage nozzle shield. Two fabricated manifolds were made to fit these bosses, with one of the pads on each manifold incorporating a tube which would position the first-stage nozzle shield.

The test results of the first engine run are shown in Figure 22. The cooling air temperature was 350°F higher than that for the nonregenerative T63-A-5 engine.

The problem was traced to excessive leakage in the joint between the liner and the first-stage nozzle shield. Since the two No. 8 lines could not supply sufficient air, the pressure in the gas producer support dropped until it was below the pressure in the gas path. This resulted in a pressure differential that allowed flow from the gas path into the turbine cooling air cavity, thus raising the temperature of the turbine cooling air. Since trying to reduce the leakage or increasing the external supply line would require extensive rework, the decision was made to supply external cooling air directly to the turbine cooling air manifold and to use secondary air for the balance piston air. This configuration is shown in Figure 23.

Because the balance piston air and the leakage were supplied by an infinite supply of secondary air, the pressure in the turbine cooling air cavity was higher than the pressure in the gas path and provided an acceptable cooling air temperature. The test results are shown in Figure 22. Although a cooling air temperature 90°F higher than the nonregenerative engine was acceptable for test purposes, a production engine would require additional work to reduce the temperature. Also, a 750°F balance piston air temperature may reduce the life of the seal material and of the second-stage wheel.

No. 5 and 8 flexible hoses and standard AN fittings were used to fabricate a manifold to attach the turbine cooling air tubes to the regenerator air inlet ducts. This manifold assembly weighs 2 lb. A more sophisticated manifold assembly could be made which would reduce the weight.

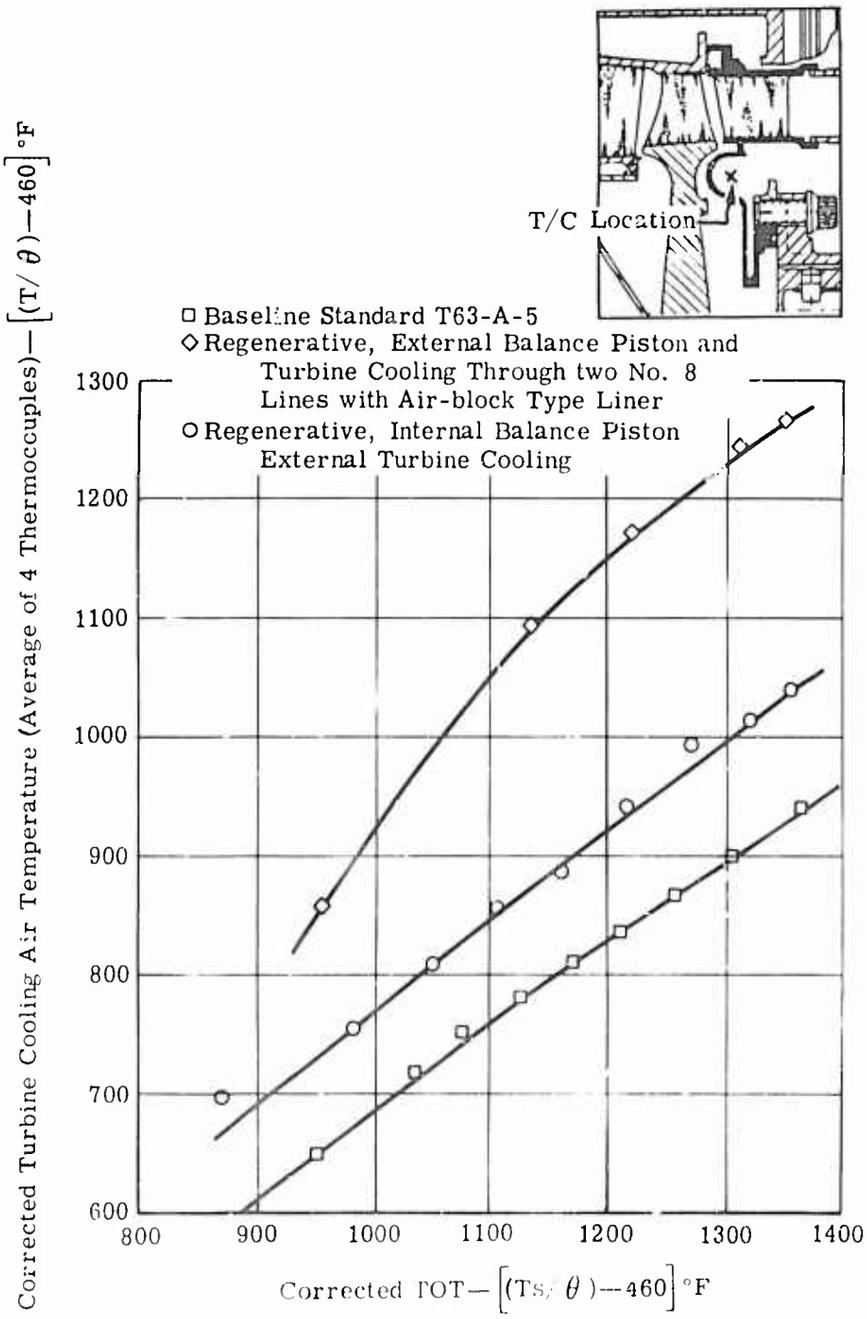

Figure 22. Turbine Cooling Air Temperature.

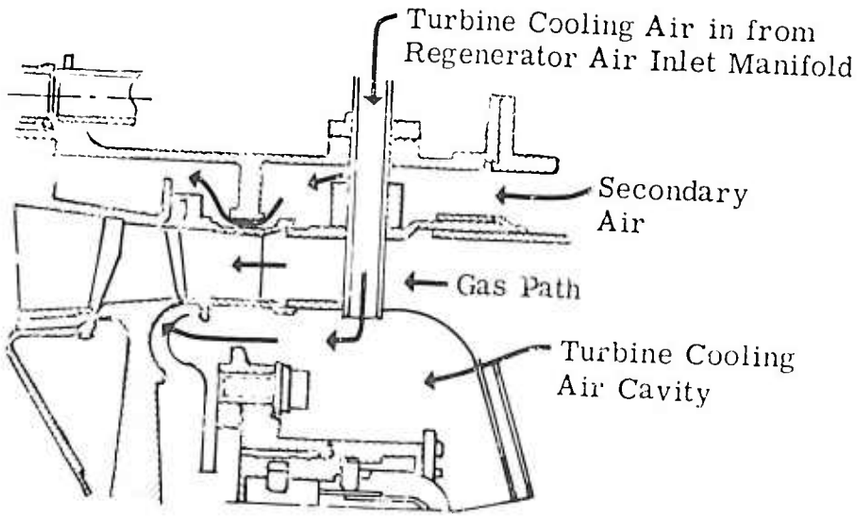

Figure 23. Revised Cooling Air System.

CONTROL SYSTEM MODIFICATION

INTRODUCTION

The power control system for the T63-A-5A consists of two pneumatic-mechanical components, the gas producer control and the power turbine governor. The gas producer control is the fuel metering component and provides transient fuel limiting (starting, acceleration, and deceleration), maximum gas producer speed limiting, ground idle speed control, and mechanical fuel shutoff. The power turbine governor provides steady-state rotor speed governing by modifying the gas producer control functioning to provide the engine power required to match the load power. Figure 24 illustrates the interrelationship of the two control components and their integration into the system with the fuel pump and fuel nozzle.

Figure 25 illustrates the limiting functions accomplished by the gas producer control. The control scheduling is represented in terms of the ratio of fuel flow to compressor discharge pressure (W_f/CDP), for this is the basis upon which the control operates. (CDP represents the control sensing pressure, which is essentially compressor discharge pressure.)

The acceleration fuel schedule, in conjunction with a modulated compressor bleed schedule, is selected to provide rapid transient response and to prevent compressor surge and excessive transient turbine temperature. Ambient temperature sensing and compensation are not required in that they are essentially provided by the CDP and bleed control schedule variation with ambient temperature. Ambient pressure compensation is provided by the CDP.

The addition of a regenerator results in a lower engine required-to-run fuel flow, which will vary as a function of temperature of the regenerator. When the engine is first accelerated and the regenerator is "cold," the amount of fuel required to accelerate the engine at a given rate is higher than the fuel flow required when the regenerator is hot.

The deceleration fuel schedule is selected to provide rapid deceleration transient response and to prevent burner flameout. The addition of a regenerator and the associated reduction in fuel flow require a much lower minimum fuel stop to provide an acceptable deceleration. Since reducing the minimum fuel flow stop increases the possibility of burner flameout, the combustion liner must be optimized to prevent flameouts.

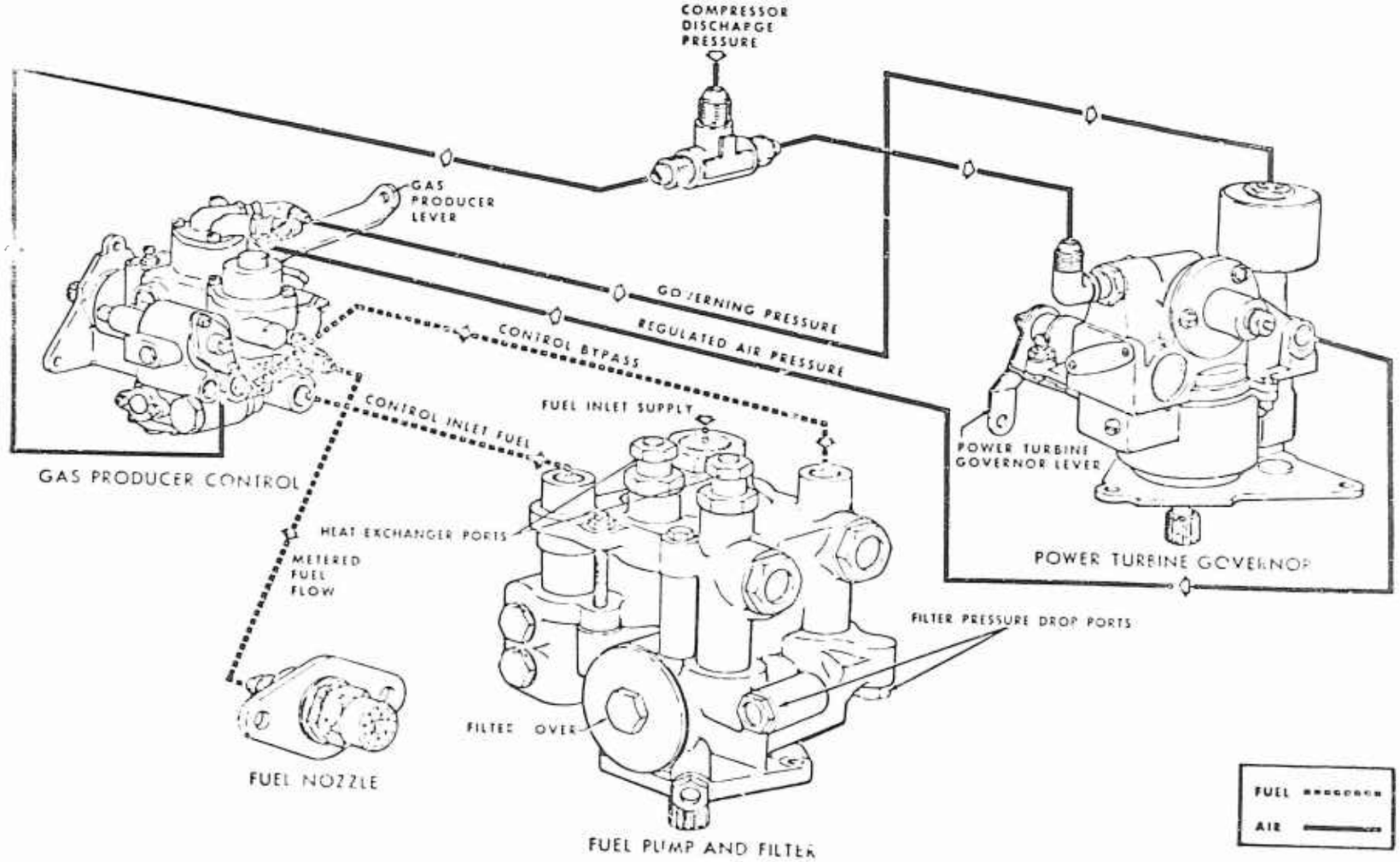

Figure 24. T63 Turboshaft Control System.

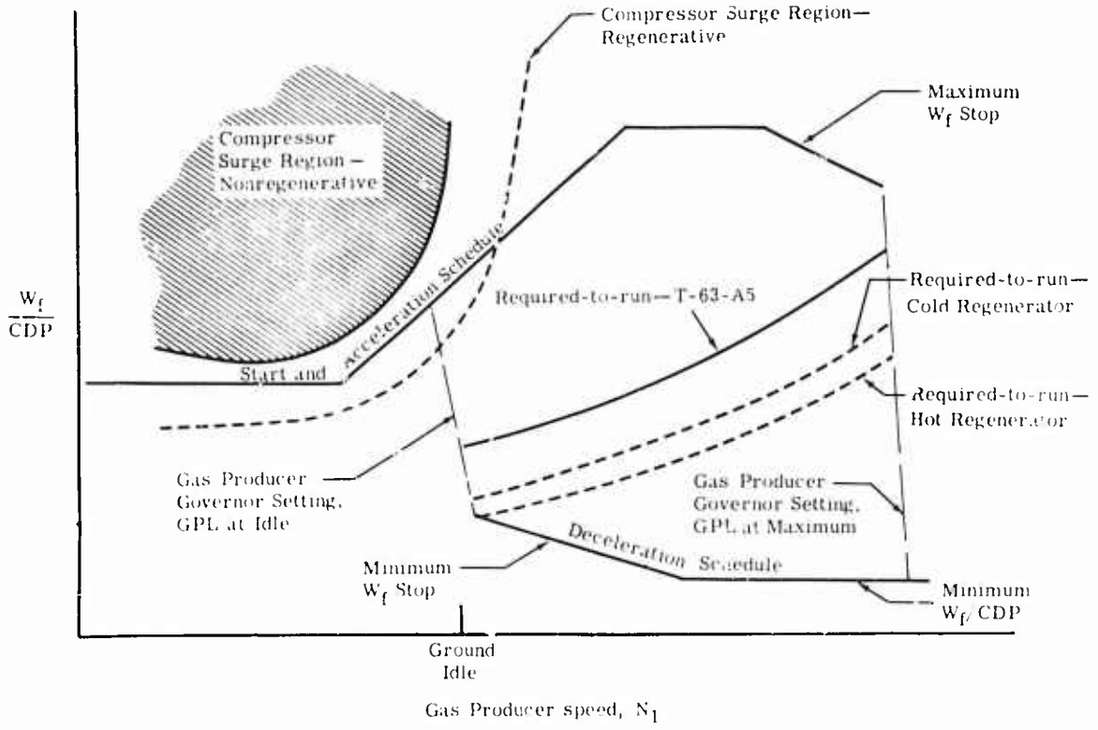

Figure 25. T63 Gas Producer Control Schedule.

For starting, the fuel flow is established by the acceleration schedule. The addition of the regenerator again poses the problem of obtaining a sufficient margin between the engine required-to-run and the acceleration schedule for both a hot and a cold regenerator. The starting portion of the acceleration schedule is the most critical. The regenerator, prior to start, can be at ambient temperature if the engine has been shut down for some time. If the engine is restarted immediately after shutdown, the regenerator temperature will be as high as 500°F. The magnitude of the effect of the change in required-to-run fuel flow on engine transient operation is dependent on the time constant of the regenerator.

It was felt that a burner inlet temperature (BIT) sensor would be required to provide a sufficiently rich fuel schedule for cold engine starts and accelerations and yet prevent surge and overtemperature during starts and transients with hot regenerators when required-to-run fuel flows would be substantially lower.

BIT SENSOR CONTROL SYSTEM

To meet program and delivery requirements, the vendor proposed a modification of an existing Bendix Model ATXC-136 BIT sensor which gave a percentage fuel flow reduction. The fuel schedule for this mode is defined in Figure 26.

The BIT sensor to accomplish the aforementioned requirements is shown in Figure 27. The sensor was mounted on a special pad on the outer combustion case of the engine. The probe extended axially into the outer combustion case to sense burner inlet temperature which is equivalent to regenerator air outlet temperature. A description of the operation of the BIT sensor follows.

A differential expansion temperature probe, consisting of a low rate of expansion core housed in a stainless steel tube, senses burner inlet temperature. Movement of the core, as the length of the tube changes with temperature, is transmitted through an amplifying linkage to position the BIT needle valve. Flow through the valve reduces metered flow to the engine by a constant percentage for each BIT area setting. This is accomplished by the use of a regulator which varies the pressure drop across the needle valve as a function of inlet fuel flow. The reference pressure for the regulator is taken from the throat of the venturi located in the control inlet. As metered flow from the main control increases, reference pressure decreases and a new force balance on the valve is established by opening the bypass area. The increase in differential pressure across the BIT needle results in the increased flow for the same area.

Special effort was devoted to analysis and sizing of the venturi for operation at the relatively low fuel flows required.

In the initial testing of the BIT sensor, difficulty was encountered in holding a constant percentage level $\left(\frac{W_f \text{ bypass}}{W_f \text{ inlet}}\right)$ for a given BIT setting.

A percentage decrease was encountered at the lower flows. This condition was undesirable because it caused reduced BIT compensation in the start range. The problem was attributed to insufficient pressure recovery after the venturi. The diffusion angle of the venturi had been increased from 6° to 21° to minimize the package size.

The flow system was changed to plumb the bypass upstream of the venturi. This allowed sufficient working pressure for the regulator, at the low flows, to provide essentially a constant percentage fuel flow throughout the range of anticipated flows without changing the design of the venturi.

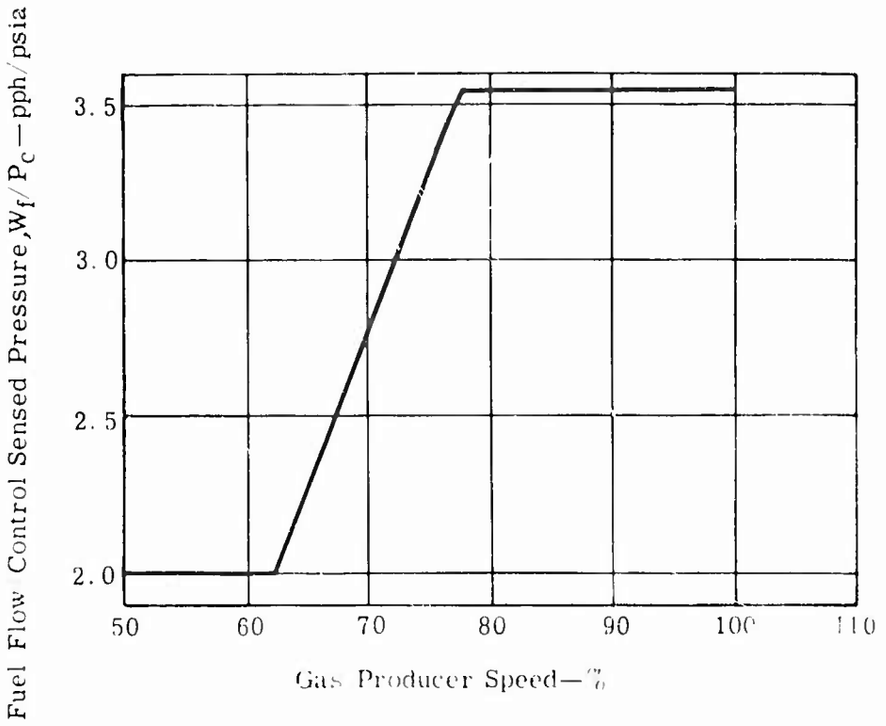

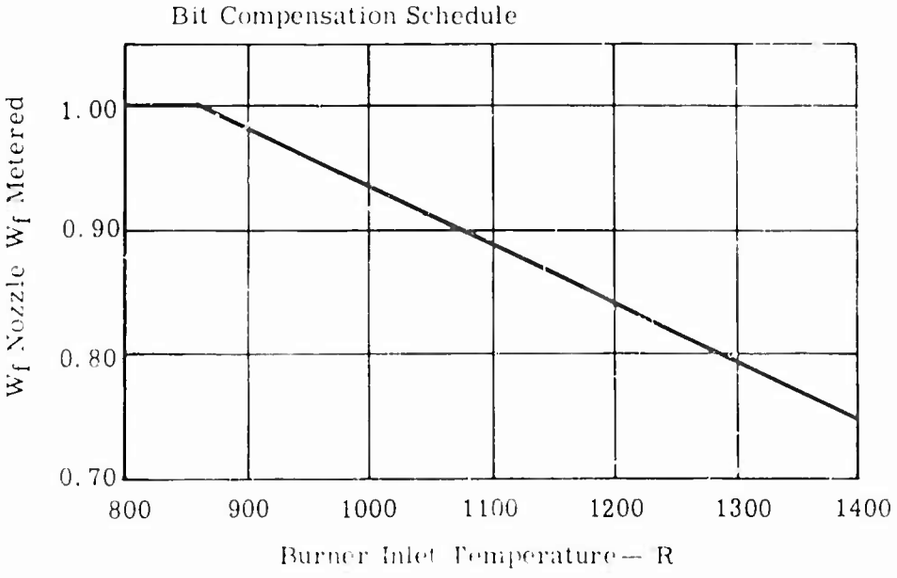

Figure 26. Regenerative T6 [illegible] Schedule PIT Compensati

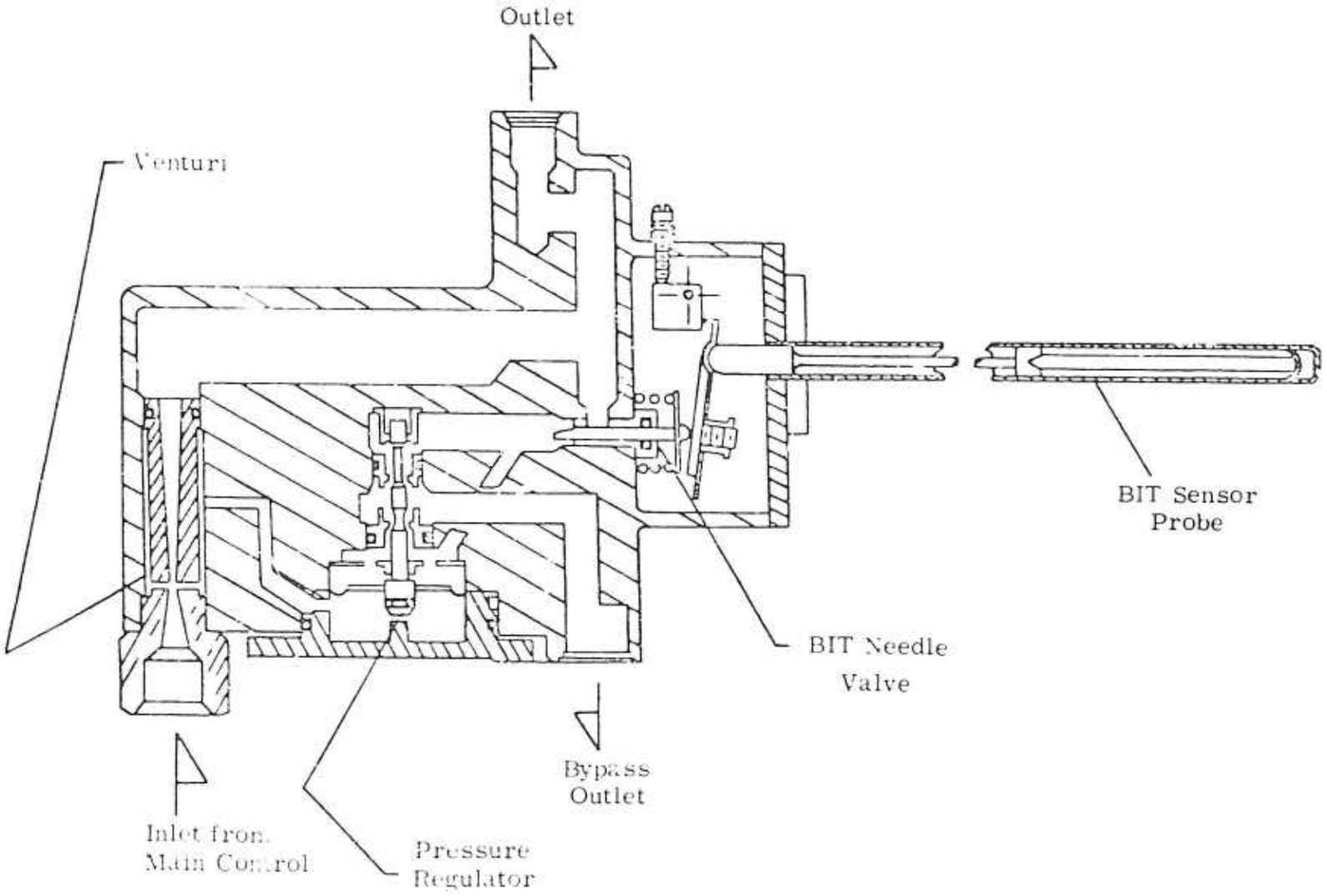

Figure 27. Burner Inlet Temperature Sensor.

SENSOR CONTROL SYSTEM WITHOUT BIT

A regenerator with a fast time constant would result in less thermal inertia, and it may be possible to provide acceptable fuel scheduling without a BIT bias for variations in regenerator heat input to the engine. The estimated time constant of the proposed regenerator was four seconds. Consequently, at the time that the fuel control system with the BIT sensor was being developed, another control system was being worked on in which a BIT sensor was not incorporated. It was decided that both systems should be investigated, since a possibility did exist that a BIT sensor may not be required. This decision would have to be made as a result of engine tests whereby the characteristics of the regenerator and BIT sensor could be determined. The fuel schedule without the BIT sensor is shown in Figure 28.

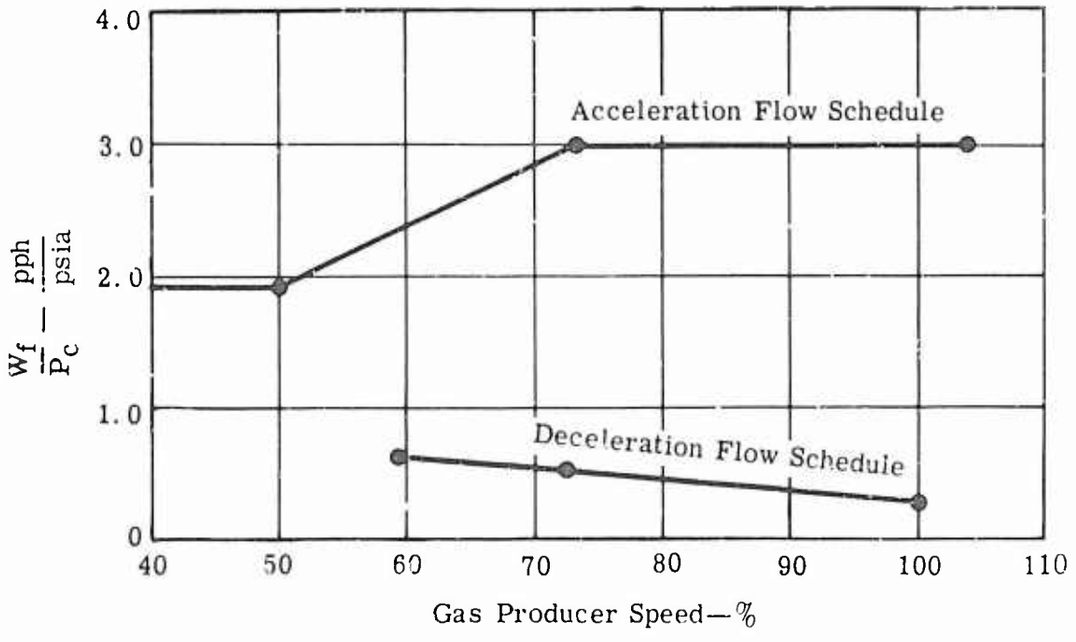

Figure 28. Regenerative T63 Control Schedule Without BIT Compensation.

ENGINE TEST RESULTS

Engine tests were conducted on the system with and without the BIT sensor. Two main areas in question in regard to the engine-control system were the time constant of the regenerator versus the BIT sensor time constant and the necessity of a BIT sensor.

The tests indicated that the time constant of the regenerator was faster than that of the BIT sensor, and the engine would accelerate faster than the BIT sensor could respond. The tests also indicated that a better control system could be obtained without the BIT sensor.

The basic problems encountered with the BIT sensor control mode were:

- There was a lag of 3 to 4 seconds on light-off due to compensator bypass valve chatter.
- The idle governor slope was very shallow, which resulted in N_1 sensitivity to required-to-run fuel flow and caused slow decelerations.
- Overspeeds of up to 2500 rpm on accelerations occurred because of the response rate of the BIT sensor and its relationship to the regenerator warm-up rate.

The fuel control without the BIT sensor provided acceptable transients over the required temperature range of 0° to 100°F ambient temperature. Thermal inertia of the regenerators was not a major problem, although decelerations were slower than those for an engine without regenerators.

The only problem encountered with this control configuration was surge during starting with hot regenerators. The fuel schedule was readjusted in the starting range to eliminate the problem. It was found that with the throttle in the idle position, the fuel flow in the 25 000-rpm range was 3 to 6 pph higher than the bench setting. Placing the throttle lever in the 90° position elimmated the blip in fuel flow and thus the starting surge with hot regenerators.

Static bench test of the fuel control could not substantiate occurrence of the blip. It is believed that a dynamic lead term existed in the control which is a function of the P_x and P_y volume and bleed size. With the throttle in the 90° position, the P_y system is closed and the lead term does not exist.

A detailed investigation of the blip problem was not necessary since satisfactory starts could be made with a hot engine. The throttle would be positioned at 90° until idle speed was obtained, and then the throttle would be retarded to idle.

Table XII compares the transient operation of the regenerative engine without a BIT sensor with the T63-A-5A specification maximum allowable transient times.

TABLE XII.
TRANSIENT OPERATION WITHOUT BIT SENSOR
COMPARED WITH SPECIFICATION REQUIREMENTS

	Transient Times (sec)	
Transient	Regenerative T63	T63-A-5A Model Specification 580-F
Deceleration from takeoff to ground idle (32,000 rpm)	5.3	5 (maximum)
Acceleration from ground idle to takeoff power	4	7
Acceleration from flight idle 35,600 rpm to takeoff power	3.5	3 (maximum)
Start to ground idle (hot regenerator)	16.0 (1200°F Maximum TOT)	60 (maximum) (1700°F TOT maximum)
Start to ground idle (cold regenerator)	21.0 (1000°F Maximum TOT)	
The following starts were made with 4.5 kva generator load, 60 % speed, and minimum battery voltage.		
Start to ground idle (hot regenerator)	38 (1450°F Maximum TOT)	
Start to ground idle (cold regenerator)	60 (1375°F Maximum TOT)	
Type II wave-offs	Surge free with ambient temperatures from 0 to 100°F and speed down to 29,000 rpm	

*A Type II wave-off consists of 3 min at takeoff power, a snap deceleration to the wave-off speed, and an immediate snap acceleration to takeoff power.

An acceptable fuel flow schedule could be made in the existing T63-A-5A fuel control on a "one-of-a-kind" basis using the existing power turbine governor. However, on a production basis, the required fuel flow schedule tolerances of the fuel control would require a compensating device in the starting range. Typical transients obtained prior to the 50-hr flight-worthiness test are shown in Figures 29 through 32. Note that no instability existed during steady-state operation throughout the speed range.

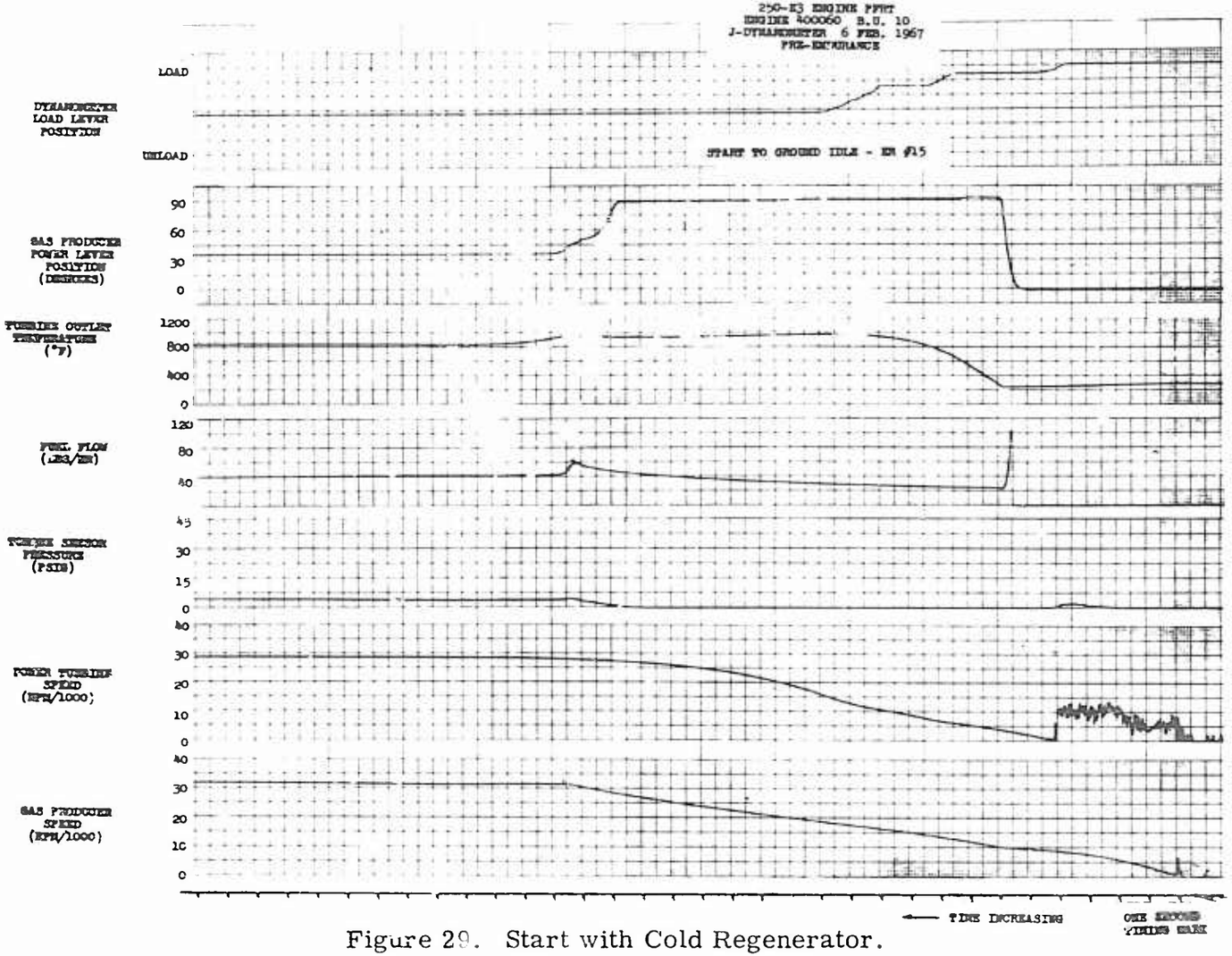

Figure 29. Start with Cold Regenerator.

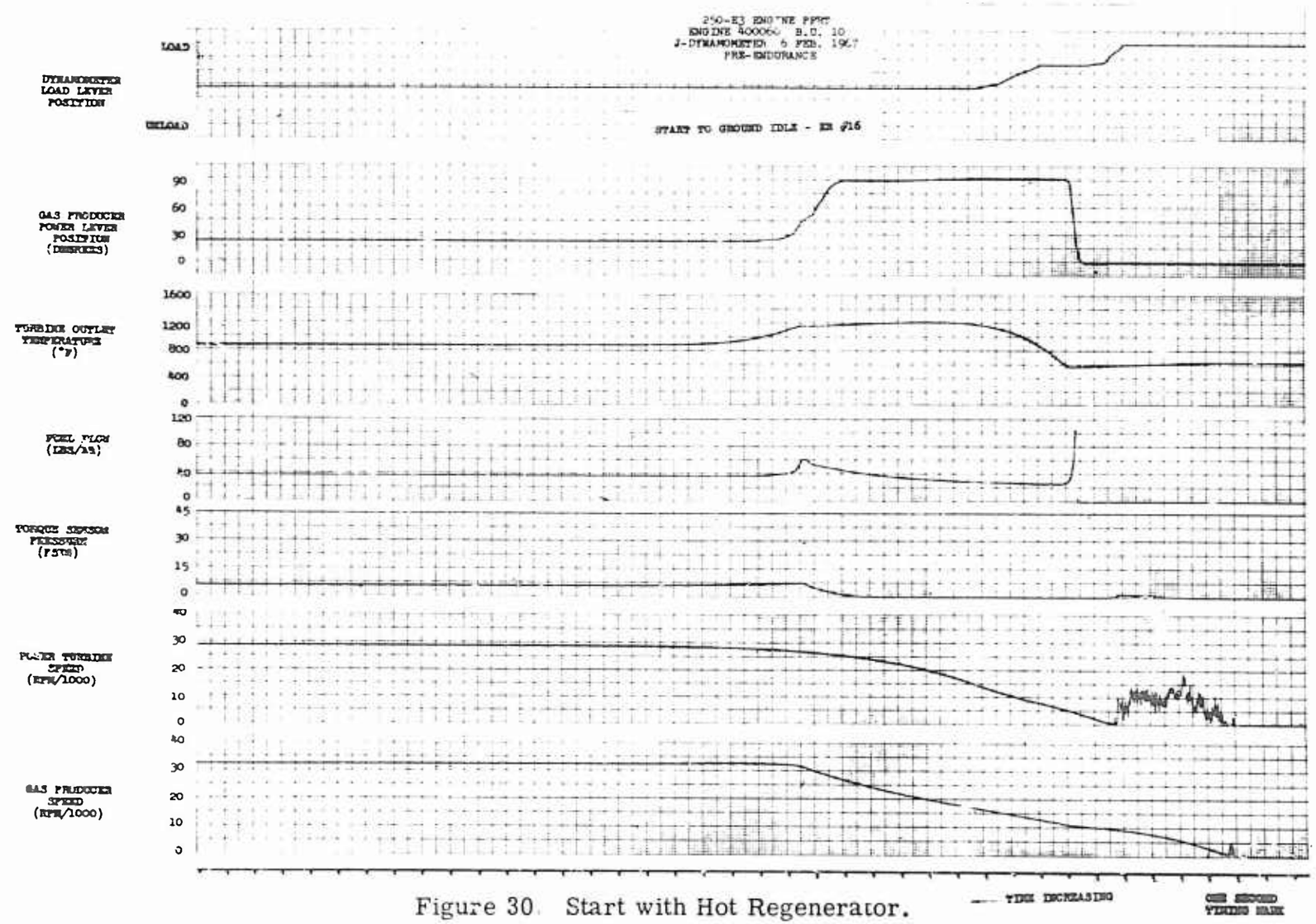

Figure 30. Start with Hot Regenerator.

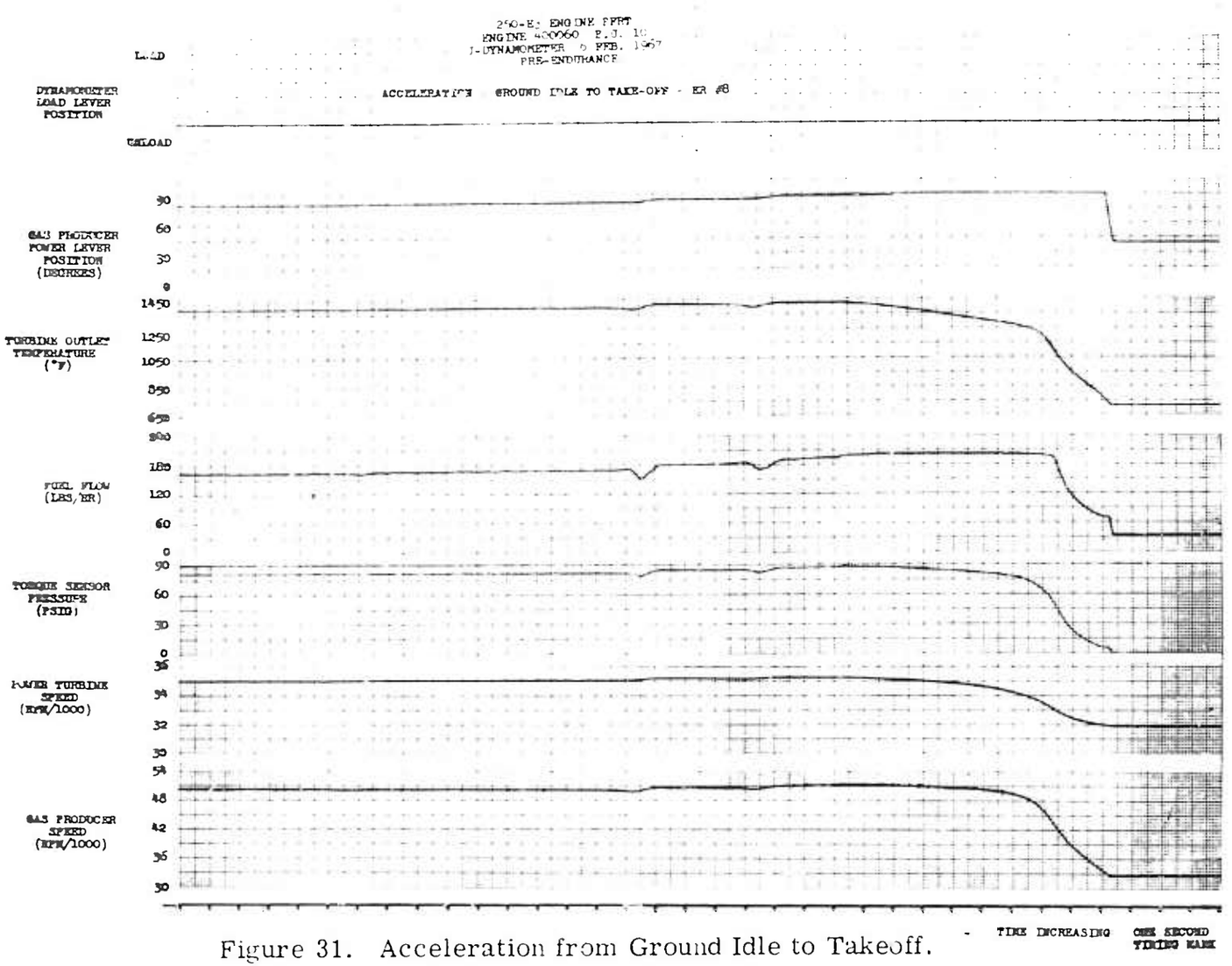

Figure 31. Acceleration from Ground Idle to Takeoff.

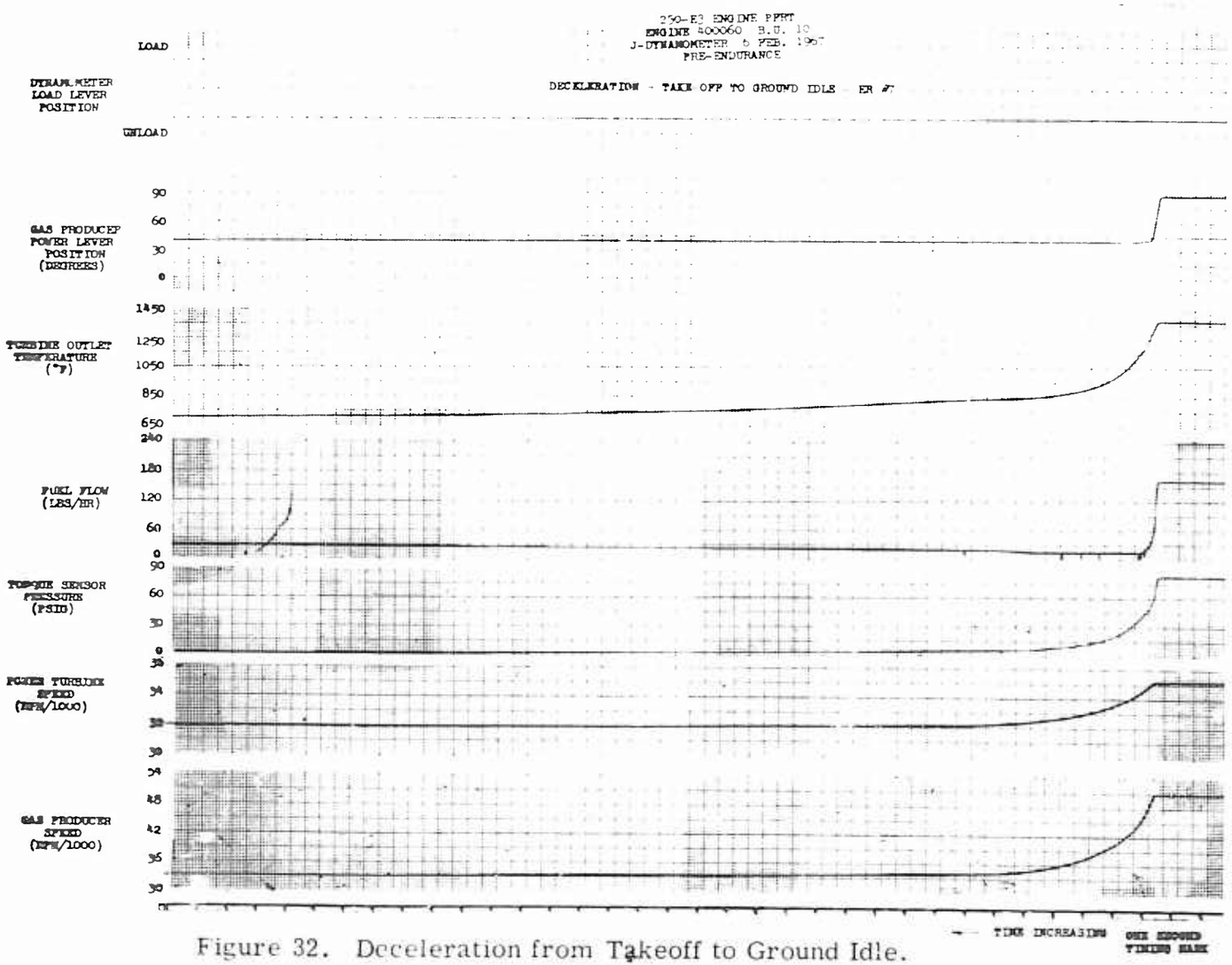

Figure 32. Deceleration from Takeoff to Ground Idle.

REGENERATIVE ENGINE PERFORMANCE

59°F SEA LEVEL PERFORMANCE

The test engine was an Army-furnished T63-A-5 modified to incorporate a fifth-stage bleed system on the compressor, an eight-thermocouple power turbine support, and an instrumented exhaust collector. The regenerative engine, Model 250-E3, S/N 400060, was comprised of compressor S/N B-169, accessories gearbox S/N C-250, and turbine S/N D-364. A second Army-furnished engine, S/N 400067, was also employed briefly during the test.

All engine testing was done on "J" dynamometer which had been modified to accommodate the regenerative engine. The test stand has the capability of testing the engine at compressor inlet temperatures from -35° to +130°F and altitudes up to 20,000 ft. Under all test conditions, the external environment of the engine was ambient.

The initial installation of the regenerative engine is shown in Figure 33.

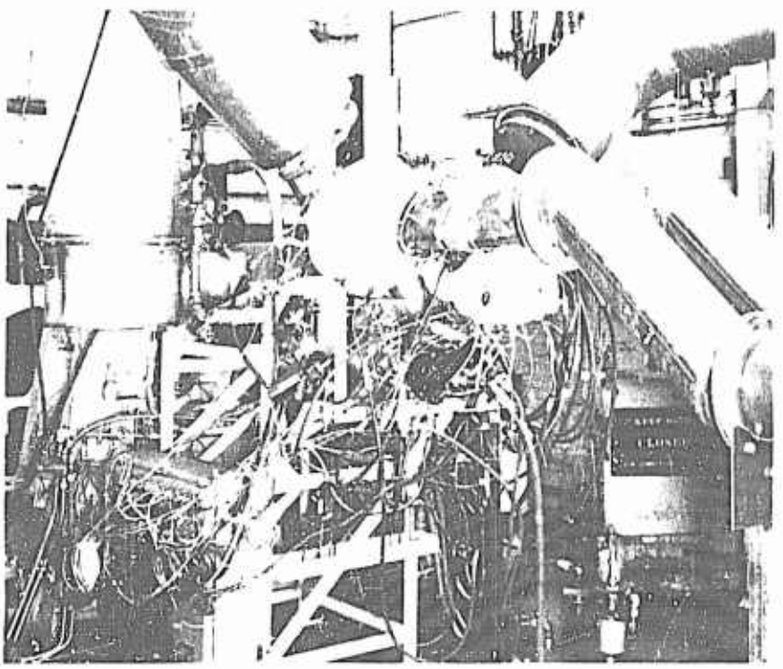

Figure 33. Initial Installation of the Regenerative Engine.

Instrumentation for evaluation of engine/regenerator performance consisted of the following:

Symbol	Data	Probe
P_{T_3}	Compressor discharge pressure	One three-element P/N T-809405 rake in the left regenerator module, downstream of the diffuser section of the regenerator
T_{T_3}	Compressor discharge temperature	One three-element P/N T-809404 rake in the right regenerator module—in the same axial location as for the P_{T_3} rake
$P_{T_{3.5}}$	Regenerator air outlet pressure	One three-element P/N T-811256 rake in the air outlet duct of each regenerator module. Sensing elements were located at centers of equal-area annuli.
$T_{T_{3.5}}$	Regenerator air outlet temperature	One three-element P/N T-811257 rake in the air outlet duct of each regenerator module and downstream of the $P_{T_{3.5}}$ rakes. Sensing elements were located at centers of equal-area annuli.
P_{T_4}	Burner outlet pressure	One single-element probe located at mean annulus depth in the 5 o'clock position.
T_{T_5}	Gas producer turbine outlet temperature	Eight single-element thermocouples of the standard type, as located by a P/N 683009-3 power turbine support.
P_{S_7}	Power turbine outlet / regenerator gas inlet pressure	Four wall static taps on each exhaust collector outlet duct, located midway between major and minor axes immediately upstream of the engine/regenerator interface.

Symbol	Data	Probe
T_{T_7}	Power turbine outlet/regenerator gas inlet temperature	Five thermocouples in each exhaust collector outlet duct at centers of equal-area elliptical annuli
P_{S_8}	Engine exhaust/regenerator gas outlet pressure	Eight equally spaced static taps at each regenerator exhaust port in the exhaust instrumentation adapter rings.
T_{T_8}	Engine exhaust/regenerator gas outlet temperature	One four-element T-310904 rake on the semimajor axis and one five-element T-810903 rake on the semiminor axis of each exhaust instrumentation adapter ring. Sensing elements were located at the centers of equal-area elliptical annuli.

Performance station locations are shown in Figure 34.

Additional instrumentation employed at various stages of the test program included: six static pressure holes located about the outer wall of the exhaust ducting on the left regenerator module; a PWA T 311993 five-element pressure probe with elements equally spaced along the major axis on the exhaust adapter of the left regenerator module; temperature and pressure probes in the manifold supplying cooling air to the upstream side of the first-stage turbine wheel (instrumentation per T 311084); various pressure probes in the turbine cooling air supply system, etc. Other instrumentation included standard dynamometer performance instrumentation and that required to maintain safe engine operating conditions.

The main problem encountered early in the test program was low performance due to regenerator tube cracking and high pressure drop on the exhaust side of the regenerator. The tube cracking, discussed in the Regenerator Design and Fabrication Section of this report, resulted in air leakage from regenerator air outlet to regenerator gas inlet. This air completely bypassed the turbine, resulting in a significant depreciation in power and increase in specific fuel consumption. After the second run of the engine, a leakage check of the units indicated a 0.14-lb/sec (5.2%) leakage rate which resulted in a 60-horsepower depreciation. In general, it can be said that a leakage of 1% of compressor airflow will

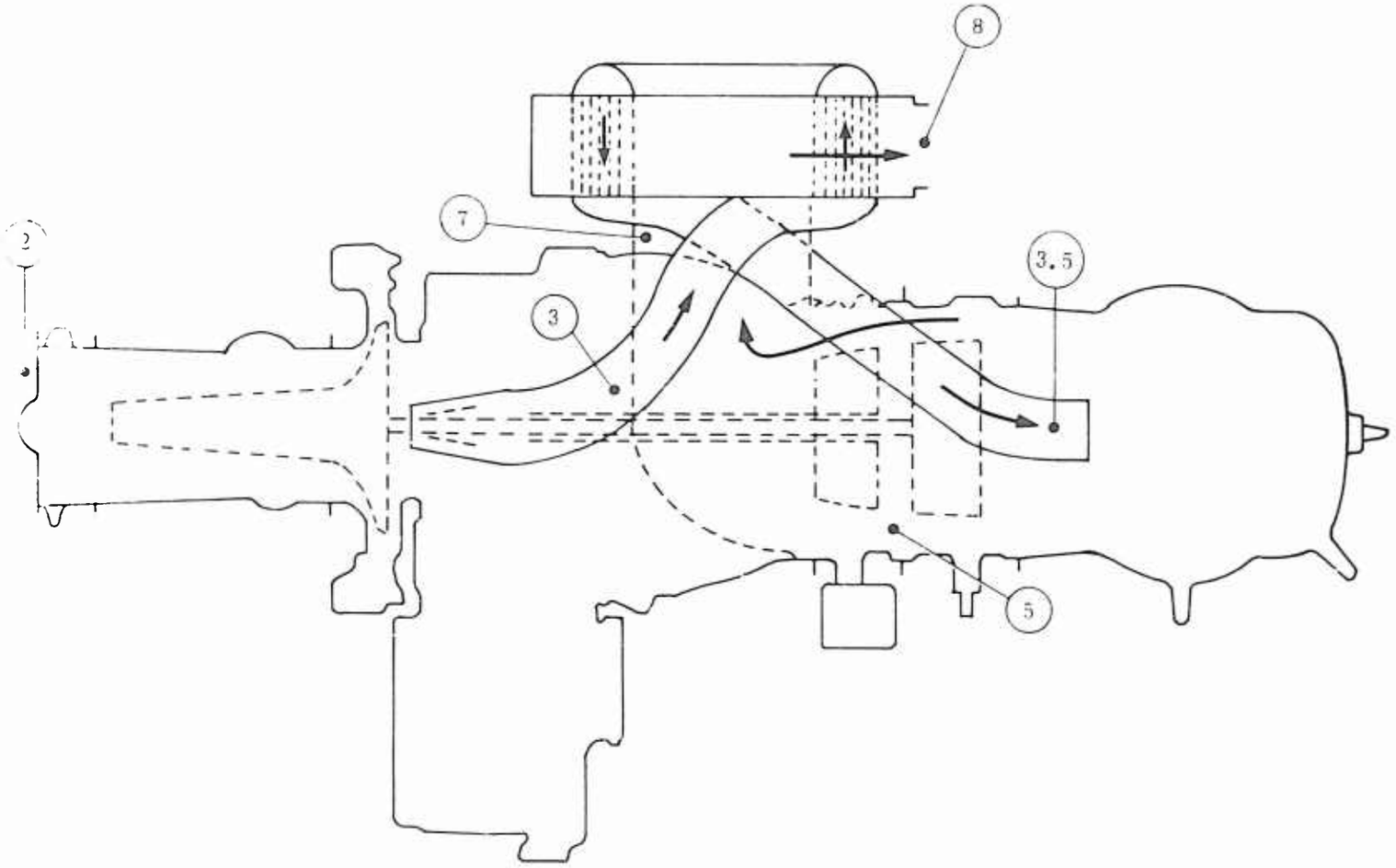

Figure 34. Gas Path Station Location.
(Circled numbers denote station locations.)

result in a 5% reduction in horsepower and a 3% increase in specific fuel consumption at the same engine turbine outlet temperature.

The exhaust-side pressure drop was also approximately 2% higher than anticipated. A 1% increase in pressure drop results in approximately 1.5% decrease in horsepower and 1.5% increase in specific fuel consumption. Table XIII lists the performance of all the regenerator configurations tested. The first ship set modification consisted of removing the first rows of tubes. Although no additional tubes cracked, some of the ends of the tubes that were plugged broke off at the header. As a result, the performance data shown for the first set modified does include some leakage. The second ship set completed the 50-hr flightworthiness test, and the third set ran a final on the test stand prior to shipment to Allison Plant 10 for flight test.

A reduction in pressure drop and the associated improvement in overall engine efficiency result in the engine operating at a high speed for the design temperature. Since the exhaust-side pressure drop increases with an increase in speed, the total pressure drop will have to be compared at a constant flow factor ($W_a \sqrt{T}/t$) instead of a constant TOT. Based on the estimated flow factor (3.42), the total pressure drop for the various configurations is listed in Table XIV.

The discrepancy between rig and engine test data on the first set was due to nesting of the tubes during engine running. This is substantiated by the closer agreement obtained on the second set, which had a baffle at midspan to preclude the possibility of tube nesting. However, the second set of regenerators had a 0.7% discrepancy between rig and engine testing which could be due to turbine exit swirl angle associated with engine running. This is somewhat substantiated by the temperature and pressure profiles shown in Figures 35 through 37.

A complete set of engine data showing all performance parameters is shown in Figures 38 through 44. This data was obtained on the third set of regenerators and defines the performance of the final regenerator configuration. The engine met or exceeded all design requirements as shown in Table XV.

HEAT REJECTION

Heat rejection to the lubricating oil was significantly higher in the regenerative configuration than in the standard engine. At equivalent gas

PERF[illegible]MANCE COMP[illegible] MODIFICATIONS

AT [illegible]

TABLE XIV.
TOTAL PRESSURE DROPS FOR VARIOUS CONFIGURATIONS

	Engine Test		Rig Test at AiResearch
	Gas Side ΔP (%)	Total ΔP(%)	Total ΔP (%)
First Set	8.7	12.5	10.85
First Set Modified	7.3	11.1	—
Second Set	6.2	9.2	8.5
Third Set	5.7	8.7	—

TABLE XV.
REGENERATIVE ENGINE PERFORMANCE

Power Rating	TOT	Horsepower			SFC		
		Spec	Test	% Spec	Spec	Test	% Spec
Takeoff and Military	1380	280	300	+7.15	0.56	0.555	-0.9%
Normal	1280	239	256	+7.1	0.575	0.570	-0.86%
90% Normal	1222	215	231	+7.45	0.587	0.580	-1.2%
75% Normal	1140	179	190	+6.15	0.611	0.611	0.0%

producer speeds, the regenerative engine was as much as 200 BTU/min higher, as shown in Figure 45. The main reason for the higher heat rejection was the close proximity of the regenerators to the oil pump and filter assembly which is situated at the top right-hand side of the gearbox. It is not anticipated that the higher heat input to the gearbox will pose any problem. This has been substantiated by the successful completion of the 50-hr endurance test of the regenerative engine.

ENVIRONMENT TEMPERATURES

Although environment temperatures were measured during test stand running, the values would hold true only for that environment. When the aircraft is installed in the helicopter, the temperature around the engine will be affected by the compartment configuration and compartment cooling configuration. In general, it can be said that the addition of the regenerator will increase the air temperature along the top of the engine in the area around the regenerators by approximately 200°F. Compartment temperatures as measured in the YOH helicopter are discussed in the flight test portion of this report.

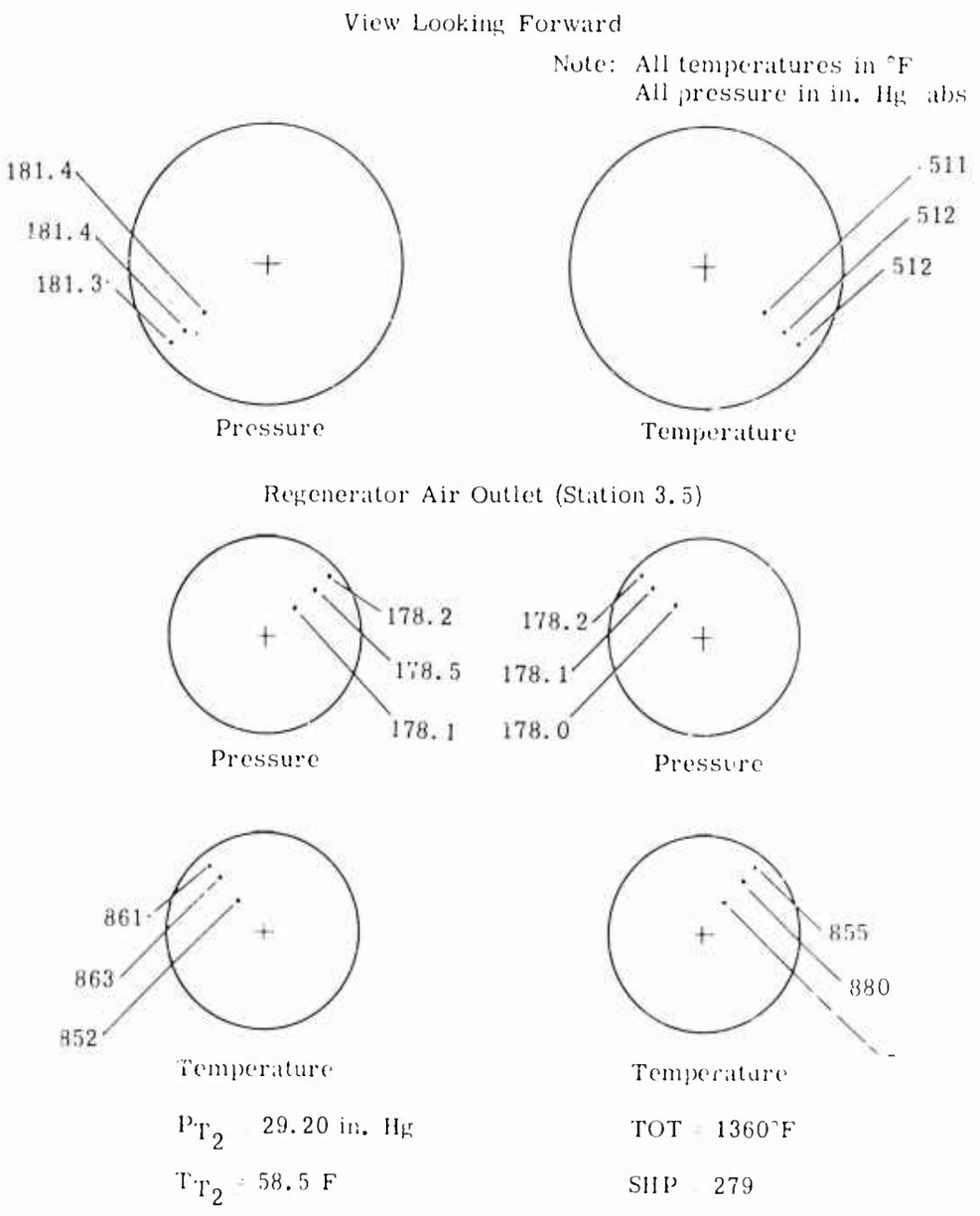

Figure 35. Temperature and Pressure Profile of Regenerator Air Inlet and Outlet.

Regenerator Gas Inlet (Station 7)

Top View

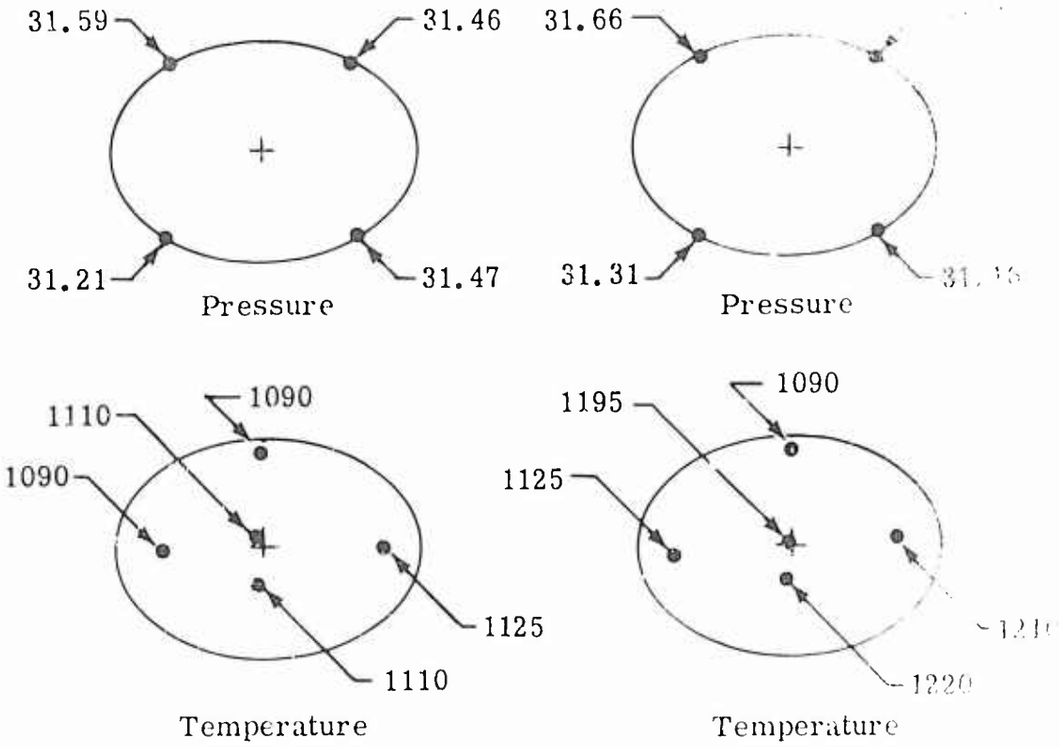

P_{T_2} = 29.20 in. Hg.	TOT = 1360°F	P_{T_3} = 181.4 in. Hg
T_{T_2} = 58.5°F	SHP = 279	$T_{T_{3.5}}$ = 863°F
RPR = 1.0	W_a = 3.049 lb/sec	$P_{T_{3.5}}$ = 178.2 in. Hg
N_1 = 50,993 rpm	W_f = 154 lb/hr	T_{T_8} = 758°F
N_2 = 35,094 rpm	T_{T_3} = 511.6°F	P_{S_8} = 29.23 in. Hg

Note: All temperatures in °F
All Pressures in in. Hg abs

Figure 36. Temperature and Pressure Profile of Regenerator Gas Inlet.

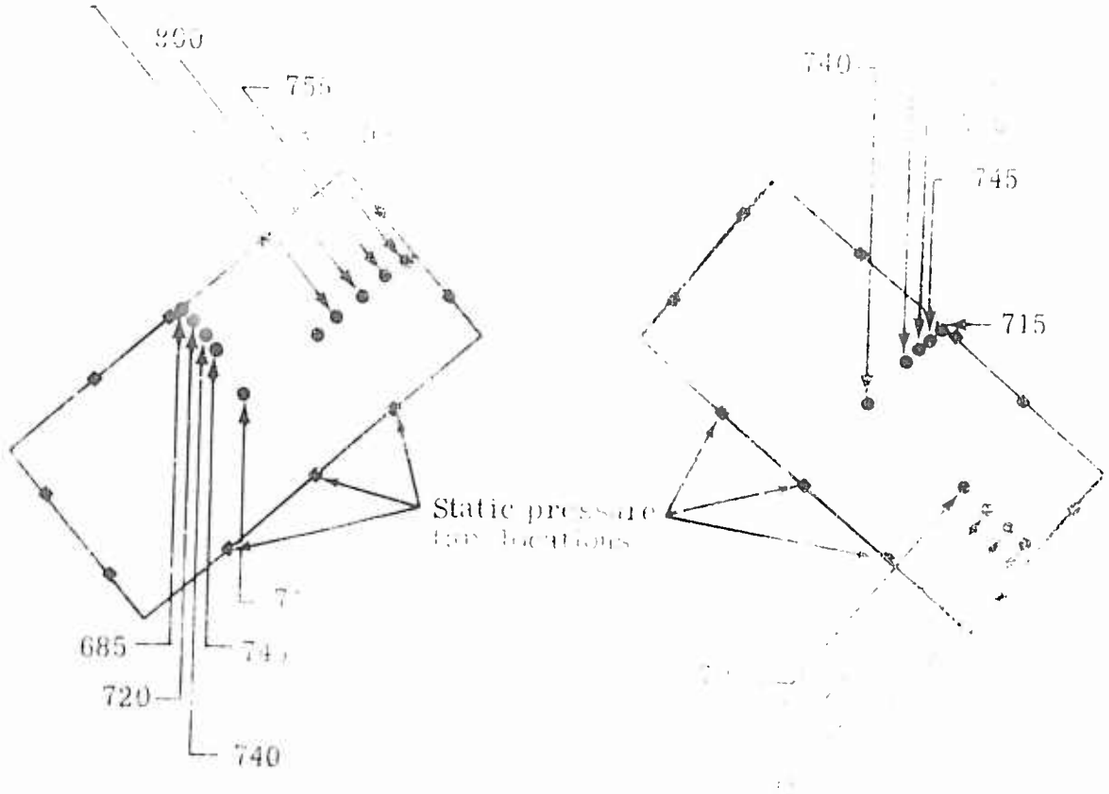

P_{T_2} = 29.20 in. Hg.			
T_{T_2} = 58.5 F	SHP = 279		= 863°F
RPR 1.0	W_a = 3.049 lb/sec	Avg	T_{T_7} 1137°F
N_1 = 50,993 rpm	W_f = 154 lb/hr		E_C 55.3%
N_2 35,094 rpm	Avg T_{T_8} 758°F		E_H = 61.5%

Note: All Temperatures in °F
All Pressures in in. Hg abs

Figure 37. Temperature and Pressure Profile of Regenerator Gas Outlet

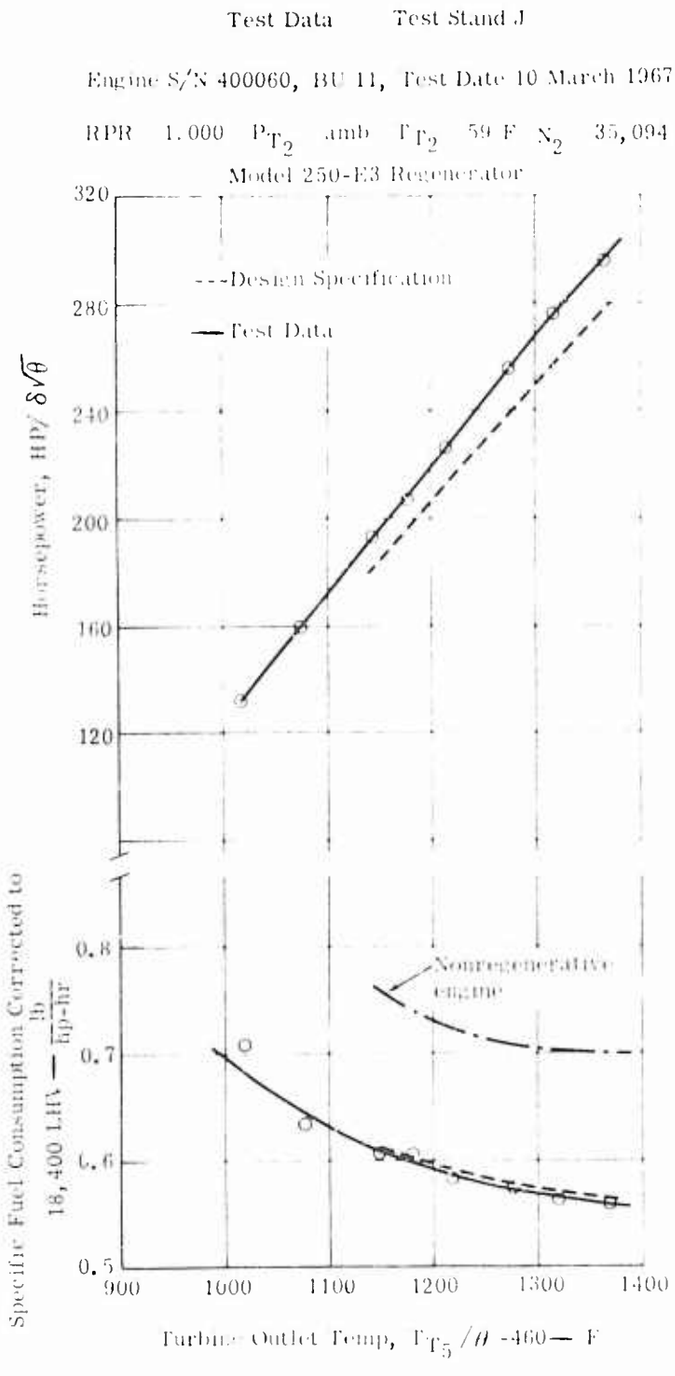

Figure 38. Regenerative Engine Performance at Sea Level, Standard Day Conditions.

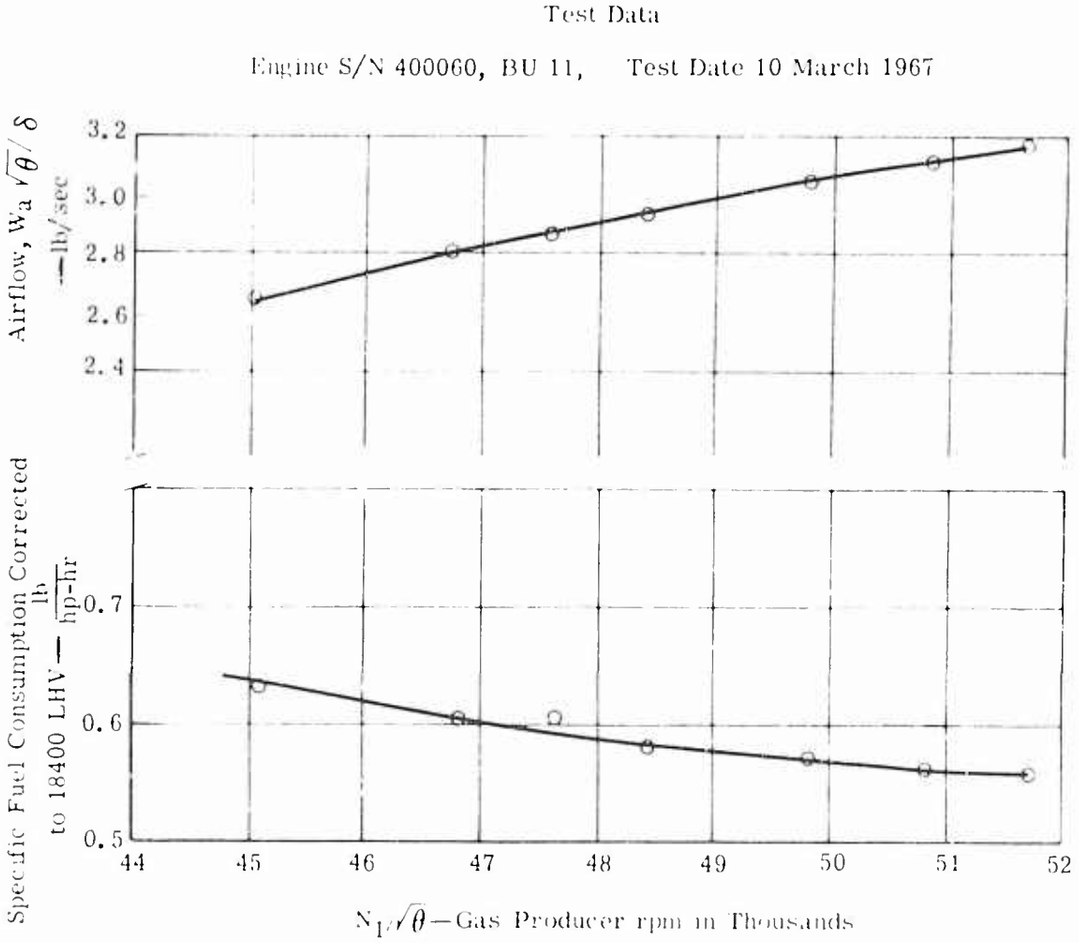

Figure 39. Regenerative Engine Performance at Sea Level, Standard Day Conditions.

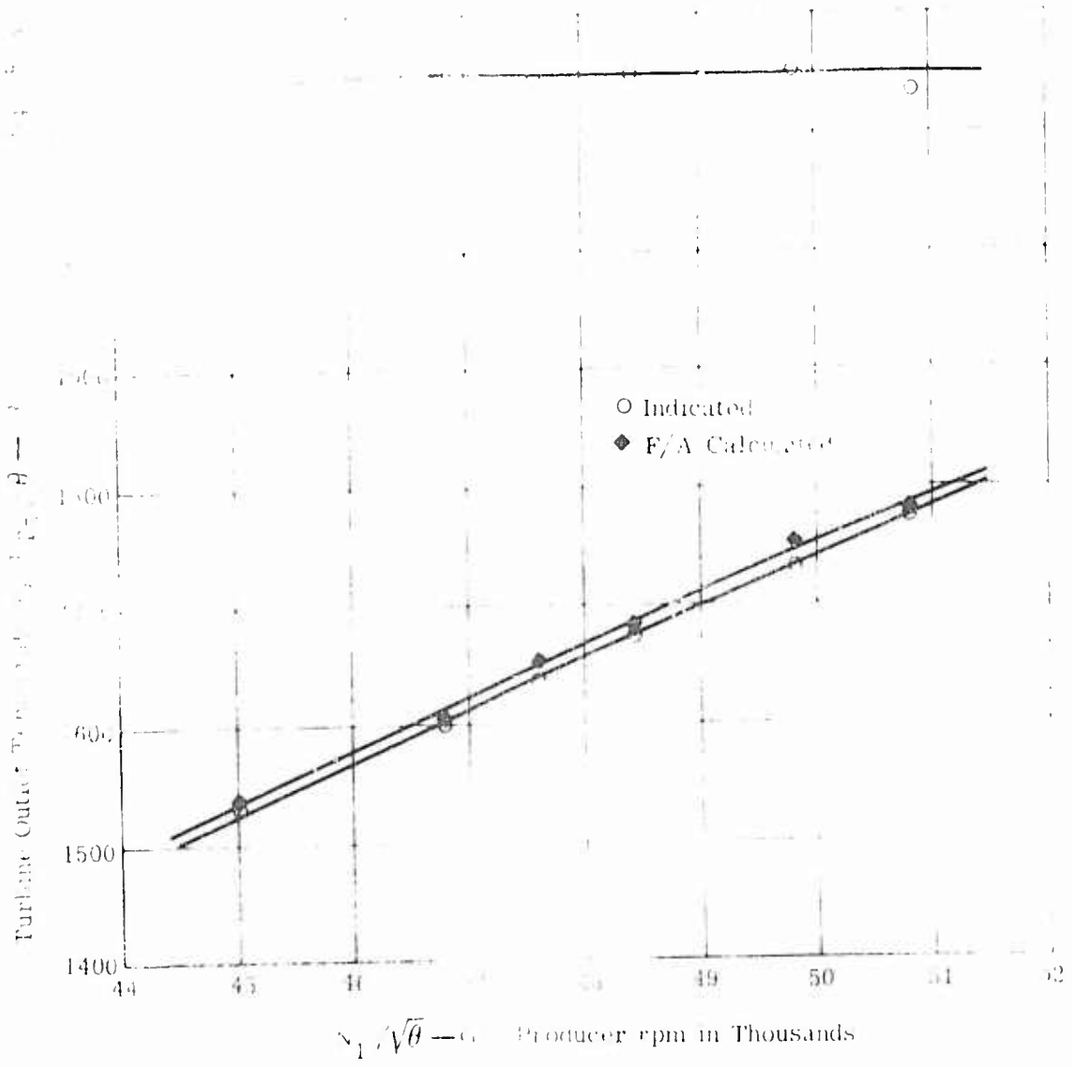

Figure 40. Regenerative Engine Performance at Sea Level, Standard Day Conditions.

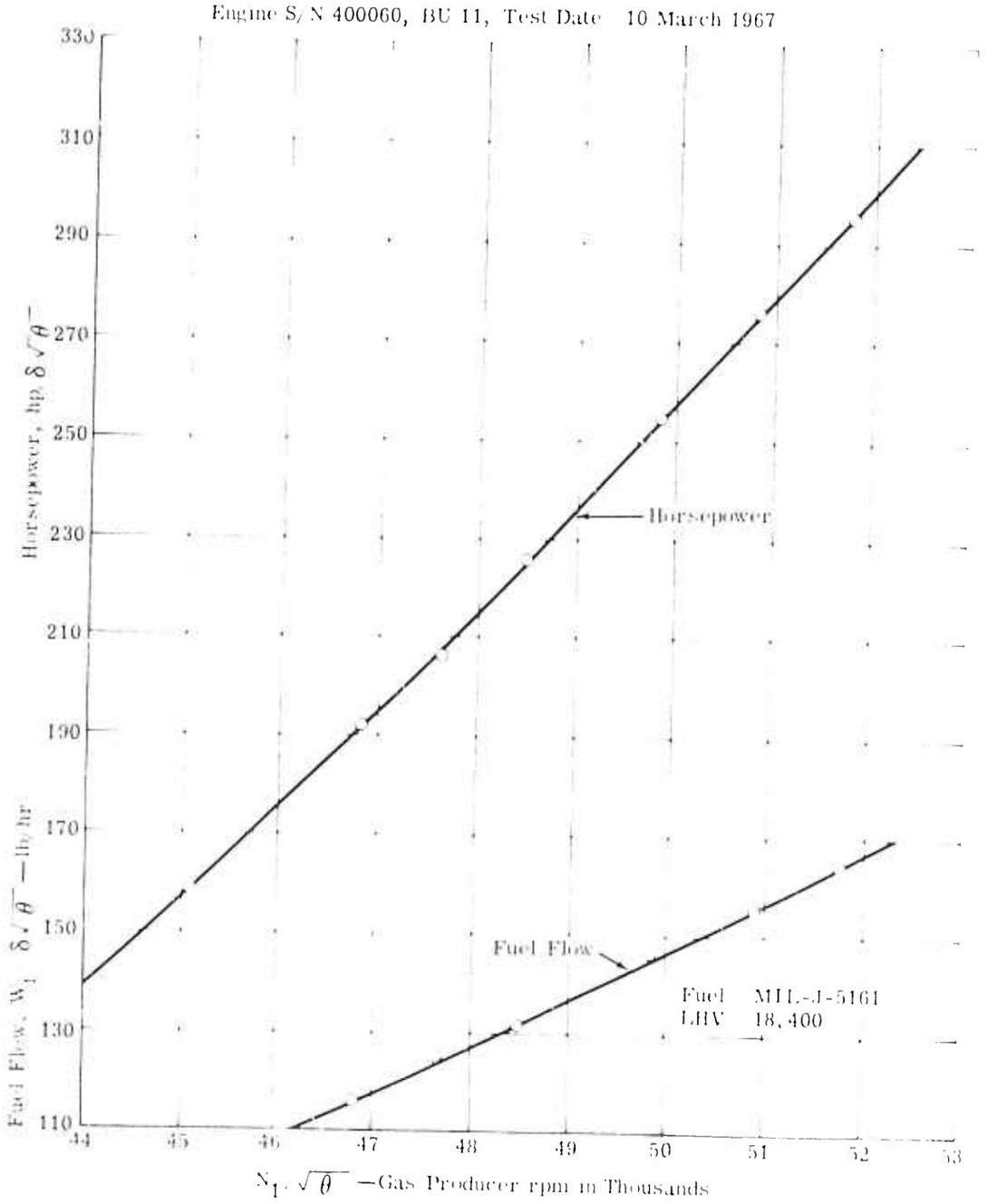

Figure 41. Regenerative Engine Performance at Sea Level, Standard Day Conditions.

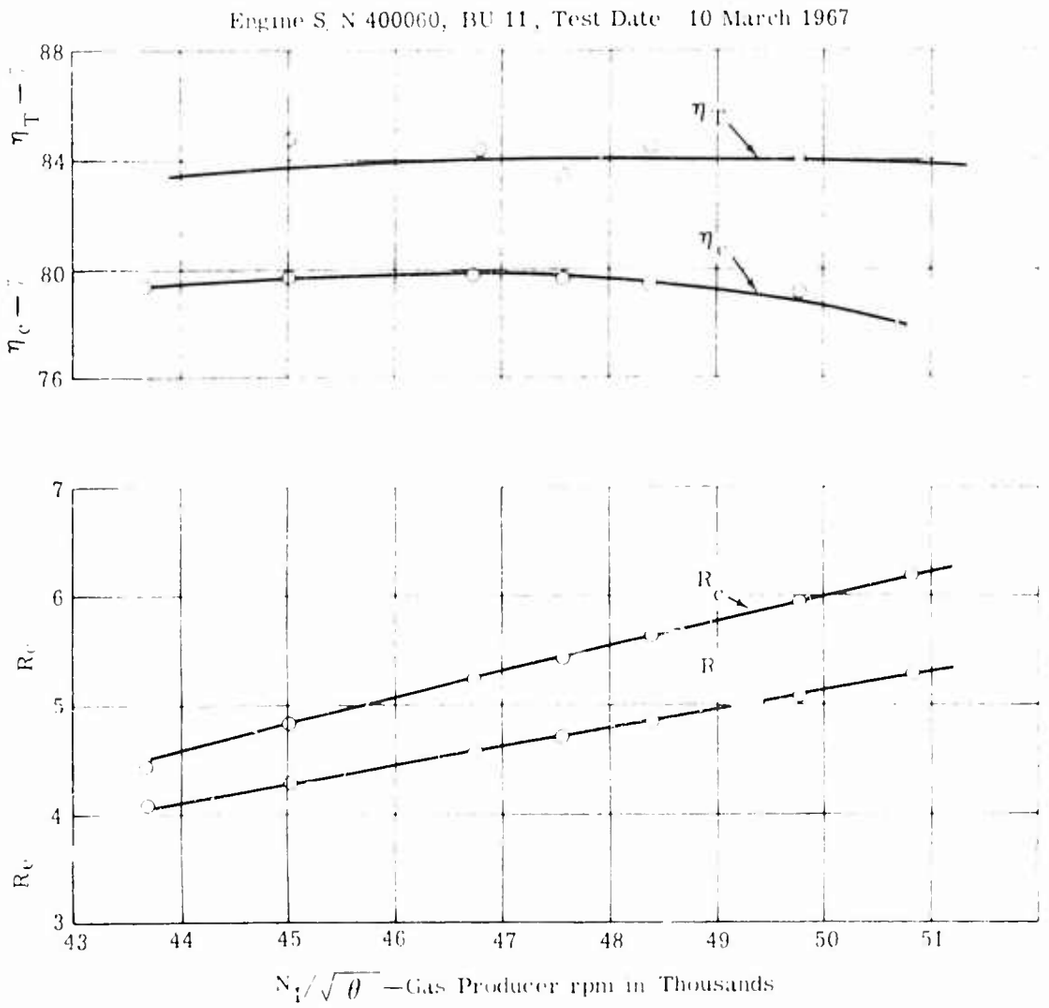

Figure 2. Regenerative Engine Performance at Sea Level, Standard Day Conditions.

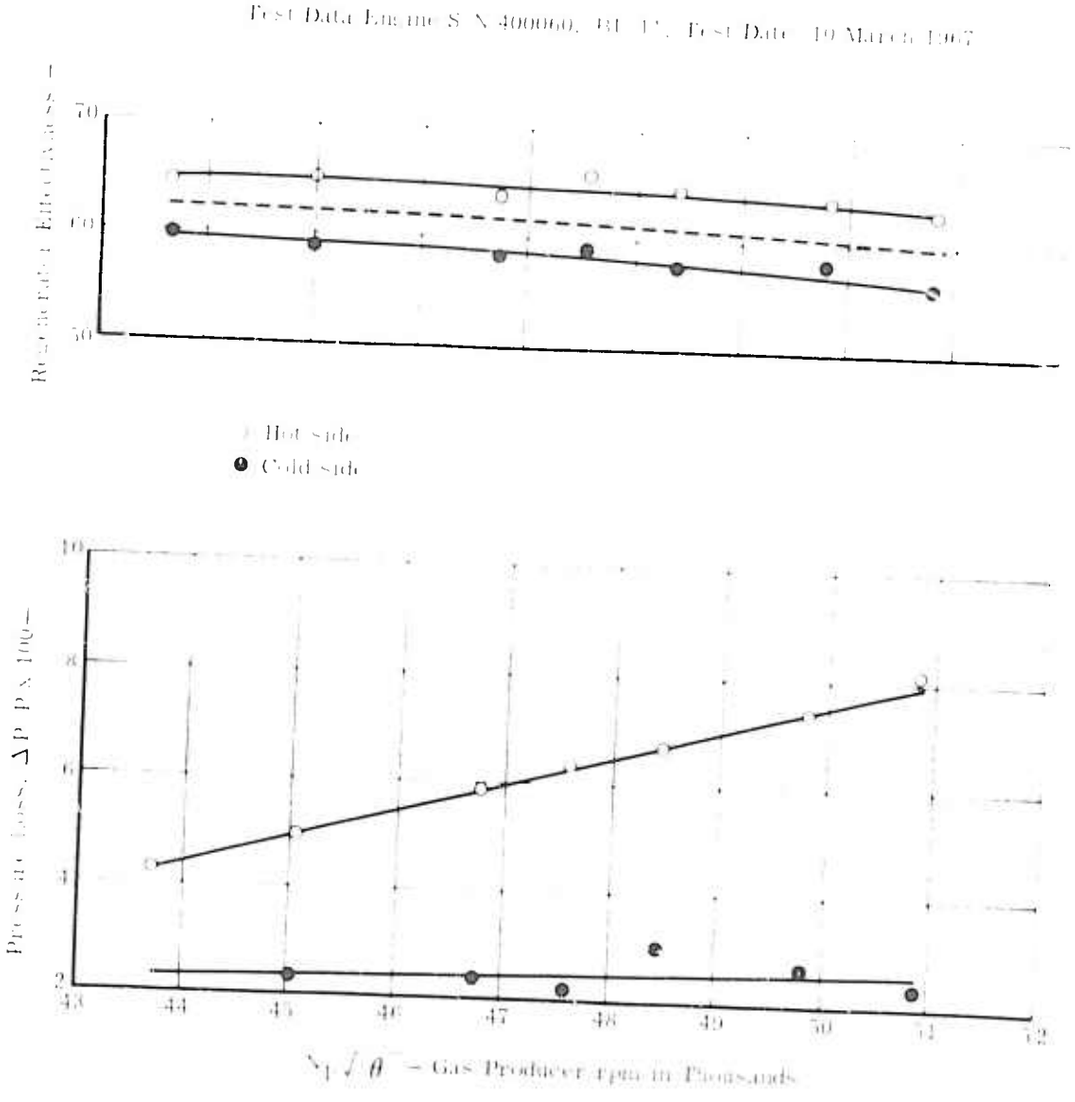

Figure 43. Regenerative Engine Performance at Sea Level, Standard Day Conditions.

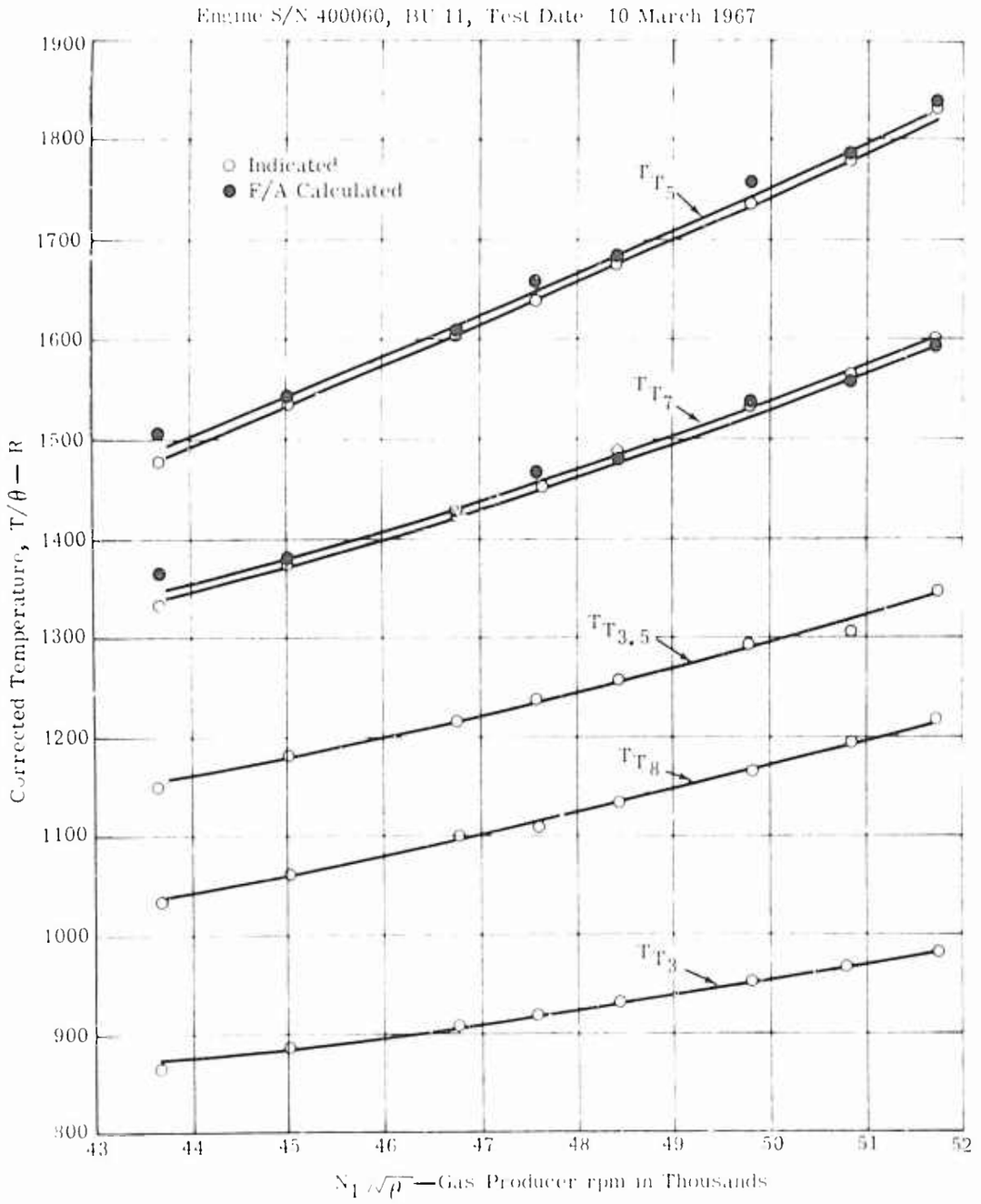

Figure 44. Regenerative Engine Performance at Sea Level, Standard Day Conditions.

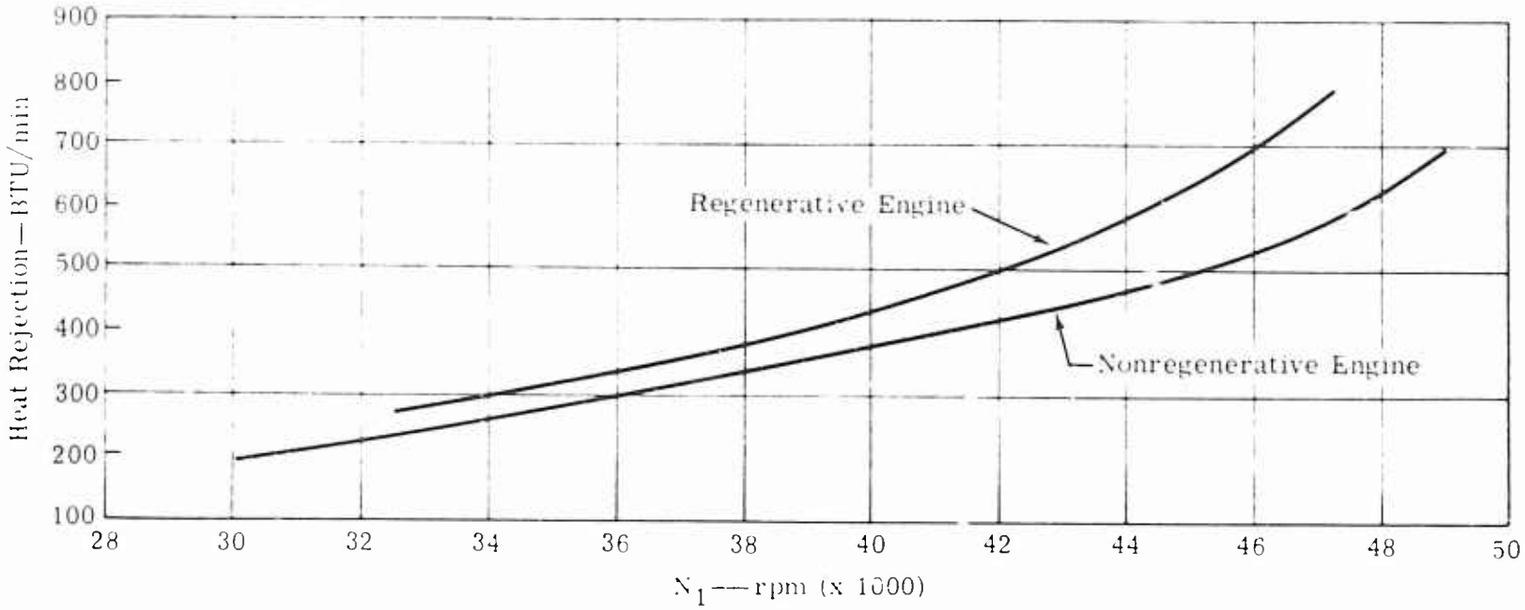

Figure 45. Regenerative Engine Heat Rejection.

TEMPERATURE PATTERN

The addition of a regenerator changes the inlet conditions to the combustion liner. Not only is the burner inlet temperature higher as a result of the heat input from the regenerator, but also the flow distribution may be changed. The basic liner used for this test had been developed on an earlier regenerative engine program.

The burner outlet temperature (BOT) pattern was not measured directly. Instead, gas producer turbine outlet temperature (TOT) was measured by means of eight individual thermocouples, and burner outlet temperature pattern was estimated by means of the following relationship which was obtained from previous engine testing:

$$\left(T_{max}/T_{avg}\right)_{BOT} = \left[\left(T_{max}/T_{avg}\right)_{TOT} + 0.01\right] \pm 0.03$$

The test results indicated a T_{max}/T_{avg} of 1.16 at 1380°F maximum TOT as compared to 1.13 for the nonregenerative engine. This would indicate a BOT pattern of 1.17 ± 0.03 for the regenerative engine compared to 1.14 ± 0.03 for the nonregenerative engine. While the 1.17 value is not as good as that obtained with the current T63-A-5 engine, it is considered satisfactory for a 50-hr endurance test and flight test.

In addition, thermal paint, which changes color as a function of temperature, was used on the combustion liner to ensure that there were no "hot" spots on the liner which would result in premature failure of the liner. Figures 46 and 47 show the first liner configuration tested. Isothermal lines have been drawn on the piece to outline the various temperature bands. The final liner configuration did not have the flange at the end but it was not felt that the flange would affect the temperature pattern. The necessity for the removal of the flange was previously discussed in this report.

EXHAUST BYPASS

At the same maximum allowable turbine outlet temperature, the regenerative engine has a lower horsepower as a result of the increased pressure drop associated with the regenerator. This is not to say that regenerative engines will always have a lower horsepower, for a regenerative engine would be designed for a specific application while meeting all the power requirements. In this program a regenerator was added to an existing engine, which results in a power reduction. One method of reducing the horsepower loss would be to bypass the regenerator when maximum horsepower is required.

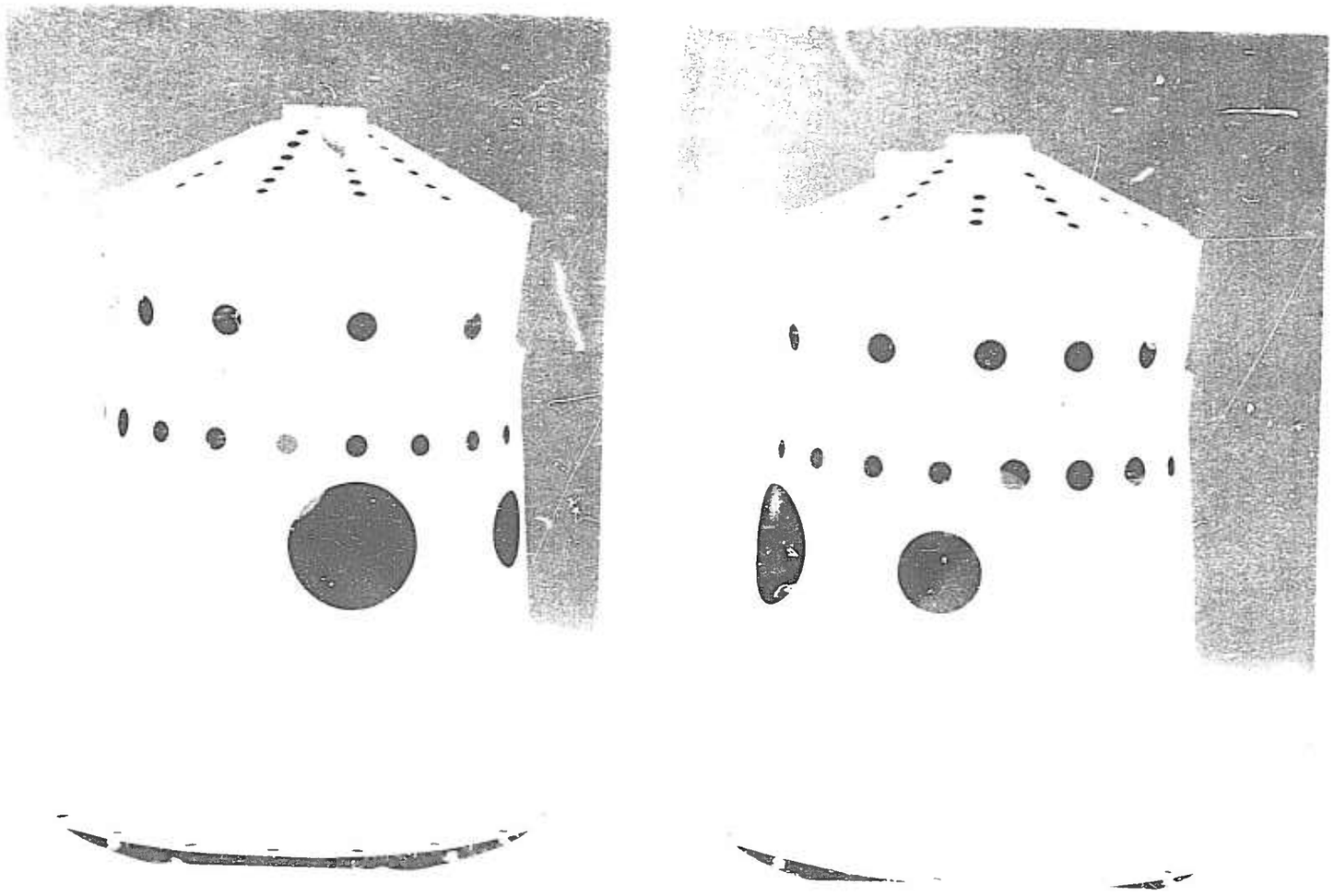

Figure 46. Combustion Liner Temperature Pattern.

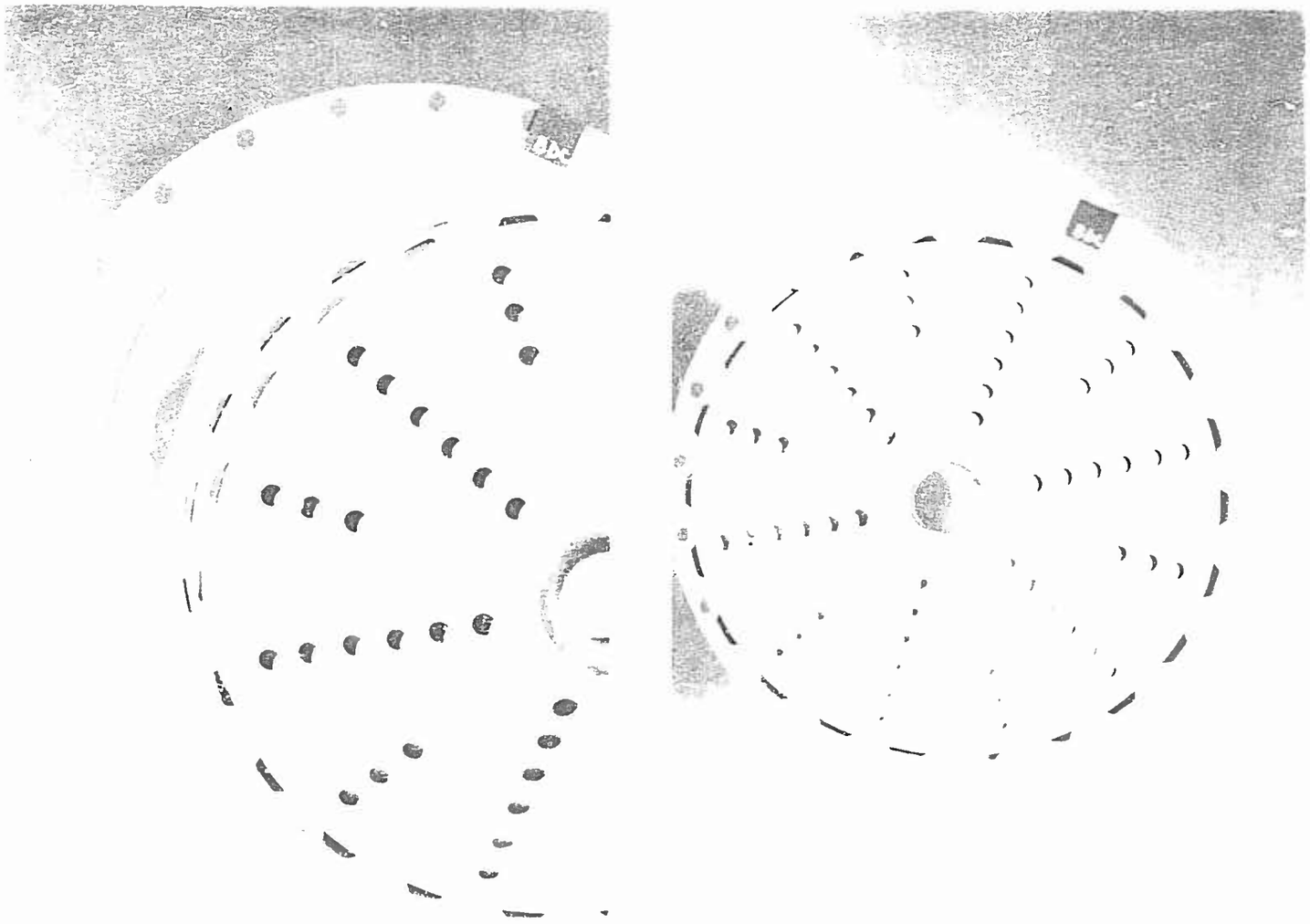

Figure 47. Combustion Liner Temperature Pattern.

The second ship set of regenerators was designed to allow bypass of the exhaust side of the regenerator. A removable cover was built into the top of the regenerator. (Reference print, Figure 116, at the back of this report). With the normal gas outlet blanked off and the cover removed, the exhaust gas exits out the top and bypasses the core. Bypassing the gas side should have resulted in a 3% to 4% reduction in pressure drop and a resulting increase in maximum horsepower.

The test data was very disappointing. Although the sfc was close to that obtained on a nonregenerative engine, the horsepower was no greater than that obtained without bypass. The pressure drop associated with the bypass was equal to the pressure drop of the gas side of the regenerator core resulting in no performance improvement. The test results indicate that further design and testing would be required to provide a satisfactory bypass configuration.

ENGINE WEIGHT AND SIZE

The design weight for the regenerative engine was 180 lb based on a regenerator weight of 44 lb. The final configuration regenerator weight was 50.5 lb, resulting in an engine weight of 184.5 lb. The weight breakdown of the engine is shown in Table XVI. Figure 48 shows the basic size of the engine package and the cg location.

TABLE XVI.
T63 REGENERATIVE ENGINE WEIGHT BREAKDOWN

	Design (lb)	Actual (lb)
Basic Engine Weight Minus Air Tubes	132.3	132.3
BIT Sensor	2.7	0.0
Cooling Air Manifold	1.0	2.0
Regenerator	44.0	50.2
Regenerator Instrumentation	0.3	0.3
Total Engine Weight (Instrumented)	180.3	184.8

ALTITUDE PERFORMANCE

A complete altitude calibration was completed during the first portion of the 50-hr test. Conditioned air from facilities was piped to the engine inlet, and the exhaust of the engine was piped to vacuum pumps in facilities. By varying the pressure and temperature of the inlet air and maintaining

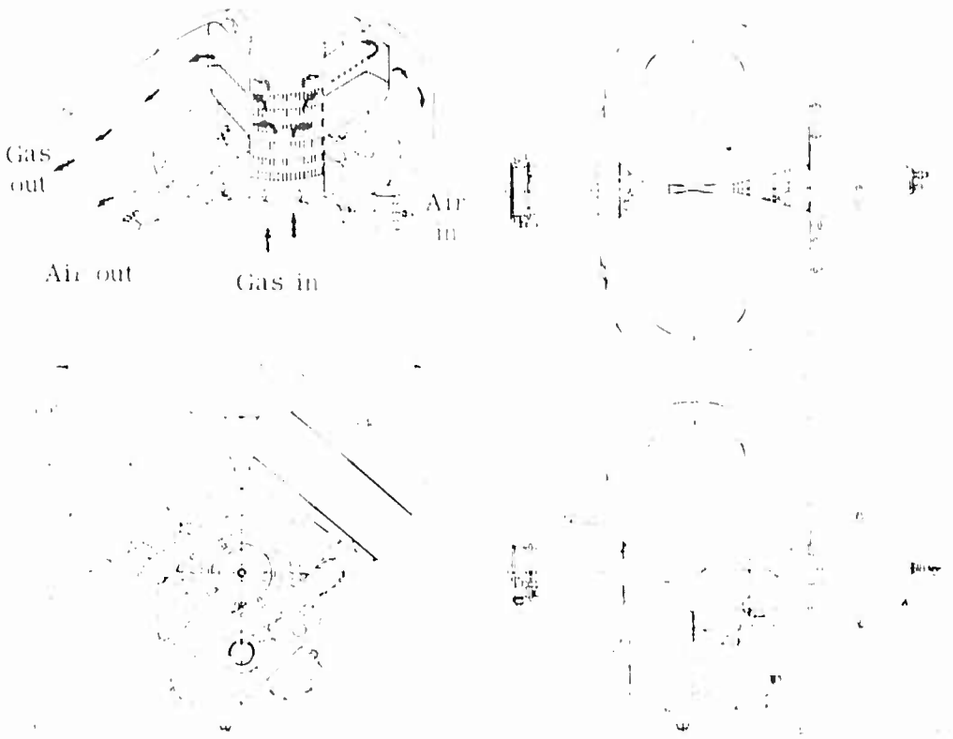

- Sized for 90 % normal power (2[illegible] hp, 0.587 sfc)
- Regenerator configuration tube-shell, single-pass folded cross-flow (air in tubes) (2 required)
- 60 % η_e, 9.86 % total ΔP, total regenerator weight = 50.2 lb
- Engine weight = 184.5 lb
- Engine cg 5.25 in. aft and 3.12 in. above side gearbox mounting

Figure 48. Regenerative T63 Engine Schematic.

unity ran across the engine, altitudes to 20,000 ft and inlet temperatures from +130° to -55°F were simulated. Complete engine performance parameters were recorded from idle to maximum power.

Engine performance was also calculated using the L-14 computer deck. The calculated data includes a "K" correction factor for the standard nonregenerative engine. This "K" factor was obtained empirically by means of an extensive altitude calibration of nine production engines.

A comparison of test and calculated data curves is included in the Appendix of this report. For convenience, all of the data is tabulated in Tables XVII and XVIII. Table XVIII compares the estimated and the test data at the conditions of 101 at 1350°F. The basic engine performance obtained during the test compared very closely with the calculated data. Horsepower was within a range from 2% to 6% above that estimated, and specific fuel consumption was from 1% below to 2% above that estimated.

At the design point (1220°F TOT), the test data indicated that at the lower temperatures the inlet temperature had a greater effect on sfc than has been shown on the nonregenerative engine. At 130°F inlet temperature, the sfc was 7.7% greater than that estimated. This performance degradation cannot be attributed solely to the regenerator, since the pressure drop was less than that estimated and should have improved sfc. Only a complete survey of several engines would determine the proper "K" correction required for the regenerative engine.

TABLE XVII.
PERFORMANCE COMPARISON AT DESIGN POINT 1222°F TOT

[illegible]	Engine Performance						Regenerator Performance					
	Horsepower			SFC			Effectiveness			ΔP Loss		
	Estimate	Test	% of Estimate	Estimate	Test	% of Estimate	Estimate	Test	% of Estimate	Estimate	Test	% of Estimate
[illegible]	[illegible]	[illegible]	+7.[illegible]	0.527	0.52	-1.3	54.7	5[illegible]	[illegible]	11.[illegible]	12.[illegible]	[illegible]
[illegible]	[illegible]	18[illegible]	+5.6	0.5[illegible]6	0.53[illegible]	-1.1	60.0	56[illegible]	[illegible].7	1[illegible]	[illegible]	[illegible]
[illegible]	21[illegible]	22[illegible]	+4.2	0.5[illegible]	0.58	-1.7	60.[illegible]	[illegible]	-1.7	[illegible]	[illegible].7	[illegible]
[illegible]	[illegible]	[illegible]	[illegible]	0.687	0.74	+7.7	62.[illegible]	[illegible]	[illegible]	[illegible]	[illegible]	-1[illegible].7
[illegible]	[illegible]	[illegible]	0	0.645	0.665	+[illegible].1	62.2	[illegible]	[illegible].7	[illegible]	7.8	[illegible]
[illegible]	[illegible]	[illegible]	[illegible]	[illegible]57	0.58	+1.7	62.[illegible]	62	[illegible]	[illegible]	11.4	[illegible]
[illegible]	[illegible]	[illegible]	+4.[illegible]	0.57	0.577	+1.2	[illegible]	64	[illegible]	[illegible]	1[illegible]	[illegible]
[illegible]	[illegible]	[illegible]	[illegible]	.7[illegible]	0.715	-2.[illegible]						

[illegible]

TABLE XVIII
PERFORMANCE COMPARISON AT MAXIMUM TOT OF [illegible]°F

Test Condition	[illegible]						Regenerator Performance					
	[illegible]			[illegible]			[illegible]			ΔP Loss		
	Estimate	Test	% of Estimate	Estimate	Test	% of Estimate	Estimate	Test	% of Estimate	Estimate	Test	% of Estimate
[illegible]	[illegible]	[illegible]	[illegible]	[illegible]	[illegible]	[illegible]	60	—	—	12.5	—	—
[illegible]	[illegible]	[illegible]	[illegible]	[illegible]	[illegible]	[illegible]	60.4	—	—	[illegible]	—	—
[illegible]	[illegible]	[illegible]	[illegible]	[illegible]	[illegible]	[illegible]	[illegible]	[illegible]	[illegible]	[illegible]	[illegible]	-2.
[illegible]	[illegible]	[illegible]	[illegible]	[illegible]	[illegible]	[illegible]	[illegible]	[illegible]	[illegible]	[illegible]	[illegible]	[illegible]
[illegible]	[illegible]	[illegible]	[illegible]	[illegible]	[illegible]	[illegible]	[illegible]	[illegible]	[illegible]	[illegible]	[illegible]	-15.
[illegible]	[illegible]	[illegible]	[illegible]	[illegible]	[illegible]	[illegible]	[illegible]	[illegible]	[illegible]	[illegible]	[illegible]	[illegible]
[illegible]	[illegible]	[illegible]	[illegible]	[illegible]	[illegible]	[illegible]	[illegible]	[illegible]	[illegible]	[illegible]	[illegible]	[illegible]
[illegible]	[illegible]	[illegible]	[illegible]	[illegible]	[illegible]	[illegible]	[illegible]	[illegible]	[illegible]	[illegible]	[illegible]	[illegible]

[illegible]

50-HOUR FLIGHTWORTHINESS TEST

A 50-hr endurance test was run on the 250-E3 regenerative engine to determine its flightworthiness prior to installation in a modified YOH-6A helicopter for flight testing at Allison Plant 10. The test was conducted in accordance with MIL-E-8597, dated 8 February 1949, with the exception that during the first 25 hr, the steady-state running was replaced by a series of altitude calibrations. The altitude performance data is discussed in the latter part of the preceding section of this report entitled Regenerative Engine Performance. The basic test schedule consisted of eight 6-hr cycles plus 2 hr at ram conditions. This 6-hr cycle consisted of the following increments.

1. Normal Rated Power

   Two hr at 1280°F

2. Takeoff Power

   Forty min of alternate 5-min periods at 1380°F and flight idle

3. Power Transients

   Thirty min of power transients consisting of six cycles from flight idle to takeoff power (1380°F)
   - 4-1/2 min at flight idle
   - 30 sec at 1380°F

4. 90% Normal Rated Power

   Forty min at 1222°F

5. Military Rated Power

   Thirty min at 1380°F

6. 75% Normal Rated Power

   Thirty min at 1140°F

7. Incremental Power

Ten min each at 20, 30, 40, 50, 60, 70, and 80% power

The Model 250-E3 regenerative engine satisfactorily completed the 50-hr flightworthiness test in excellent condition. Performance of the regenerative engine at sea level conditions exceeded the estimated performance throughout the power range. At 1380°F TOT, the horsepower was 105 and sfc was 99.1% of specification limits.

Engine performance depreciation at 75% normal rating was 2.1% in horsepower and 1.4% in sfc. At takeoff conditions, a loss of 0.5% in horsepower with little or no change in sfc was noted. This depreciation was within the allowable limit of 7.5% depreciation.

The regenerators were pressure checked prior to and upon completion of the test. No leakage was noted, thus indicating that the regenerators were intact and not cracked. Visual inspection of the regenerators showed a light soot buildup on the air tubes.

The only problem occurring during the test was an intermittent control instability. The cause could not be determined during the test. Bench test after completion of the test also did not reveal any deficiencies. The problem was not considered serious.

The teardown inspection did not reveal any serious discrepancies and all parts were in excellent condition. The only parts changes made to the engine prior to flight test were as follows:

1. The instrumented exhaust collector was replaced.

2. The first-stage turbine wheel was replaced as a precautionary measure because the cooling air temperature of the regenerative engine was 90°F hotter than the standard engine.

3. The first and fourth stage compressor blades were replaced with production blades from engine 400067.

A complete record follows of the 50-hr test which lists all the stops made during the test. The test was started on 27 January 1967 and completed on 15 February 1967.

Stop No.	Date (1967)	Engine Time Endurance (hr)	Engine Time Total (hr)	Remarks
	27 January		53:54	Drained and flushed stand oil system. Filled tank with Mil-L-23699 oil—vendor W. R. Grace, Hatco Div (Lot No. 11). Oil samples taken graded B & E. Mil-J-5161F fuel used had a LHV of 18,604 BTU/lb. Installation and checkout of F63-A-3A engine completed.
103	30 January	0:00	54:00	Normal start at 1070°F TOT using maximum starter voltage of 24. Indicator light noted for magnetic drain plug in scavenge oil line—continued run. Lost fire—control appears to have little or no idle band. Set stop on gas producer Sperry lever to mark 30,000 rpm N_1 speed—appears to be bottom of idle band. Removed magnetic plug; found small hair-like particles—cleaned and reinstalled. Engine was dry.
104		0:00	54:45	Normal start at 950°F TOT using maximum starter voltage. N_1 speed = 32,377 rpm at ground idle; main oil pressure = 120 psig; oil flow = 13.99 lb/min. Checked bleed operation; bleed valve opened and closed at 43,708 rpm N_1 speed. Note high AGB case pressure—set new limit of 15 in. H_2O. Maximum obtainable TOT = 1330°F; AGB* case pressure = 13 in. H_2O. Shutdown No. 104. Inspected breather vent hose—condition good—

*Accessory gearbox

Stop No.	Date (1967)	Engine Time Endurance (hr)	Engine Time Total (hr)	Remarks
				replaced with 18-in. long No. 12 hose. Determined control was set up to sense P_c pressure at outer combustor case and not at scroll.
105		0:00	55:00	Normal start at 1050°F TOT. Slow acceleration to maximum TOT 1350°F. Shut down to adjust maximum fuel stop on control. Increased stop one full turn counterclockwise. Removed short breather hose and hooked up per standard practice.
106		0:00	55:46	Completed preliminary engine checkout; engine operation satisfactory, condition good. Slight turbine scrape noted on coastdown. Reset oil temperature from 160° to 200°F.
107		0:00	57:37	Scheduled shutdown. Completed baseline performance calibration on nonregenerative configuration. Slight turbine scrape noted on coastdown. Removed magnetic drain plug from oil-out line and found few powder-like particles. Noted slight oil leak at fuel pump pad. Drained 90 ml of oil from breather vent bottle after 2 hr 52 min of operation. Removed engine from stand for conversion to 250-E3 configuration.
	3 February			
108		0:00	58:04	Engine converted to regenerative configuration. Oil system flushed; new oil added; samples graded B

Stop No.	Date (1967)	Engine Time Endurance (hr)	Engine Time Total (hr)	Remarks
				& B. Motored engine; filled oil tank to 16-in. level. Max TOT at fireup = 1015°F. Shut down to inspect engine; condition good; operation normal except for low oil inlet pressure.
109		0:00	58:21	Normal fireup at TOT 945°F. Noted oil leak at supply tank filler cap. Shut down to tighten cap; smooth coastdown; engine operation normal and condition good.
110		0:00	62:25	Scheduled shutdown. Completed preliminary checkout of engine, transients and pre-endurance calibration. Engine performance satisfactory; operation normal and condition good.
	6 February			
111		0:00	63:18	Normal fireup. Dynamics equipment set up to record steady-state and transient data. Shut down due to AGB magnetic light indication at bottom drain plug. Inspected plug; noted fuzz, cleaned and reinstalled.
112		0:00	65:06	Scheduled shutdown. Completed steady-state and transient running. Engine operation normal; condition good. Dynamics personnel setting up to record start data.
113		0:00	65:11	Scheduled shutdown. Completing start requirements for Dynamics data recording.

Stop No.	Date (1967)	Engine Time Endurance (hr)	Engine Time Total (hr)	Remarks
114		0:00	65:13	Scheduled shutdown. Completed start requirements for Dynamic data recording. Engine operation normal, condition good. Setting up for regenerator bypass performance calibration. Two cap screws broke off when removing bypass cover. Installation complete.
115		1:22	66:45	On endurance. Completed calibration with regenerators bypassed. Engine very slow to accelerate: 1.158 min to ground idle. Magnetic drain plug light indication in scavenge oil line. Continued run. Shut down to inspect engine and regenerators—condition good. Converting stand and engine for regenerative operation. Broken cap screws on right-hand regenerator not removed. Installed re-enforcement plates. Repaired and checked instrumentation. Set up to run at -35°F inlet. Drained 160 ml of oil from AGB vent bottle.
116		5:27	70:55	Scheduled shutdown. Unable to obtain -35°F inlet. Completed -12°F inlet calibration. Experienced momentary control instability. Smooth coastdown; engine condition good.
	8 February			
117		7:20	72:06	Scheduled shutdown. Completed 130°F inlet calibration at sea level.

Stop No.	Date (1967)	Engine Time Endurance (hr)	Engine Time Total (hr)	Remarks
				No abnormalities noted during run. Converting stand and engine for 6000-ft calibration at +95°F inlet.
118		9:43	75:22	Completed 6000-ft calibration. While operating at a stabilized TOT of 1285°F, experienced governor instability. A step increase in N_1, N_2, hp, and TOT was noted. Smooth coastdown; engine dry. Serviced GP* and PT** Sperry actuators. Setting up to run sea level calibration at -35°F inlet.
	9 February			
119		10:05	75:52	Normal fireup at maximum TOT of 960°F. Conducted 30 min run while facilities cooled down to prevent icing. Engine condition good; operation normal.
120		11:39	77:31	Scheduled shutdown. Completed sea level calibration at -35°F inlet. Magnetic drain plug indication at scavenge oil line; continued run. Bleed valve inoperative due to freezing. Setting up to conduct 20,000-ft calibration. Checked instrumentation and repaired as required.
121		11:46	77:44	Shutdown due to loss of vibration indication at compressor. Inspected pickup; checked OK. engine dry.

*Gas producer
**Power turbine

Stop No.	Date (1967)	Engine Time Endurance (hr)	Engine Time Total (hr)	Remarks
122		13:51	79:57	Normal fireup. Compressor vibration pickup operation normal. Magnetic drain plug indication at scavenge oil line; continued run. Completed 20,000-ft calibration. Found fuzz on mag plug; cleaned and reinstalled. Set up to conduct 10,000-ft calibration.
123		15:06	81:14	Scheduled shutdown. Completed 10,000-ft calibration. No abnormalities noted during run except magnetic drain plug indication at scavenge oil line; cleaned off fuzz and reinstalled. Engine condition good. Set up to conduct post altitude calibration.
	10 February			
124		16:00	82:16	Shutdown due to facilities being unable to stabilize at desired inlet conditions. Engine operation normal; condition good.
125		18:22	84:41	Scheduled shutdown. Completed postaltitude calibration. Mag plug light for scavenge oil line; determined plug defective, replaced same. Engine condition good. Engine and stand changes made as required for endurance schedule.
126		19:40	86:01	Scheduled shutdown. Completed first cycle of takeoff and power transients operation. Engine condition good. Governor instability experienced during steady-state operation. Actual [illegible]

Stop No.	Date (1967)	Engine Time Endurance (hr)	Engine Time Total (hr)	Remarks
				valve as required by running schedule. Maximum TOT during anti-ice operation—1410°F.
127		20:50	87:11	Normal fireup. Completed second cycle. No abnormaalties noted during run. Inspected engine and regenerators; condition good.
128		23:12	89:36	Scheduled shutdown. Completed third and fourth cycles. Actuated anti-ice valve as required. Experienced instability; engine suddenly accelerated; requires trimming. Engine dry. Drained 150 ml of oil from AGB breather vent bottle.
	13 February			
129		24:27	90:50	Shutdown No. 129. Completed ram power run. Operation unsteady on governor during run; N_1 increased 756 rpm. TOT increased 50°F, and TMOP* went up 13 psi. Instability continued throughout run. Heavy smoke from breather vent bottle. Drained 50 ml of oil from bottle. AGB case pressure was 11.5 in. H_2O. Checked all lines, jets, etc., in control and governor; appeared O.K.
130		29:50	96:40	Scheduled shutdown. Experienced instability; continued run. Noted air bubbles in sight glass of oil

*Torquemeter oil pressure

Stop No.	Date (1967)	Engine Time Endurance (hr)	Engine Time Total (hr)	Remarks
				tank approximately every 15 or 20 min. Engine oil pressure normal. Smooth shutdown; engine and regenerator condition good. Added [illegible] oil to tank; drained 220 [illegible] from breather vent bottle. Removed DCV* and replaced with "dimmer" valve in an attempt to improve stability.
	14 February			
131		5:10	106:06	Scheduled shutdown. Completed second 5-hr cycle. Smooth shutdown, no abnormalities noted during run. Removed "dimmy" double check valve and installed new DCV*.
132		11:10	111:16	Scheduled shutdown. Completed third 5-hr cycle. Erratic hunting at high power. Experienced severe instability [illegible] oil [illegible]. [illegible] oil to breather [illegible].
[illegible]		[illegible]	111:51	Normal [illegible]. Experienced governor instability [illegible] shutdown. Removed DCV* [illegible] "dimmer" DCV.
134		[illegible]	117:[illegible]	Scheduled shutdown. Magnetic [illegible] scored; oil line came [illegible] after 20 hr of operation [illegible] run. Noted large [illegible] hr [illegible].

*Double check valve

Stop No.	Date (1967)	Engine Time Endurance (hr)	Engine Time Total (hr)	Remarks
				Experienced instability after approximately 3 hr of operation. Completed endurance requirements. Removed mag plug; noted black fuzz; cleaned and reinstalled. Drained 220 ml of oil from breather vent bottle. Set up for postendurance performance calibration.
135		50:33	121:13	Scheduled shutdown. Completed postendurance calibration. Control instability required completing run on gas producer governing. Smooth coastdown; engine and regenerators condition good. Added 1740 ml of oil to supply tank. Fuel and oil samples taken for analysis. Oil consumption rate 0.017 gal/hr.

FLIGHT TEST

YOH-6A MODIFICATION, INSTRUMENTATION, AND CHECKOUT

The original contract specified that the flight test be conducted in a Bell UH-13 helicopter. However, a better flight evaluation could be made in the YOH-6A helicopter since the compartment temperature would be more realistic and comparable test data without a regenerator would be available. The contract was amended to include the modification of a YOH-6A to permit the installation of a regenerative engine. A YOH-6A (Aircraft S/N 62-4214) was flown from Fort Knox, Kentucky, to the Allison flight test hangar (Plant 10) for modification. The modification consists of placing a "dog-leg" in the horizontal rib above the clamshell doors and modifying the clamshell doors and sheet metal to provide a "bubble" on either side of the aircraft to accommodate the increased engine width in the vicinity of the regenerators.

Since the horizontal rib is a main load-carrying member, a comprehensive stress analysis was made of the modified area. For the stress analysis of the horizontal rib, the maximum loading conditions were obtained from Hughes. These loads are shown in Figure 49.

Based on the loads, a stress analysis was made of the new rib. The basic design philosophy was aimed at providing a rib that had the same stress level and stiffness. It is necessary to have the same stiffness to ensure that the distribution of the loads throughout the aft section of the aircraft is not changed appreciably. The basic geometry of the new rib is a U-channel with riveted return angles as required to provide the proper stiffness.

In the area to be modified, the loads are compressive in the forward direction with a reaction shear flow along the skin. The critical stress in the rib will be a buckling stress in the legs of the channel as a result of the moment induced by the "dog-leg" in the rib.

Initially the rib was to be made from the same material as the original rib (AMS-4911 titanium alloy). Hammer-forming the titanium was found to be very difficult. As a result of the forming problems, the rib was made from Inco 718 material (AMS-5596).

During modification of the YOH-6A, it was necessary to support the tail boom after the horizontal rib had been removed. Prior to modification, the helicopter was leveled and alignment stations on the aircraft were located with a transit. The tail boom was then removed and the ship was supported as shown in Figure 50. Figures 51 and 52 show the modification at various stages of completion.

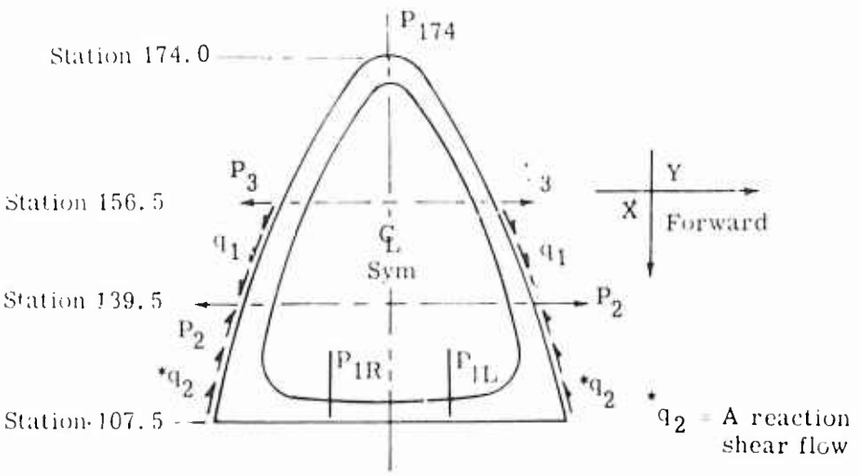

Three independent maximum loading conditions

GH = Ground Handling Load
4b = Symmetrical Flight Load
5a = Unsymmetrical Flight Load

All loads ultimate

Condition	P_{174} (lb)	P_{1L} (lb)	P_{1R} (lb)	P_2 (lb)	P_3 (lb)	q_1 (lb/in.)
GH	2880	—	—	—	—	25.5
4b	548	848	848	272	74	7.2
5a	450	434	624	224	60	6.0

The stiffness of the rib is as important as the strength. The magnitude of the load acting on the rib and both the lateral and vertical natural frequencies are dependent on the rib stiffness.

Figure 49. YOH-6A Maximum Loading Conditions for Stress Analysis.

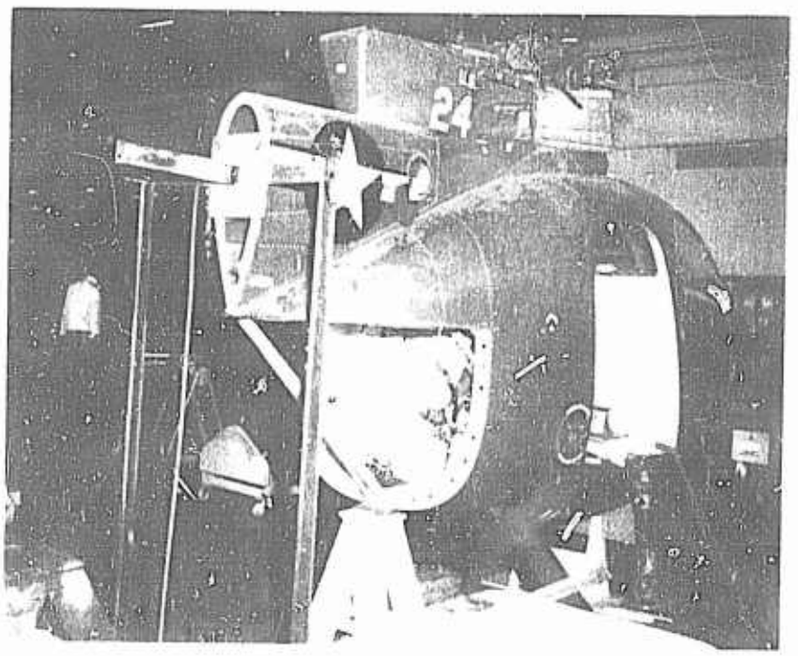

Figure 50. Tail Boom Support During Modifications of YOH-6A.

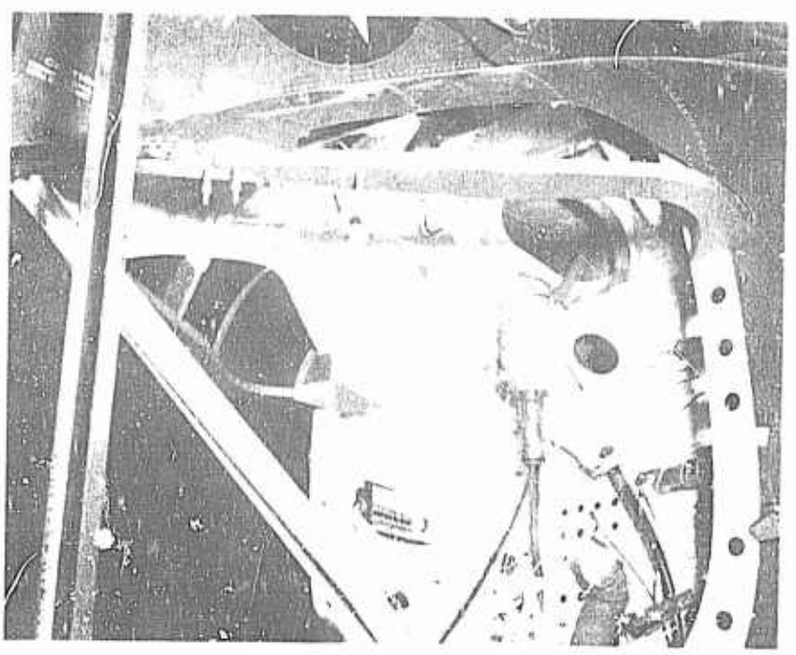

Figure 51. YOH-6A Modification in Process.

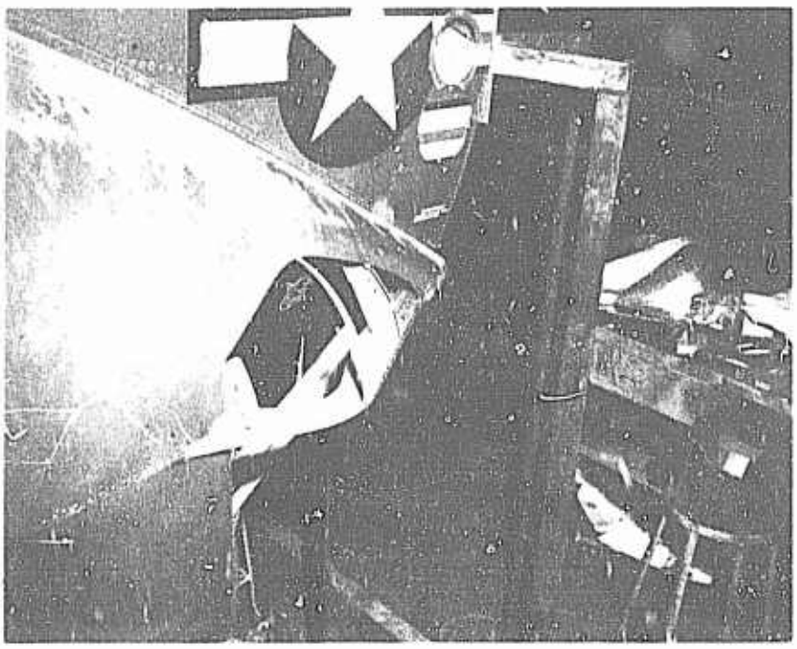

Figure 52. YOH-6A Modification in Process.

No unforeseen problems were encountered during the modification. On completion of the modification, the tail boom was reinstalled and the alignment point on the end of the horizontal stabilizer was only 0.150 in. from its original position, which is well within leveling accuracy.

The exhaust extensions for the regenerative engine incorporate a transition from a rectangular to a circular cross-section 8 in. in diameter. The 8-in.-diameter pipe extends straight back through the clamshell doors. This configuration will minimize the pressure drop in the exhaust extension. From the "tail-on" position, the exhaust area will be 100 in.^{2} The centerline distance between the two 8-in.-diameter pipes will be 17 in.

The drawings that outline the proposed modifications are as follows:

- EX-88200 Modifications—Rib Installation
  OH-6A Helicopter
  250-E3 Engine Installation

- EX-88201 Modification--Access Door
  OH-6A Helicopter
  250-E3 Engine Installation

- EX-88202 Tail Pipe Assembly
  OH-6A Helicopter
  250-E3 Engine Installation

- EX-88203 Loft Lines
  OH-6A Helicopter Fuselage
  Modification for 250-E3 Engine Installation

The completed installation is shown in Figures 53 through 56. A weight and balance check obtained after completion of the fabrication is as follows:

	Weight (lb)
Empty weight without modification	1057
Instrumentation	372
Regenerators	50
Modification in aircraft	26
Pilot and copilot	330
Maximum fuel load	421
Total weight	2256

A weight of 2200 lb will be used as a nominal gross weight for the test program. The minimum gross weight will be 1900 lb and the maximum gross weight will be 2400 lb. The aircraft as flown is within the center of gravity limits outlined in the YOH-6A operational manual. The manual defines the center of gravity limits as 97 in. to 104 in. with a baseline 30 in. in front of the helicopter.

The instrumentation installed in the aircraft consisted of a photo panel and a 26-channel CEC oscillograph with associated matching networks and wiring. The following parameters were recorded during the flight test:

- Camera counter No.
- Oscillograph counter No.
- Altimeter
- Airspeed
- Outside air temperature

Figure 53. Completed Installation of Regenerative T63 in the YOH-6.

Figure 54. Completed Installation of Regenerative T63 in the YOH-6A.

Figure 55. Completed Installation of Regenerative T63 in the YOH-6A.

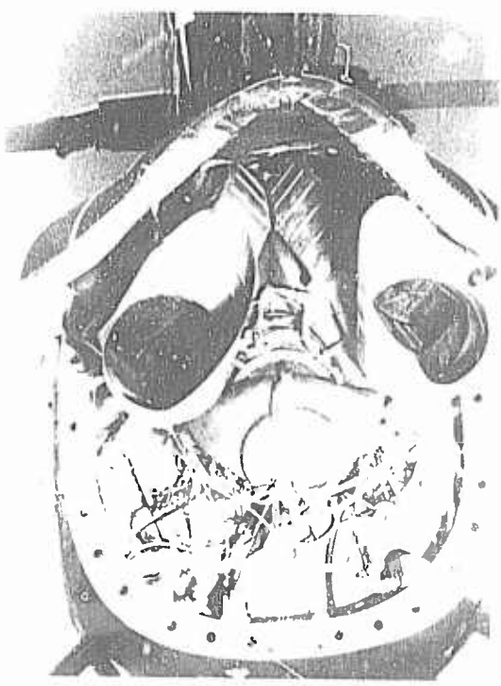

Figure 56. Completed Installation of Regenerative T63 in the YOH-6A.

- Fuel inlet temperature
- Power turbine governor position
- Gas producer lever position
- Collective pitch position
- Horsepower
- Fuel inlet pressure
- Clock
- Gas producer speed (N_1)
- Power turbine speed (N_2)
- Main rotor speed (N_R)
- Fuel nozzle pressure
- Engine oil pressure
- Turbine outlet temperature
- Oil inlet temperature
- Compressor inlet temperature
- Battery voltage
- Compressor inlet pressure
- Starter current
- Generator load
- Indicator and event lights
- Engine compartment temperatures (17)
- Fuel flow
- Control sensing pressure
- Bleed valve dump pressure

Figure 57 shows the instrumentation installed in the aircraft.

INSTALLATION LOSSES

The aircraft flight test data (Ref. 12) indicated that the performance was approximately 10% lower than measured in the aircraft compared to the test cell engine at the same installation. Since the installation loss was expected to be low, the engine was removed for investigation. In addition, the carbon seal in the exhaust collector leaked, resulting in heavy smoking on fire and shutdown.

The exhaust collector was removed and the carbon seal was replaced. While the turbine was shut down, the balance piston seal was measured. There was no measurable change in balance piston seal clearance which could have caused the depreciation. Half of the compressor case was removed to inspect the rotor for dirt under the impeller shroud. No dirt was found under the impeller which could have caused engine depreciation. The regenerator was also checked and found free of any leakage. These areas are the most likely places for engine depreciation to occur.

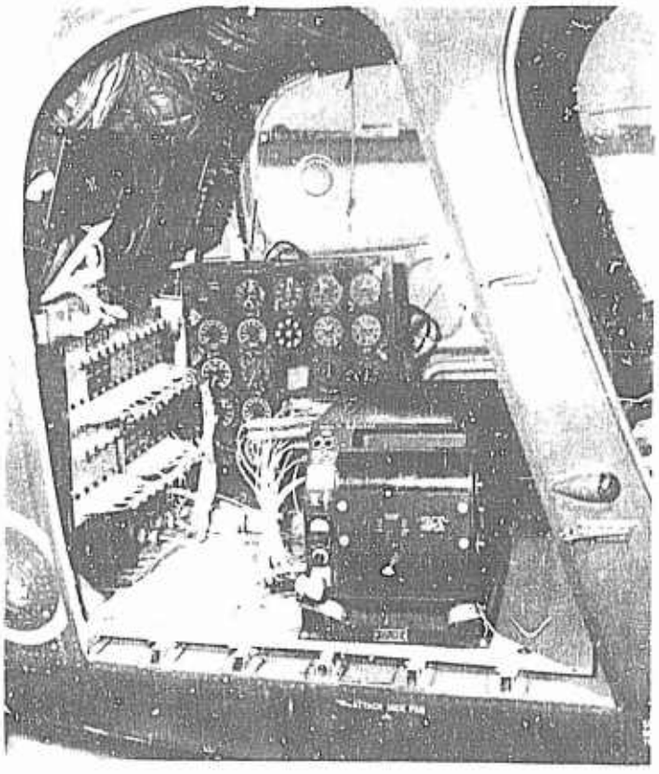

Figure 57. Instrumentation Installed in the YOH-6A.

Engine calibrations run both with and without a regenerator indicated that [illegible] depreciation had occurred. Both the nonregenerative and the regenerative engines were basically "specification" engines as shown in Figure 58. Based on the "green" run prior to installation, the regenerative engine depreciated [illegible] in horsepower at 1330 F. This depreciation was due to an unexplained loss in compressor airflow which occurred in both the regenerative and nonregenerative engine runs.

In the aircraft, an instrumentation ring is installed directly on the front support of the compressor. An engine run with the ring installed indicated [illegible] additional loss of [illegible] when facing the compressor inlet temperature measured by the aircraft instrumentation ring. The aircraft instrumentation ring therefore [illegible] read 3.7 F cooler than the standard thermocouple. Correcting for the compressor inlet temperature error results in a total depreciation of [illegible]. As mentioned previously, [illegible] of this 7.4 is based on the depreciation and [illegible] is performance loss due to blockage associated with the instrumentation ring.

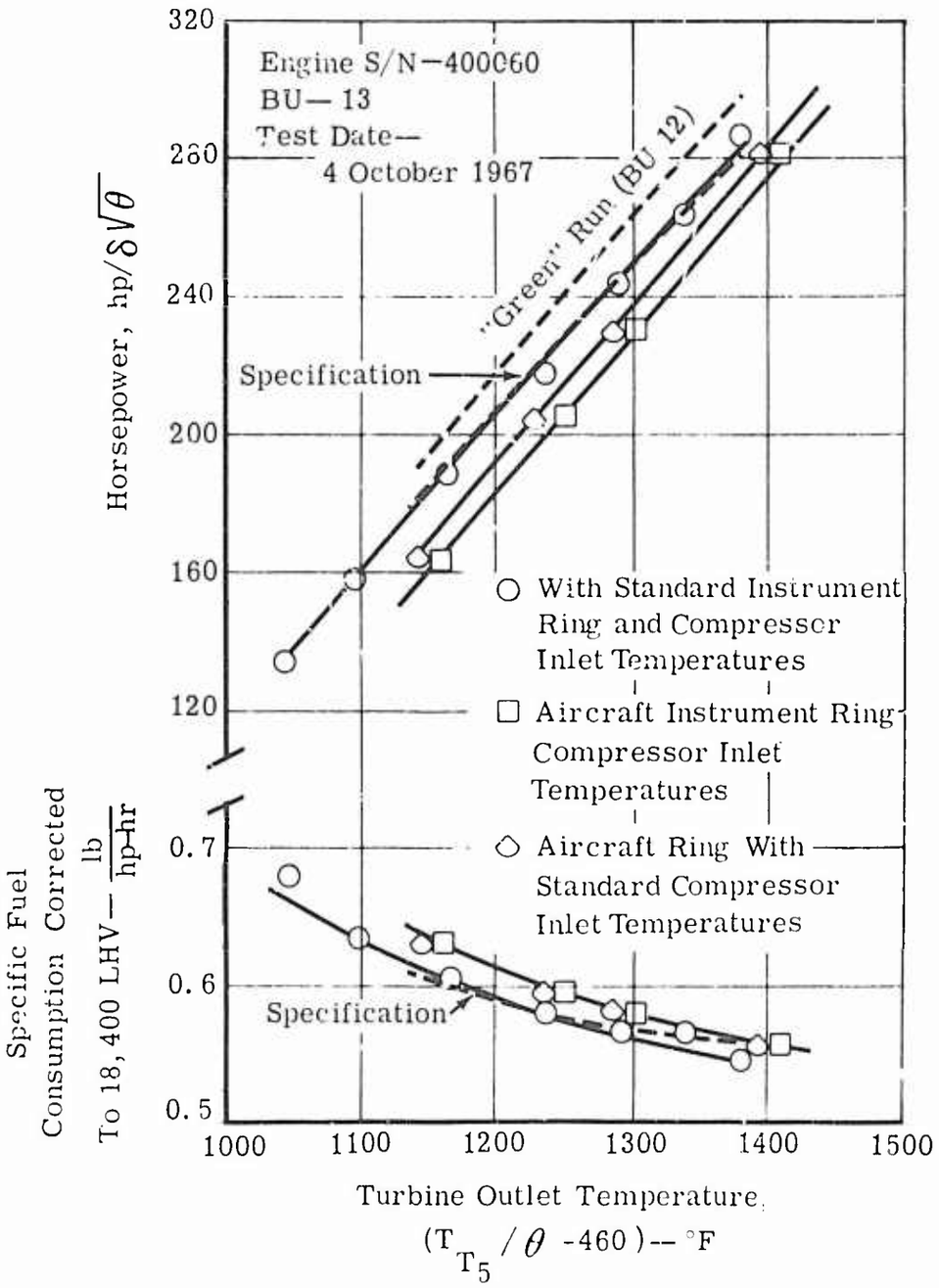

Figure 58. Engine Performance with Aircraft Instrumentation Ring Installed.

To determine the actual installation losses, the test stand data obtained in BU 13, with the aircraft instrumentation ring installed, was used as the base line. Figure 59 shows the installation loss of the regenerative engine in the modified YOH-6A aircraft. The flight test data are a composite of all the data obtained at 1500 and 5000 ft corrected to sea level standard day conditions. At maximum turbine outlet temperature (1380°F), the installation loss was 2.2% in horsepower and 1.8% in specific fuel consumption. In terms of performance level, the installed engine was 4.6% below specification horsepower as a result of the 2.2% installation loss and 2.4% loss associated with blockage of the instrumentation ring.

FLIGHT PERFORMANCE EVALUATION

In addition to the fixed airspeed calibration shown in Figure 59, variable airspeed calibrations were run at 1500-, 5000-, and 10,000-ft altitudes. The calibrations were run at 1900-, 2200-, and 2400-lb gross weight. The test data are shown in Figures 60, 61, and 62. The data are corrected to standard day altitudes to account for the slight variations in altitude and temperature encountered during the flight test.

One of the major problems of installing a regenerator on an existing engine is the reduction in horsepower associated with the increased pressure drop. A comparison of the specification values for the regenerative and nonregenerative engines is presented in Table XIX.

In terms of level flight, the regenerative powered aircraft was capable of flying to the maximum V_{NE} (velocity not to exceed) of the aircraft without exceeding 1380°F (takeoff and Military) at all altitudes from sea level to 10,000 ft. However, there are two areas where the lower power available will limit the aircraft performance: on a maximum power climb to 10,000 ft and hover out of ground effect at 95°F and 6000 ft.

A maximum power climb and an autorotation descent are shown in Figures 63 and 64. The maximum power climb to 10,000 ft took 10 min compared to 6.5 min for a nonregenerative engine. This slower climb rate was due to the lower power available.

During hover out of ground effect, the only comparison available would be a direct comparison of the specification horsepowers available on a 95°F, 6000-ft day. For the nonregenerative engine, the maximum horsepower available is 207; for the regenerative engine, the maximum power available is 186 horsepower. This is a 10% reduction in maximum available power. The power available on a 95°F, 6000-ft day is 65% of that available on a standard day of 59°F, sea level, which is comparable to the lapse rate of the nonregenerative engine.

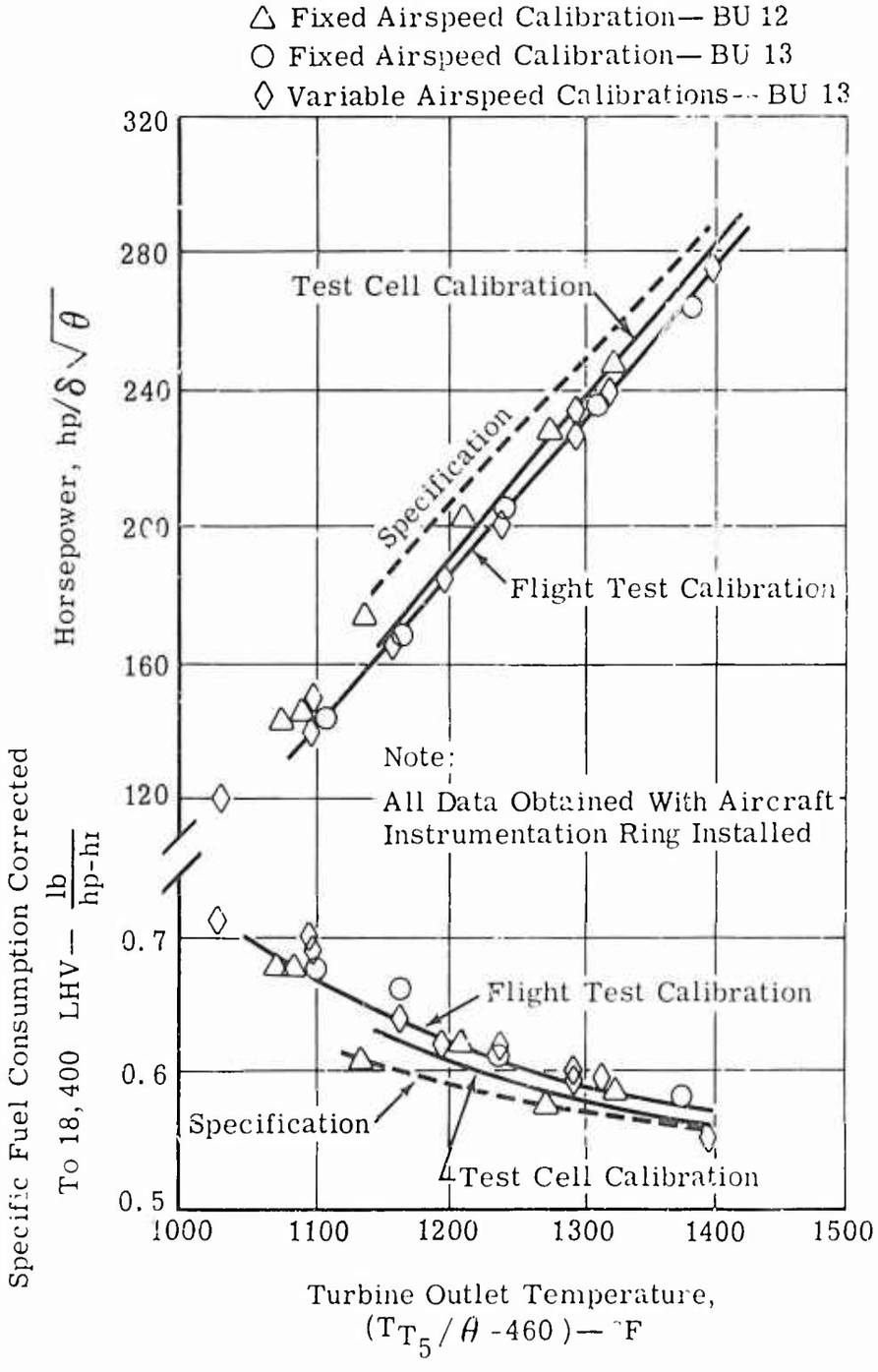

Figure 59. Installation Loss of the Regenerative Engine Installed in the Modified YOH-6A.

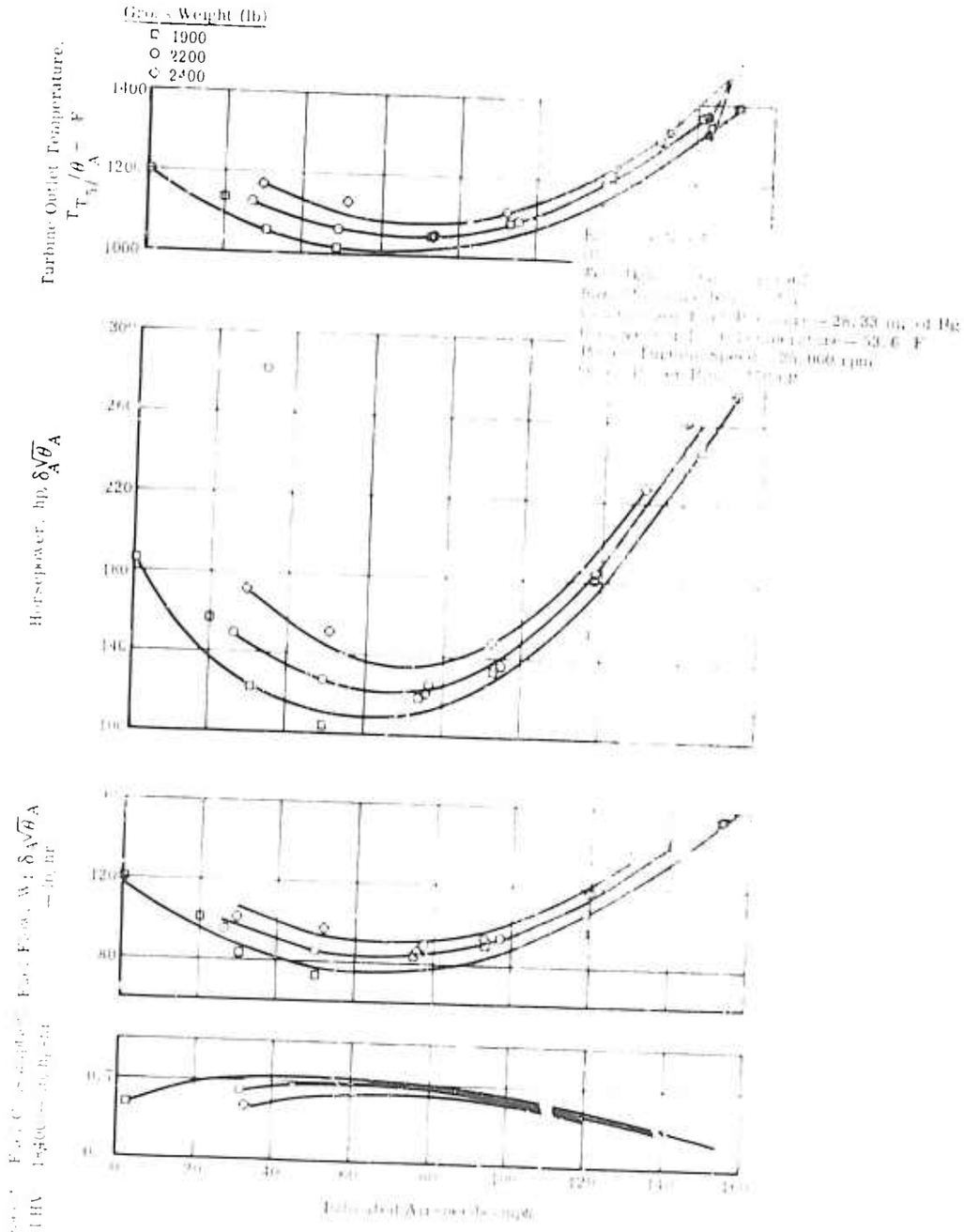

Figure 60. Variable Airspeed Calibration at 1500 Feet.

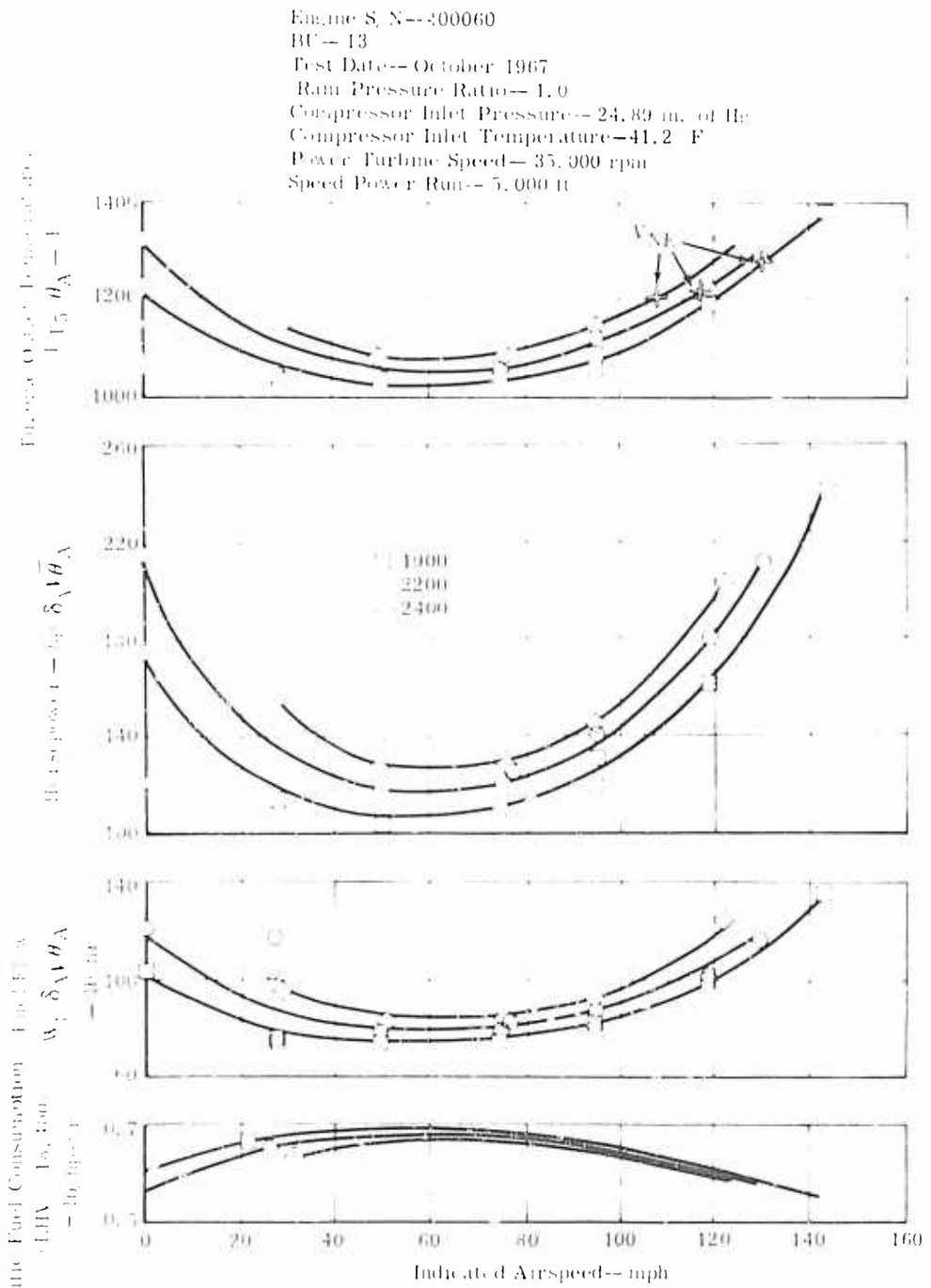

Figure 61. Variable Airspeed Calibration at 5000 Feet.

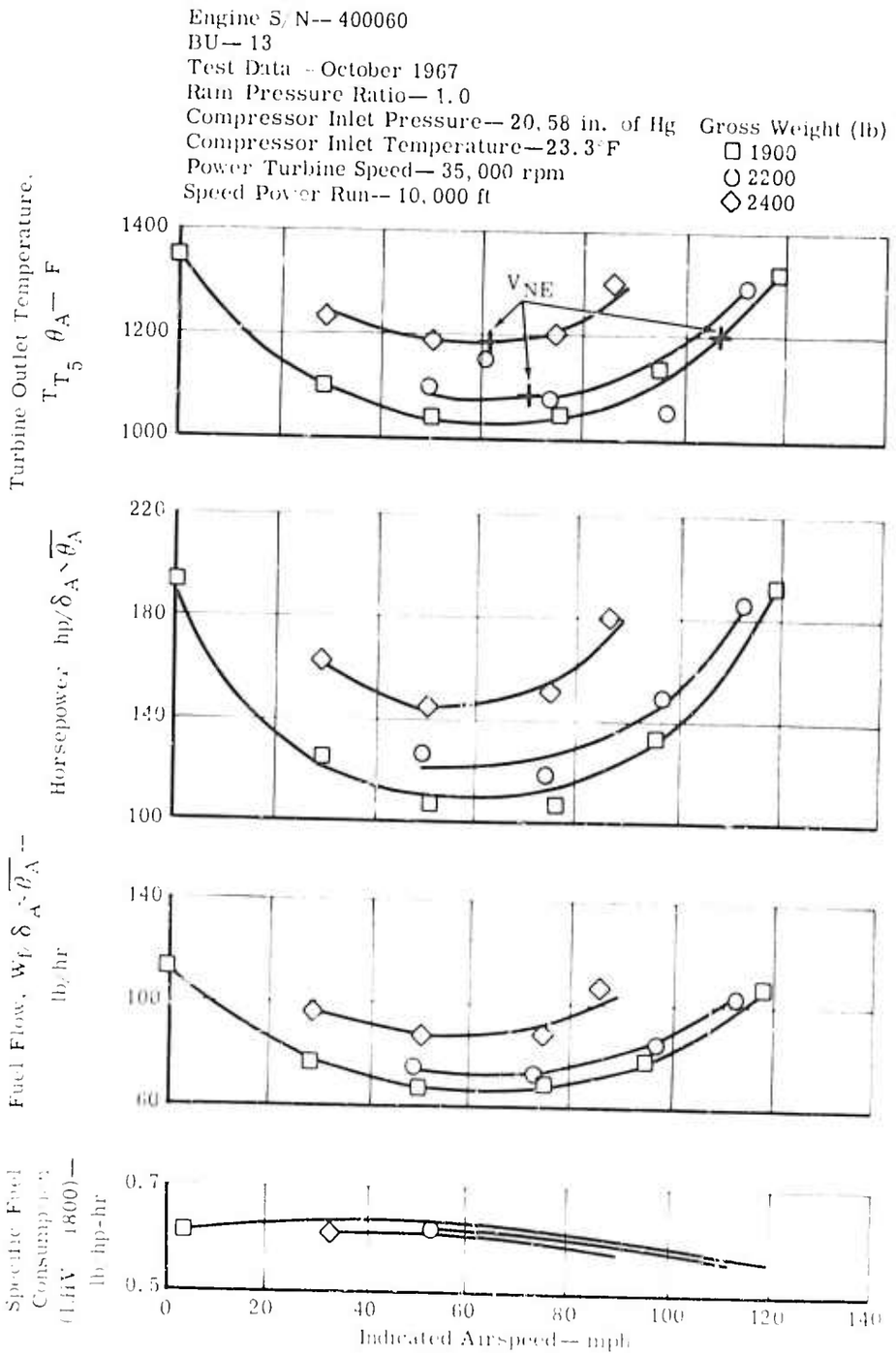

Figure 62. Variable Airspeed Calibration at 10,000 Feet.

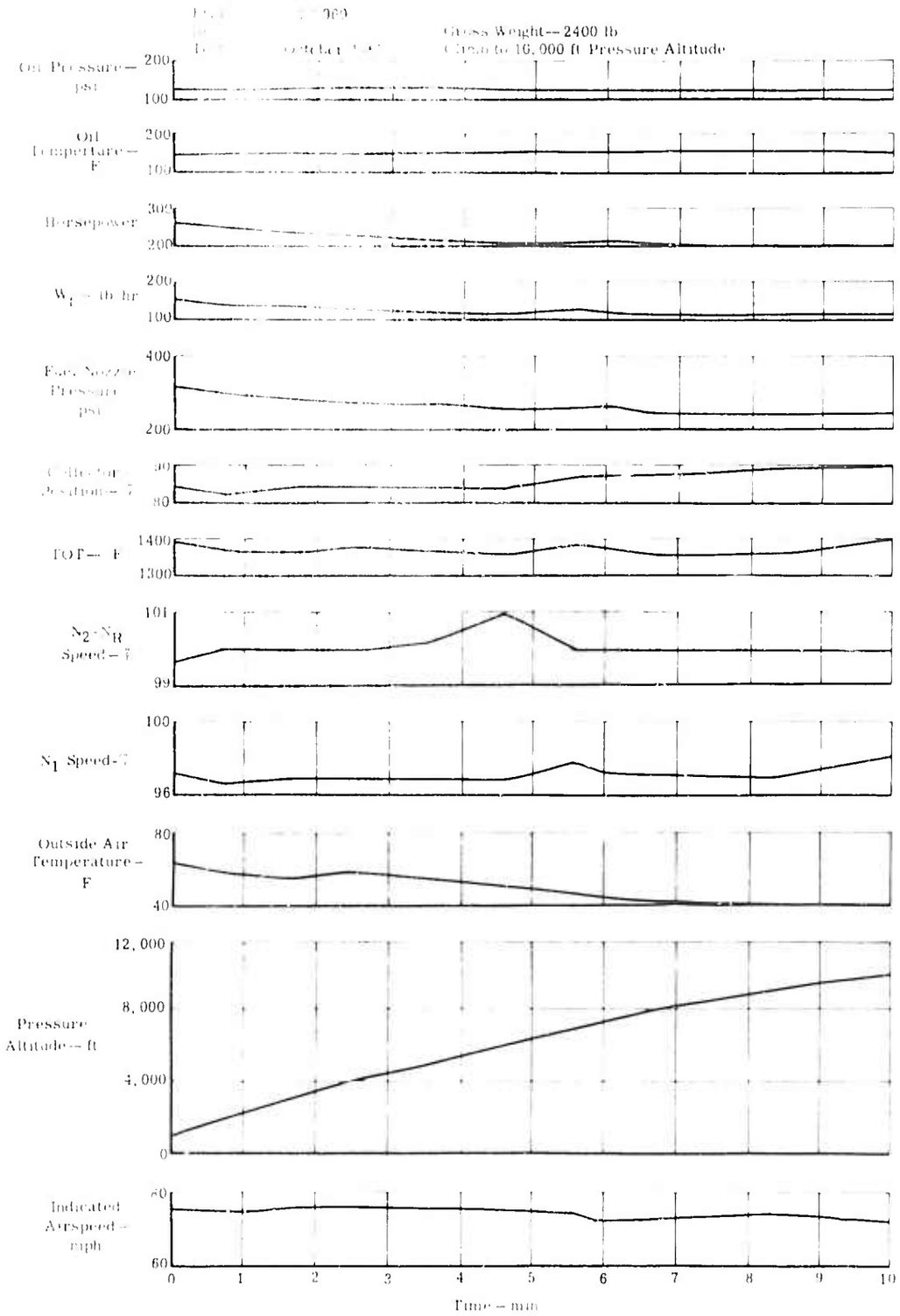

Figure 63. Maximum Power Climb to 10,000 Feet.

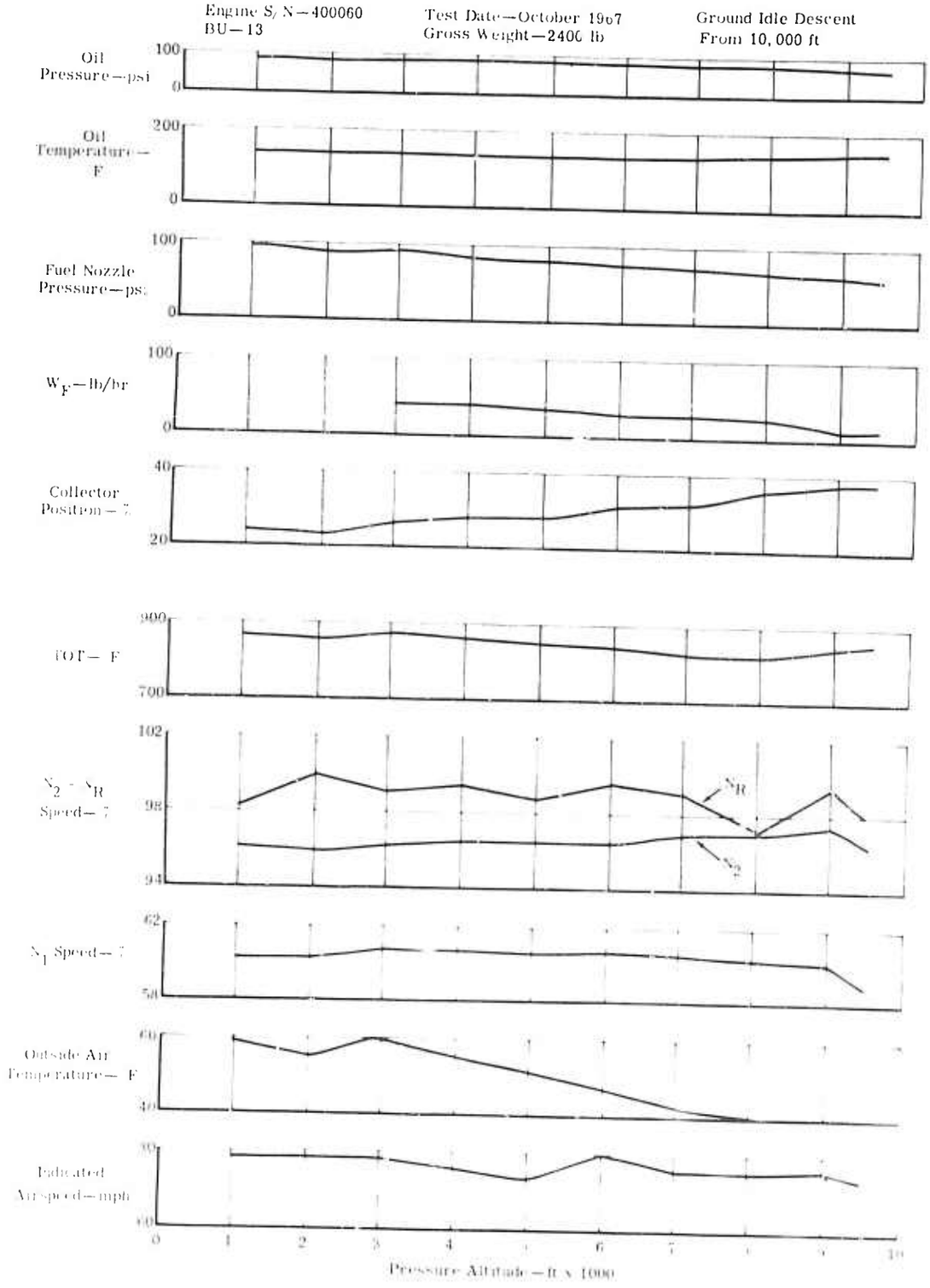

Figure 64. Autorotation Descent from 10,000 Feet.

TABLE XIX.

PERFORMANCE RATINGS AT
STANDARD SEA LEVEL STATIC CONDITIONS

	T63-A-5A			Regenerative T63 (Target Values)		
Ratings	Maximum Measured Rated Gas Temperature (°F)	Shaft HP (min)	Maximum Specific Fuel Consumption (lb/shp-hr) (max)	Maximum Measured Rated Gas Temperature (°F) (max)	Shaft HP (min)	Maximum Specific Fuel Consumption (lb/shp-hr)
Takeoff and military	1380	317	0.697	1380	280	0.560
Normal	1280	270	0.706	1280	239	0.575
90% Normal	1226	243	0.725	1222	215	0.587
75% Normal	1148	203	0.762	1140	179	0.611

To determine the effect of the regenerator on the range of the aircraft, the fuel consumption data were adjusted for the blockage due to the instrumentation ring using the data obtained from Figure 58 to adjust the aircraft performance data shown in Figures 60 and 61. The resulting data were plotted as specific range and compared with nonregenerative engine data obtained from USATECOM Report No. 4-3-0250/51/52/53 which was obtained on S/N 62-4212 aircraft at Edwards AFB, California. The results are shown in Figures 65 and 66.

At 1500 ft, the improvement in specific range varied from 18.9% to 24%. It was estimated that the improvement in specific range would be from 25% to 36%, with the maximum improvement being at the minimum horsepower point. The lower improvement in specific range is due to the higher horsepower requirements of the regenerative aircraft. The modification which resulted in a bubble on either side of the aircraft could account for the difference. However, since the drag curves were obtained on two different aircraft, it is conceivable that the difference could be due to variations in aircraft rather than the modification.

At 5000 ft, the drag curves for the regenerative and nonregenerative aircraft are the same at the low and high airspeeds. At these points, the specific range agrees very closely with the originally estimated values. The regenerative engine powered aircraft, therefore, can be expected to have a specific range that is 25% to 30% better than the nonregenerative aircraft.

COMPARTMENT TEMPERATURES

Due to the location of the regenerators above the engine, the temperature around the engine directly below the regenerators will increase. A fan was installed to blow outside air around the engine in this area. Test data indicate that the blower reduced temperatures 20° to 50°F around the left side of the turbine only.

The major problem encountered was the distribution of the temperatures around the engine. The right-hand side and the top of the turbine were considerably above the 450°F limit. To provide a more even flow of air through the compartment, an opening at the back of the aircraft was provided by placing a hole in the rear cap which is between and above the exhaust extensions. This reduced the temperatures from 90° to 200°F on the right-hand side and the top of the turbine.

Originally the exhaust extensions were scarfed as shown in Figure 53. To prevent the possibility of exhaust gas flow into the compartment, an 8-in.-diameter pipe was installed over the extensions. The pipe extended 3 in.

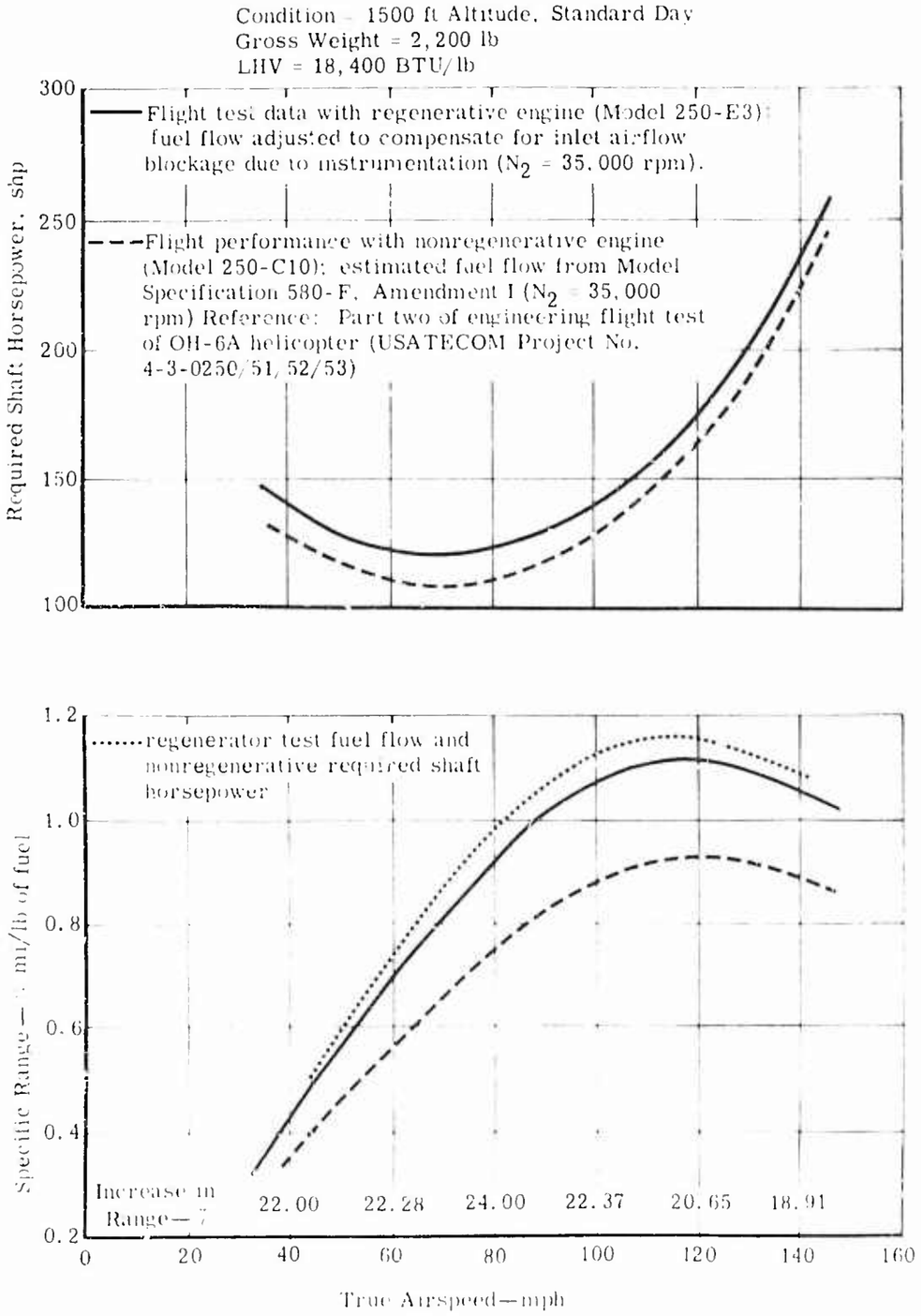

Figure 65. Helicopter Performance Comparison at 1500 Feet.

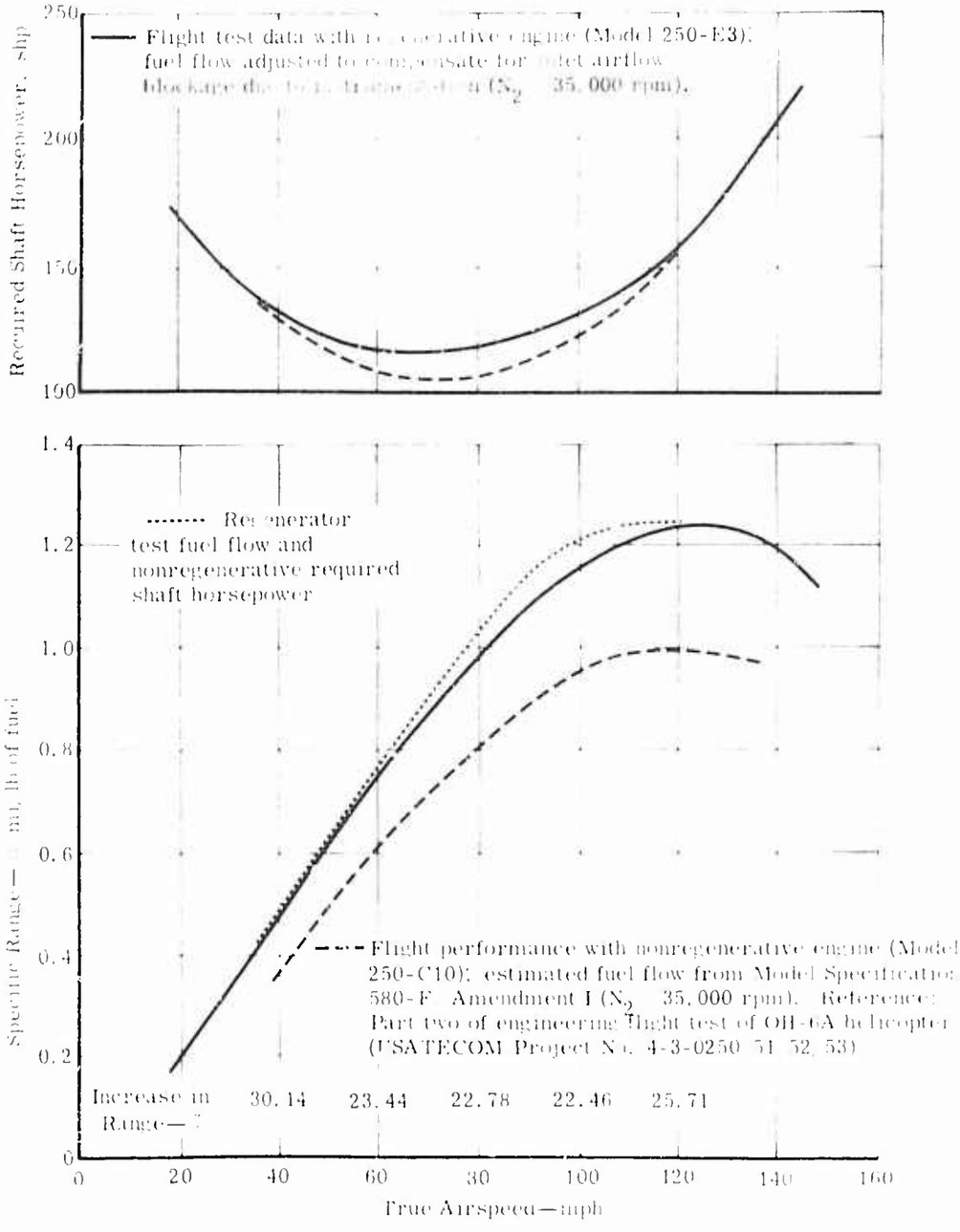

Figure 66. Helicopter Performance Comparison at 5000 Feet.

past the clamshell doors. With this configuration, it was possible to get a compartment temperature which was satisfactory for flight test.

The location of the thermocouples and a comparison of compartment temperatures for a regenerative and a nonregenerative aircraft are shown in Figure 67. Although the temperatures were from 27° to 96°F higher than those in the nonregenerative installation, all temperatures were within limits. Table XX compares the compartment temperatures at different flight conditions. The highest temperatures occurred at level flight at high speed. Although the temperatures were still within limits, problems could occur at ambient temperatures above 80°F. Insulating the regenerators would help this problem and eliminate the need for the cooling air fan.

TRANSIENT RESPONSE

Transient operation was checked throughout the operating range from sea level to 10,000 ft. One of the main areas of interest centered around the effect of the thermal inertia of the regenerators. The effect of thermal inertia would be most readily seen on a collective deceleration. The objective of the maneuver is to reduce forward speed without changing altitude. The pilot lowers collective to unload the rotor and flares the ship. The rotor speed starts to increase and the engine decelerates. The maximum speed attained by the rotor is determined to a great extent by how fast the engine decelerates. With a 2-sec collective movement, the rotors split at 105% speed at 1500 ft, 108% at 5000 ft, and 110% at 10,000 ft. Faster collective movements resulted in no split before the rotor reached 110%. Surge checks were also made at all altitudes to check the effect of the increased pressure drop on the surge margin of the engine. No surges were encountered from sea level to 10,000 ft.

Accelerations were also made to check the acceleration characteristics, which are primarily a function of the control system. On a collective acceleration, the droop of the rotor speed is a function of the acceleration rate of the engine. Rotor droop as low as 81% was encountered. This problem can be remedied by increasing the slope of the fuel schedule at the lower gas speeds. At 10,000 ft, the collective accelerations resulted in peak temperatures in excess of 800°C (1472°F). This problem also could be eliminated by a change in the fuel control schedule.

Gas producer acceleration and deceleration made by a throttle movement were satisfactory at all altitudes. Minimum gas producer speed droop was 55% on the decelerations.

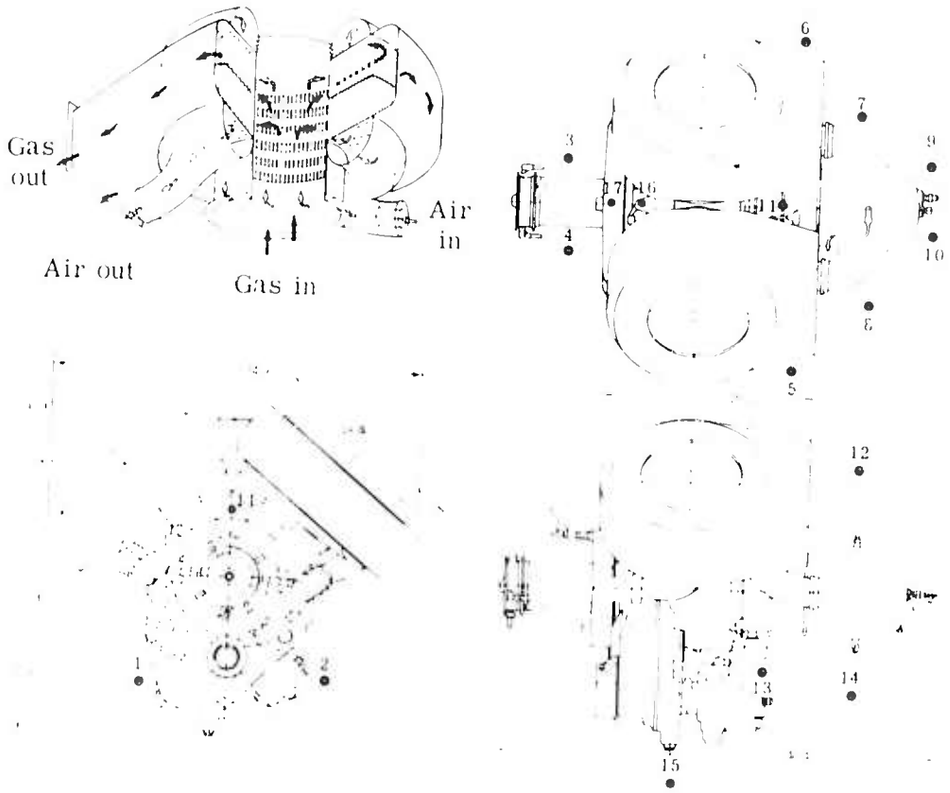

Thermocouple Number	Thermocouple Location	Temperature Limits (°F)	Hover, Sea Level, 80°F		
			Regenerative Engine		
1	Gearbox Right	250	240	169	
2	Gearbox Left	250	230	162	
3	Compressor Left	250	212		
4	Compressor Right	250	212		
5	Turbine Left	↓	324	231	
6	Turbine Right	↓	356	248	
7	Turbine Right	450	294	213	
8	Turbine Left	Average	278	233	258
9	Turbine Right	↓	289	259	Average
10	Turbine Left	↓	248	225	
11	Turbine Top	↓	397	305	
12	Turbine Top	↓	449	270	
13	Turbine Bottom	450	254	152	
14	Turbine Bottom	450	272	196	
15	Gearbox Bottom	250	222	195	
16	Gearbox Metal Temperature	220	280	238	
17	Compressor Metal Temperature	500	432	394	

Figure 67. YOH-6A Compartment Temperatures.

TABLE XX.

COMPARTMENT TEMPERATURES

Thermocouple Number	Temperature Limit (°F)	Hover		Level Flight 138 mi/h		Maximum Power Climb	
1	250	240		212		212	
2	250	230		212		281	
3	250	212		212		212	
4	250	212		212		212	
5		324		406		305	
6		356		562		565	
7		294		352		418	
8	450	278	354	352	424	238	410
9	Avg	289		321		380	
10		248		296		256	
11		597		625		597	
13		449		480		531	
12	450	264		359		252	
14	450	271		356		269	
15	250	222		221		212	
16	370	280		334		280	
17	500	432		490		398	
OAT		80°		80°		50°F	

A direct comparison of the transient response of the regenerative and nonregenerative engines is given in Table XXI. Representative plots of the transient data are shown on Figures 68 through 71.

Steady-state operation was entirely satisfactory. No abnormal torsional or low cycle instability was encountered.

INFRARED SIGNATURE MEASUREMENT

Since the addition of the regenerators lowers the exhaust gas temperature by approximately 320°F, the infrared signature of the aircraft would be significantly reduced. The infrared signature of the regenerative powered aircraft was tested at the Allison flight test facilities by personnel of the Infrared Countermeasures group of the Naval Air Testing Station at China Lake, California. A substantial reduction in infrared signature was measured. A separate report by the Naval Air Testing Station will summarize the results of this test.

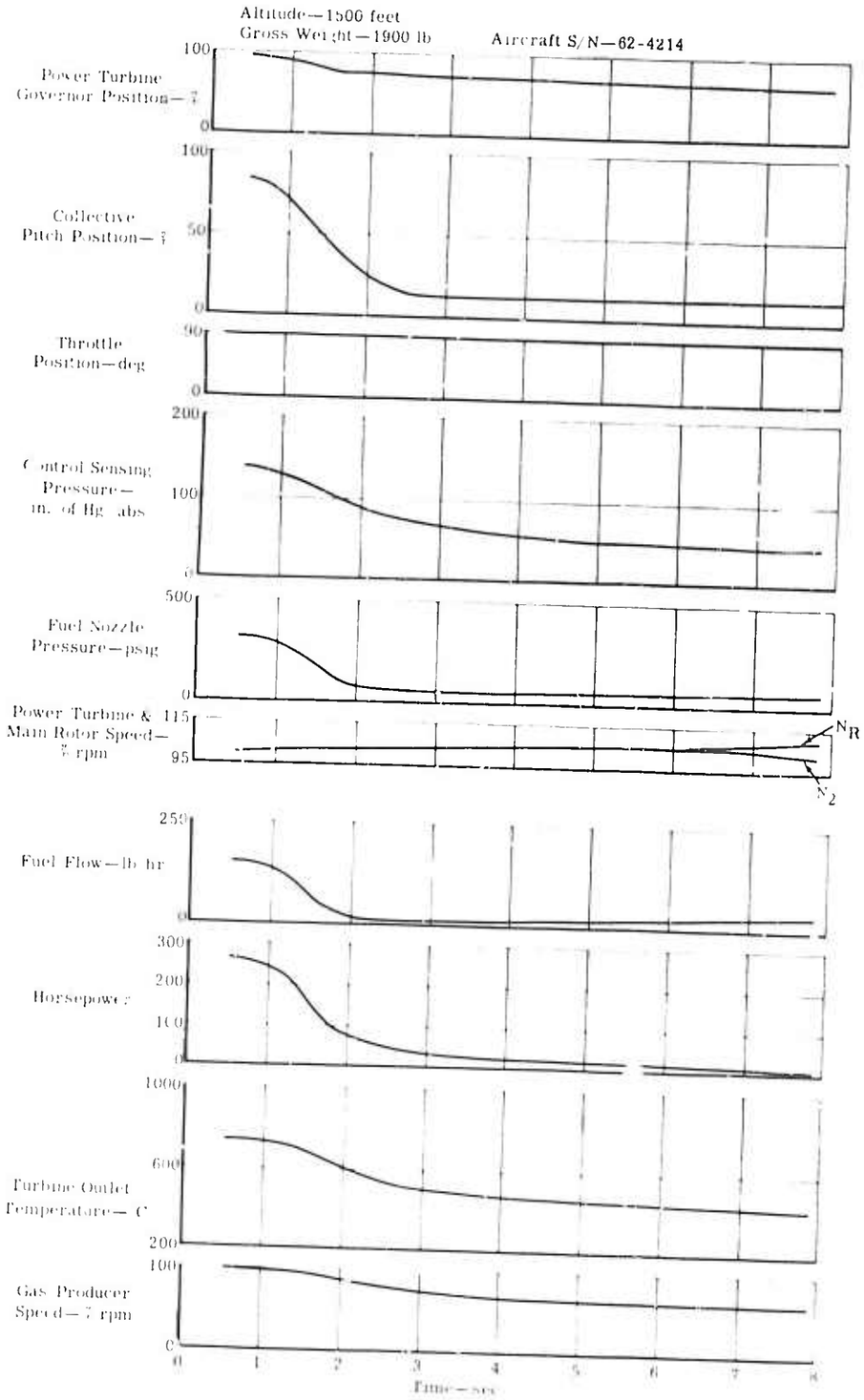

Figure 68. Collective Deceleration at 1500 Feet.

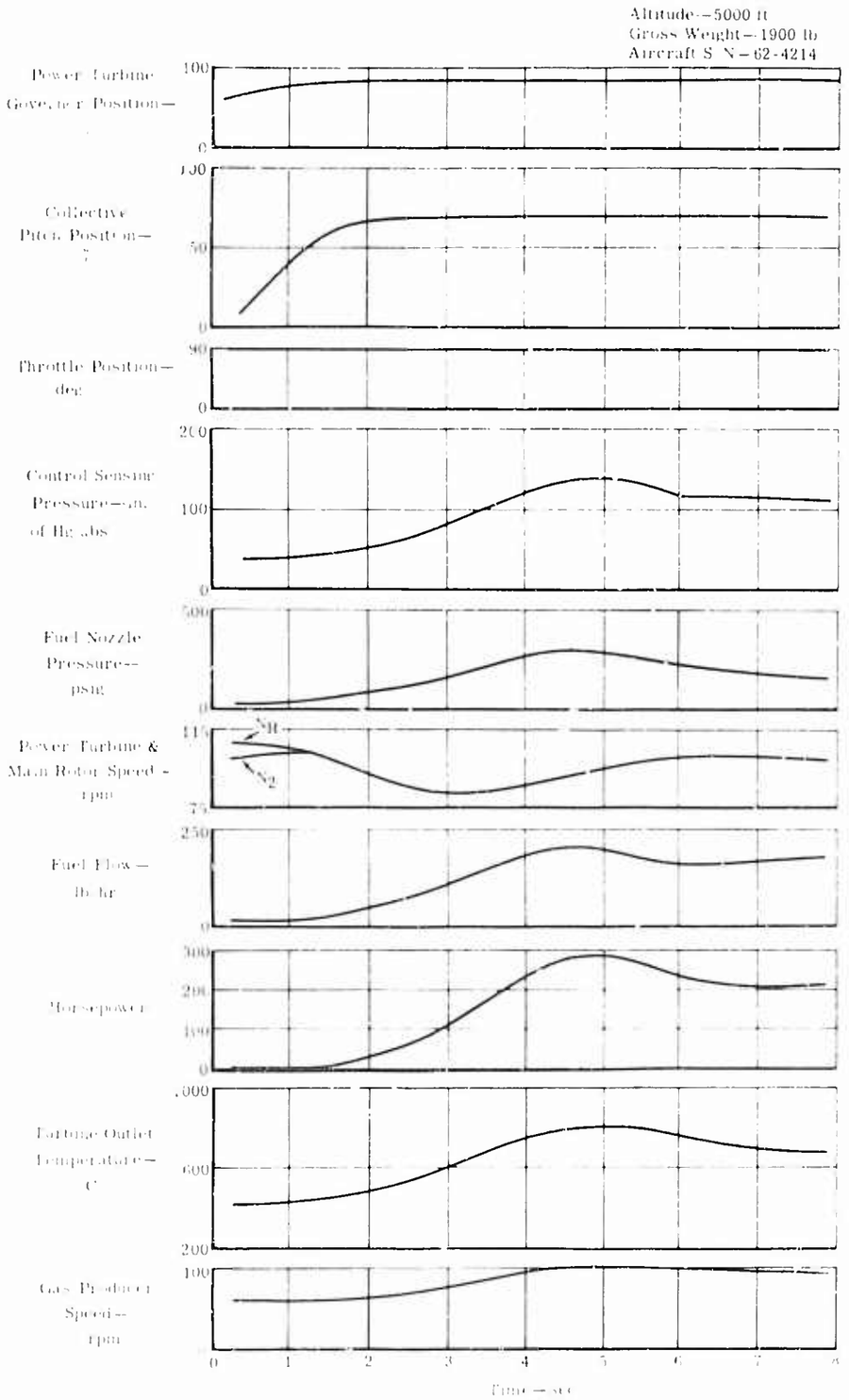

Figure 69. Collective Acceleration at 5000 Feet.

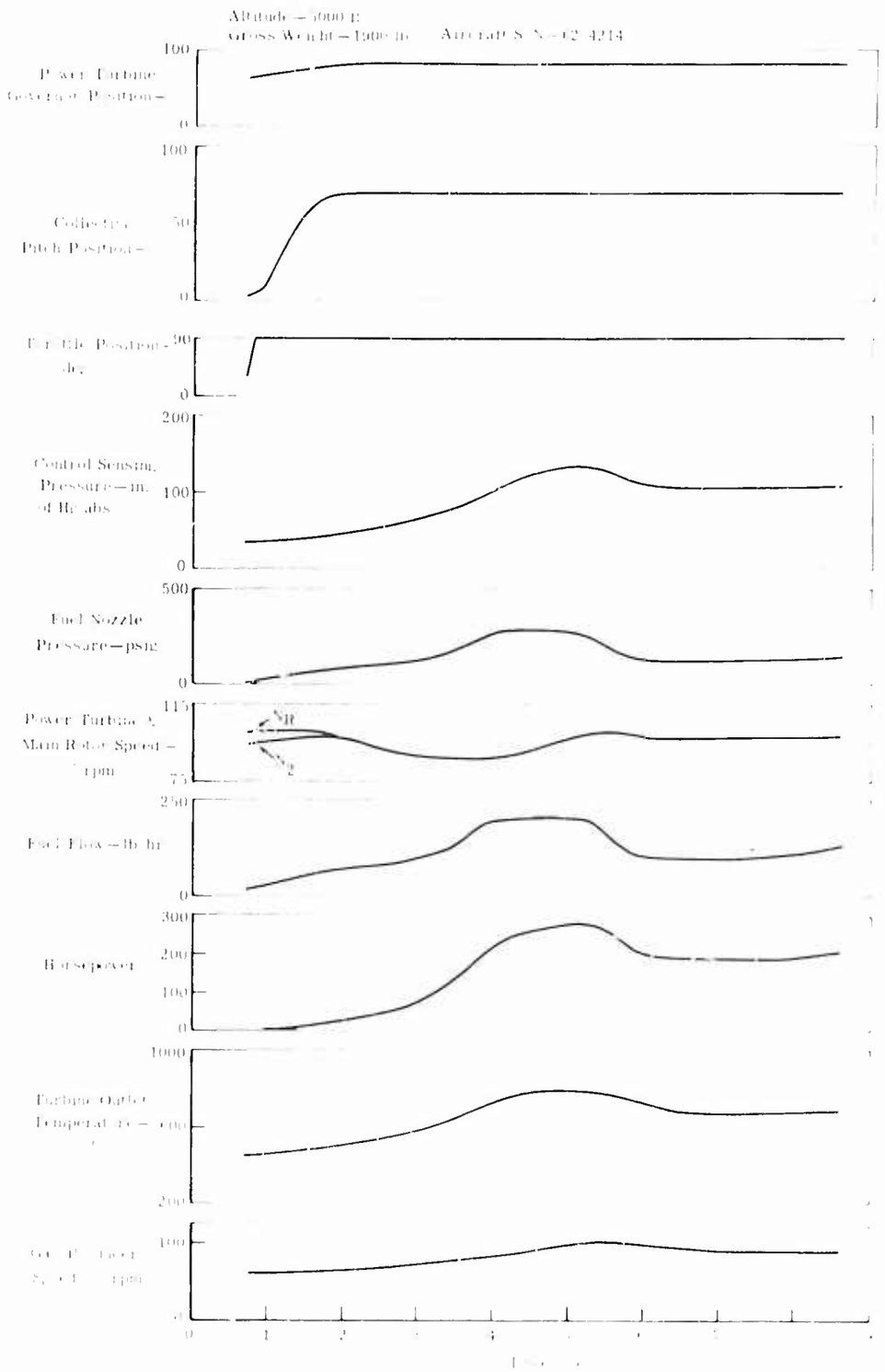

Figure 70. Gas Producer Acceleration at 5000 Feet.

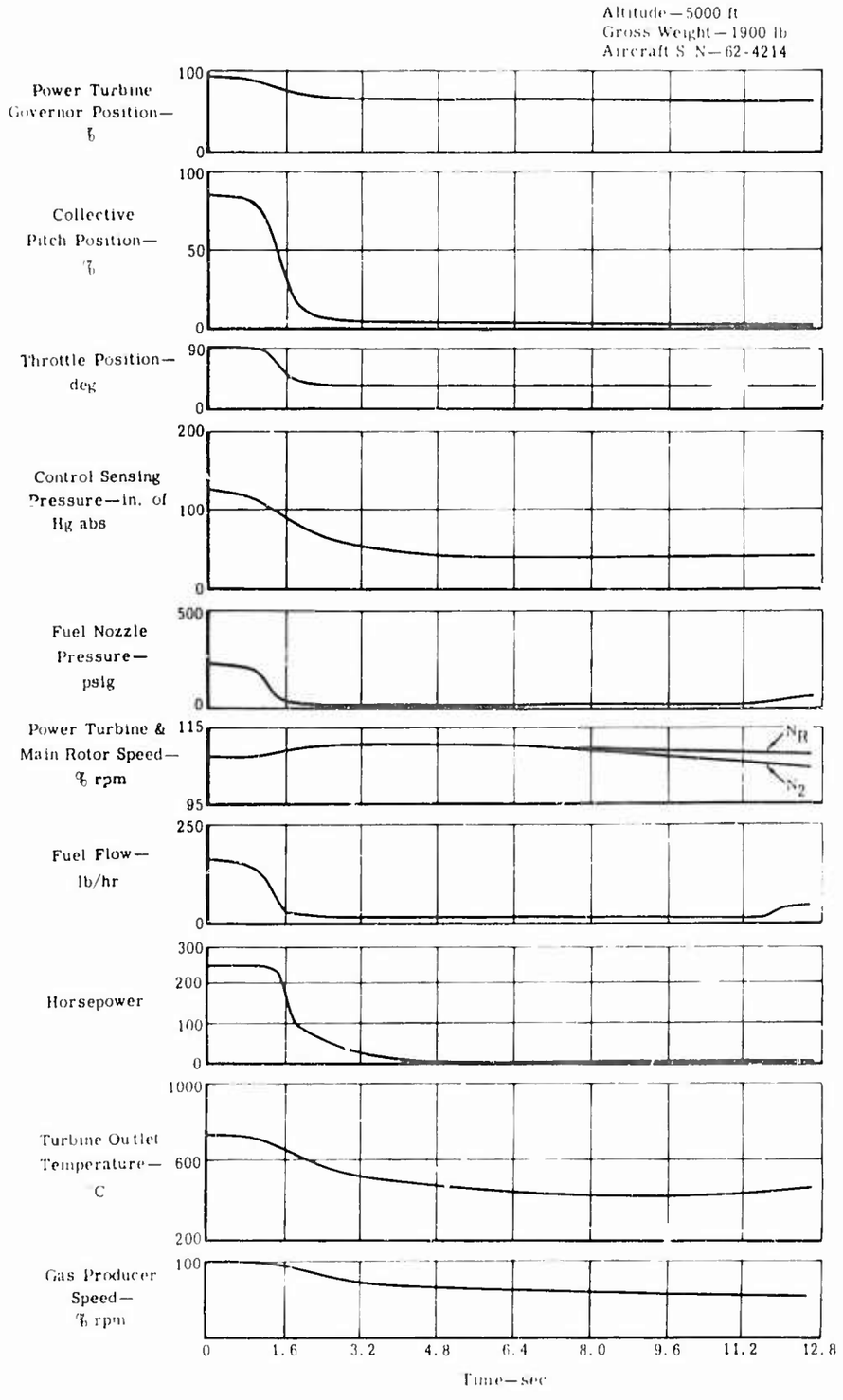

Figure 71. Gas Producer Deceleration at 5000 Feet.

TABLE XXI.

TRANSIENT RESPONSE COMPARISON

	T63-A 5.x	Regenerative Engine
Gross Weight	2100 lb	2200 lb
Altitude	1500 ft	1500 ft
Outside Air Temperature	65°F	65°F
Collective Acceleration	92% N_2N_R	81% N_2N_R
Throttle Acceleration	95% N_2N_R	88% N_2N_R
Surge Check	OK	OK
Collective Deceleration		
Slow	106% N_2 Split	105% N_2 Split
Medium	105% N_2 Split	112% N_2 No Split
Fast	110% N_2 No Split	

APPENDIX

PERFORMANCE CURVES

The curves included in the Appendix are a complete set of all pertinent performance parameters obtained on the engine, S/N 400060, BU No. 10, during the altitude calibration runs. In addition, the estimated altitude performance as obtained from the L-14 IBM deck is included.

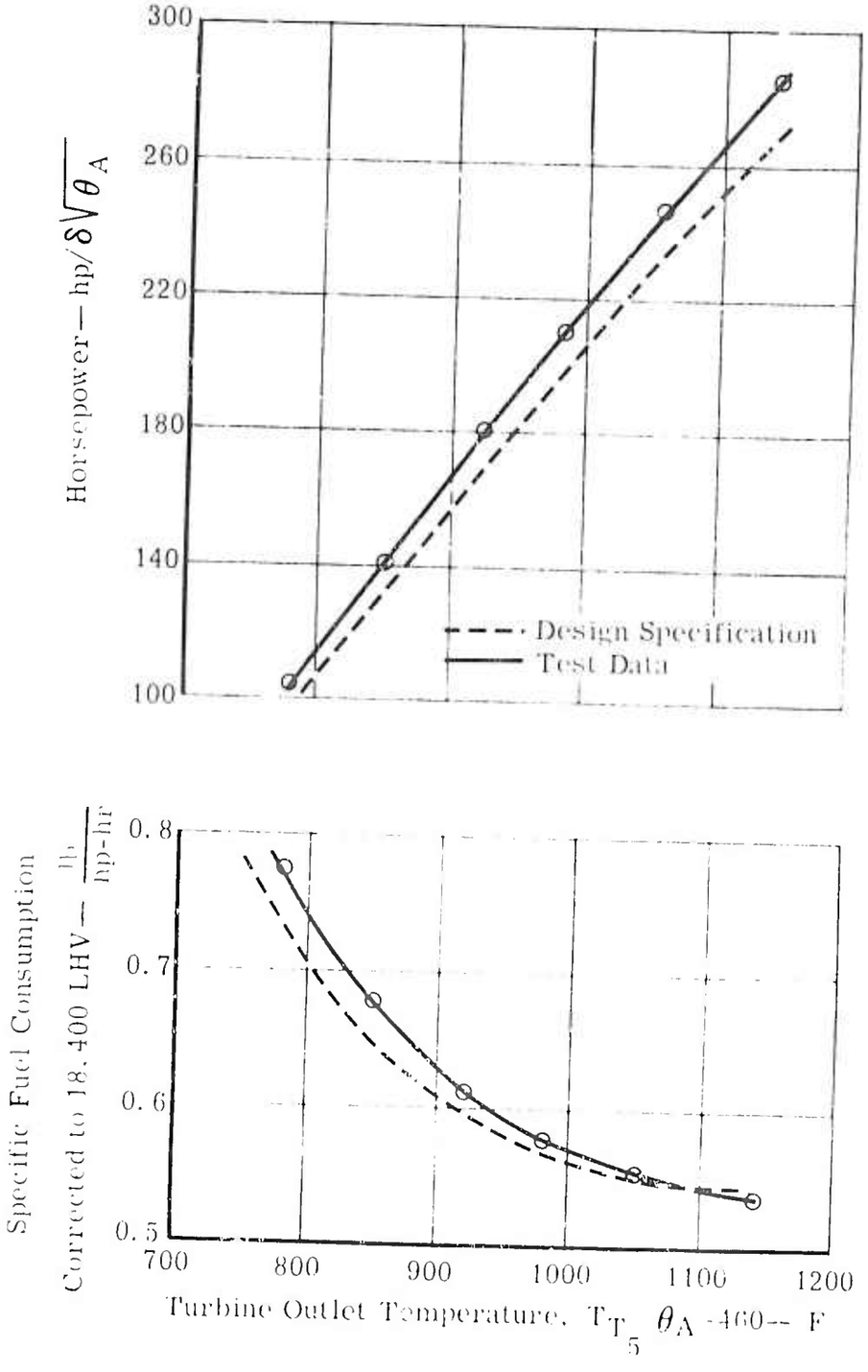

Figure 72. Test Data at Sea Level and -12 F.

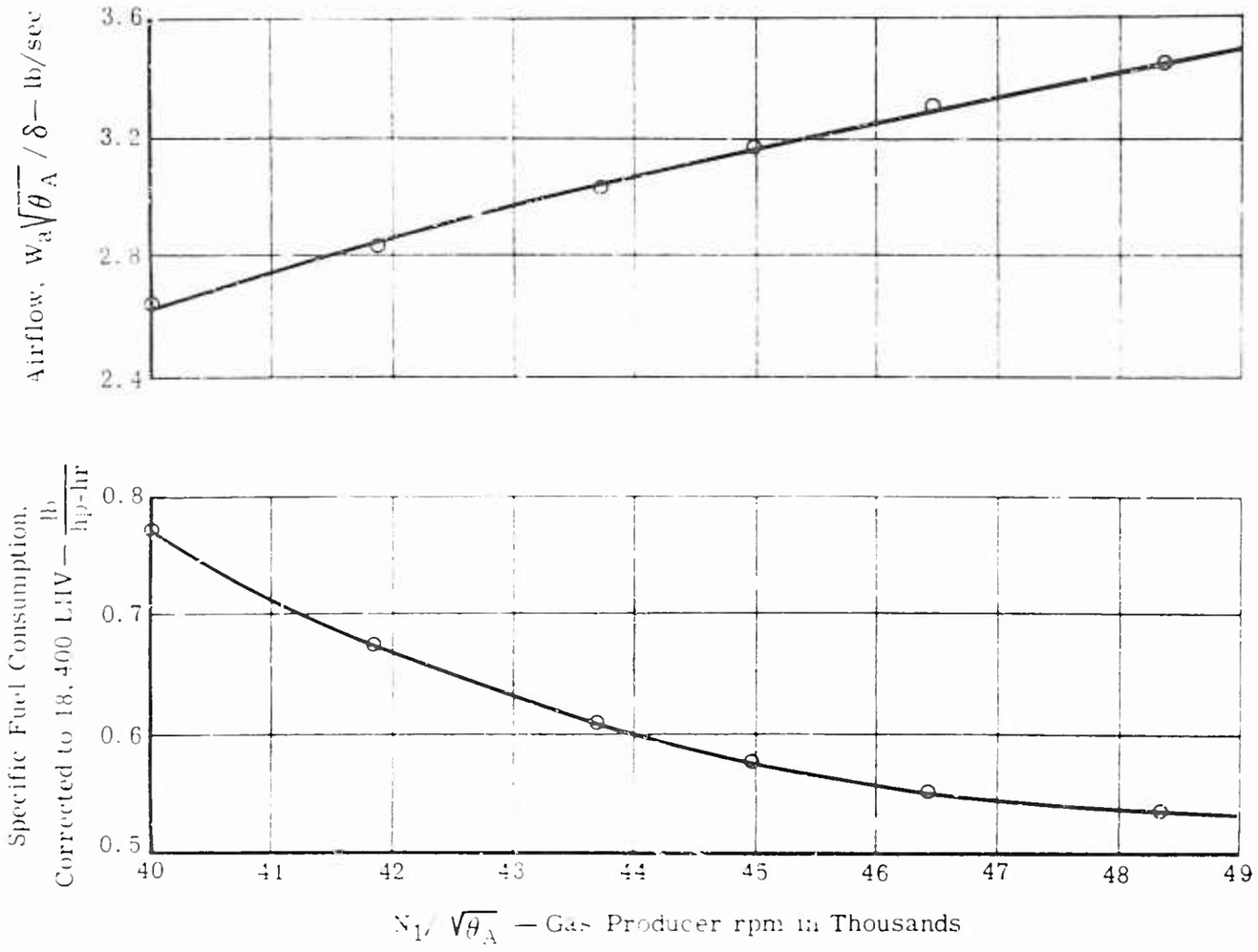

Figure 73. Test Data at Sea Level and -12 F.

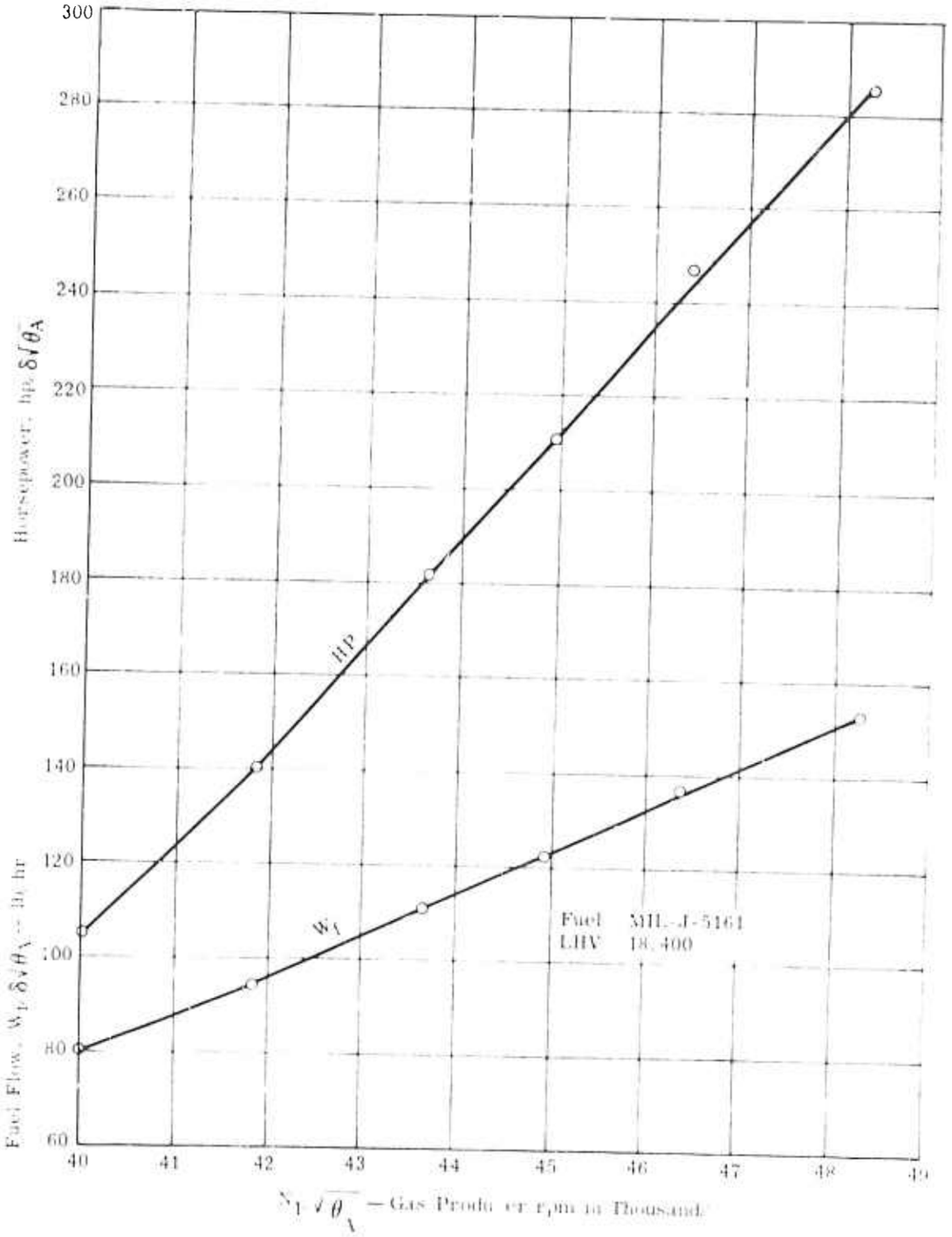

Figure 74. Test Data at Sea Level and -12 F.

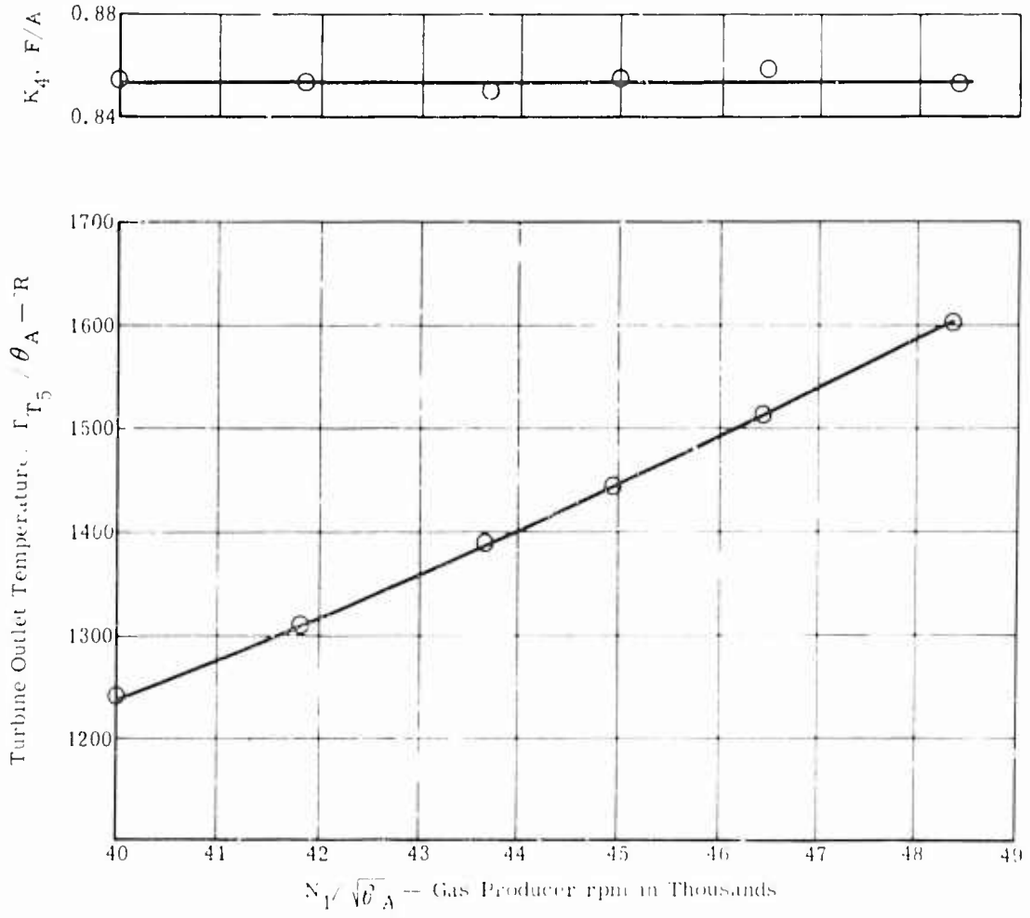

Figure 75. Test Data at Sea Level and -12 F.

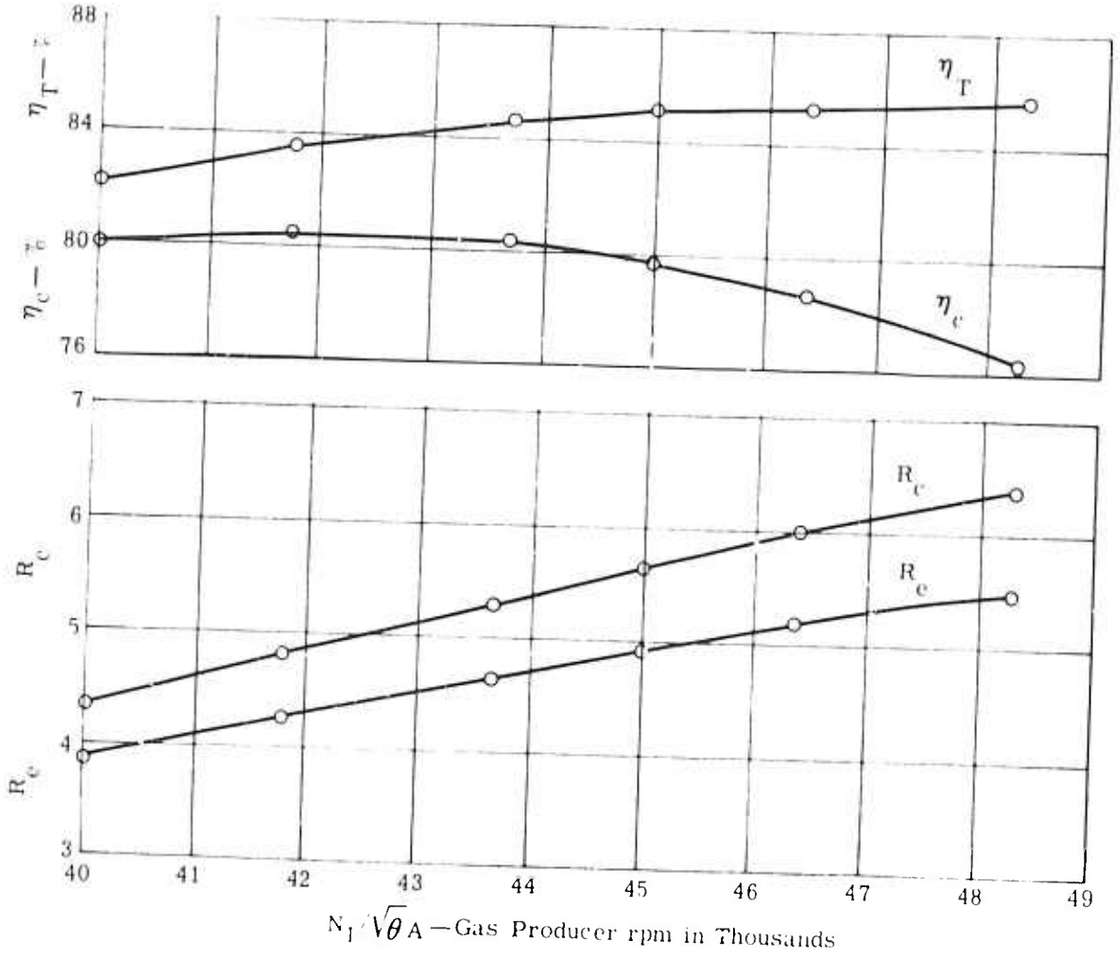

Figure 76. Test Data at Sea Level and -12 F.

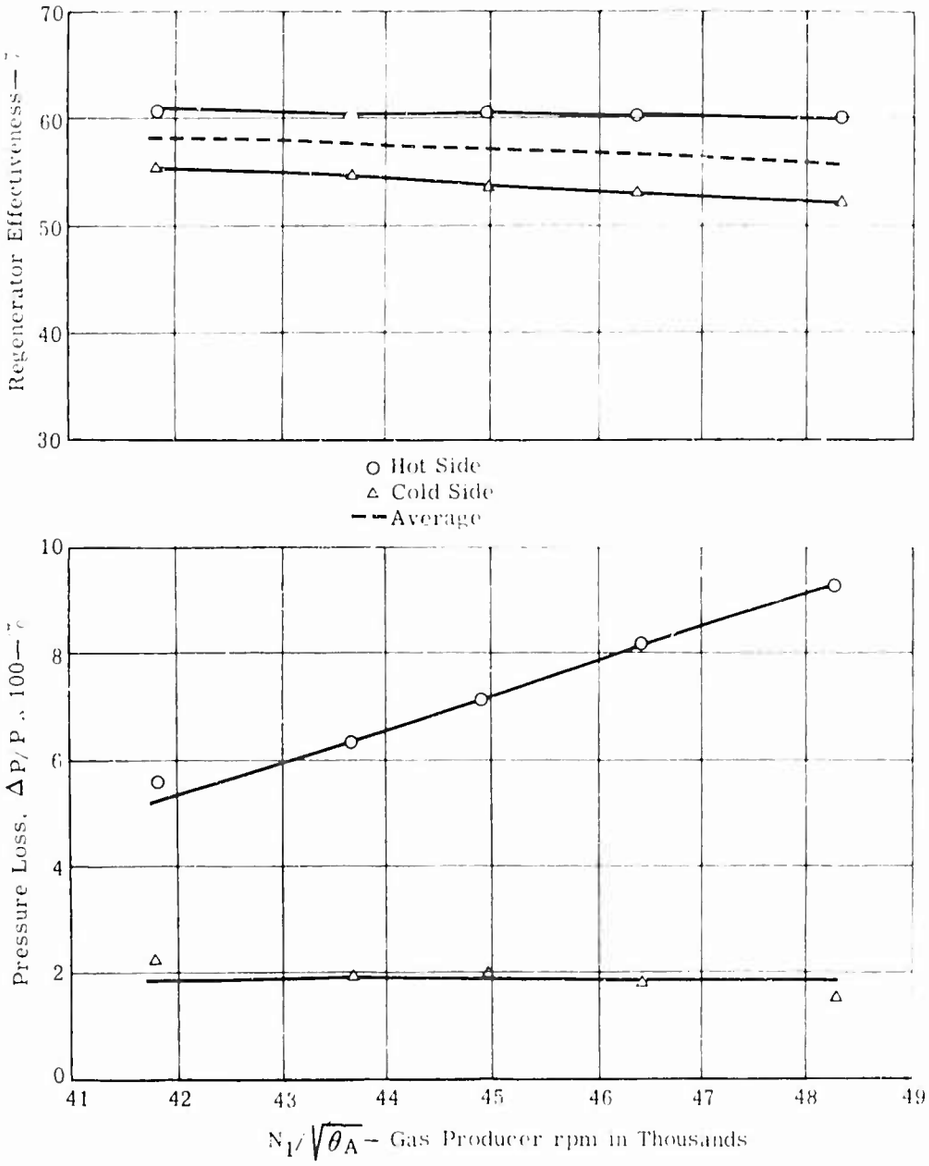

Figure 77. Test Data at Sea Level and -12 F.

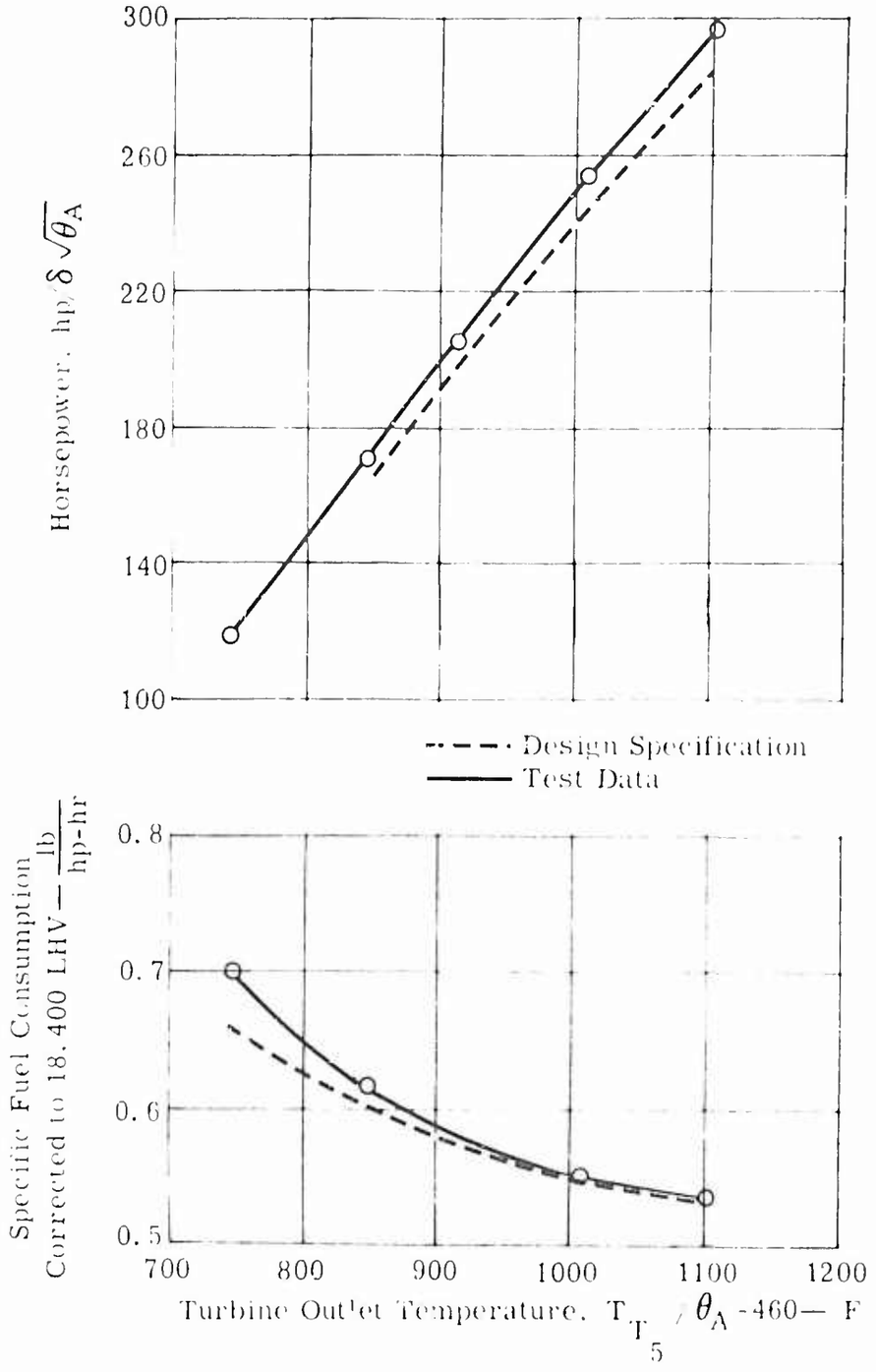

Figure 78. Test Data at Sea Level and -35 F.

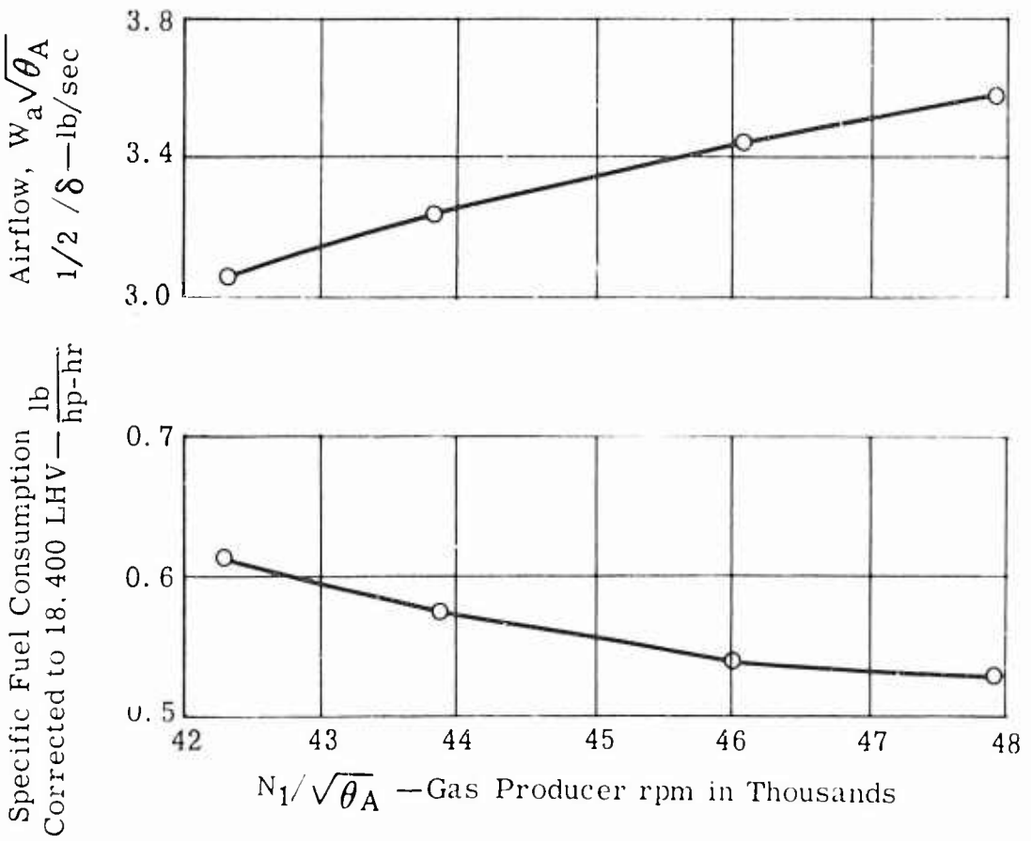

Figure 79. Test Data at Sea Level and -35 F.

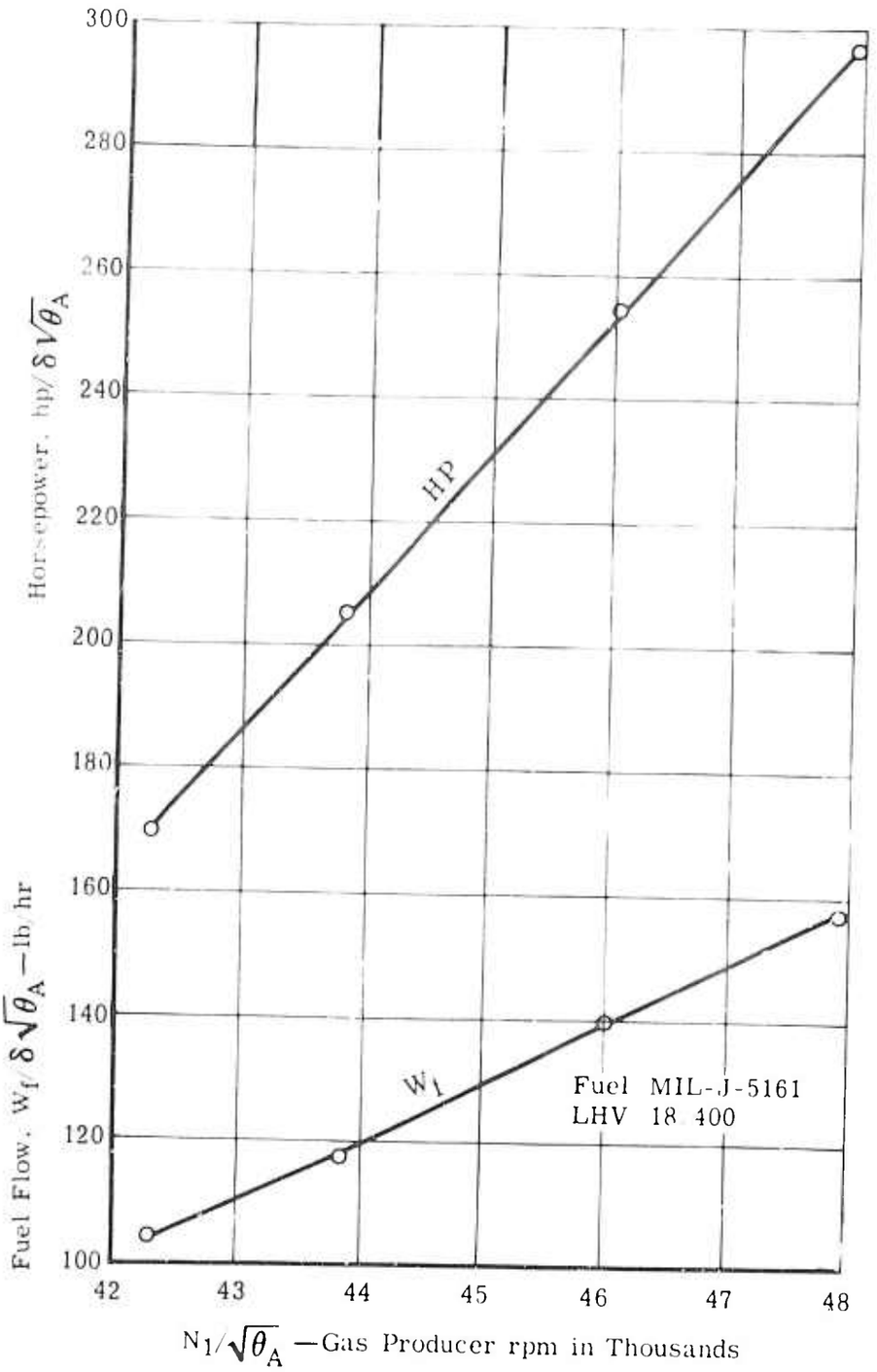

Figure 80. Test Data at Sea Level and -35 F.

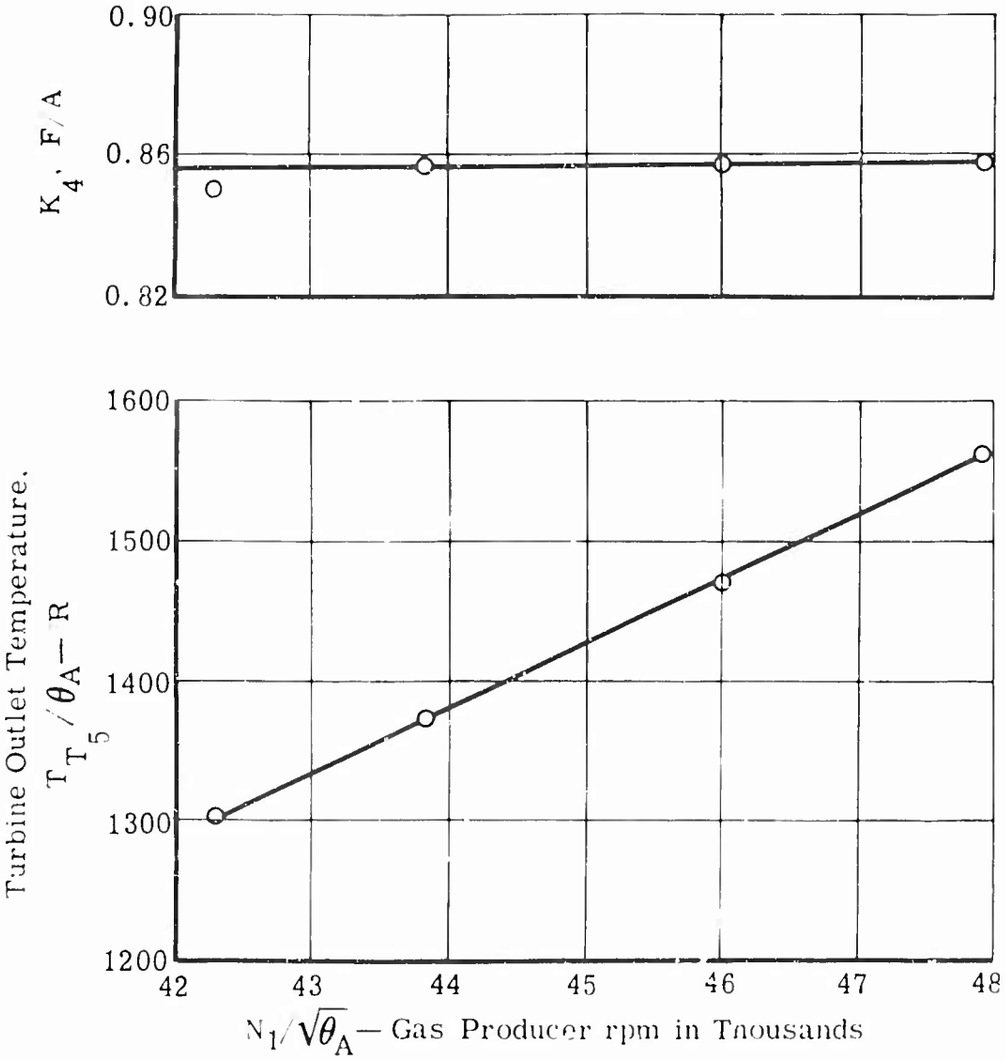

Figure 81. Test Data at Sea Level and -35° F.

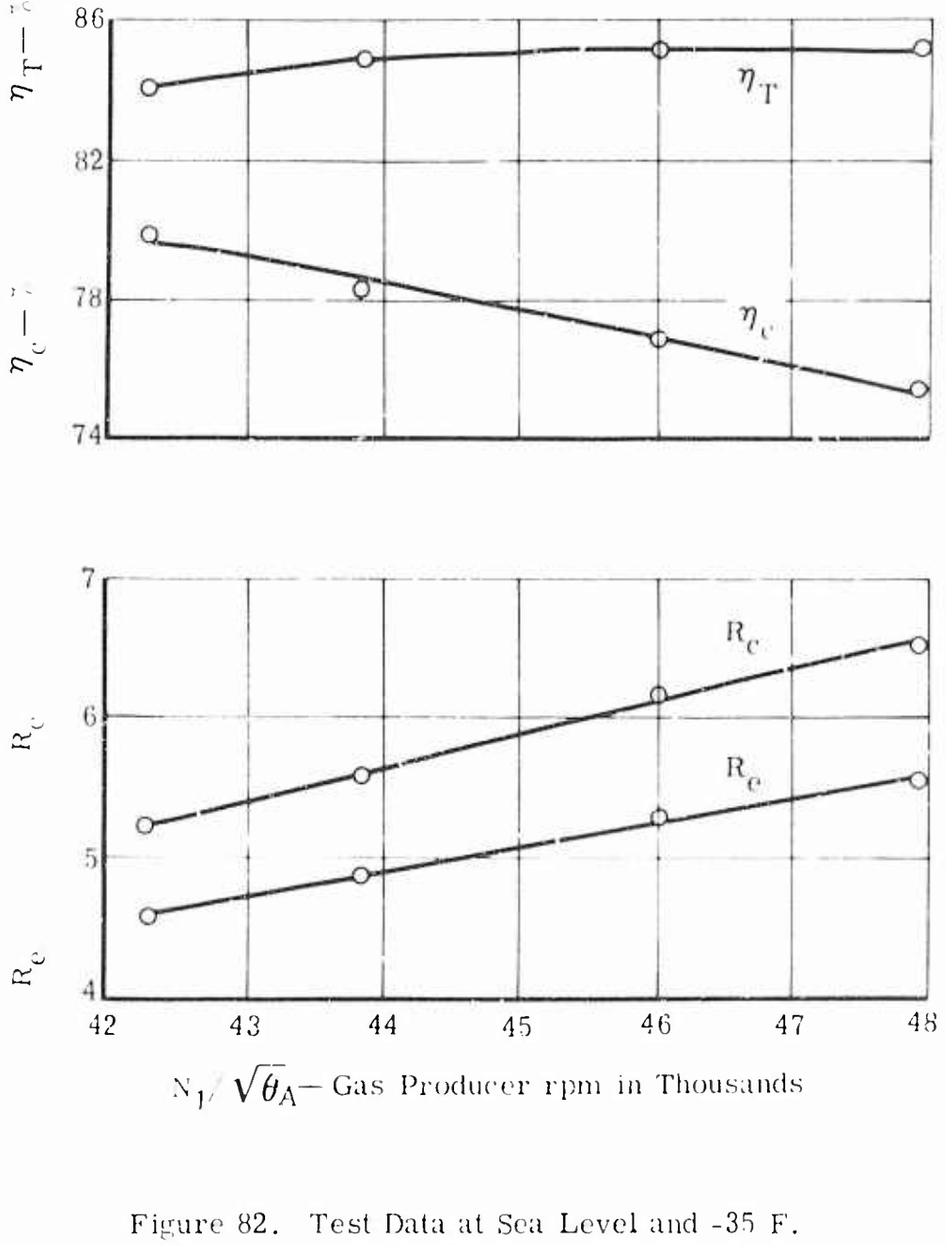

Figure 82. Test Data at Sea Level and -35 F.

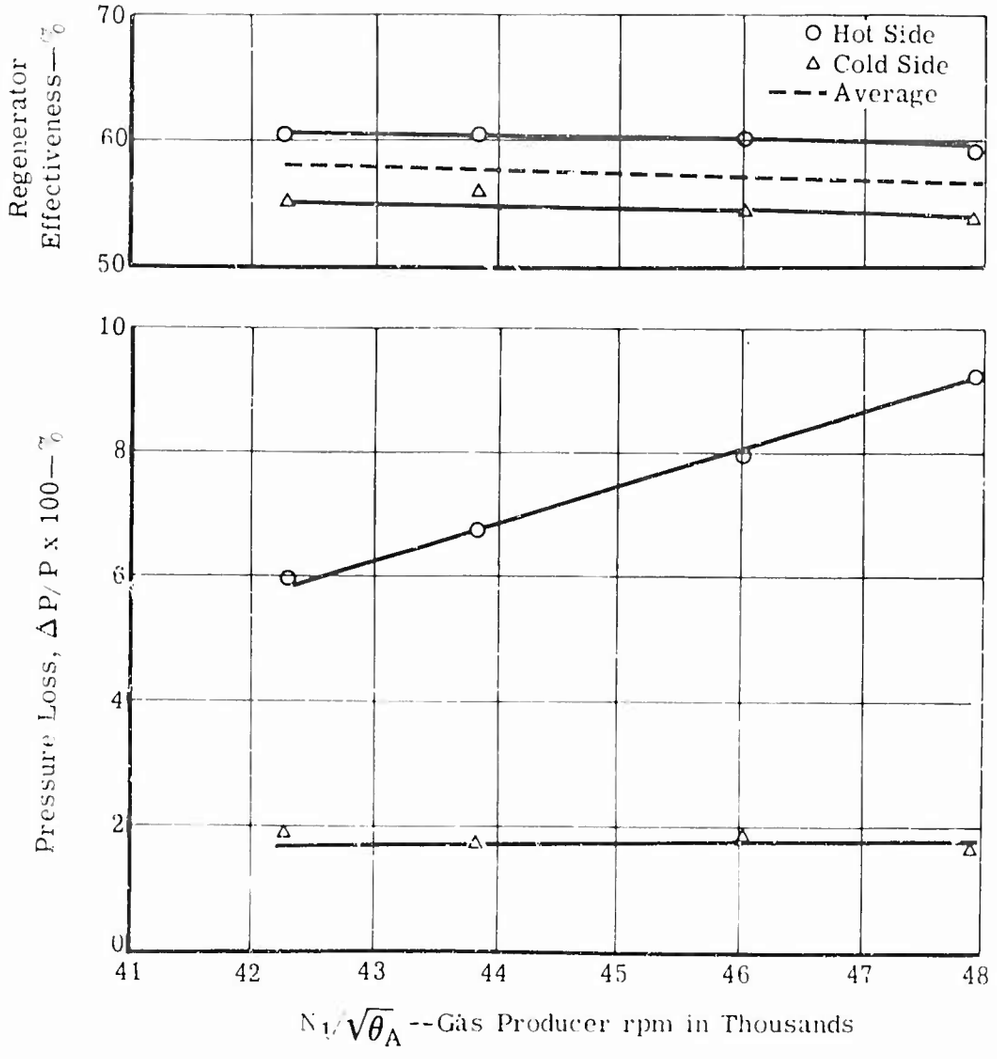

Figure 83. Test Data at Sea Level and -35°F.

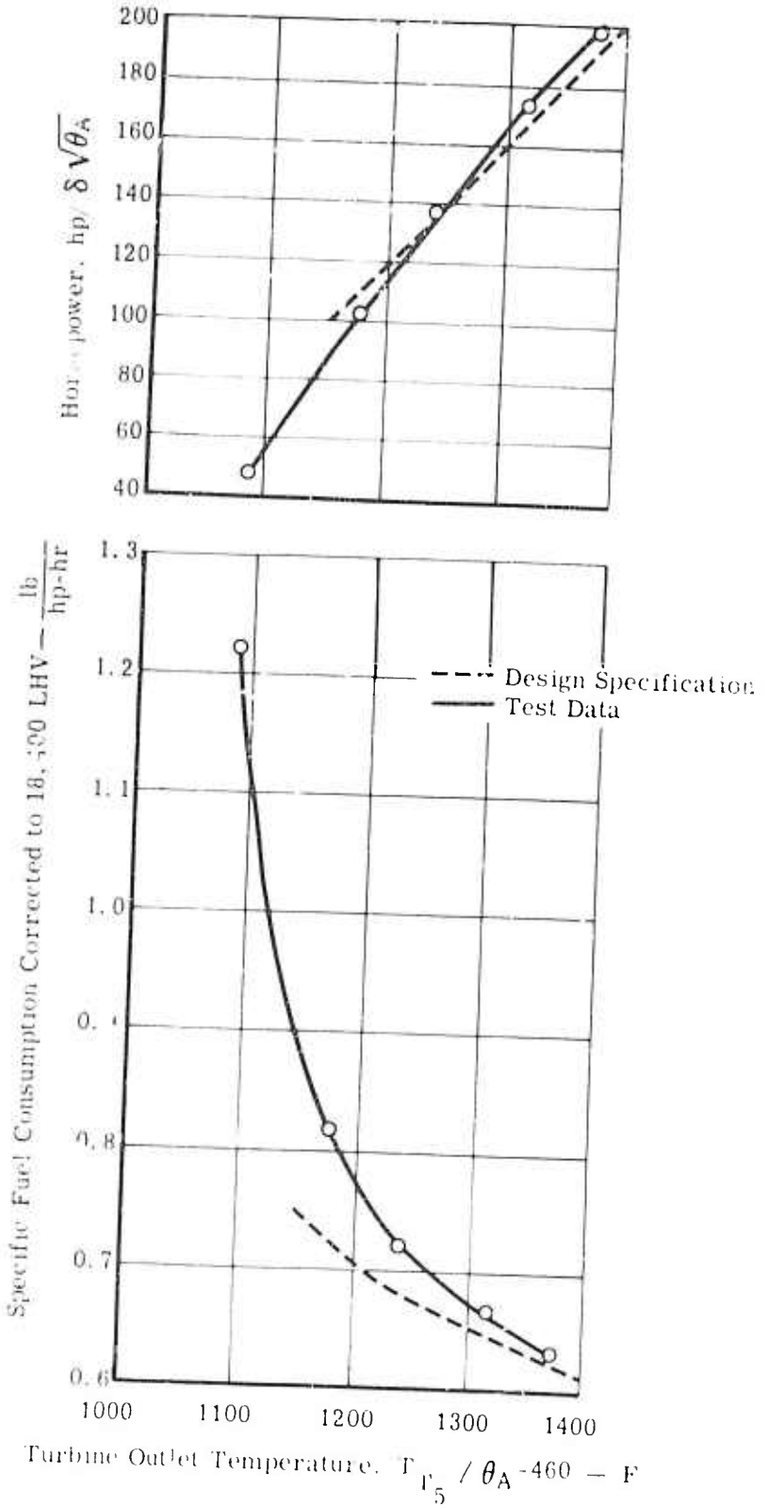

Figure 84. Test Data at Sea Level and +130°F.

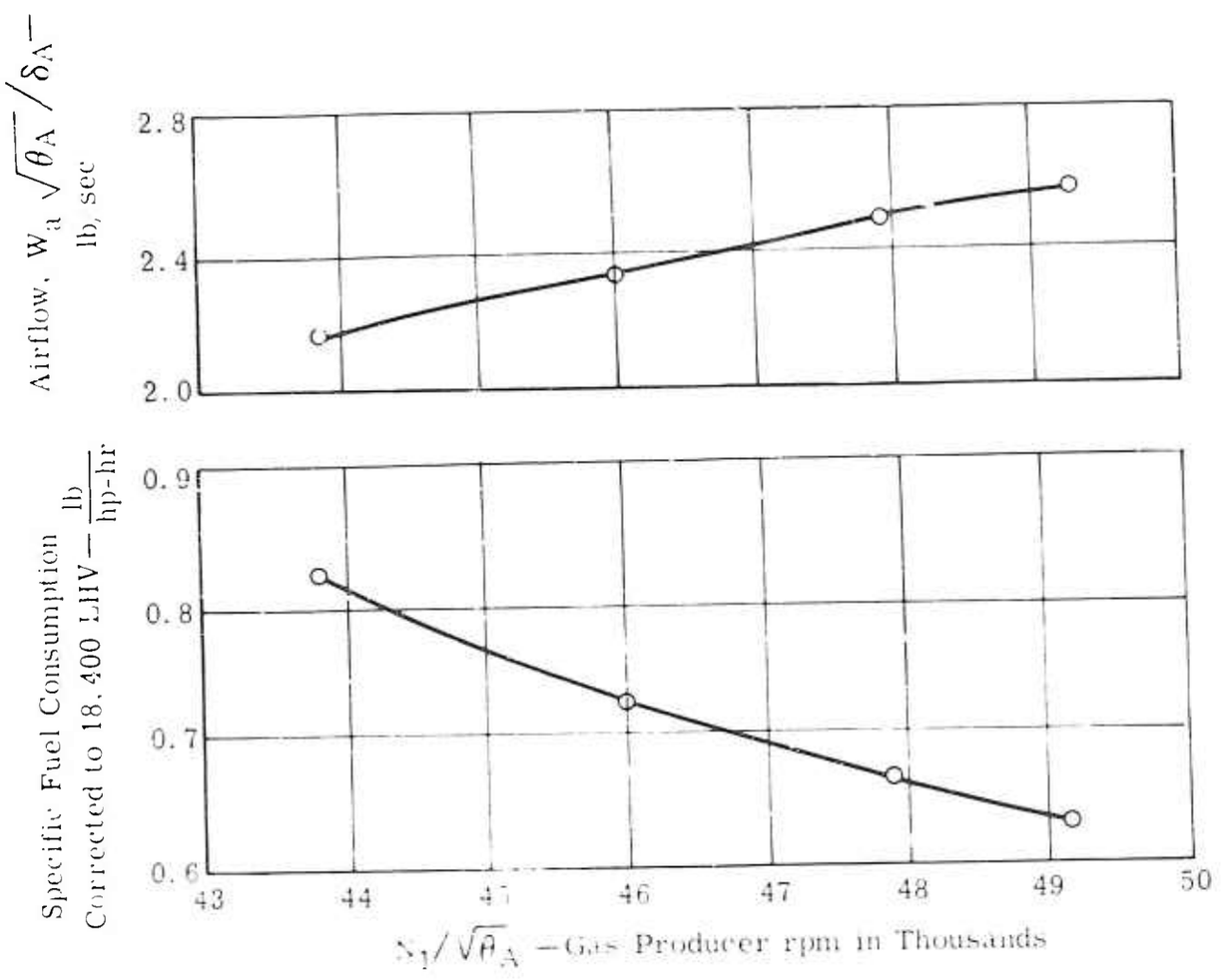

Figure 65. Test Data at Sea Level and -130 F.

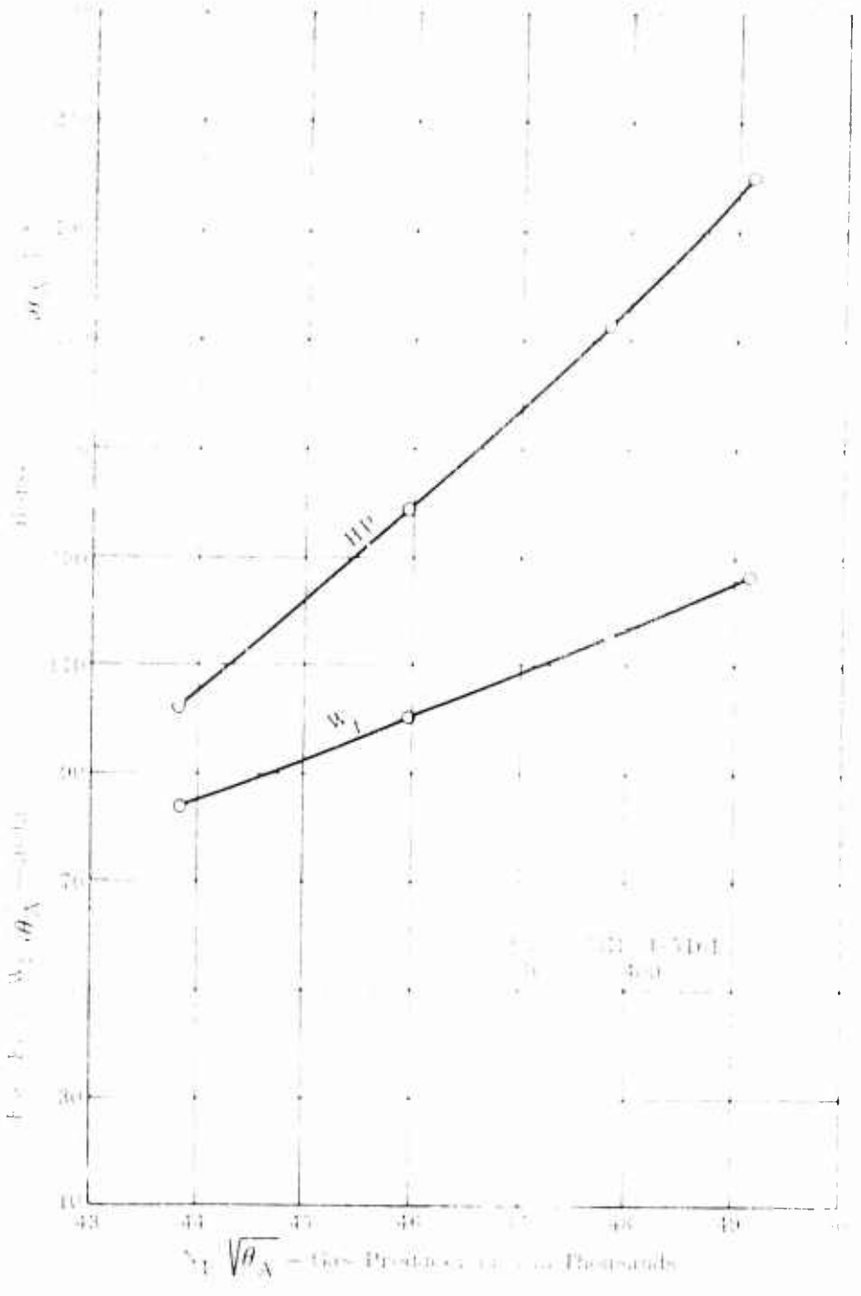

Figure 86. Test Data at Sea Level and +130 F.

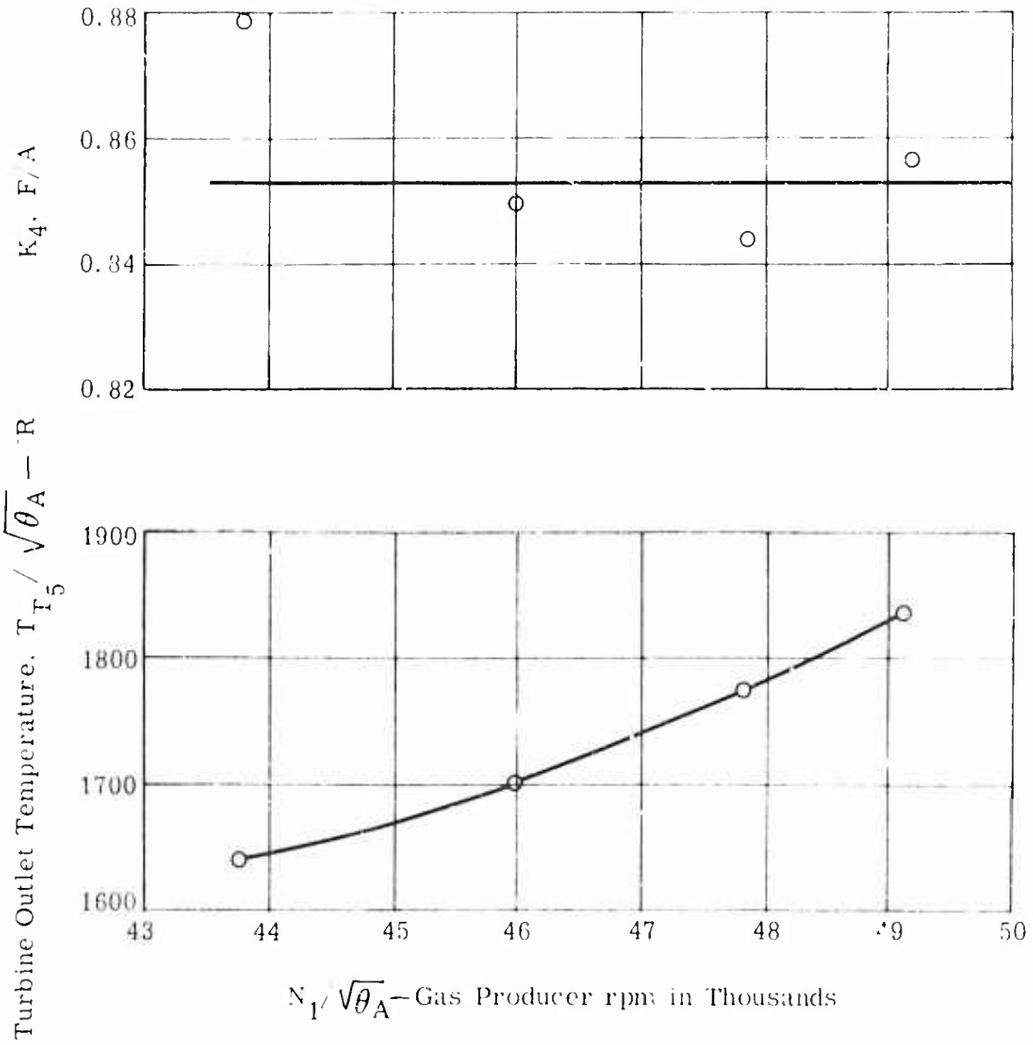

Figure 87. Test Data at Sea Level and +130°F.

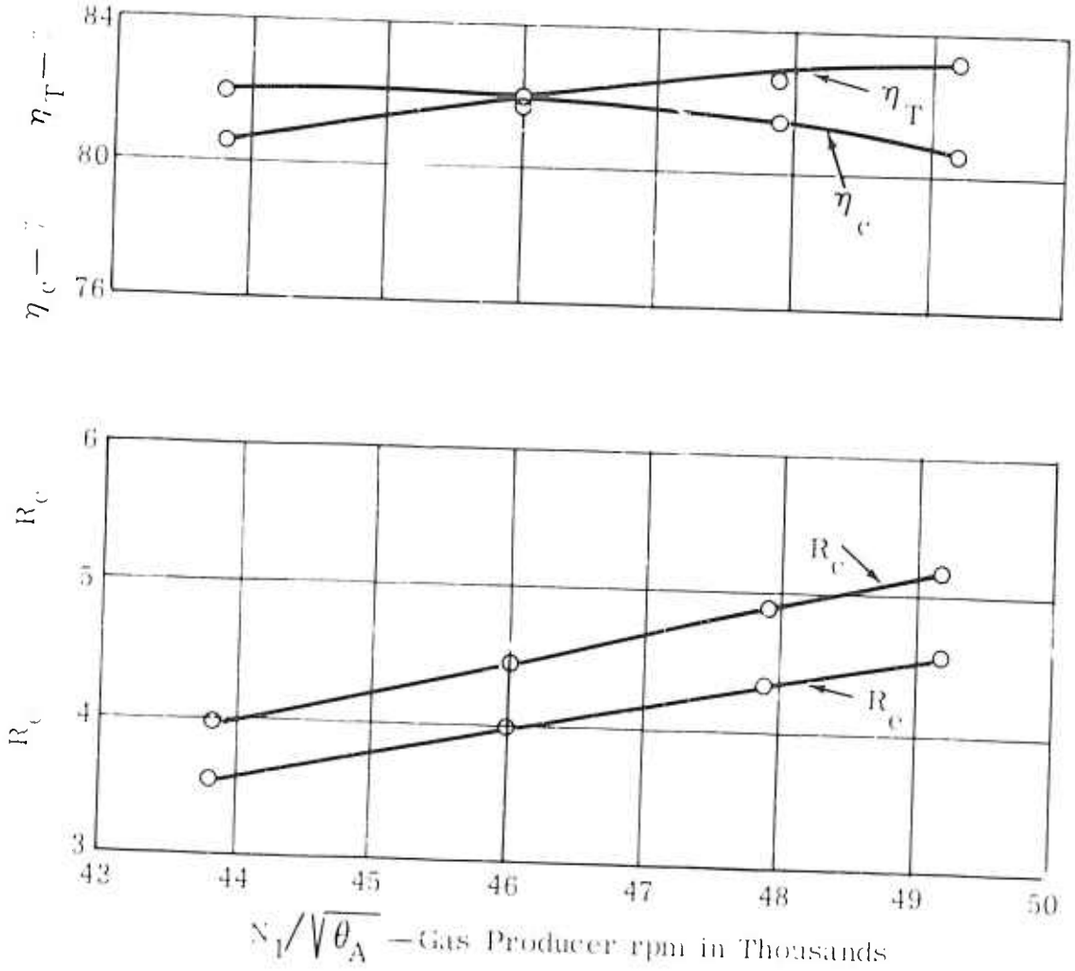

Figure 88. Test Data at Sea Level and +130 F.

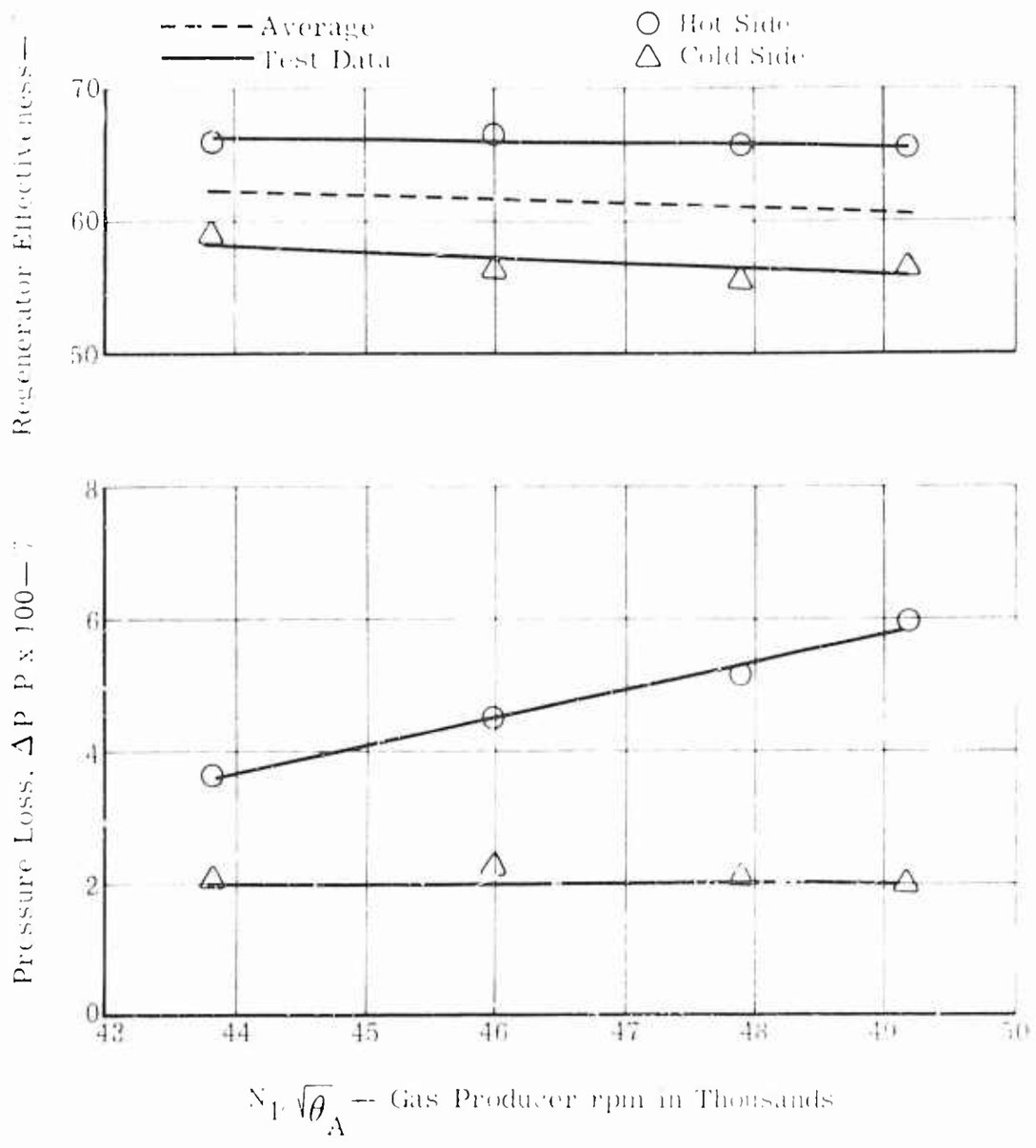

Figure 89. Test Data at Sea Level and +130 F.

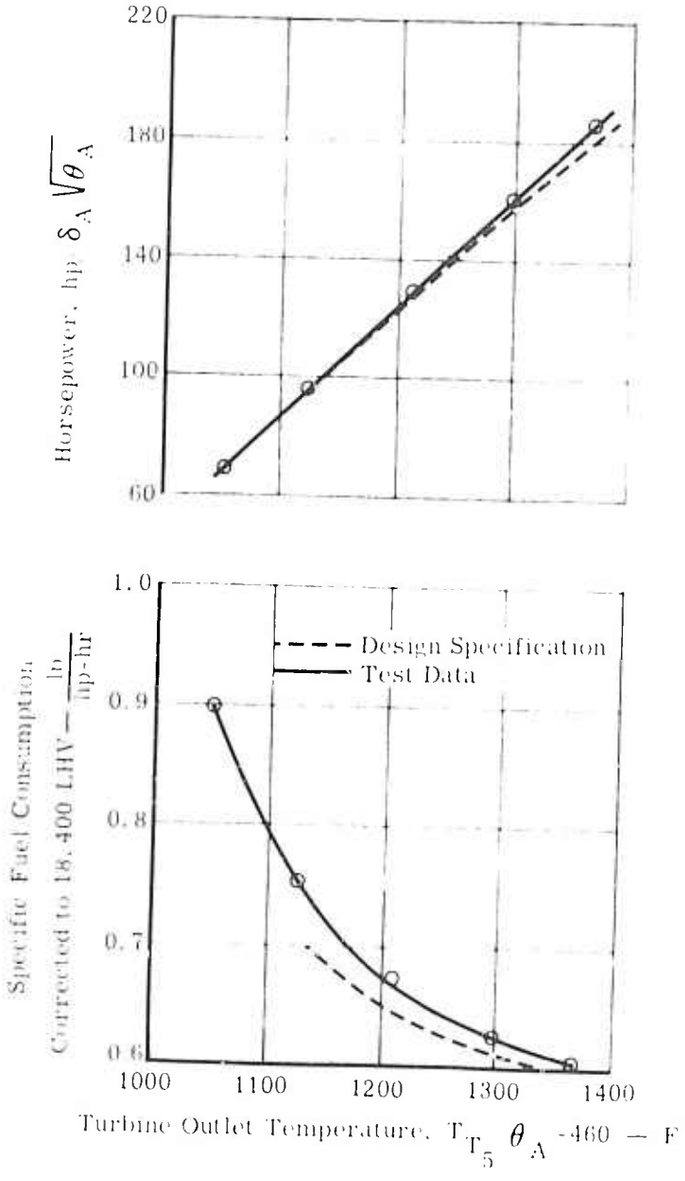

Figure 90. Test Data at 6000 Feet and 95 F.

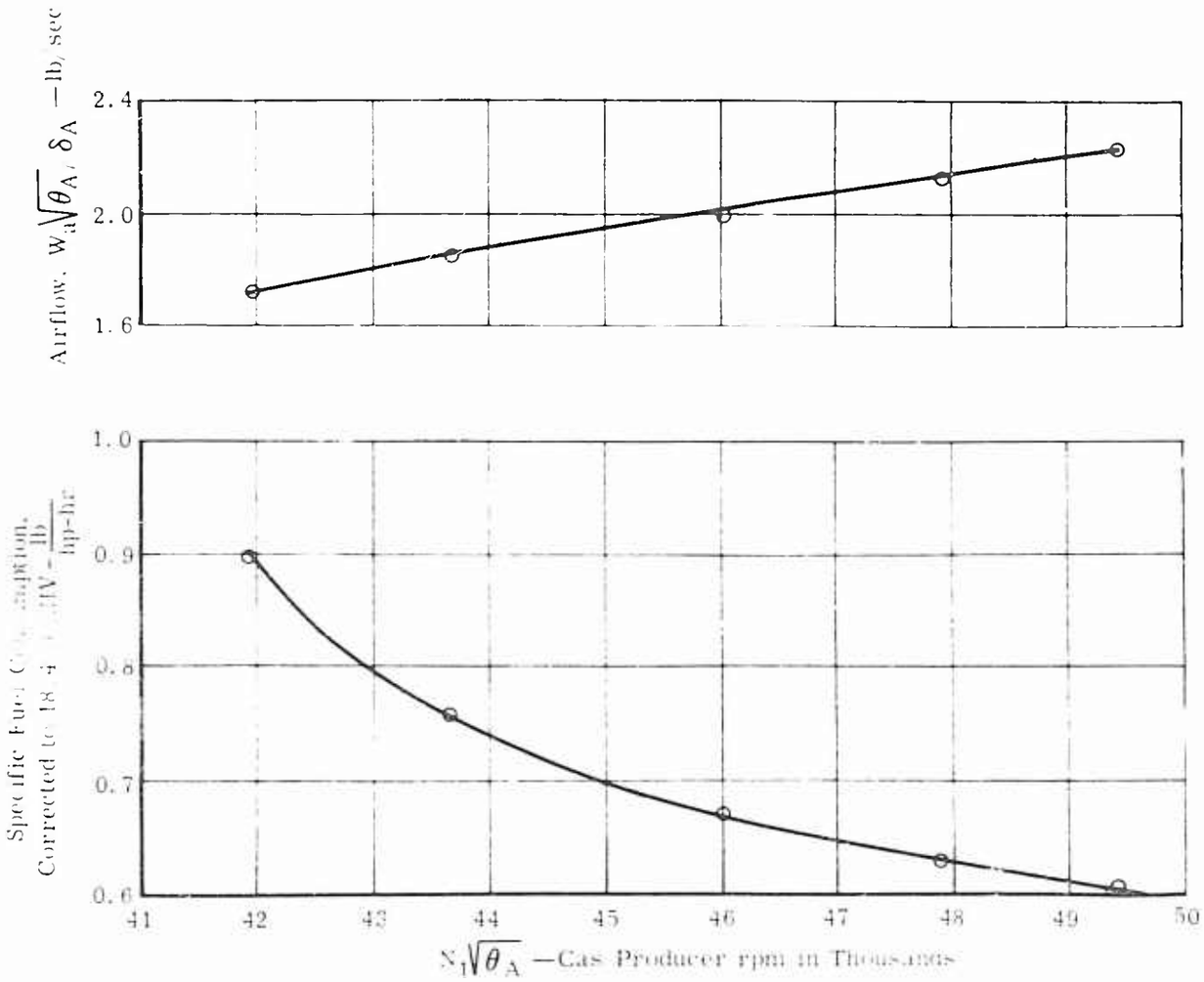

Figure 91. Test Data at 6000 Feet and 95 F.

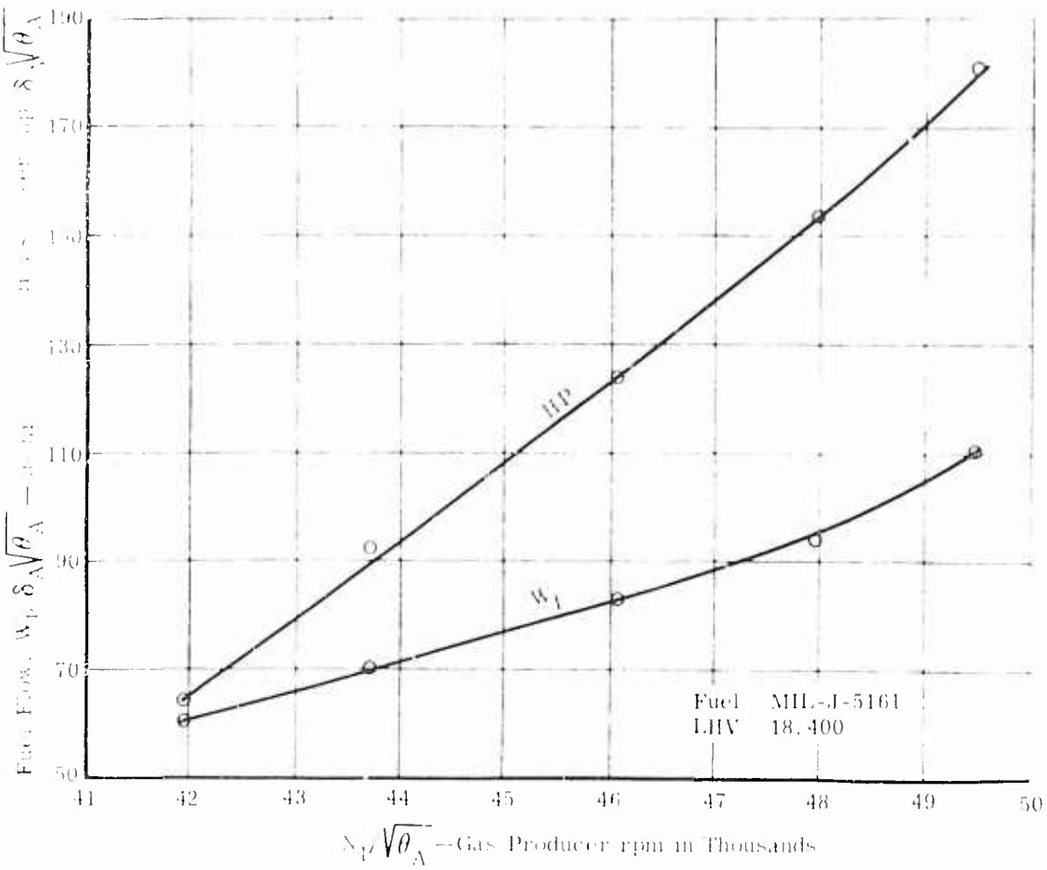

Figure 92. Test Data at 6000 Feet and 95 F.

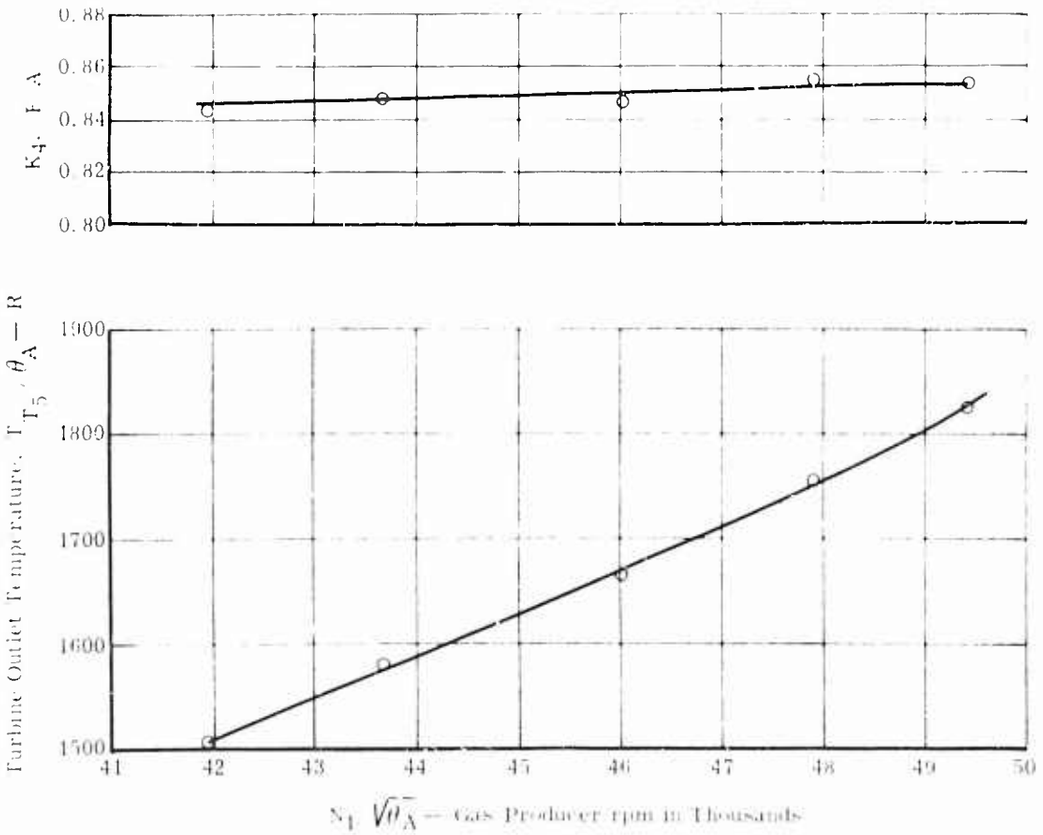

Figure 93. Test Data at 6000 Feet and 95 F.

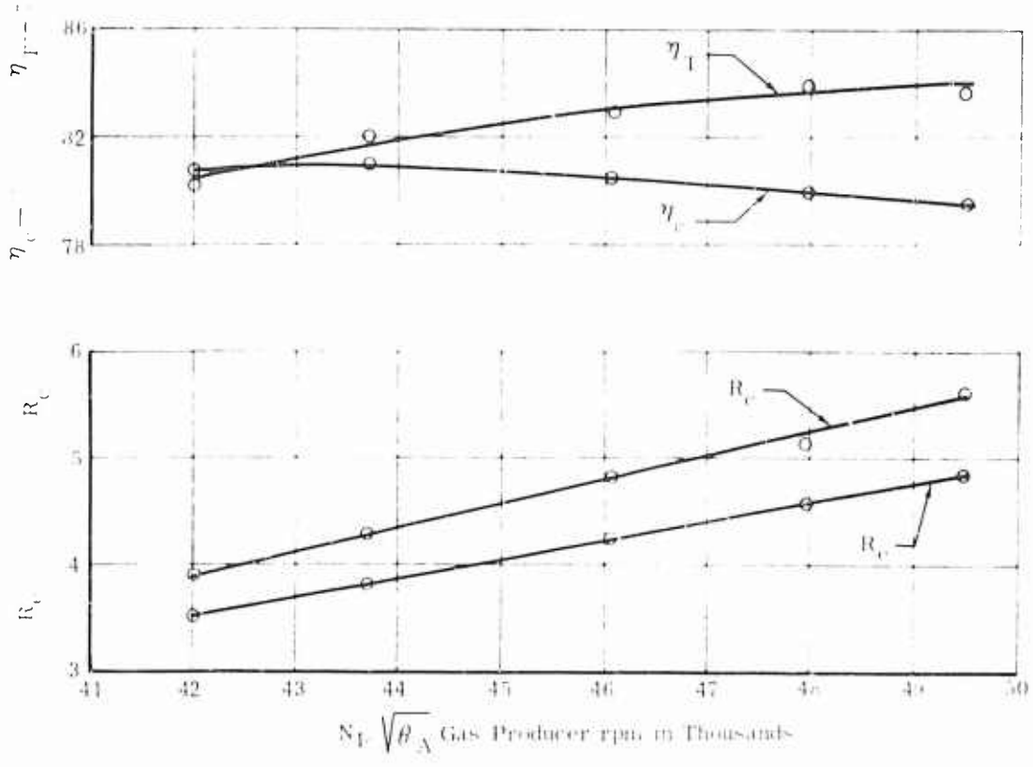

Figure 94. Test Data at 6000 Feet and 95 F.

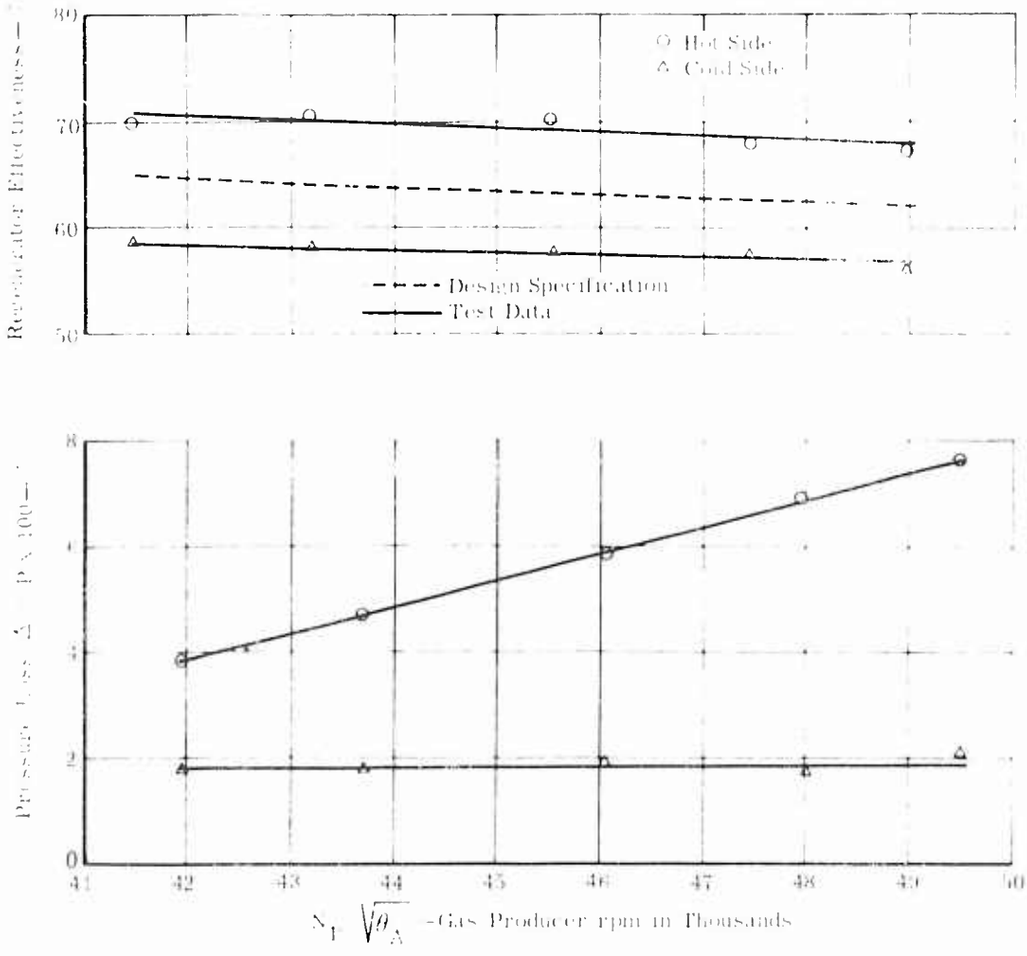

Figure 95. Test Data at 6000 Feet and 95 F.

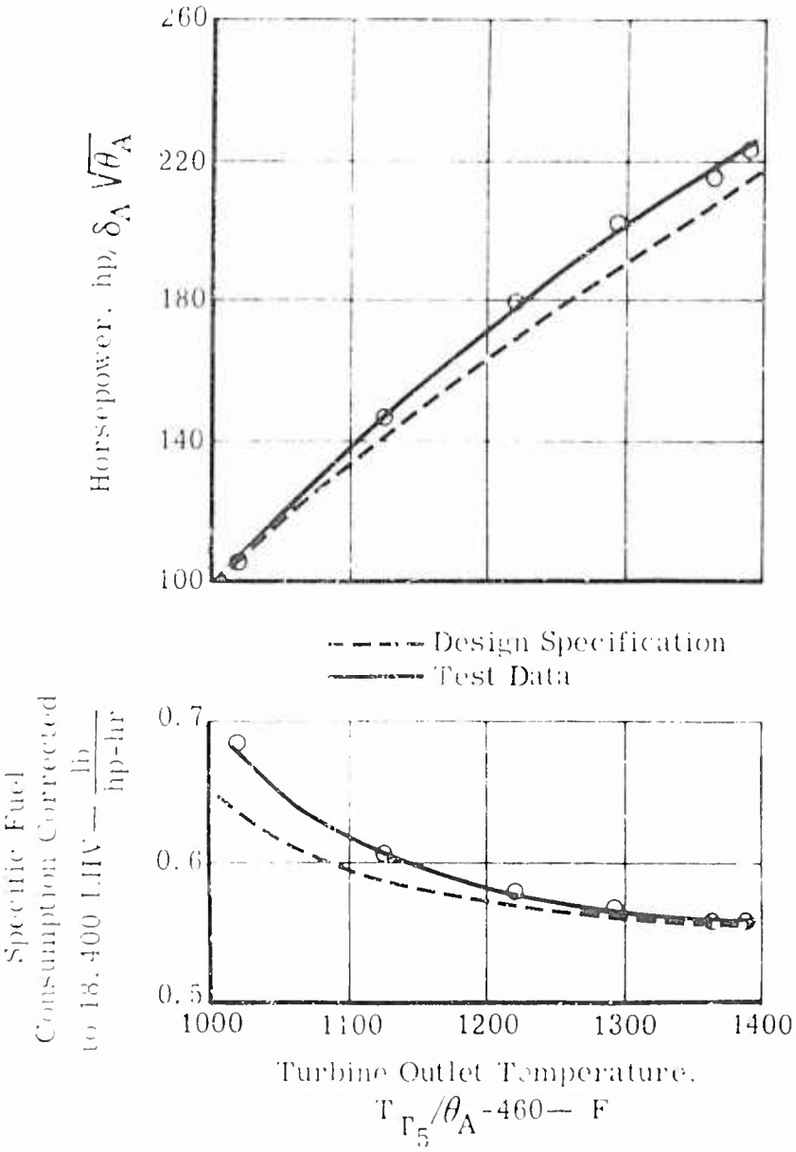

Figure 96. Test Data at 10,000 Feet and 23 F.

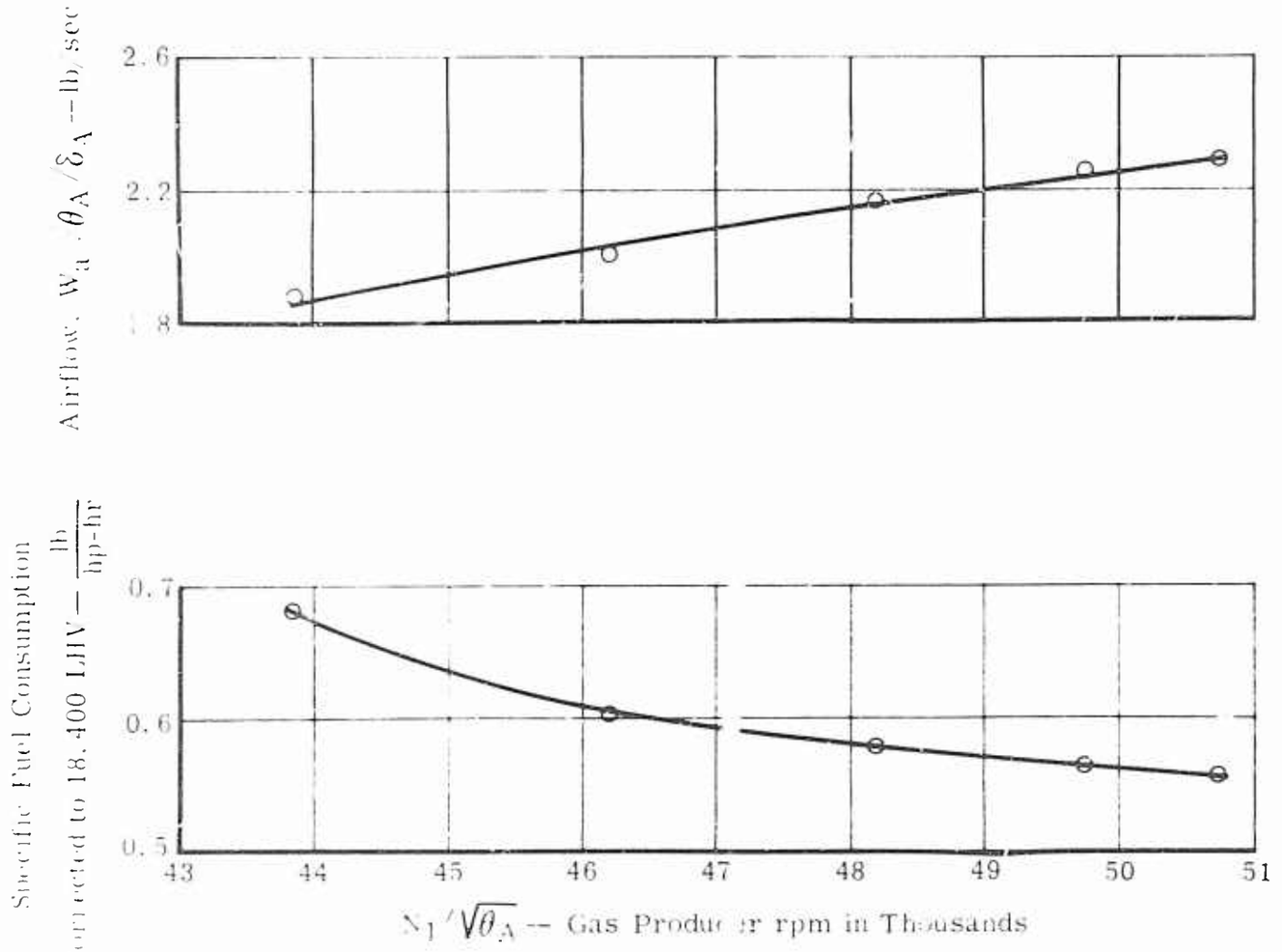

Figure 97. Test Data at 10,000 Feet and 23 F.

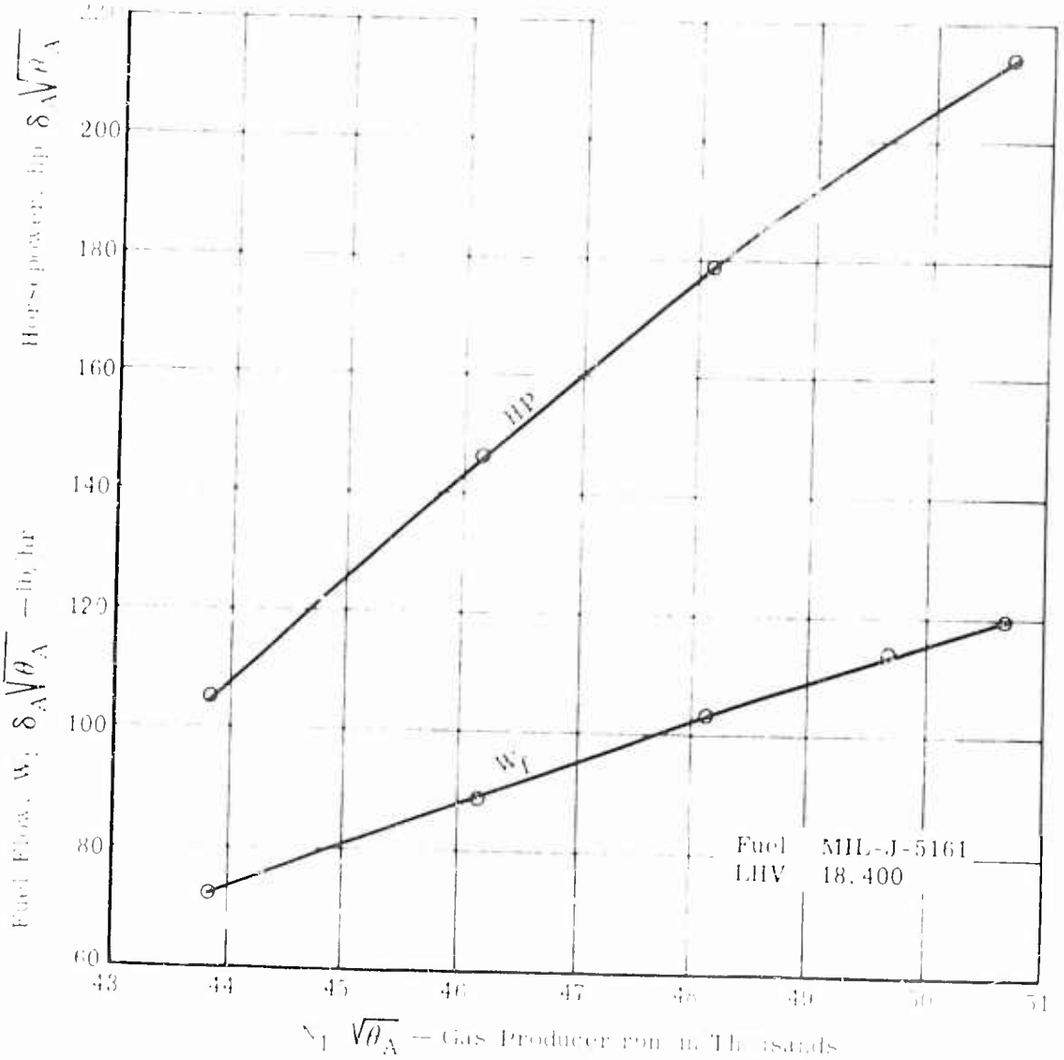

Figure 98. Test Data at 10,000 Feet and 23 F.

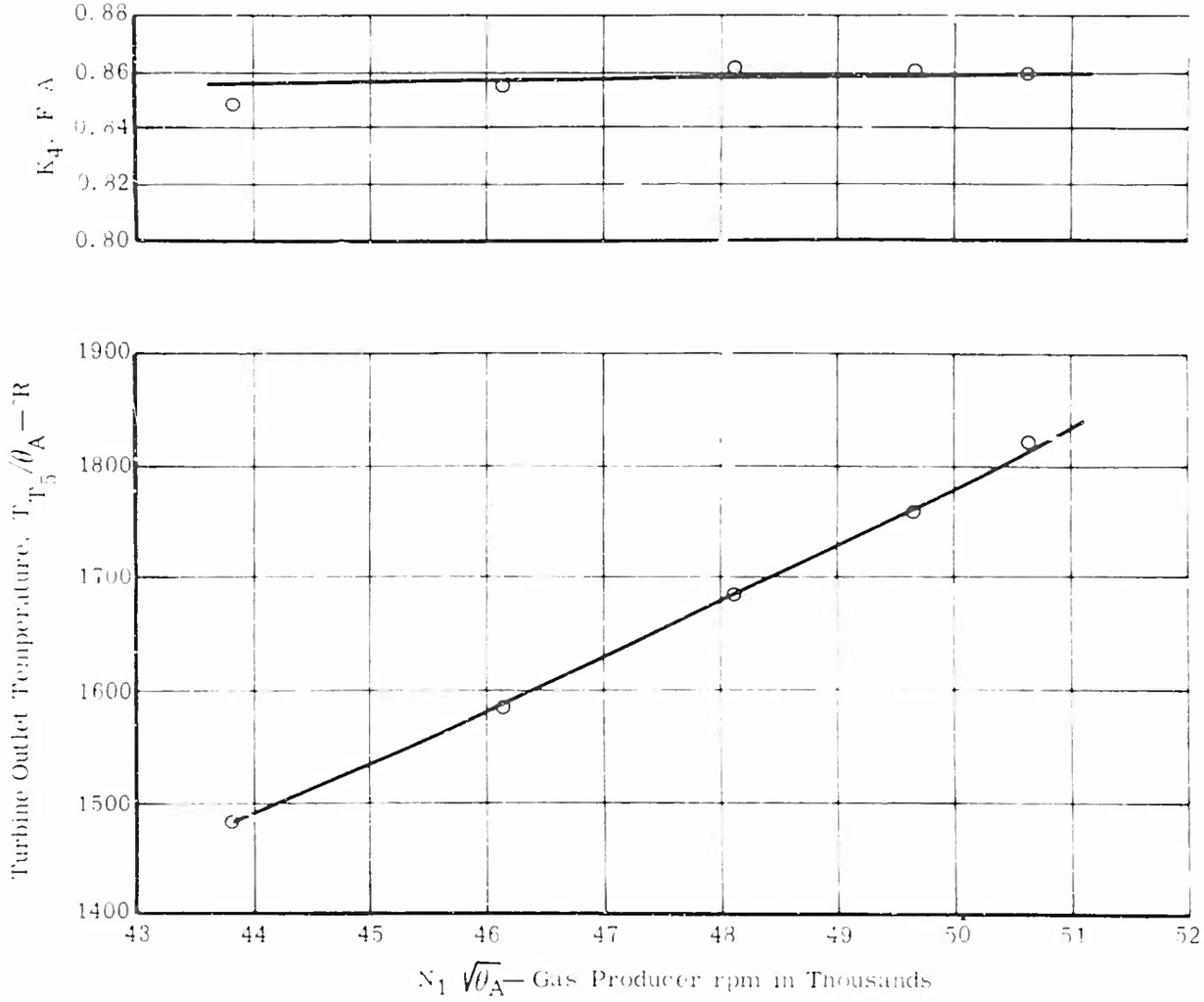

Figure 99. Test Data at 10,000 Feet and 23 F.

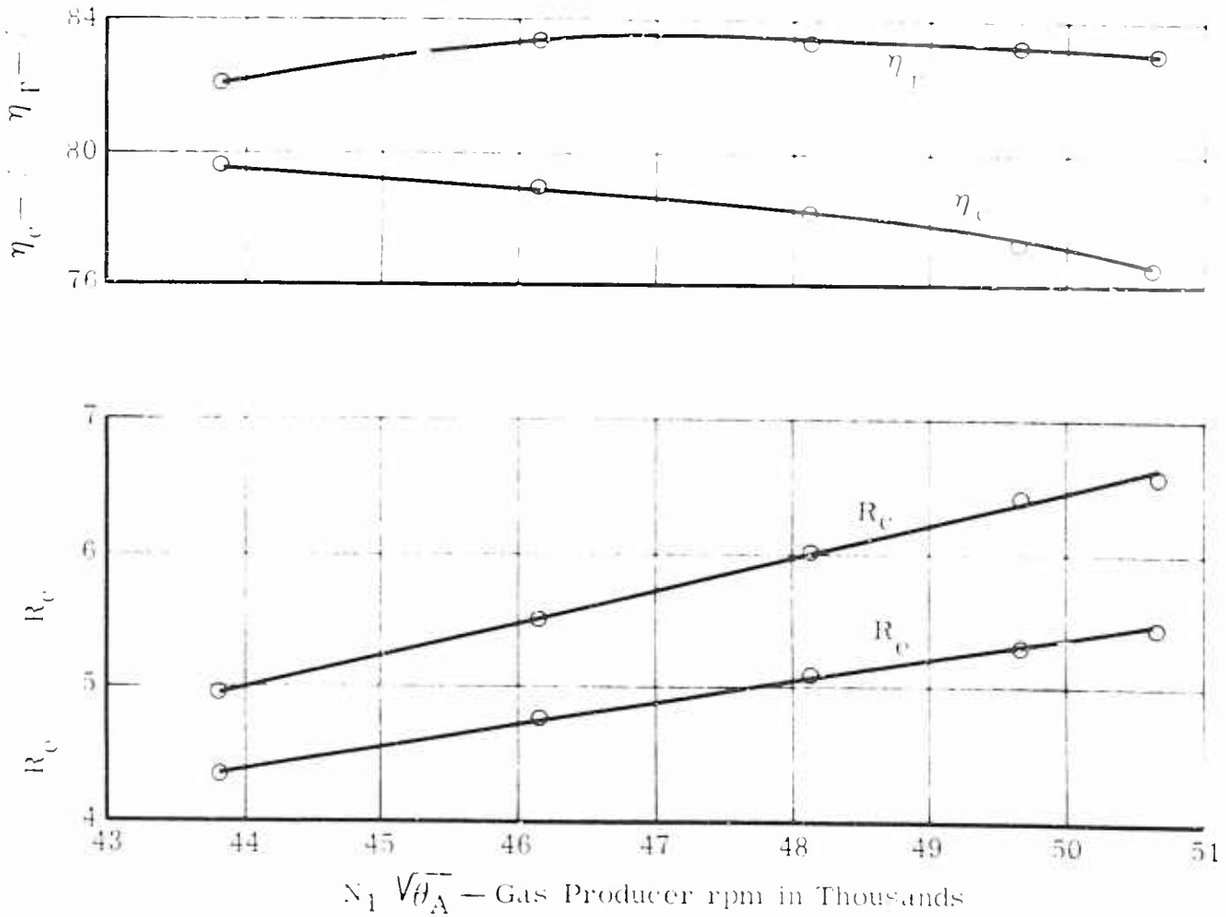

Figure 100. Test Data at 10,000 Feet and 23 F.

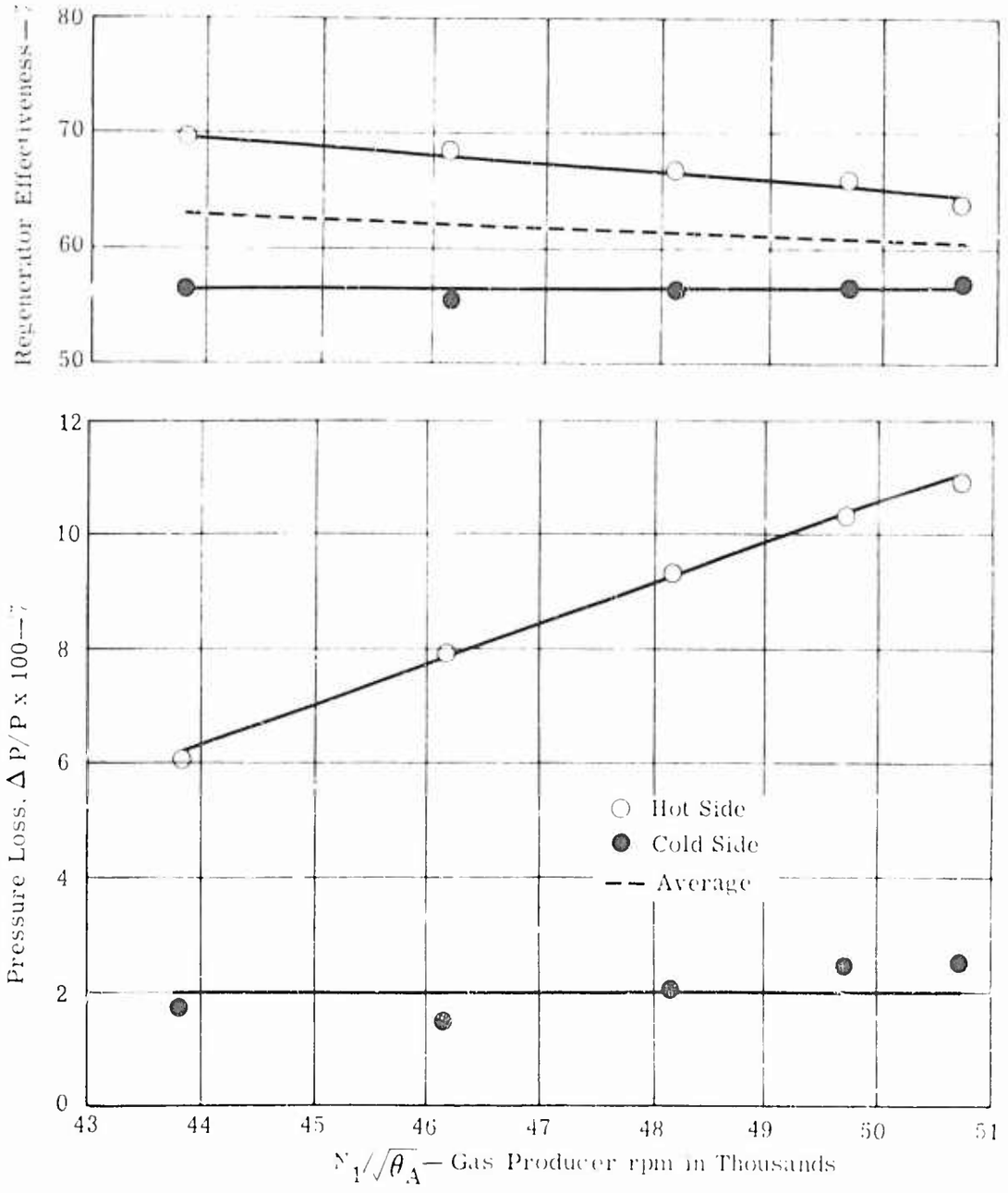

Figure 101. Test Data at 10,000 Feet and 23 F.

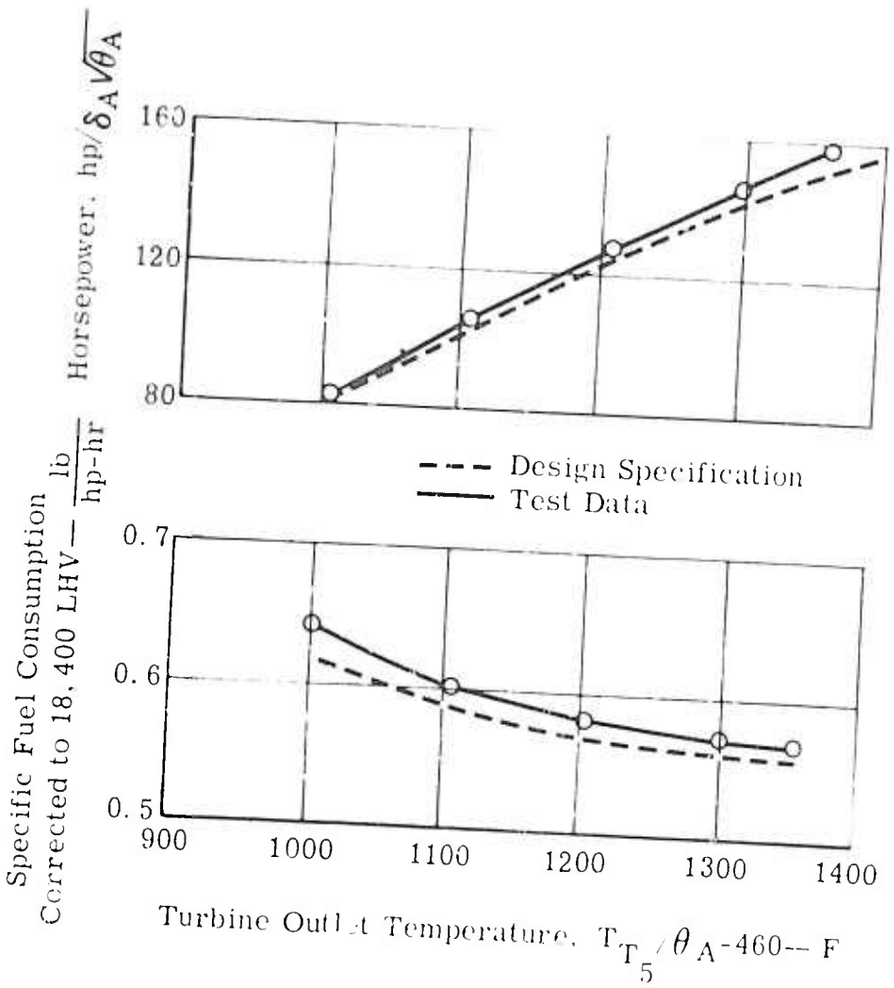

Figure 102. Test Data at 20,000 Feet and -12 F.

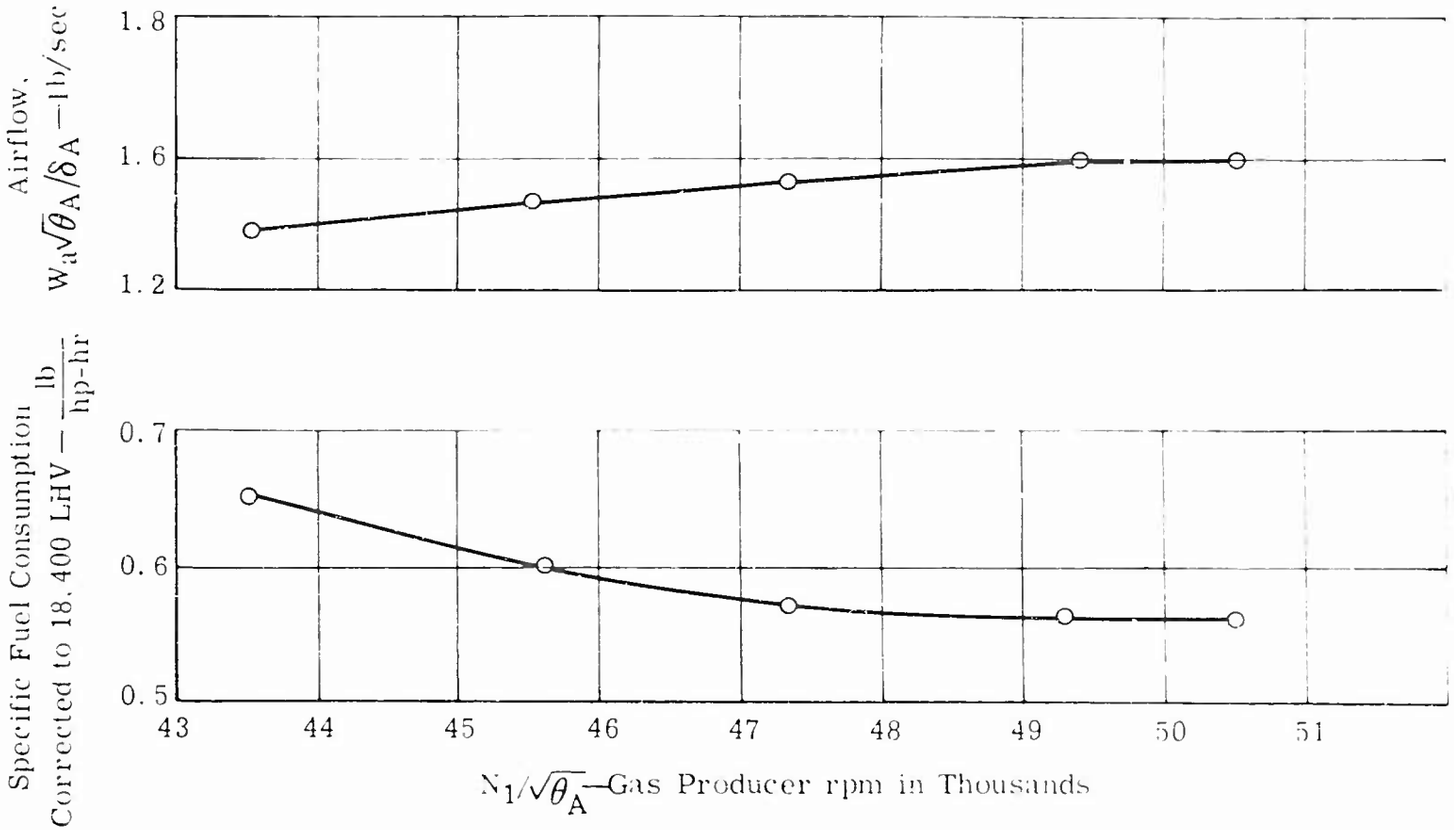

Figure 103. Test Data at 20,000 Feet and -12°F.

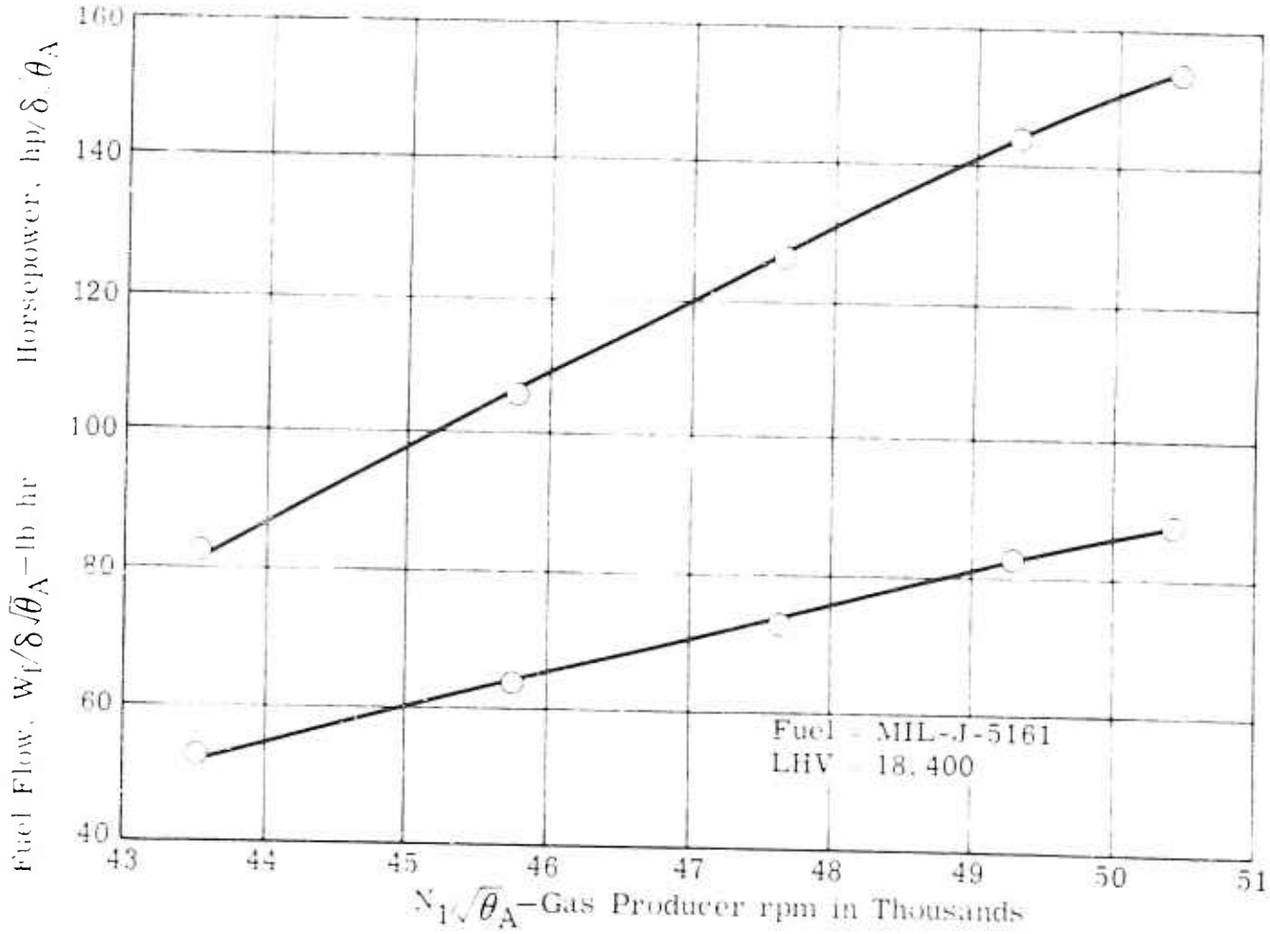

Figure 104. Test Data at 20,000 Feet and -12°F.

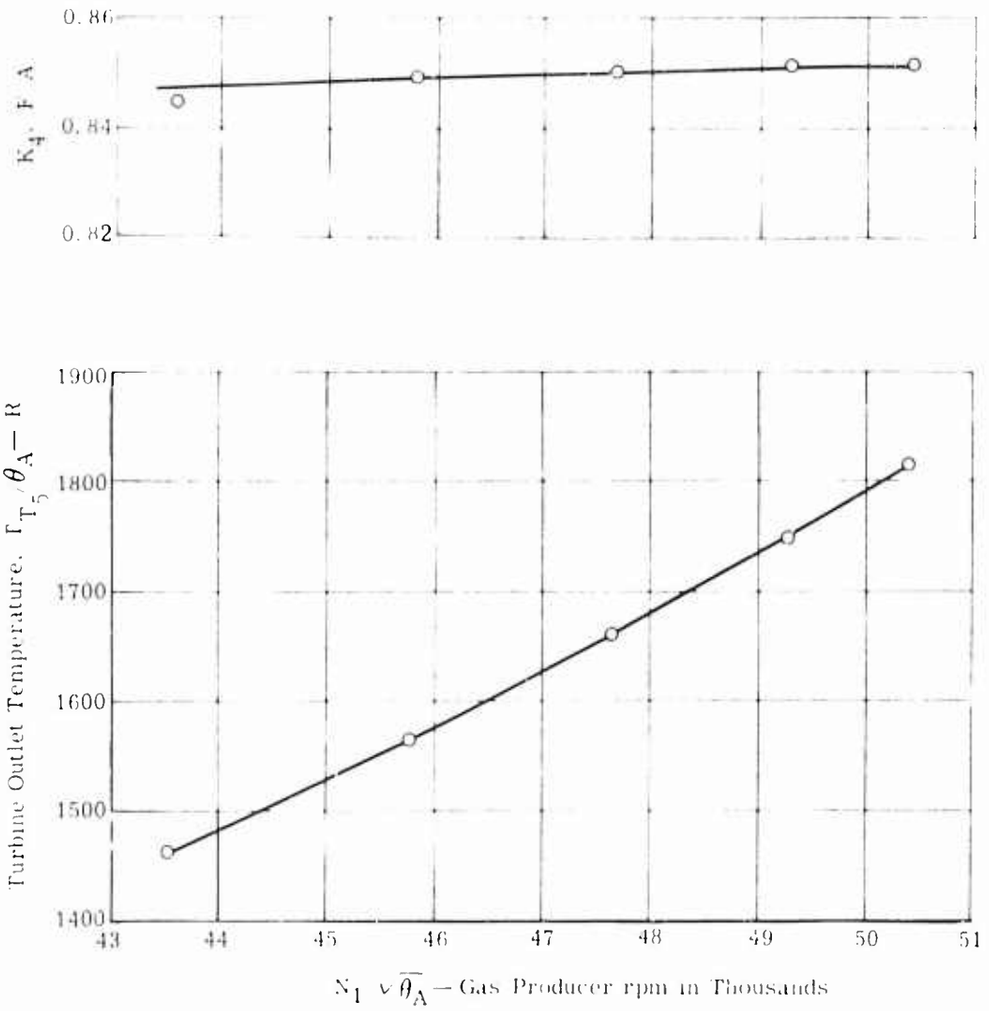

Figure 105. Test Data at 20,000 Feet and -12 F.

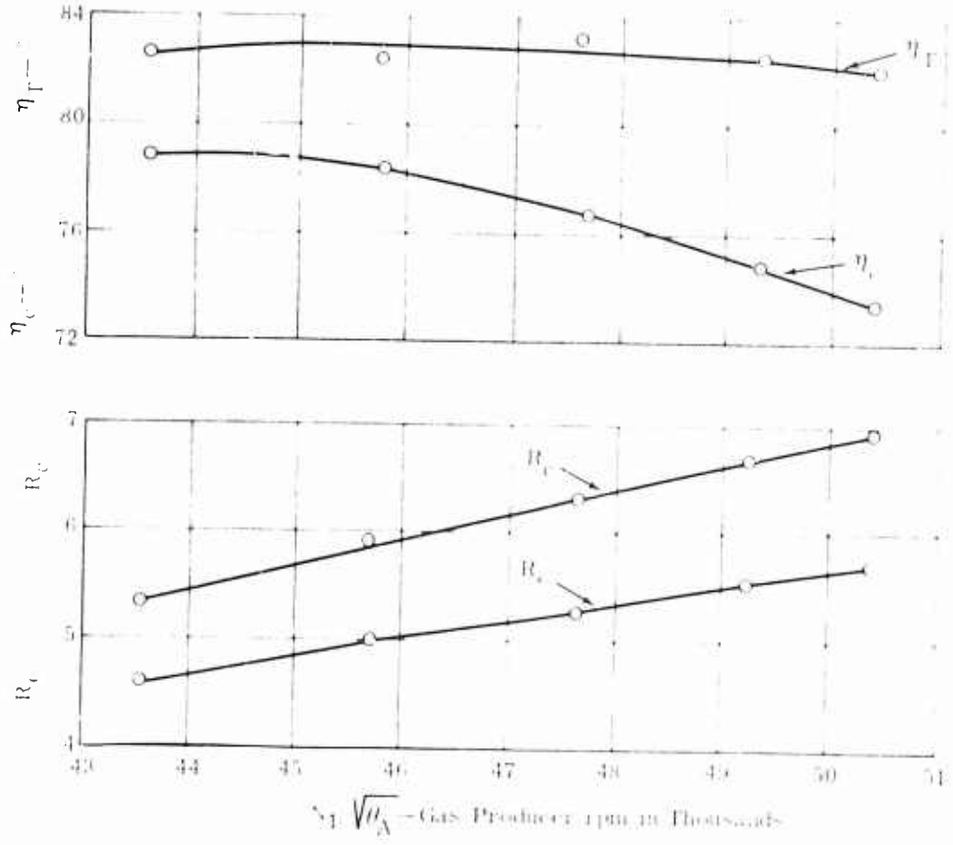

Figure 106. Test Data at 20,000 Feet and -12° F.

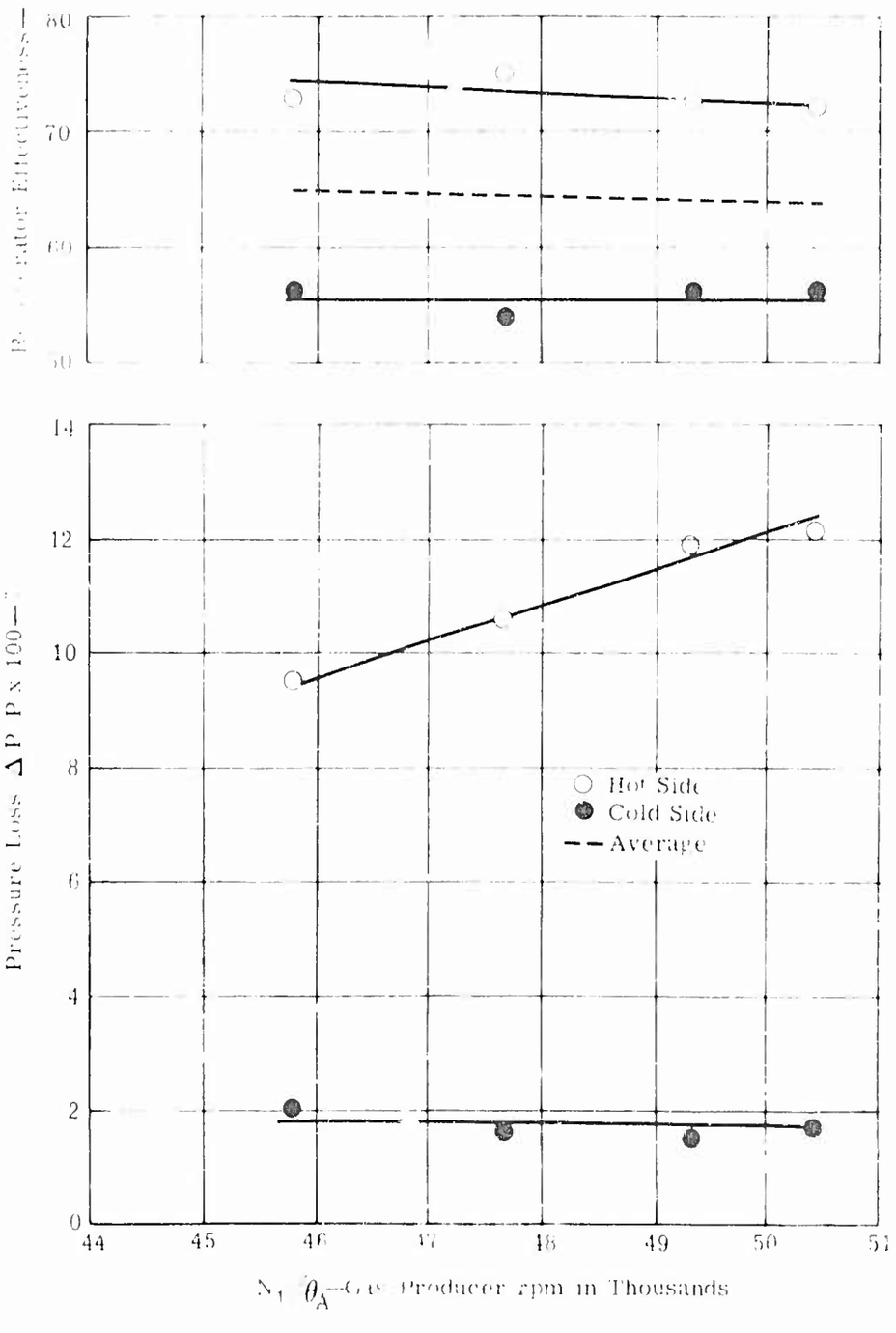

ource 107. T[illegible] 060

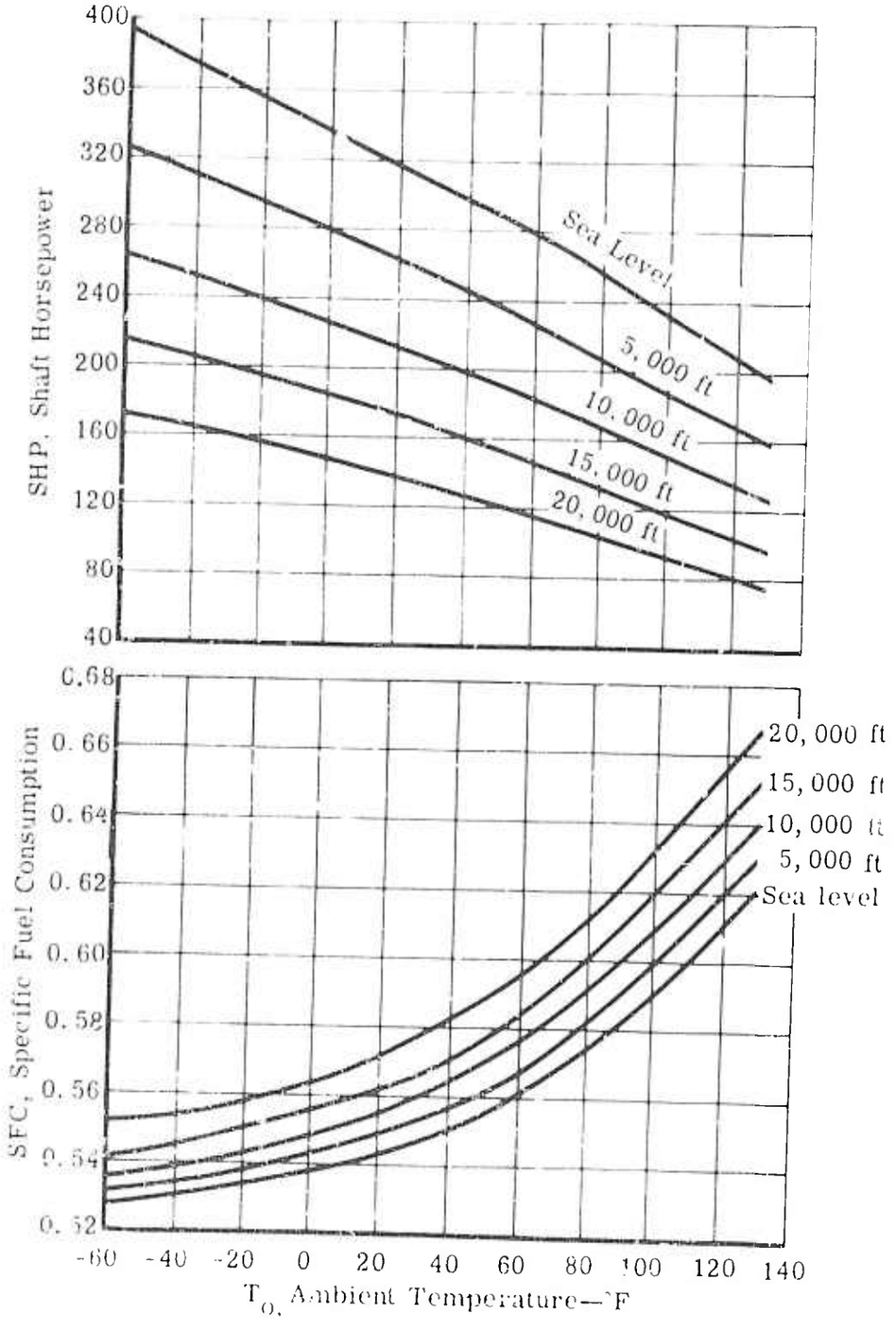

Figure 108. Calculated Engine Performance at Takeoff and Military Power.

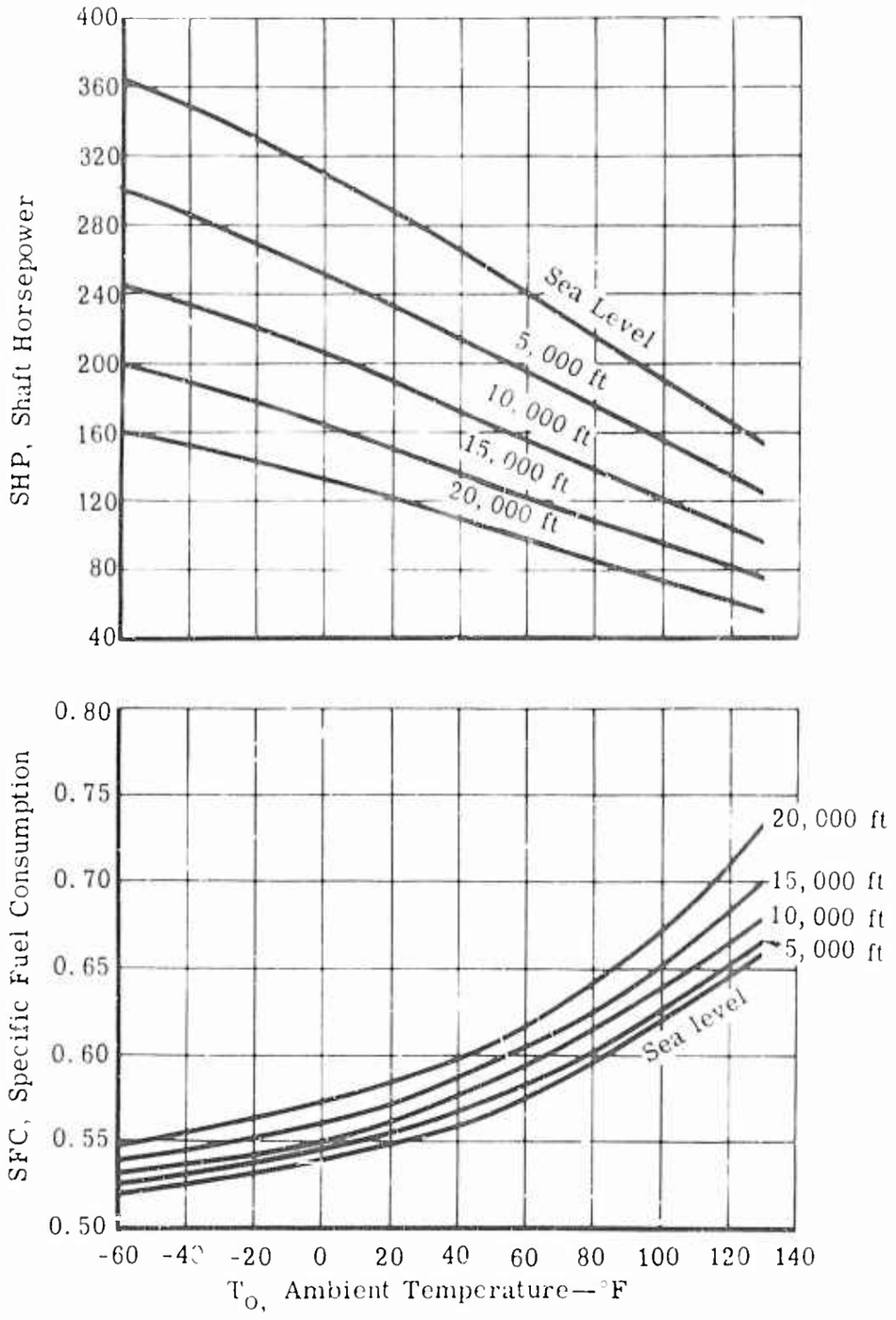

Figure 109. Calculated Engine Performance at Normal Power.

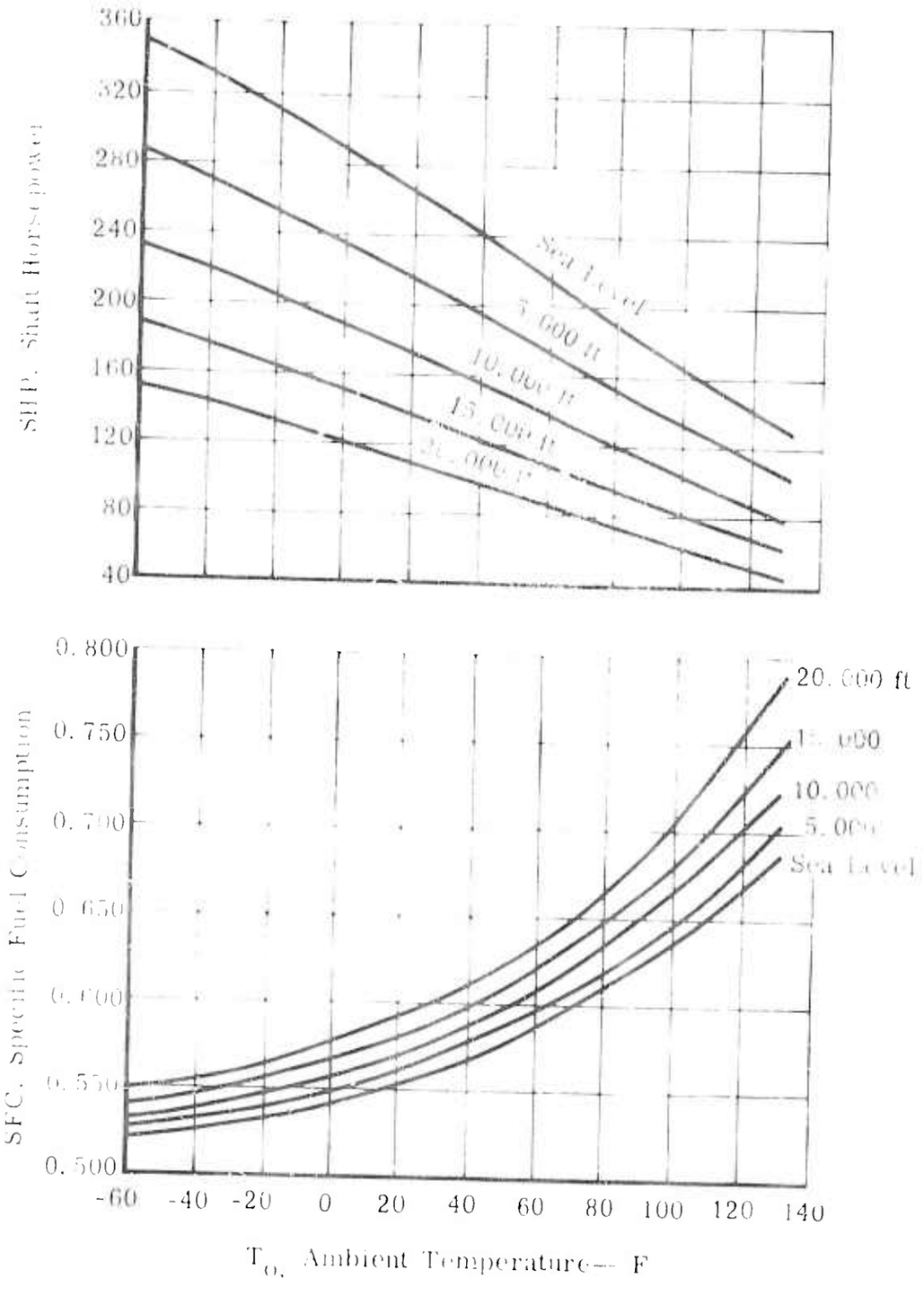

Figure 110. Calculated Engine Performance at 90% Normal Power.

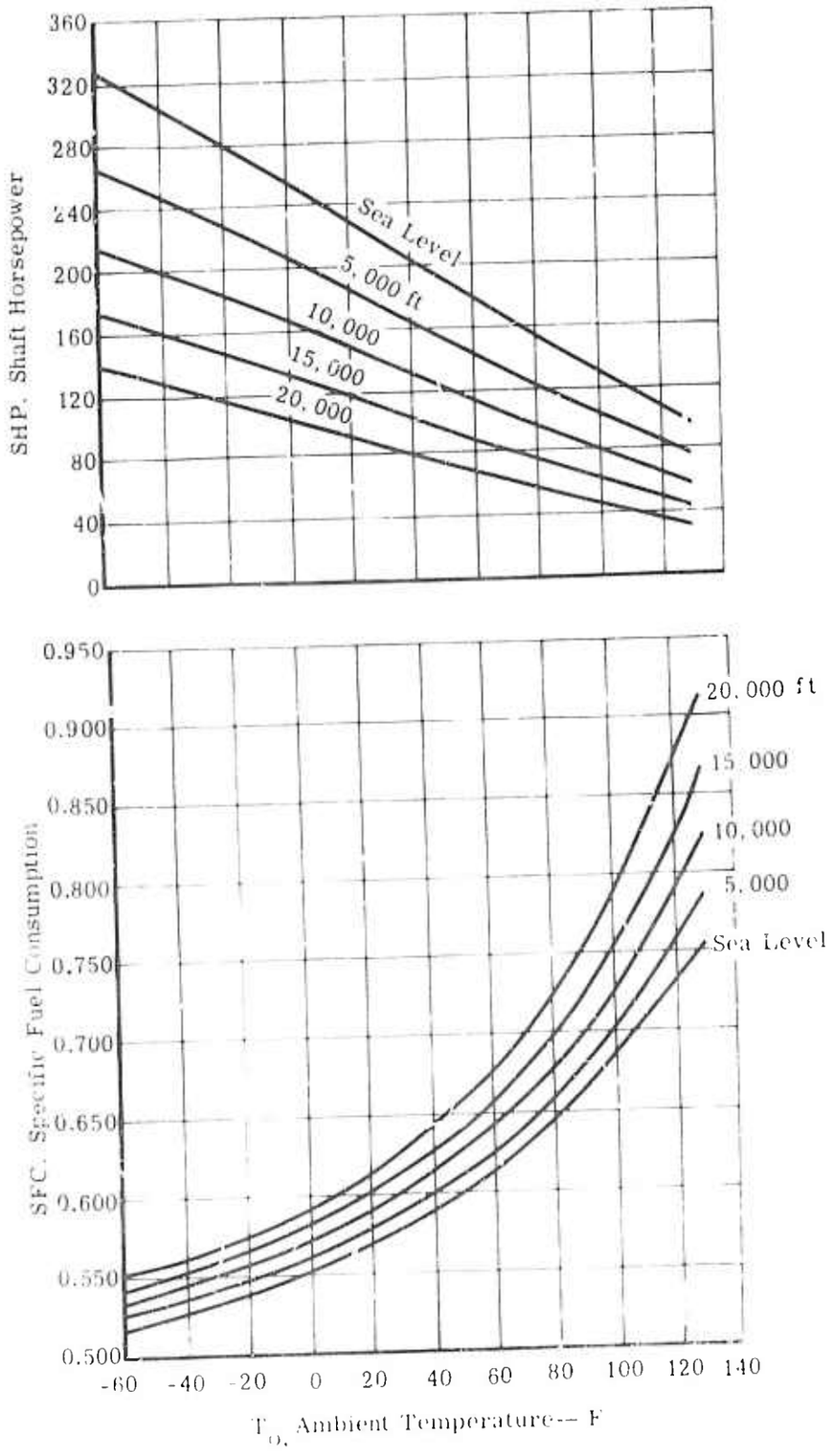

Figure 111 Calculated Engine Performance at [illegible]

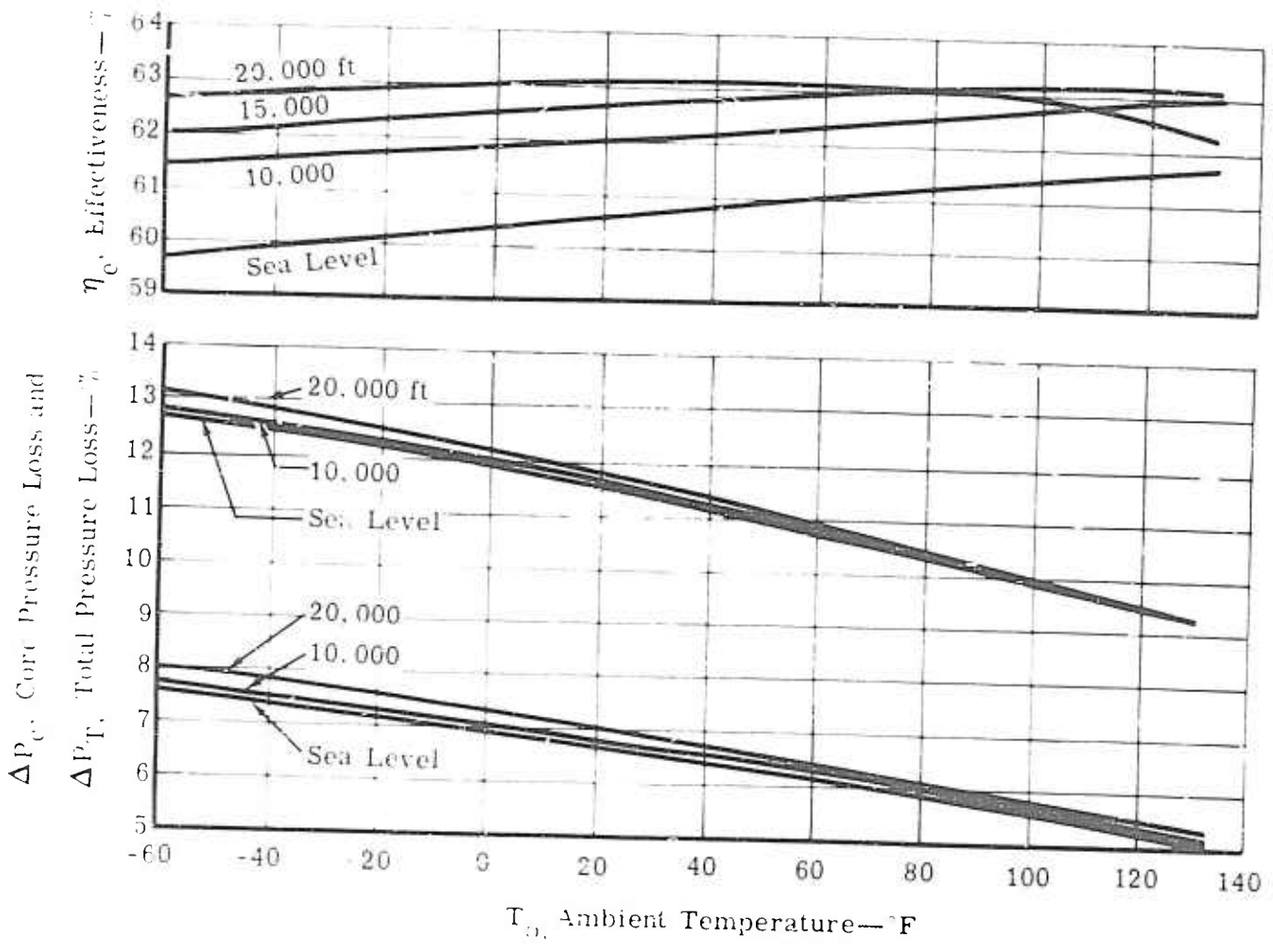

Figure 112. Calculated Regenerator Performance at Takeoff and Military Power.

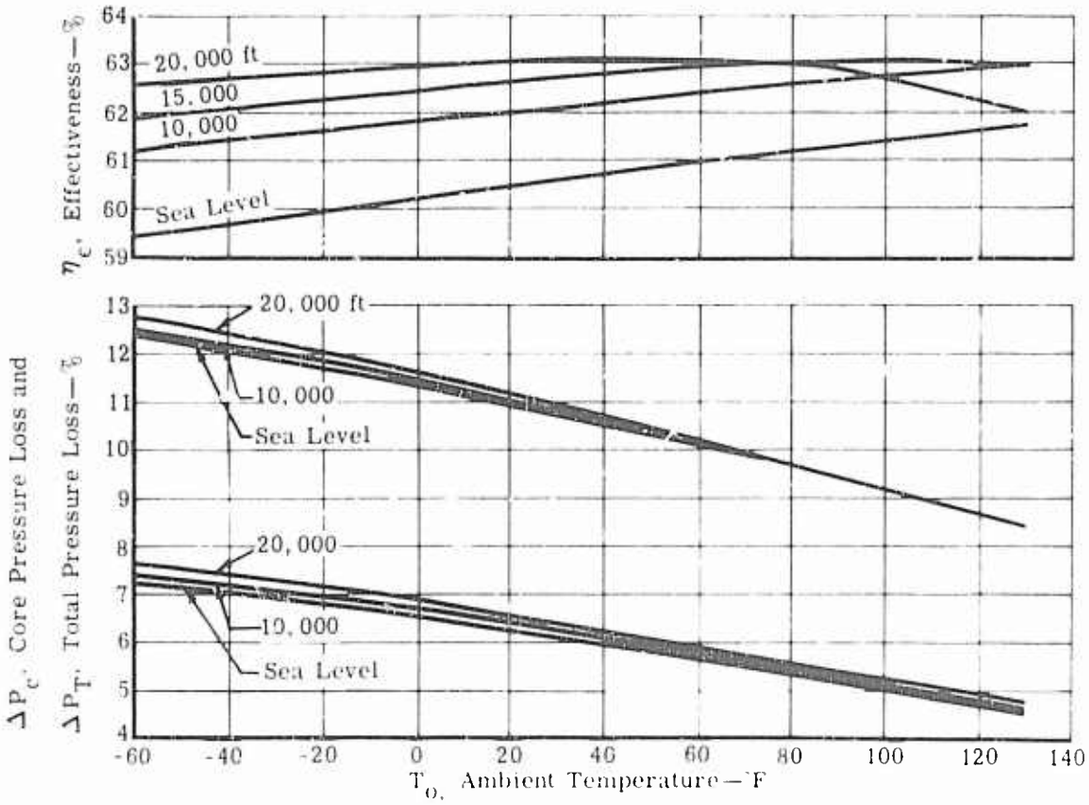

Figure 113. Calculated Regenerator Performance at Normal Power.

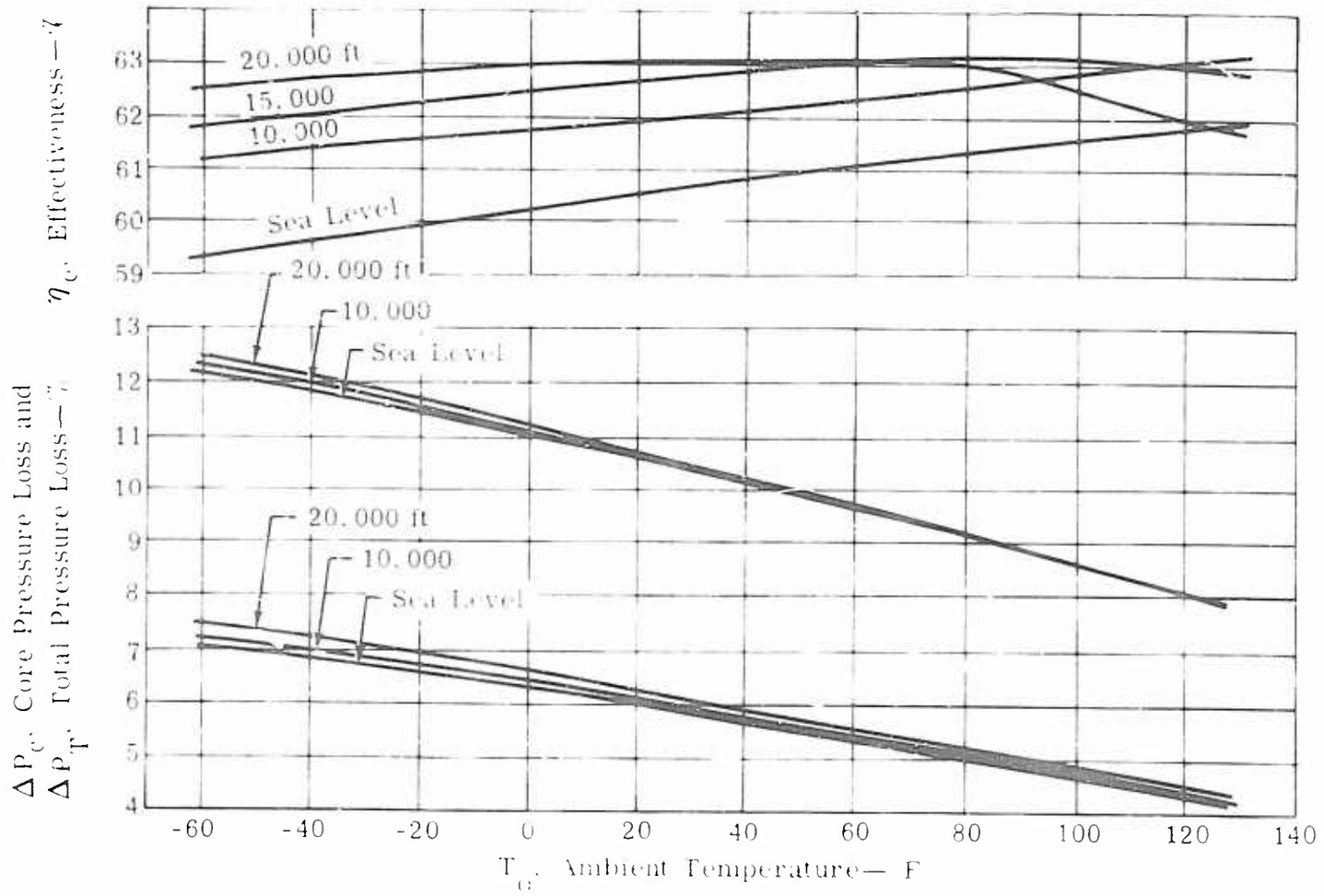

Figure 114. Calculated Regenerator Performance at 90% Normal Power.

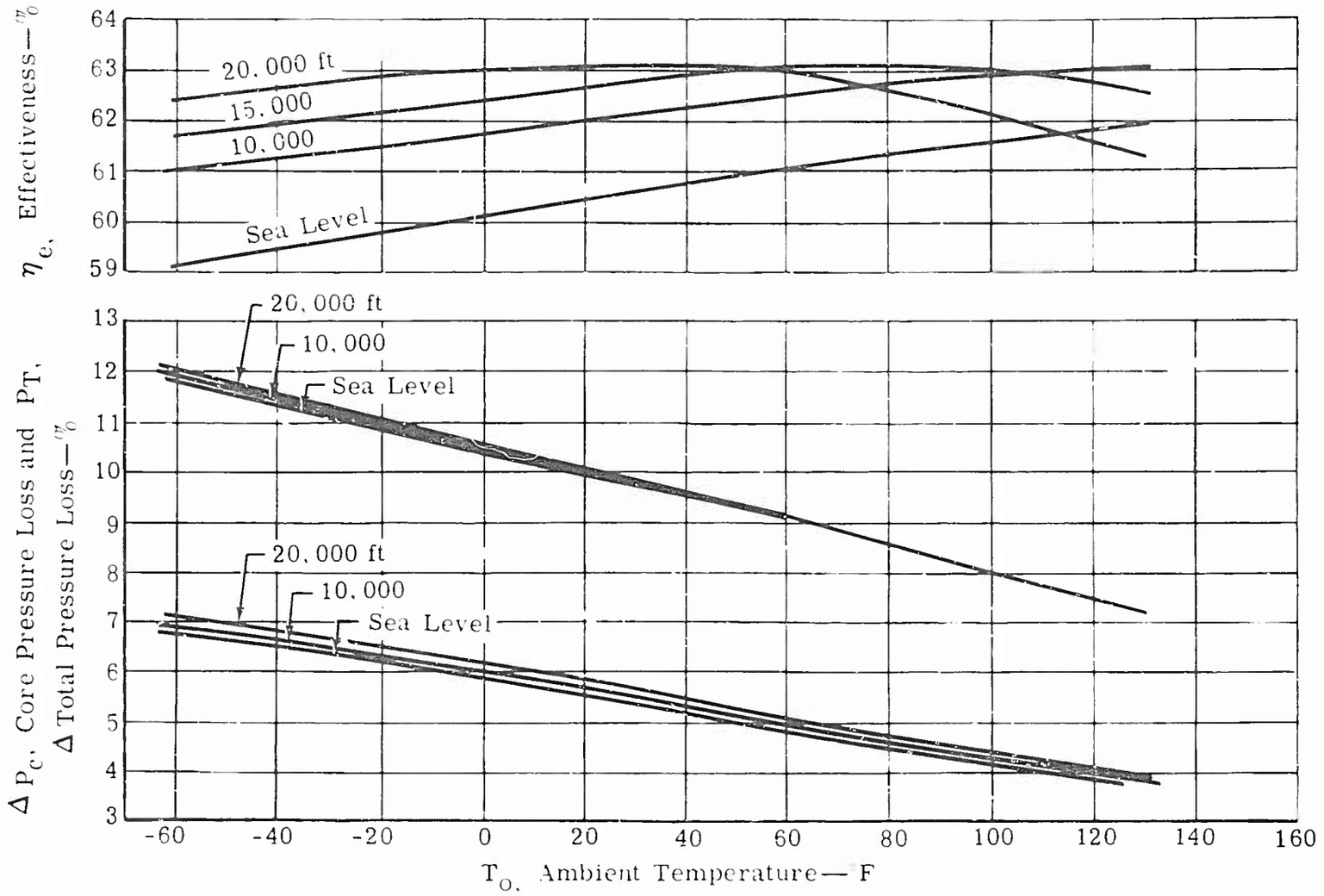

Figure 115. Calculated Regenerator Performance at 75% Normal Power.

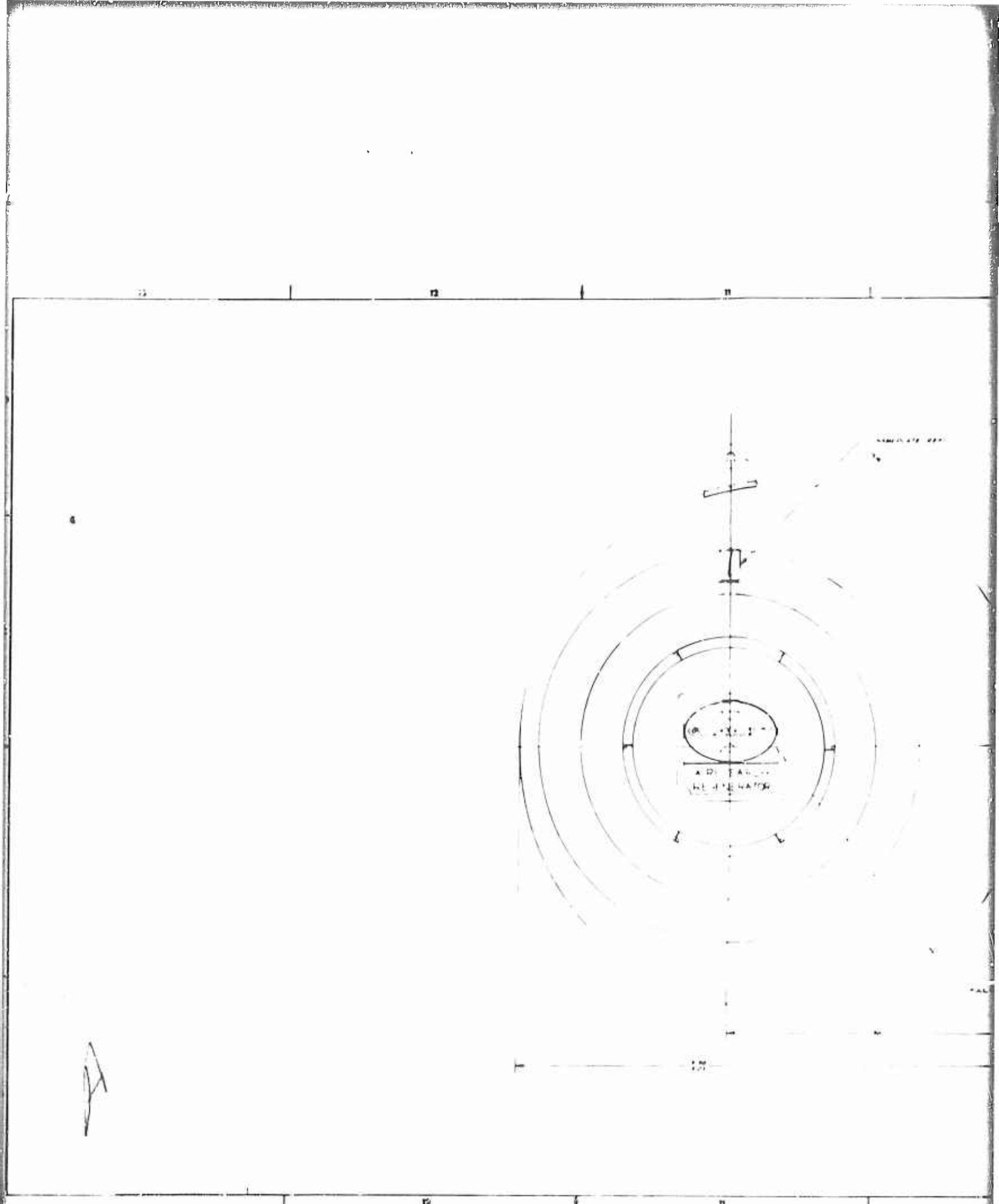

Figure D-1. Regenerator Outline

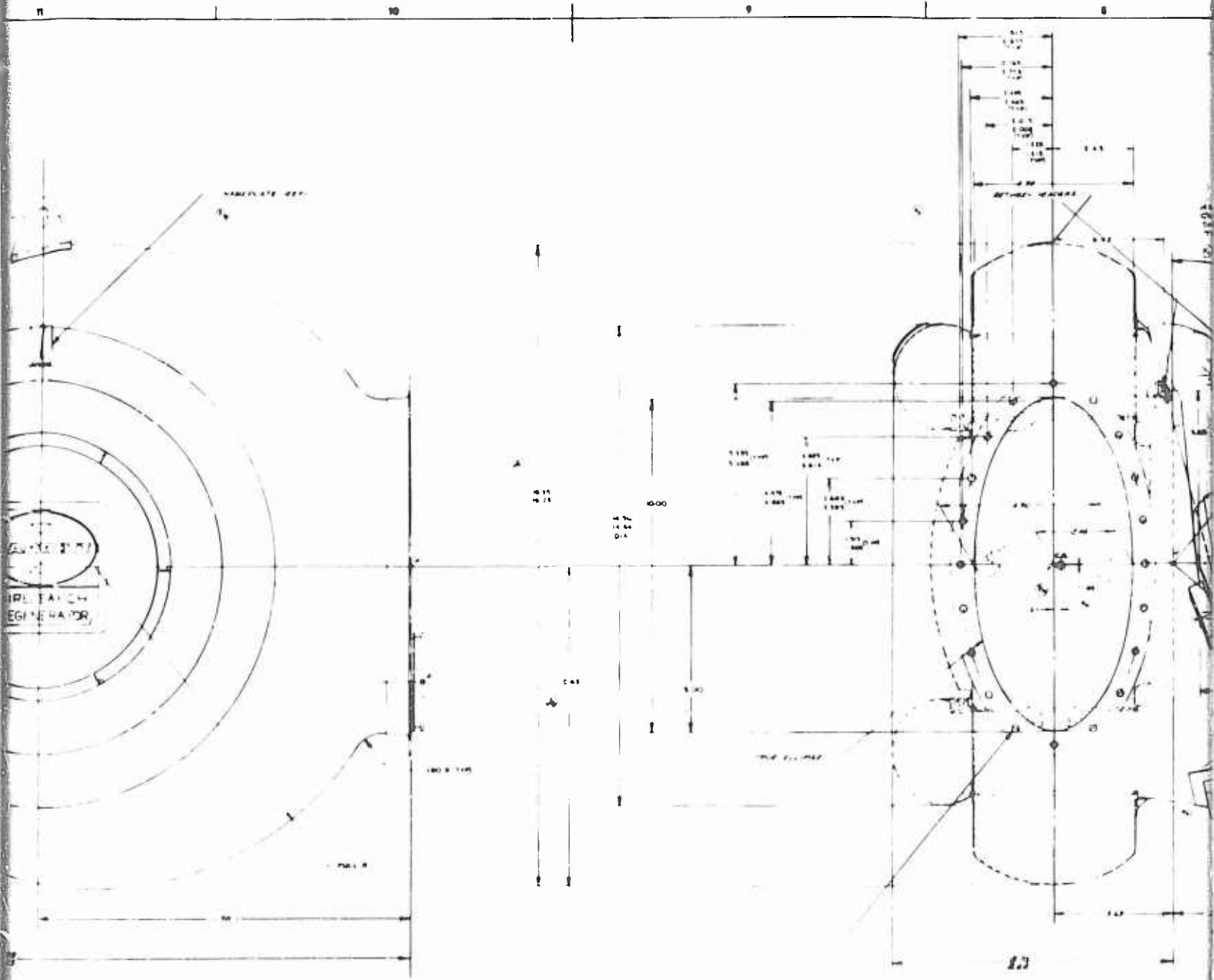

182330

B

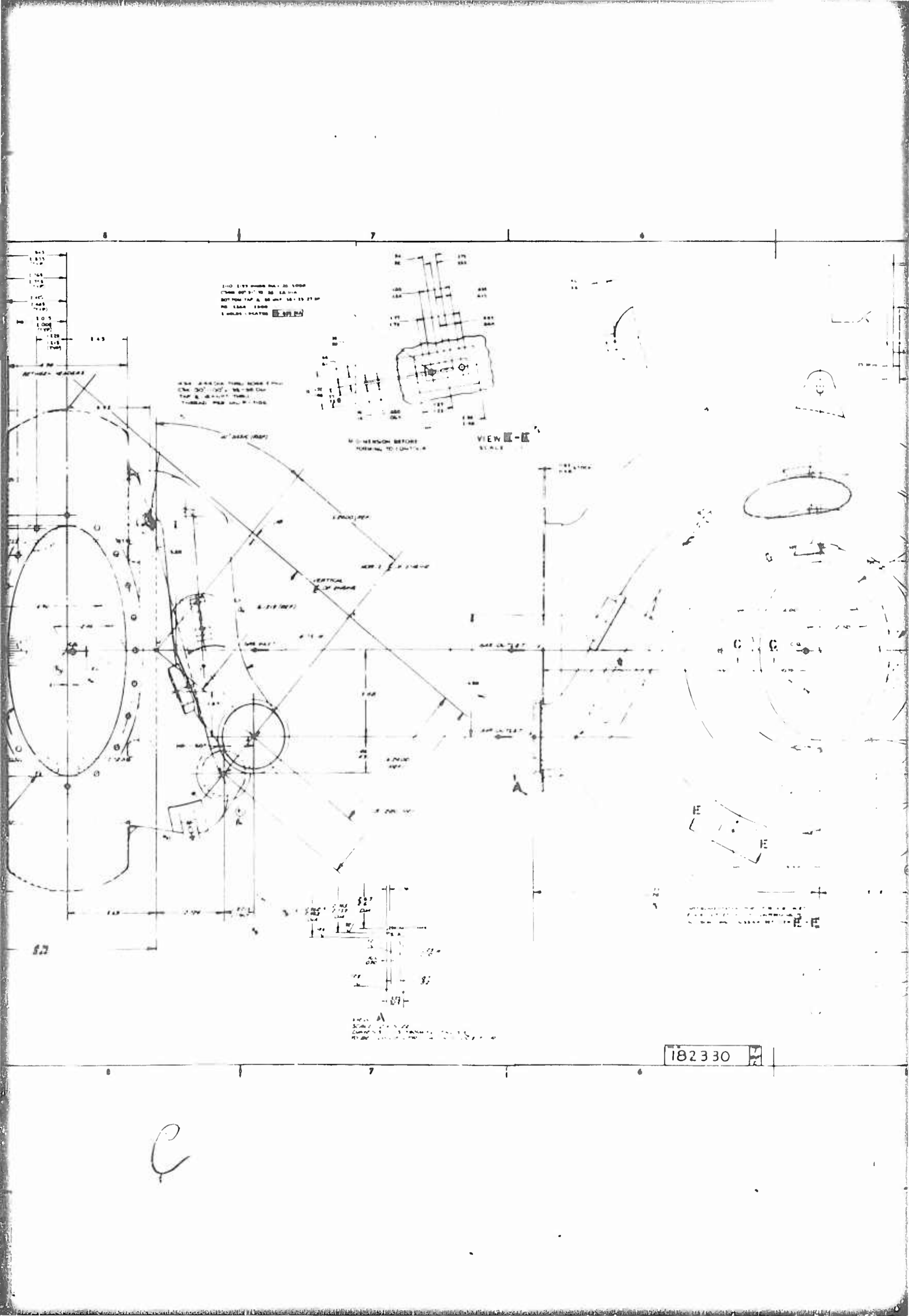
VIEW E-E
182330

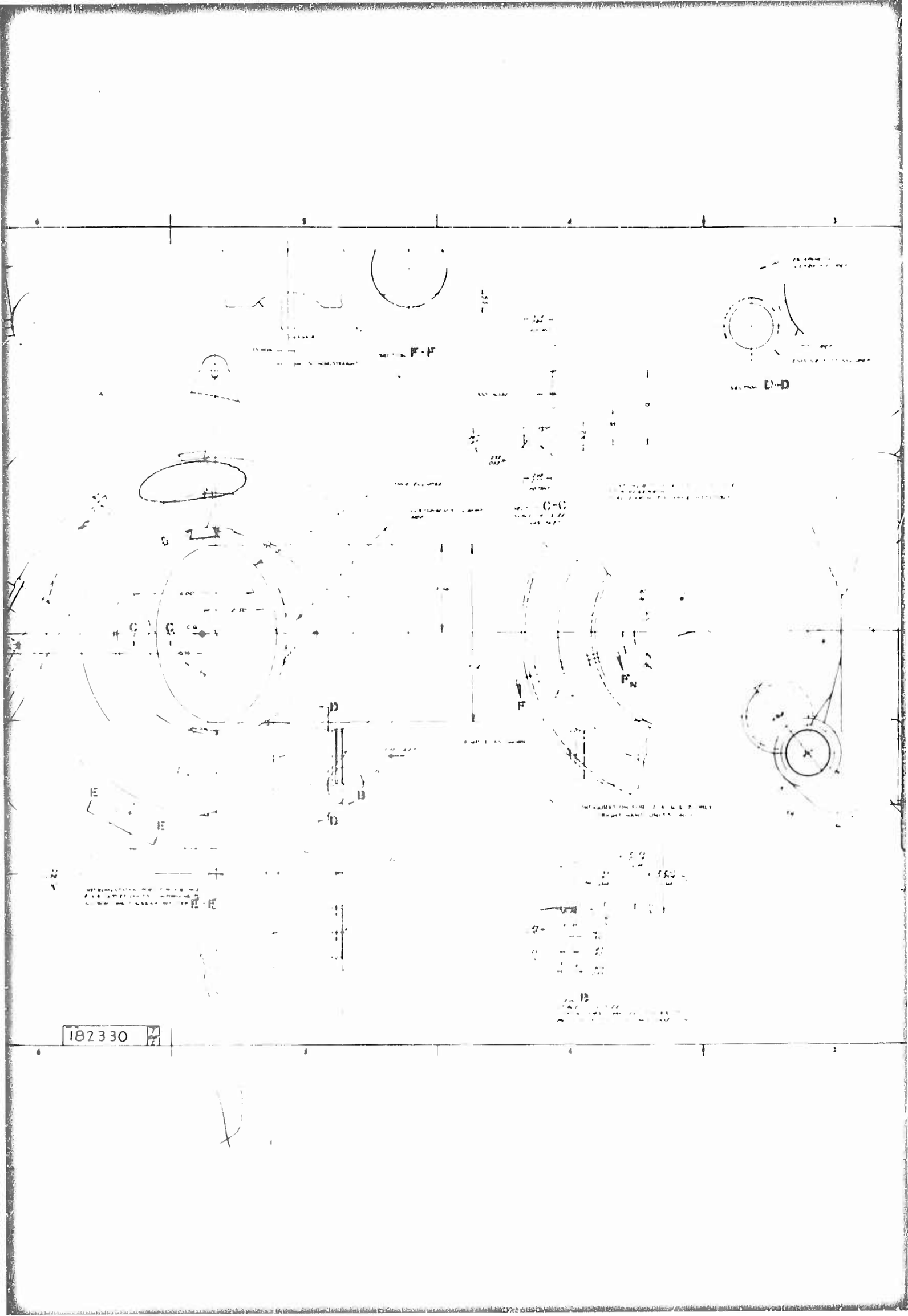
F-F
D-D
C-C
182330

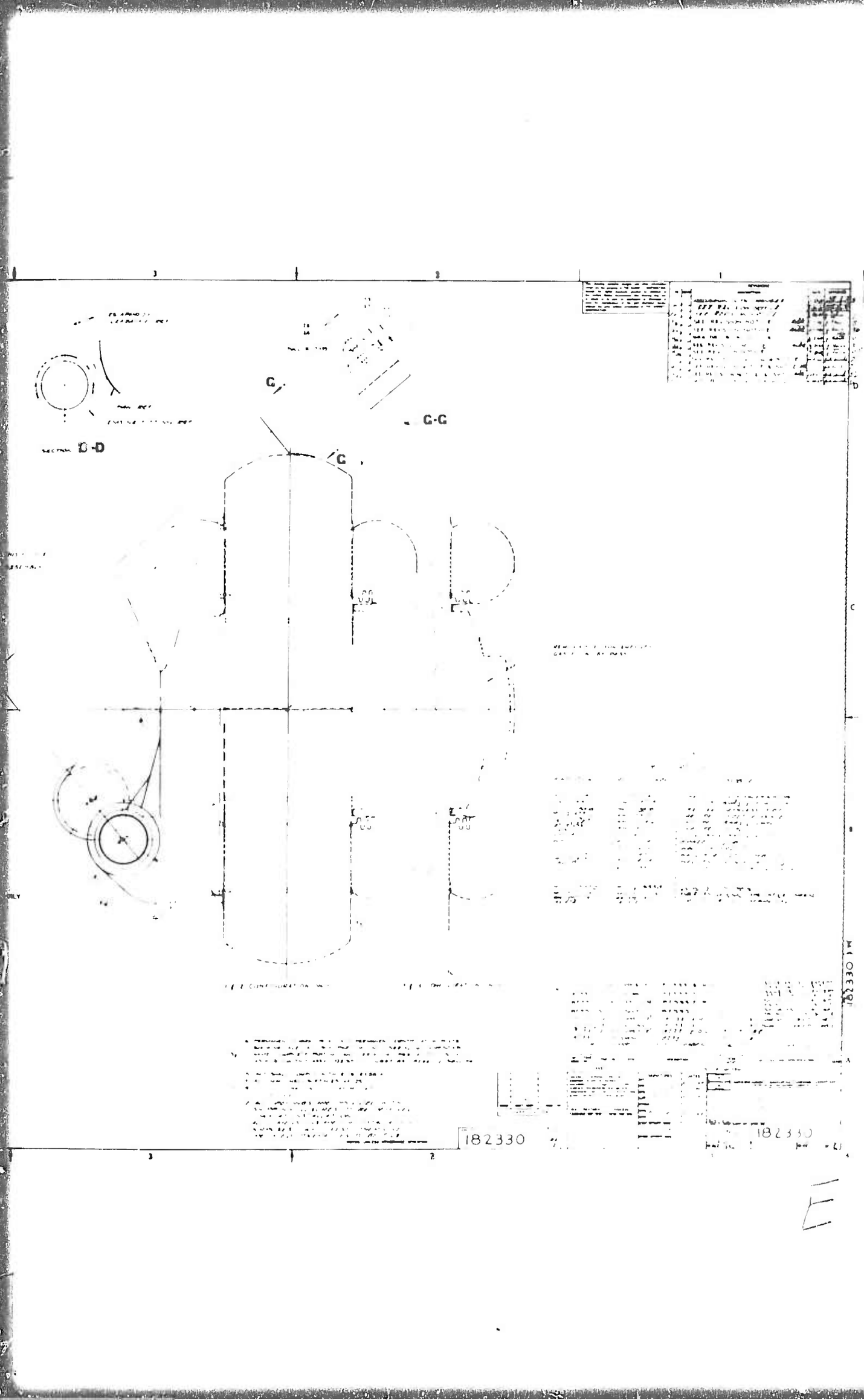
C
C-C
D-D
C
182330
182330

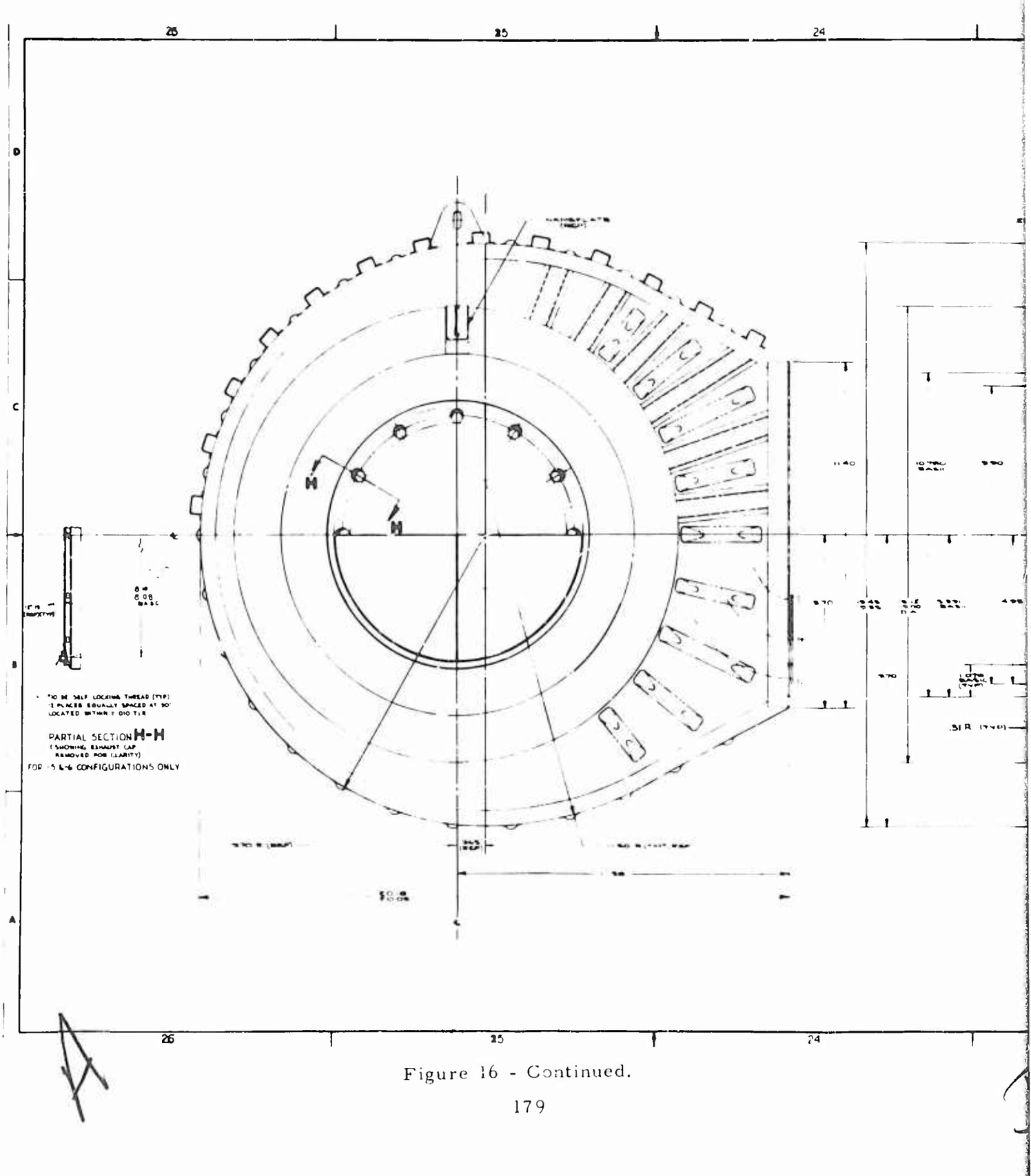

Figure 16 - Continued.

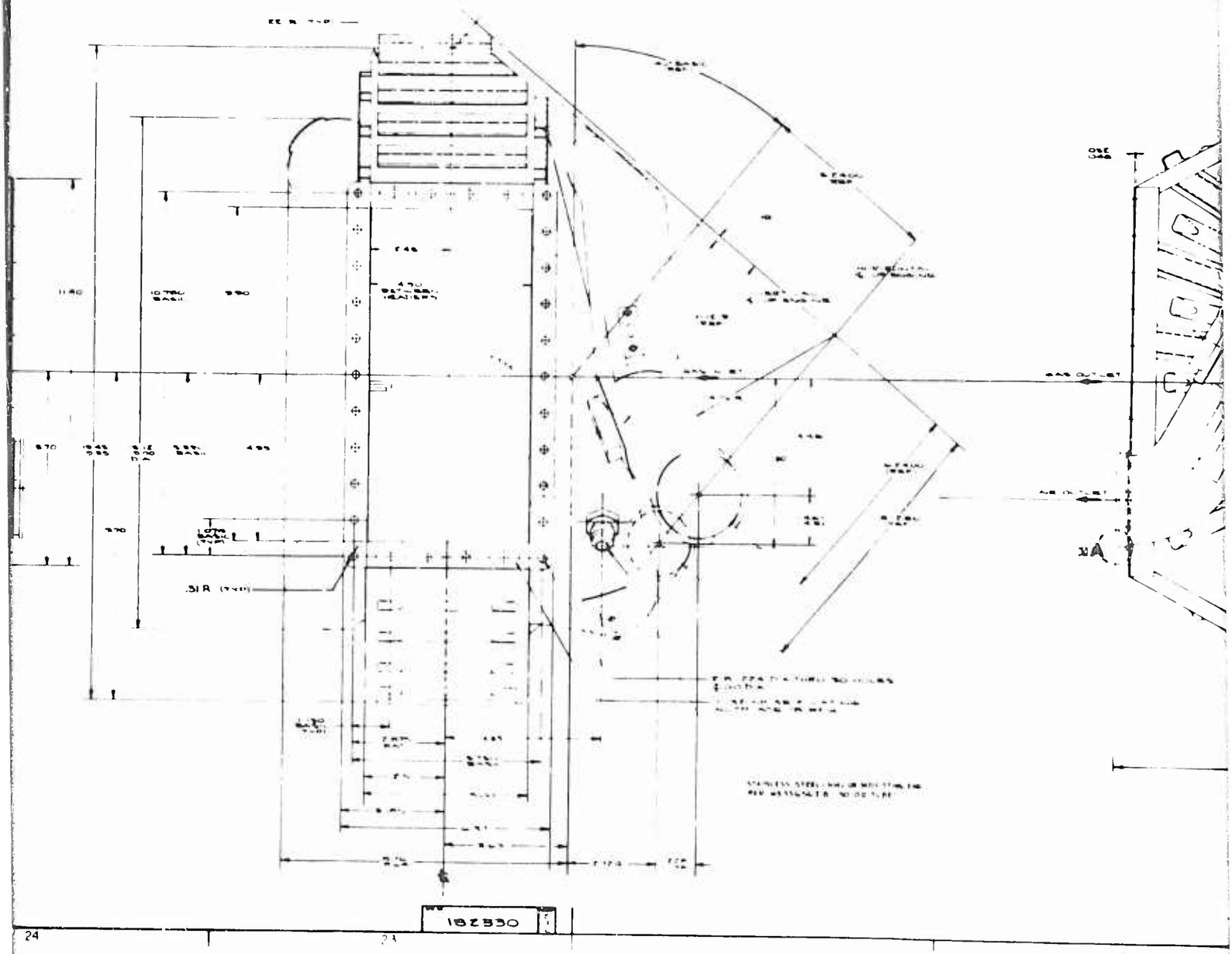

182330

B

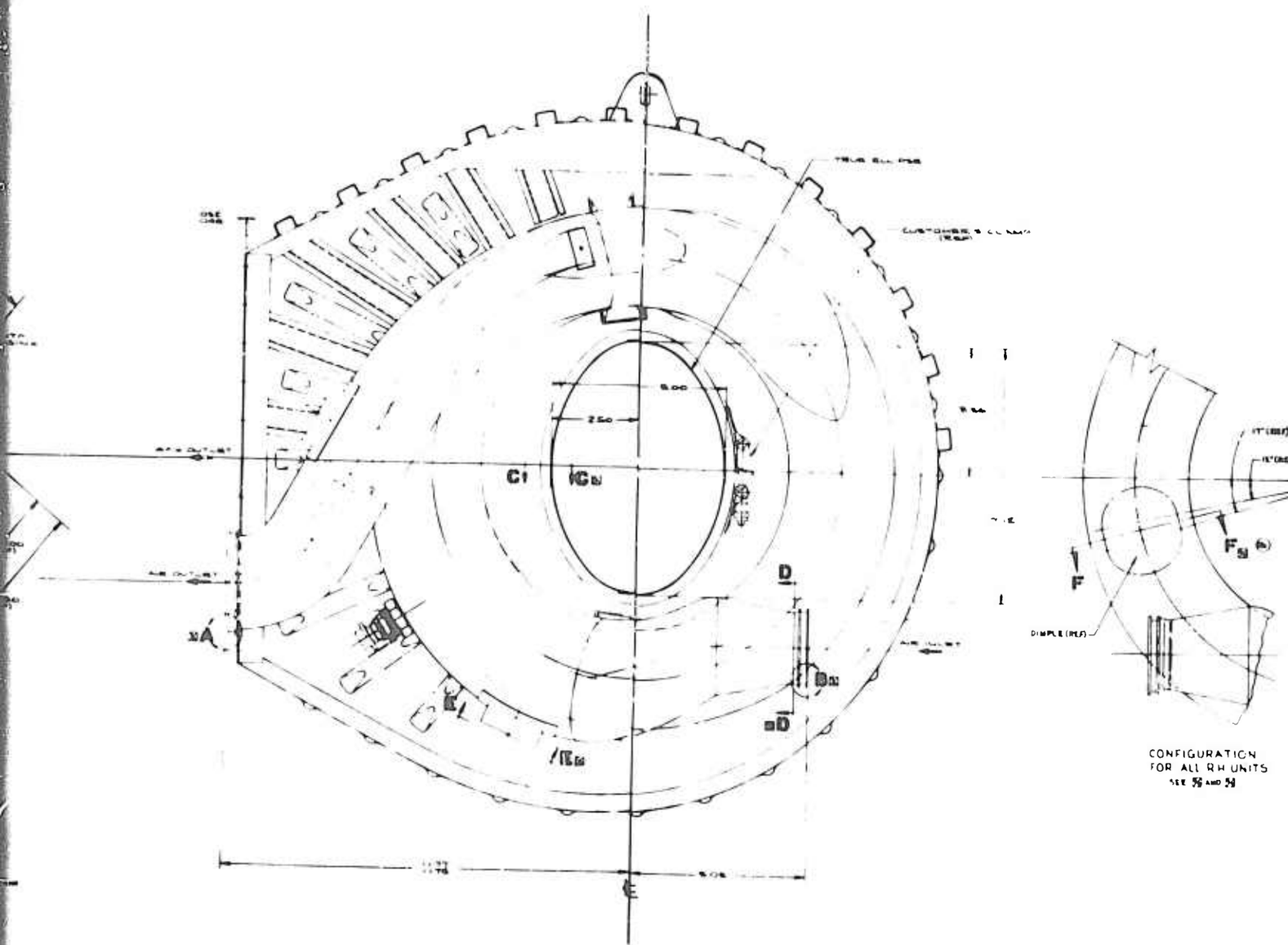

IBZ330

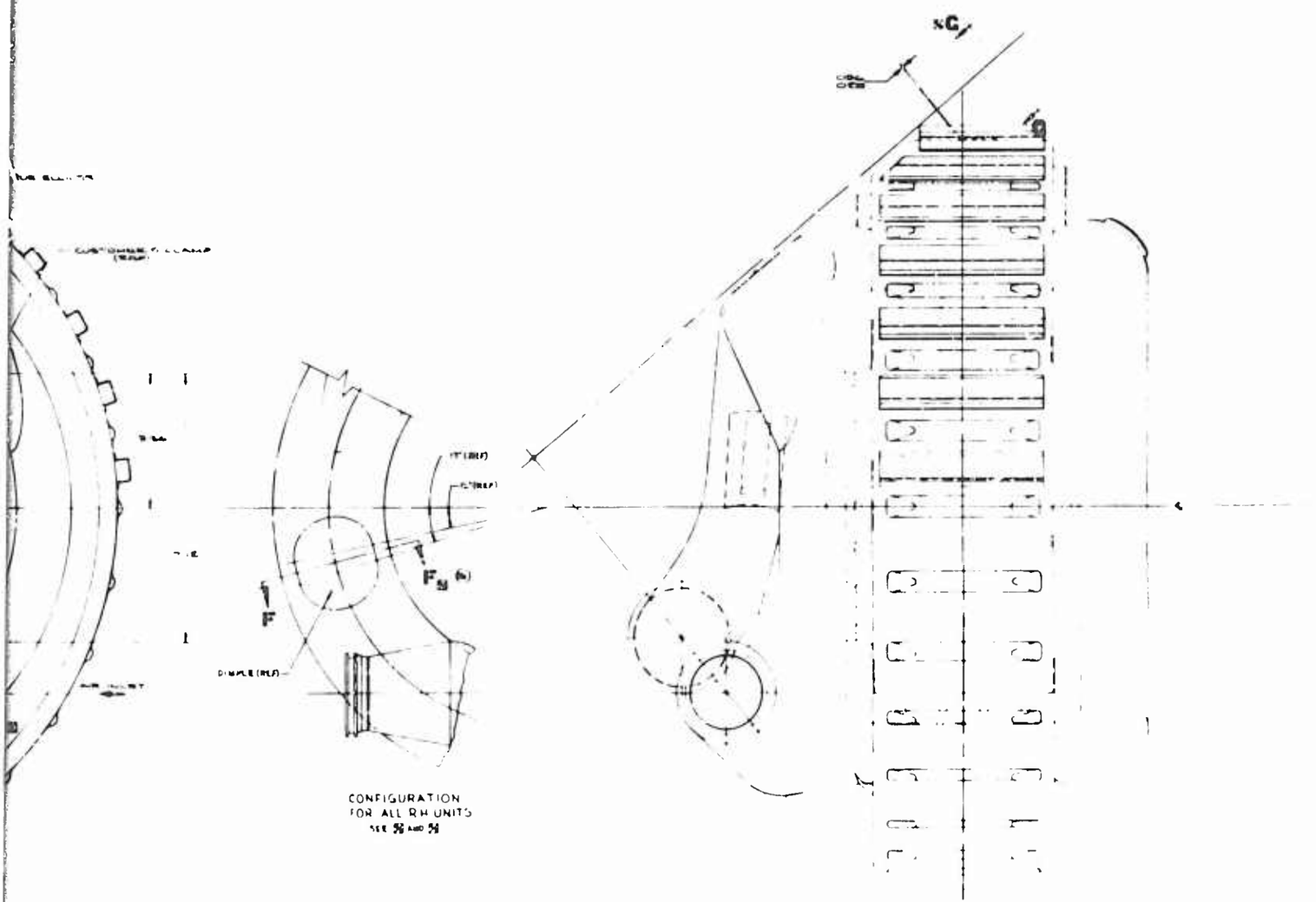

CONFIGURATION
FOR ALL RH UNITS
SEE 56 AND 58

182330

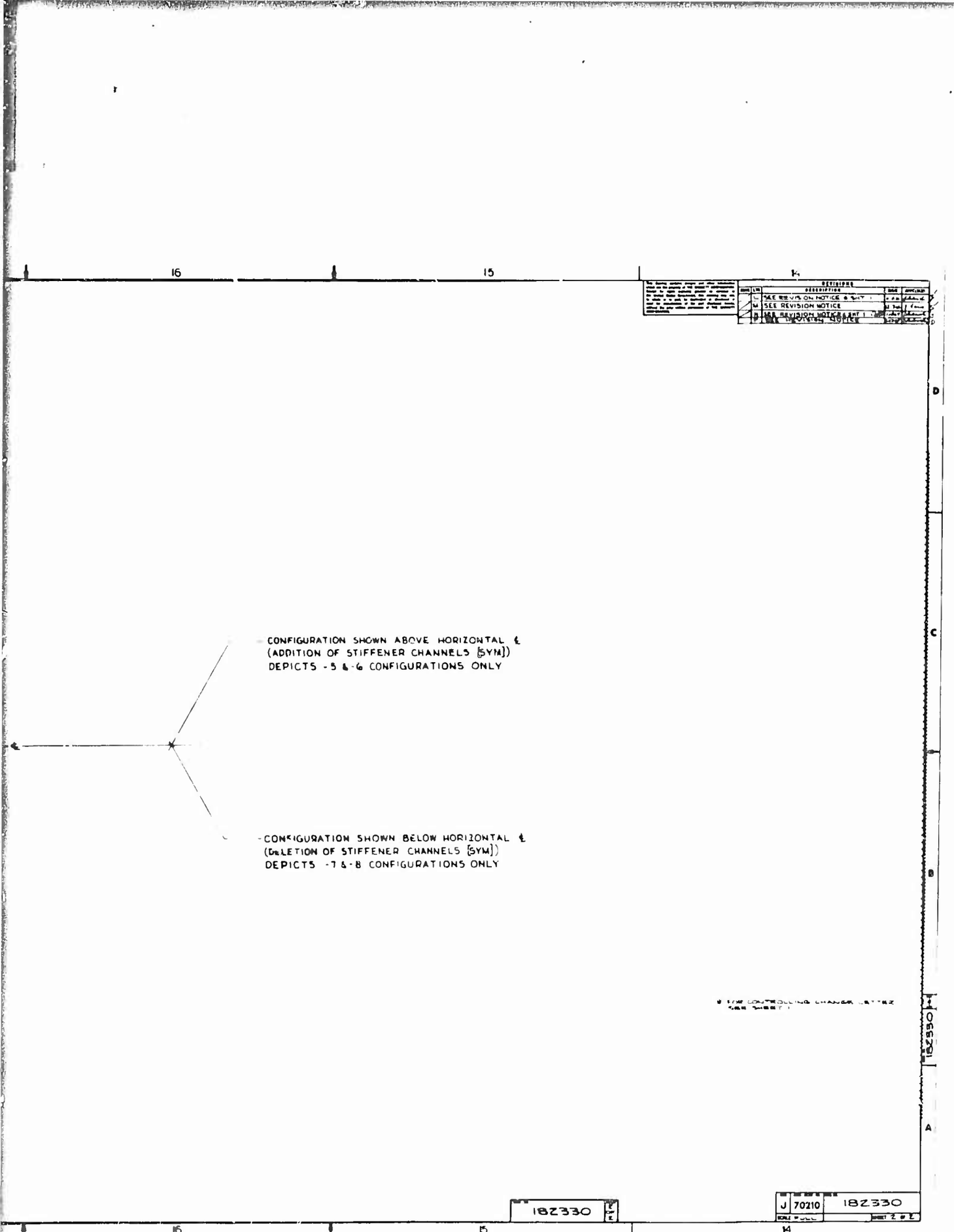
16
15
14
REVISIONS
DESCRIPTION
SEE REVISION NOTICE
SEE REVISION NOTICE
D
C
B
A
CONFIGURATION SHOWN ABOVE HORIZONTAL ℄
(ADDITION OF STIFFENER CHANNELS [SYM])
DEPICTS -5 & -6 CONFIGURATIONS ONLY
℄
CONFIGURATION SHOWN BELOW HORIZONTAL ℄
(DELETION OF STIFFENER CHANNELS [SYM])
DEPICTS -7 & -8 CONFIGURATIONS ONLY
182330
J 70210
182330

E

Unclassified
Security Classification

DOCUMENT CONTROL DATA - R & D

(Security classification of title, body of abstract and indexing annotation must be entered when the overall report is classified)

1 ORIGINATING ACTIVITY *(Corporate author)*
Allison Division, General Motors
Indianapolis, Indiana

2a. REPORT SECURITY CLASSIFICATION
Unclassified

2b. GROUP

3 REPORT TITLE
T63 REGENERATIVE ENGINE PROGRAM

4 DESCRIPTIVE NOTES *(Type of report and inclusive dates)*
Final report

5 AUTHOR(S) *(First name, middle initial, last name)*
Edward J. Privoznik

6 REPORT DATE	7a TOTAL NO OF PAGES	7b NO OF REFS
May 1968	192	None

8a CONTRACT OR GRANT NO	9a. ORIGINATOR'S REPORT NUMBER(S)
Contract DA-44-177-AMC-293(T) b. PROJECT NO c. Task 1M121401A14413 d.	USAAVLABS Technical Report 68-9 9b. OTHER REPORT NO(S) *(Any other numbers that may be assigned this report)* EDR 5380

10 DISTRIBUTION STATEMENT
This document has been approved for public release and sale, its distribution is unlimited.

11 SUPPLEMENTARY NOTES	12. SPONSORING MILITARY ACTIVITY
None	U. S. Army Aviation Materiel Laboratories Fort Eustis, Virginia

13 ABSTRACT

Application of regeneration to the small gas turbine engine can provide a significant improvement in Army aircraft range capability and in fuel logistics. However, very little is known about regenerator performance when tested under actual operating conditions. This is especially true of regenerative engine-aircraft compatibility. The program was oriented toward gaining this experience.

The program was divided into three phases. Phase I consisted of the design and fabrication of the regenerator and required engine modifications. Phase II encompassed the engine testing required to ensure the flightworthiness of the regenerative engine. Phase III included modifications of a YOH-6A helicopter and flight test of the regenerative engine powered aircraft throughout the operating range.

The test program demonstrated the feasibility of a regenerative engine as a power plant for aircraft operation. A horsepower-to-weight ratio of 1.62 and a maximum specific range of 1.2 miles per pound of fuel were demonstrated. The addition of a regenerator increased the specific range of the YOH-6A aircraft by 25.7%. The performance at altitude agreed with the originally predicted values obtained by means of a computer program.

The transient response of the regenerative engine powered aircraft was similar to that obtained using the prototype T63-A-5 nonregenerative engine.

DD FORM 1473

Unclassified
Security Classification

Unclassified
Security Classification

14 KEY WORDS	LINK A		LINK B		LINK C	
	ROLE	WT	ROLE	WT	ROLE	WT
Regenerative Engine T63-A-5 Modification YOH-6A Modification Tube-Shell Stationary Regenerator Regenerative Engine Flight Test						

Unclassified
Security Classification